Mechanisms of immune-mediated liver injury in acute liver failure

Triantafyllou, Evangelos

Awarding institution:
King's College London

Mechanisms of immune-mediated liver injury in acute liver failure

Evangelos Triantafyllou

Thesis submitted to the Faculty of Life Sciences & Medicine at
King's College London for the degree of Doctor of Philosophy

King's College London
Faculty of Life Sciences & Medicine
Division of Transplantation Immunology & Mucosal Biology
Institute of Liver Studies

February 2017

Declaration

I confirm that the thesis does not exceed the word limit prescribed in the College regulations. I further confirm that the work presented in the thesis is my own and all references are cited accordingly.

Dedication

To my parents,

Christos and Fani Triantafyllou

Acknowledgements

During the period of my studies I had the pleasure to work with a number of people to whom I am thankful for their support and contribution. Foremost, I am grateful for the constant inspiration and support provided by my primary supervisor, Dr Harry Antoniades, who has been a great mentor for me. I feel honored to be member of this research group under his guidance and leadership. I would like to thank my second supervisor, Dr Yun Ma, for her kindness, supervision and advice throughout my studies. I would also like to acknowledge Professors Julia Wendon and Mark Thursz for their support and intellectual input to my project, and thank Professor David Adams for the opportunity to carry out part of my research at the National Institute for Health Research (NIHR) Birmingham Liver Biomedical Research Unit of University of Birmingham. I am grateful for his invaluable supervision and advice in the first year of my PhD.

I feel privileged to having joined three different universities throughout my PhD. I have met fantastic colleagues and I am immensely grateful to them for their help, support and encouragement. Sharing a research office with dedicated scientists has enriched my knowledge and experience. In the NIHR Birmingham Liver Biomedical Research Unit (University of Birmingham), I am enormously grateful to Dr Evaggelia Liaskou and Dr Chris Weston for experiencing their enthusiasm about research and providing me assistance with immunological techniques and experiments in these labs. I also thank Dr Stuart Curbishley and Dr Zania Stamataki for technical and methodological support.

In the Institute of Liver Studies (King's College London), I would like to thank Dr Oltin Pop for his valued assistance with immunohistochemistry techniques and Dr Christine Bernsmeier and Dr Arjuna Singanayagam for patient recruitment and lab support with experiments. In the Division of Digestive Diseases (Imperial College London), Dr Wafa Khamri has enormously offered teaching, guidance and help with flow cytometry and cell culture techniques. I also thank and acknowledge Dr Annika Wilhelm, Dr Gemma Petts and Dr Lucia Possamai and the staff of Central Biomedical Services for their guidance and methodological support to carry out animal research. I acknowledge the Medical

Research Council and the Rosetrees Charitable Trust for funding support of this research project. Finally, I would like to thank my parents, Christos and Fani, and my extended family and friends back home for their great support and encouragement during my studies, I am extremely grateful to them.

Abstract

Background: Acute liver failure (ALF) is characterized by overwhelming hepatocyte death and liver inflammation where the infiltration of myeloid cells in areas of necrosis is contrasted by immune cell depletion and dysregulation in the systemic circulation. The mechanisms underlying resolution of acute hepatic inflammation are largely unknown to date. In this thesis, I used both human and murine experimental models in order to investigate the impact of Mer Tyrosine Kinase (MerTK) during ALF and examine how the micro-environmental mediator, Secretory Leukocyte Protease Inhibitor (SLPI), governs this immunological response.

Methods: Flow cytometry, immunohistochemistry, confocal imaging and gene expression analyses determined the phenotypic, functional and transcriptomic profile and tissue topography of MerTK+ monocytes and macrophages in ALF, healthy and disease controls. The temporal evolution of macrophage MerTK expression and its impact on hepatic resolution was examined in APAP-induced acute liver injury using wild-type (WT) and Mer-deficient ($Mer^{-/-}$) mice. Furthermore, SLPI effects on hepatic myeloid cells were determined *in vitro* and *in vivo* using APAP-treated WT mice.

Results: I demonstrate a significant expansion of resolution-like MerTK+HLA-DR^{high} cells in both circulatory and tissue compartments of ALF patients. Compared to WT mice, that show an increase of MerTK+$MHCII^{high}$ hepatic macrophages during the resolution phase in ALF, APAP-treated $Mer^{-/-}$ mice exhibit persistent liver injury and inflammation, characterized by a decreased proportion of liver-resident Kupffer cells and increased number of hepatic neutrophils. Both *in vitro* and in APAP-treated mice, SLPI reprograms macrophages towards resolution responses through induction of a MerTK+HLA-DR^{high} phenotype which promotes neutrophil apoptosis and their subsequent clearance.

Conclusions: The work presented in this thesis has identified a prorestorative, MerTK+, macrophage phenotype that evolves during the resolution phase of APAP-induced ALF and represents a novel immunotherapeutic target to promote resolution responses following acute liver injury.

Significance of this study

What is already known about this subject:

- Liver inflammation is central to the pathogenesis of ALF where infiltration of myeloid cells in areas of hepatic necrosis is contrasted by systemic immune cell depletion and dysregulation.
- MerTK regulates innate immune responses and promotes the clearance of apoptotic cells following acute tissue injury.
- SLPI is produced within the inflamed liver in ALF and is a key modulator of monocyte anti-inflammatory responses.

What are the new findings:

- ALF patients have an expansion of resolution-like MerTK+HLA-DR^{high} monocytes and hepatic macrophages, characterized by suppressed innate and enhanced efferocytic/phagocytic responses.
- MerTK+ monocytes exhibit a distinct pattern of adhesion, phagocytosis, pattern-recognition and cytokine receptors and genes associated with antigen presentation and macrophage polarization.
- A similar phenotype (MerTK+MHCII^{high}) with enhanced phagocytic capabilites evolves during the resolution phase of APAP-induced acute liver injury in mice.
- MerTK-deficient mice exhibit persistent liver injury and inflammation after APAP overdose and are characterized by a depletion in MHCII^{high}-bearing prorestorative resident Kupffer cells and by increased numbers of activated neutrophils.
- SLPI reprograms myeloid cells towards resolution responses by inducing the prorestorative MerTK+HLA-DR^{high} phenotype which promotes neutrophil apoptosis and their subsequent clearance.

How might it impact on clinical practice in the foreseeable future?

- SLPI is a pivotal pro-resolving mediator in ALF that promotes MerTK-dependent hepatic resolution responses following acute liver injury.
- Harnessing the prorestorative capabilities of MerTK+ cells represents a novel therapeutic strategy to promote resolution following acute hepatic inflammatory disorders.

List of abbreviations

AALF, acetaminophen-induced acute liver failure

AHR, airway hyperresponsiveness

AI, autoimmune liver disease

ALD, alcoholic liver disease

ALF, acute liver failure

APACHE II, acute physiology and chronic health evaluation II score

APAP, acetaminophen (paracetamol)

AST, aspartate aminotransferase

BEC, biliary epithelial cell

CCR, chemokine (C-C motif) receptor

CD, cluster of differentiation

CLD, chronic liver disease

ConA, concanavalin A

DAMP, damage-associated molecular pattern

DMSO, dimethyl-sulfoxide

FACS, fluorescence-activated cell sorting

FasL, Fas ligand

FFPE, formalin-fixed paraffin-embedded

Gas6, growth-arrest-specific 6

$GdCl_3$, Gadolinium Chloride

GM-CSF, granulocyte macrophage colony stimulating factor

HBV, hepatitis B virus

HC, healthy control

HCV, hepatitis C virus

HFE, haemochromatosis

HGF, hepatocyte growth factor

HIF-1, hypoxia-inducible factor 1

HLA-DR, human leukocyte antigen-DR

HSC, hepatic stellate cell

HSEC, hepatic sinusoidal endothelial cell

IFN, interferon

IL, interleukin

INR, international normalized ratio

KC, Kupffer Cell

LPS, lipopolysaccharide

LTA, lipoteichoic acid

Ly6C, lymphocyte antigen 6 complex, locus C

Ly6G, lymphocyte antigen 6 complex, locus G

MELD, model for end stage liver disease

$MerTK^{-/-}$, Mer tyrosine kinase receptor deficient mice

MerTK, Mer tyrosine kinase receptor

MMA, mild-moderate asthma

MoMF, monocyte-derived macrophage

MPO, myeloperoxidase

NAALF, non-acetaminophen-induced acute liver failure

NAFLD, non-alcoholic fatty liver disease

NASH, non-alcoholic steatohepatitis

NE, neutrophil elastase

NET, neutrophil extracellular trap

NETosis, neutrophil extracellular trap formation

NF-κB, nuclear factor NF-kappaB

NL, normal liver

NOS, nitrive oxygen species

PBC, primary biliary cirrhosis

PBMC, peripheral blood mononuclear cell

PBMC, peripheral blood mononuclear cells

PBS, phosphate-buffered saline

$PGE_{2,}$ prostaglandin E2

PI3K, phosphoinositide 3 kinase

PMA, phorbol myristate acetate

Pros1, protein S

PS, phosphatidylserine

PSC, primary sclerosing colangitis

PtdSer, phosphatidylserine

PTGER2, PGE_2 receptor EP2 subtype

ROS, reactive oxygen species

RTK, receptor tyrosine kinase

SA, severe asthma

SALF, seronegative acute liver failure

SIRS, systemic inflammatory response syndrome

$SLPI^{-/-}$, secretory leukocyte protease inhibitor deficient mice

SLPI, secretory leukocyte protease inhibitor

SOCS, suppressor of cytokine signaling protein

SOFA, sequential organ failure assessment score

TAM, (Tyro3-Axl-MerTK)

TGF, transforming growth factor

TLR, toll-like receptor

TNF-α, tumor necrosis factor-alpha

TRAIL, TNF-related apoptosis-inducing ligand

TSLP, thymic stromal lymphopoietin

TUNEL, terminal deoxynucleotidyl transferase dUTP nick end labeling (TUNEL)

WCC, white cell count

Presentations, abstracts and publications related to this work

Presentations:

- **European Association for the Study of the Liver (EASL) Masterclass 2016** (Frankfurt, Germany) - Oral presentation: "Mer Tyrosine Kinase (MerTK) promotes hepatic resolution responses in acute liver failure".
- **Clinical Hepatology Practice in 2016: From Science to Therapy** (Birmingham, UK) - Poster presentation: "Secretory leukocyte protease inhibitor (SLPI) drives hepatic resolution responses in acute liver failure".
- **European Association for the Study of the Liver (EASL) Annual Meeting 2016** (Barcelona, Spain) - Poster presentation: "Secretory leukocyte protease inhibitor (SLPI) drives hepatic resolution responses in acute liver failure through modulation of the Mer Tyrosine Kinase (MerTK) pathway".
- **European Association for the Study of the Liver (EASL) Annual Meeting 2015** (Vienna, Austria) - Poster presentation: "Secretory Leukocyte Protease Inhibitor (SLPI) suppresses innate immune responses and promotes resolution of inflammation in an auto/paracrine manner during acute liver failure".
- **American Association for the Study of Liver Diseases (AASLD) The Liver Meeting 2014** (Boston, MA, USA) - Poster presentation: "Secretory Leukocyte Protease Inhibitor (SLPI) promotes hepatic resolution responses in acute liver failure".
- **British Association for the Study of the Liver (BASL) Annual Meeting 2014** (Newcastle, UK) – Poster presentation: "Secretory Leukocyte Protease Inhibitor (SLPI) promotes hepatic resolution responses in acute liver failure".
- **Keystone Symposia - Molecular Cell Biology of Macrophages in Human Diseases 2014** (Santa Fe, New Mexico, USA) - Poster presentation: "Secretory Leukocyte Protease Inhibitor (SLPI): a pivotal mediator of anti-inflammatory responses in acetaminophen induced acute liver failure".

Published abstracts:

- **E. Triantafyllou**, A. Wilhelm, L. Possamai, et al. Secretory leukocyte protease inhibitor drives hepatic resolution responses in acute liver failure through modulation of the MER tyrosine kinase pathway. **Journal of Hepatology**, April 2016. Vol. 64, S425–S630.
- **E. Triantafyllou,** O.T. Pop, E. Liaskou, et al. Secretory Leukocyte Protease Inhibitor (SLPI) promotes hepatic resolution responses in acute liver failure (ALF). **Hepatology**, Volume 60, Issue S1, October 2014, Pages: 546A–564A.
- **E. Triantafyllou**, O.T. Pop, R.D. Abeles, et al. Seronegative acute liver failure represents a macrophage - T cell activation syndrome. **Journal of Hepatology**, April 2014. Vol. 60, Issue 1, S111–S112.

Publications:

- **E. Triantafyllou**, O.T. Pop, L.A. Possamai, A. Wilhelm, E. Liaskou, A. Singanayagam, C. Bernsmeier, W. Khamri, G. Petts, R. Dargue, S.P. Davies, J. Tickle, M. Yuksel, V.C. Patel, R.D. Abeles, Z. Stamataki, S.M. Curbishley, Y. Ma, I.D. Wilson, M. Coen, K.J. Woollard, A. Quaglia, J. Wendon, M.R. Thursz, D.H. Adams, C.J. Weston, and C.G. Antoniades. 2017. MerTK expressing hepatic macrophages promote the resolution of inflammation in acute liver failure. ***Gut.*** doi:10.1136/gutjnl-2016-313615.
- Bernsmeier, C., O.T. Pop, A. Singanayagam, **E. Triantafyllou**, V.C. Patel, C.J. Weston, S. Curbishley, F. Sadiq, N. Vergis, W. Khamri, W. Bernal, G. Auzinger, M. Heneghan, Y. Ma, W. Jassem, N.D. Heaton, D.H. Adams, A. Quaglia, M.R. Thursz, J. Wendon, and C.G. Antoniades. 2015a. Patients with acute-on-chronic liver failure have increased numbers of regulatory immune cells expressing the receptor tyrosine kinase MERTK. ***Gastroenterology*** 148:603-615 e614.
- Antoniades, C.G., W. Khamri, R.D. Abeles, L.S. Taams, **E. Triantafyllou**, L.A. Possamai, C. Bernsmeier, R.R. Mitry, A. O'Brien, D. Gilroy, R. Goldin, M. Heneghan, N. Heaton, W. Jassem, W. Bernal, D. Vergani, Y. Ma, A. Quaglia, J. Wendon, and M. Thursz. 2014.

Secretory leukocyte protease inhibitor: a pivotal mediator of anti-inflammatory responses in acetaminophen-induced acute liver failure. ***Hepatology*** 59:1564-1576.

- Possamai, L.A., W. Khamri, **E. Triantafyllou**, J.A. Wendon, M.R. Thursz, and C.G. Antoniades. 2014a. Could targeting secretory leukocyte protease inhibitor be an effective therapeutic option to prevent infections in acute liver failure? ***Immunotherapy*** 6:667-669.

Table of contents

List of figures

List of tables

CHAPTER 1

1. BACKGROUND

1.1 Acute liver failure

1.1.1 Acute liver failure as a clinical syndrome

Acute liver failure (ALF) is a clinical syndrome that was initially defined as the simultaneous appearance of hepatic encephalopathy and coagulation defects in the setting of an acute liver insult, in the absence of pre-existing liver disease (Trey and Davidson, 1970). Over the years, definitions have varied in regard to duration from time of onset to signs of liver failure. ALF is characterized by overwhelming hepatocyte death, that exceeds the regenerative capacity of the liver, combining the clinical features of an acute severe liver insult with the rapid development of hepatic encephalopathy, coagulopathy, jaundice and progression to multi-organ failure (Bernal et al., 2013). ALF is a rare disease with an incidence in the developed world of fewer than 5 cases per million population per year (Bernal et al., 2015).

Over the last decades, the causes have changed with hepatitis A and B declining in incidence and acetaminophen (paracetamol) toxicity increasing at least in Western Europe and the United States (Bernal et al., 2010). The differences in aetiology between developing and developed countries are well characterized. In Europe and the United States, acetaminophen(APAP)-induced ALF (AALF) and drug-induced liver injury (DILI) form a significant proportion of ALF whilst acute viral hepatitis (e.g. hepatitis B, Hepatitis E) is more common in South Asia, Hong Kong and Australia (Acharya et al., 2002). Seronegative ALF (SALF) is another increasingly well-recognized cause of ALF due to yet unknown etiology. Its clinical diagnosis is based on exclusion of other causes of hepatocellular injury such as viral, autoimmune or drug-induced hepatitis (Bernal et al., 2010; Bernal et al., 2013). It is currently hypothesized that SALF could be due to a dysregulated immune response to an unidentified hepatotropic or environmental trigger (Donaghy et al., 2013).

The relationship of injury pattern, as determined by the etiology, course of illness and its duration, is key in understanding the clinical features and prognosis in ALF. Thus, the terms hyper-acute, acute and sub-acute ALF have been adopted in clinical practice (O'Grady et al., 1993). The period of active injury in ALF is self-limited and the overall pattern of illness is short, there is rapid onset and offset, and a finite period of necrosis. These patients are characterized by a hyper-acute pattern, and, in many cases, a rapid recovery despite developing massive multi-organ failure (Bernal et al., 2015). In acute or sub-acute forms of ALF, injury evolves over one to four weeks, it is not self-limited, but long lasting. DILI, autoimmune hepatitis and most indeterminate ALF cases will have a sub-acute pattern and a worse survival (Bernal et al., 2015).

1.1.2 Immune-mediated liver injury

1.1.2.1 The liver as an immunological and tolerogenic organ

The liver is the largest organ of the human body (1.2–1.5kg) and plays a central role in the immune responses against invading pathogens. It has a dual blood supply, with oxygenated blood entering through the hepatic artery (20%) and blood rich in nutrients and bacterial endotoxin coming through the portal vein (80%) (Liaskou et al., 2012). The liver is constantly exposed to circulating antigens and endotoxins derived from the gut, thus it is prerequisite for its immune system to be appropriately equipped to protect itself from pathogens and tolerate self and foreign antigens (Zimmermann et al., 2012). The liver capillary system is lined with different specialized cells: parenchymal cells including hepatocytes and biliary epithelial cells (BECs) but also non-parenchymal cell, such as hepatic stellate cells (HSCs) and hepatic sinusoidal endothelial cells (HSECs), that act as primary sensors of immune responses (Crispe, 2009). Importantly, the liver contains a large number of immune cells that take part in maintenance of homeostasis but are equally relevant in responses to hepatic injury, thereby playing key roles in both initiation and progression of liver diseases. It contains a high density of myeloid [liver-resident Kupffer cells (KCs), macrophages and neutrophils] and lymphoid (natural killer (NK)

cells, T or B lymphocytes) cells that initiate and shape both innate and adaptive immune responses (Heymann and Tacke, 2016).

1.1.2.2 Sterile inflammation in acute liver failure

Innate immune activation can be etiology-specific; pathogen-associated molecular patterns (PAMPs) are more important in ALF caused by hepatotropic viruses whereas damage-associated molecular patterns (DAMPs) are more important in toxic etiologies such as AALF. Recognition of pathogens by a coordinated interaction of innate immune cells (monocytes, macrophages, dendritic cells (DCs) and NK cells) expressing PAMP and DAMP recognition receptors eventually leads to the activation of adaptive immunity (Chung et al., 2012). Sterile inflammation occurs in tissues in response to different stimuli and can cause tissue stress and injury. This is a key process in drug-induced liver injury including AALF and also in nonalcoholic steatohepatitis (NASH), liver fibrosis and cancer (Kubes and Mehal, 2012).

The liver is primed to respond to injurious stimuli through the release of endogenous damage-associated molecular patterns (DAMPS) that are usually hidden from the extracellular environment, but are released upon tissue injury and which activate receptors on immune cells (Kubes and Mehal, 2012). Following AALF, paracetamol toxic metabolites induce oxidative stress and direct damage to hepatocytes which consequently release DAMPs (e.g. HMGB-1 and histone-associated DNA) that are recognized by liver-resident KCs and neutrophils, leading to their activation. In turn, activated KCs release various pro-inflammatory cytokines (e.g. TNF-α, IL-1β, IL-6) and chemokines (e.g. CCL2), thereby enhancing hepatic inflammation and increasing the influx of bone-marrow derived immune cells like monocytes and neutrophils (Heymann and Tacke, 2016; Kubes and Mehal, 2012). DCs, the major antigen-presenting cells, exert immune tolerance in the liver in collaboration with KCs by suppressing effector T cells and promoting regulatory T cells (Heymann and Tacke, 2016). During AALF, DCs exhibit increased expression of MHC-II, TLRs and secretion of high IL-6, CCL2 and TNF-α levels (Connolly et al., 2011), however, their role in the pathogenesis is yet obscure, due to the

fact that several liver cells types can express “DC markers” like MHC-II and CD11c (Krenkel et al., 2014). Besides myeloid cells, distinct lymphoid populations, especially gamma-delta (γδ) T cells, are linked to the inflammatory response in ALF, and the role of NK, NK (NKT) cells and T cells is still not fully elucidated, as further reviewed in (Heymann and Tacke, 2016; Krenkel et al., 2014) and will be discussed below.

In contrast to the pathogenesis of AALF, SALF is associated with a lymphocytic infiltrate of effector T cells, NK cells and to a lesser extent B cells (Tuncer et al., 2013), suggestive of driving immune-mediated cytotoxic damage to hepatocytes and culminates in massive hepatic necrosis and liver failure (Tuncer et al., 2013; Wu et al., 2010). These histological features and the detection of increased circulating levels of autoantibodies in SALF patients suggest an autoimmune-mediated disorder (Stravitz et al., 2011). In both underlying etiologies of ALF, the recruited immune cells themselves can contribute to hepatocyte damage mediated via direct activation of death receptors or the secretion of cytokines (Bernal et al., 2010; Quaglia et al., 2008). Thus, mechanisms designed to orchestrate liver regeneration and tissue repair can further amplify liver injury and the progression of liver failure (Tuncer et al., 2013).

1.1.2.3 Immuneparesis

Numerous clinical studies suggest that although the inciting event is overwhelming hepatocyte death in ALF, mortality occurs due to the presence of systemic inflammatory response syndrome (SIRS) and its attendant complications of multi-organ failure, immune dysfunction and recurrent infections (Antoniades et al., 2008; Rolando et al., 2000; Schmidt and Larsen, 2006; Vaquero et al., 2003). This condition shares striking similarities with sepsis with regard to the features of systemic inflammation, multi-organ failure and immuneparesis, thus may also share pathogenic mechanisms (Antoniades et al., 2008). Immuneparesis is considered the predominant driving force for morbidity and mortality in septic patients. Accumulating evidence showed that sepsis causes major immunological defects that impair host immunity (Hotchkiss et al., 2013b). These patients exhibit increased apoptosis-induced

loss of innate and adaptive immune cells that leads to immunosuppression and compromises the host's ability to kill pathogens (Hotchkiss et al., 2013a). Another hallmark of sepsis is that monocytes have a diminished ability to produce pro-inflammatory cytokines (e.g. TNF-α, IL-6 and IL-12) in response to endotoxin, TLR agonists or other bacterial compounds, findings that are consistent with the phenomenon of endotoxin tolerance (Hotchkiss et al., 2013b) whereas their anti-inflammatory mediator (e.g. IL-10) release is unaltered or enhanced (Biswas and Lopez-Collazo, 2009; Cavaillon and Adib-Conquy, 2006). Consequently, the increased release of immune-suppressive mediators and decreased antigen presentation due to reduced HLA-DR expression might augment susceptibility to secondary infections; both are associated with a worse outcome in sepsis (Hotchkiss et al., 2013b).

Central to the pathogenesis of ALF is hepatic inflammation where infiltration of myeloid cells in necrotic areas of the liver is contrasted by immune cell depletion and dysregulation in the circulation (Antoniades et al., 2014; Antoniades et al., 2012). ALF patients exhibit features of immuneparesis, mainly characterized by innate immune suppression, in particular of monocytes and neutrophils, that causes deleterious effects on anti-microbial responses and may account for increased susceptibility to infections encountered in these patients (Antoniades et al., 2006; Antoniades et al., 2014; Antoniades et al., 2012; Taylor et al., 2013). Of note, circulating monocytes in ALF show an immunosuppressive phenotype, with reduced HLA-DR expression, and exhibit impaired phagocytic and NF-kB dependent pro-inflammatory responses following microbial challenge (Antoniades et al., 2006; Antoniades et al., 2014; Bernsmeier et al., 2015). Recent work in ALF proposed that anti-inflammatory/regenerative mediators produced within the inflamed liver are of sufficient magnitude to "spill-over" into the systemic circulation, where they can dampen monocyte anti-microbial responses (Antoniades et al.; Possamai et al., 2014b).

1.1.3 Treatment strategies for ALF

The disease's rarity, severity and phenotypic heterogeneity result in a uniquely challenging illness, particularly in relation to its study and the development of effective treatments. The last decades have

seen major changes in ALF patients' care approach, resulting to decreased mortality rate, with the most visible impact coming from the use of emergency orthotopic liver transplantation (OLT) and improved organ support (Bernal et al., 2013). A recent retrospective review study on ALF cases in the United Kingdom showed improvement in hospital survival of ALF patients from 17% (mid-1970s) to 62% (mid-2000s) (Bernal et al., 2013). Despite of established treatment modalities, such as N-acetylcysteine (NAC) and OLT, ALF still presents a high mortality rate over 40 % (Bernsmeier et al., 2014). The immune system contributes crucially to the pathophysiology of ALF. Thus, future studies aiming to a better understanding of the mechanisms regulating immune cell function during ALF will be an essential step towards new treatments. These potential immune-modulatory therapies could be developed such as to re-orientate the immune system to promote the desirable functions of attenuating liver injury and promoting liver repair/regenerative responses (Possamai et al., 2014b).

1.2 Macrophages during liver injury

1.2.1 Macrophages

1.2.1.1 Macrophage origin

Monocytes and macrophages are members of the human mononuclear phagocytic system. Although historically known for their functions in host defense and clearance of apoptotic cells, they are now considered central to tissue development, homeostasis and inflammation, contributing to a broad variety of inflammatory pathologies (Ginhoux et al., 2016). Three major human monocyte subsets are reported to exist in the blood and liver (Ingersoll et al., 2010; Liaskou et al., 2013); the "classical" (CD14+CD16-), "non-classical" ($CD14_{low}$CD16+) and "intermediate" (CD14++CD16+) monocyte subsets (Wong et al., 2011). Different tissue macrophage populations do not necessarily have the same origin; tissue macrophages can arise either from embryonic yolk sac progenitors or adult bone-marrow derived monocytes (Ginhoux and Jung, 2014).

The human liver contains 80% of all body macrophages and is patrolled by myeloid cells which scan the liver vasculature and eventually infiltrate into the organ (Tacke and Zimmermann, 2014). During steady state, bone marrow-derived monocytes traffic to the liver and develop into monocyte-derived macrophages (MoMFs), a process that is markedly increased following acute liver injury (Holt et al., 2008; Varol et al., 2009) (**Fig. 1.1**). It is proposed that MoMFs do not contribute to the pool of liver-resident self-renewing Kupffer cells (KCs) which are exclusively derived from embryonic progenitors (Gomez Perdiguero et al., 2015; Schulz et al., 2012). However, a recent study using a diphtheria toxin-mediated resident KC depletion to generate niche availability, demonstrated that monocytes engraft in the liver and can gradually adopt the transcriptional profile of their depleted counterparts (KCs), giving rise to self-renewing fully differentiated KCs (Scott et al., 2016) (**Fig. 1.1**).

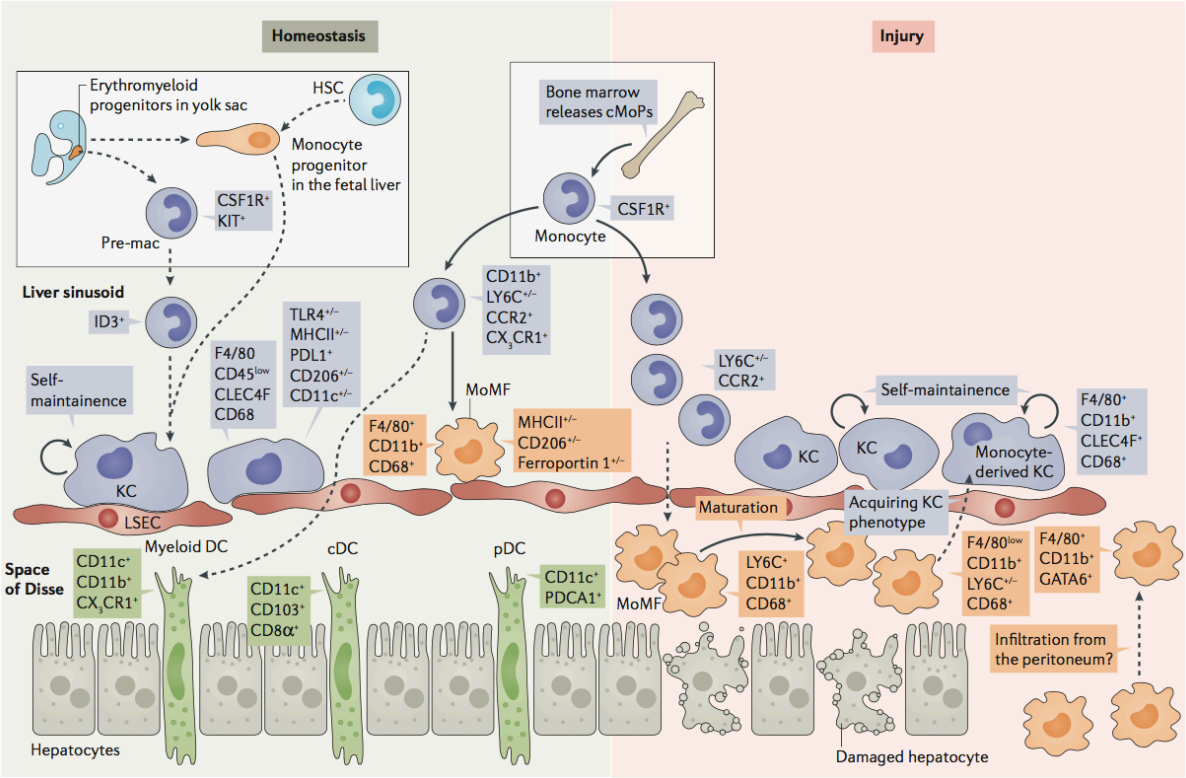

Figure 1.1 The origin of hepatic macrophage subsets.

Murine CD11b+F4/80+ Kupffer cells (KCs) originate from erythromyeloid progenitors that express macrophage colony-stimulating-factor-1-receptor (CSF1R) and are derived from the embryonic yolk sac and/or fetal liver. KCs are capable of self-replication during homeostasis and after liver injury. In adult mice, liver-infiltrating monocytes express LY6C, CC-chemokine receptor 2 (CCR2) and CX3C-chemokine receptor 1 (CX3CR1) can give rise to monocyte-derived macrophages (MoMFs) or myeloid dendritic cells (DCs). During steady state, the contribution of monocytes to hepatic macrophages is low but following liver injury monocytes are strongly recruited to areas of inflammation. Directly after tissue infiltration, monocytes are CD11b+F4/80− and mature into CD11b+F4/80+ MoMFs. If KCs are fully depleted, MoMFs can acquire a KC-like state (‘monocyte-derived KC’) with the ability to self-renew. Infiltrating peritoneal GATA6+ macrophages might contribute to the pool of hepatic macrophages during liver injury. Dashed arrows indicate cell migration or infiltration. cMoP, common monocyte progenitor; HSC, haematopoietic stem cell; ID3, inhibitor of DNA binding 3; LSEC, liver sinusoidal endothelial cell; MHCII, MHC class II; PDCA1, pDC antigen 1; PDL1, programmed cell death protein 1 ligand 1; pre-mac, pre-macrophage; TLR4, Toll-like receptor 4 [adapted from: (Krenkel and Tacke, 2017)].

1.2.1.2 Macrophage plasticity

Characteristic features of macrophages are their diversity and plasticity in function (Ginhoux et al., 2016). When macrophages encounter pathogens, they secrete pro-inflammatory cytokines and reactive oxygen and nitrogen species that aid their antimicrobial and immune function to eliminate pathogens. In contrast, during homeostatic conditions, different micro-environmental cues induce macrophages to adopt phenotypes linked with tissue repair and remodeling functions. Macrophages were traditionally categorized into either pro-inflammatory (M1), wound-healing (M2) or immune-suppressive (Mreg) (Mosser and Edwards, 2008). However, recent transcriptomic analyses of human monocyte-derived macrophages cultured with different stimuli revealed a spectrum of macrophage activation states, that challenges the M1/M2 classification (Xue et al., 2014). The signals received by macrophages are diverse, temporally and spatially dynamic. Macrophages not only respond with diverse phenotypes and various activation states, but also reversibly switch from one phenotype to another (Epelman et al., 2014; Sica and Mantovani, 2012). A newly proposed way of looking at the activation state of macrophages is to consider a multidimensional model that includes the different local signals to which they are exposed, their specific microenvironments and a collection of macrophage activation markers (Ginhoux et al., 2016; Murray et al., 2014).

1.2.2 Macrophages and liver inflammation

1.2.2.1 Macrophage functions

Macrophages are a key component of liver inflammation and exhibit great functional diversity, thus they are involved in tissue homeostasis, inflammation but also regression of liver injury. Due to their great inherent plasticity, hepatic macrophages flexibly respond to differential environments and adopt to the educative signals arising from parenchymal and immune cells within the liver (Davies et al., 2013; Lavin et al., 2014). Hence, they execute diverse functions during liver inflammation, ranging from tissue-destructive to resolution/pro-restorative roles (Sica and Mantovani, 2012). Macrophages secrete high levels of reactive oxygen/nitrogen species and inflammatory cytokines and chemokines, therefore are able to propagate both innate and adaptive immune responses. They critically influence

the different phases following liver injury, by promoting the clearance of cell debris, extracellular matrix remodeling, tissue regeneration and resolution of inflammation (Heymann and Tacke, 2016). Moreover, hepatic macrophages isolated from injured murine livers express M1 and M2 markers simultaneously (Ramachandran et al., 2012), which contradicts the M1/M2 dichotomic approach discussed above.

1.2.2.2 Macrophages in chronic liver disease

Macrophages critically influence inflammation and insulin resistance in different metabolic disorders and alcoholic liver disease (McNelis and Olefsky, 2014). Patients characterized by obesity and heavy alcohol drinking exhibit similar patterns in expression of macrophage activation markers, that are related to severity of liver steatosis and fibrosis (Wan et al., 2014). Macrophages play a central role in fibrogenesis in murine models of alcoholic steatohepatitis and NASH, where they propagate liver inflammation through TNF-α secretion and leukocyte recruitment via ICAM-1 and VCAM-1 (Tomita et al., 2006). In contrast, predominance of M2-polarized, IL-10-expressing macrophages was found to be protective in experimental alcoholic liver disease or non-alcoholic fatty liver disease (NAFLD) (Wan et al., 2014). Macrophage activation during NASH in mice is also related to accumulation of toxic lipids, such as ceramide, that promotes activation of NLRP3 and AIM2 in both infiltrating and liver-resident macrophages (Csak et al., 2014; Leroux et al., 2012; Miura et al., 2010). During metabolic disorders, CCR2+ bone-marrow derived monocytes traffic to the liver where they promote NASH while CCL2 inhibition is shown to diminish monocyte liver infiltration and steatohepatitis in chronic hepatic injury (Baeck et al., 2012; Miura et al., 2012).

Although hepatic macrophages show several features for antiviral immunity, for example expression of TLR and NOD-like receptors or secretion of IL-12 and IL-18, their role against viral hepatitis remains controversial (Boltjes et al., 2014). Both HBV and HCV infections modulate some of the macrophage antiviral effector mechanisms, through inhibition of TLR activation or induction of anti-inflammatory pathways (e.g. PD-L1) (Boltjes et al., 2014; Tu et al., 2010). In addition, macrophages

may even promote HCV entry in a TNF-dependent manner *in vitro* (Fletcher et al., 2014). By contrast, both KCs and MoMFs isolated from human livers explants of HCV patients are described as a primary source of IL-1β, (Negash et al., 2013).

Hepatic macrophages are central to the pathogenesis of chronic liver injury. They are numerically expanded in patients with hepatic cirrhosis and fibrosis (Zimmermann et al., 2011) where both profribrotic and antifibrotic roles have been described (Tacke and Zimmermann, 2014). Intermediate $CD14^{high}CD16+$ monocytes accumulate in the chronically inflamed liver due to the enhanced recruitment and local differentiation from classical CD14+CD16− monocytes, a process mediated by chemokines (e.g. CX3CL1) (Aspinall et al., 2010; Liaskou et al., 2013). $CD14^{high}CD16+$ macrophages are highly phagocytic, secrete inflammatory mediators and can activate the collagen-producing HSCs, thus playing a crucial role in fibrogenesis (Zimmermann et al., 2010). Also, monocytes infiltrate the chronically inflammed liver of mice, in a CCL2–CCR2 and CCL1–CCR8 chemokine-dependent manner, and differentiate into inflammatory macrophages that enhance fibrosis by activating HSCs activation and enhancing myofibroblast survival while also promote angiogenesis (Baeck et al., 2012; Ehling et al., 2014; Heymann et al., 2012; Karlmark et al., 2009; Pradere et al., 2013).

Prorestorative hepatic macrophages, characterized by Ly6C low expression, were recently identified in mice as key players in resolving fibrosis and accumulated in the liver during the restorative phase after tissue damage (Ramachandran et al., 2012). These $Ly6C_{low}$ hepatic macrophages derive from infiltrating $Ly\text{-}6C^{high}$ monocytes/macrophages (Ramachandran et al., 2012), thus undergo a functional switch during the course of liver injury, the mechanisms of which warrant further investigation. Gene expression analysis revealed that $Ly6C_{low}$ cells displayed a profile that cannot be classified based on the M1/M2 nomenclature, and importantly secreted matrix metalloproteinases (e.g. MMP9, MMP12 and MMP13) needed for matrix degradation and favor resolution of liver fibrosis (Ramachandran et al., 2012; Tacke and Zimmermann, 2014). Another feature of those restorative macrophages is that they are post-phagocytic and administration of liposomes boosted the degradation of extracellular matrix (Ramachandran et al., 2012). Of note, even after cessation of liver injury, a sustained $Ly\text{-}6C^{high}$

macrophage influx was observed, that dampens spontaneous fibrosis regression through secretion of pro-inflammatory cytokines (e.g. TNF-α). Blocking the CCR2/CCL2-dependent influx during the resolution phase of fibrosis therefore even enhances clearance of scar fibers (Baeck et al., 2012; Ehling et al., 2014). Together, these findings suggest that freshly infiltrating macrophages worsen liver injury whereas restoration is elicited by locally matured MoMFs. Further studies to understand the regulatory mechanisms underlying hepatic macrophage heterogeneity may help to develop novel macrophage subset-targeted therapies for liver injury and fibrosis (Krenkel and Tacke, 2017).

1.2.3 Macrophages in acute liver failure

The role of macrophages during acute liver injury is controversial, which is not surprising given the several functions of these cells at different phases of sterile liver inflammation. This can be attributed to their great heterogeneity and difficulty in distinguishing between the subpopulations, especially under inflammatory stress. Initial studies using Gadolinium Chloride ($GdCl_3$) to deplete KCs prior to paracetamol (APAP) dosing was protective mice from liver injury (Laskin et al., 1995; Michael et al., 1999). Subsequent studies used $CCR2^{-/-}$ knockout mice, thus preventing monocyte recruitment into the liver. Here, inhibition of monocyte infiltration to the liver following APAP dosing, exacerbated inflammation and delayed recovery (Dambach et al., 2002; Hogaboam et al., 2000). Two other studies using clodronate-loaded liposomes, that deplete the liver-resident macrophages, revealed that macrophage inhibition had either no effect or a detrimental effect on liver injury (Ju et al., 2002a; Karlmark et al., 2009). However, the past years several researchers using advanced experimental approaches, such as intravital multiphoton microscopy, flow cytometry based sorting of immune cells and gene expression analyses, have shown that hepatic macrophages orchestrate both pro-inflammatory/tissue-destructive and resolution/tissue-repair responses during acute liver injury (Antoniades et al., 2014; Antoniades et al., 2012; Mossanen et al., 2016; Zigmond et al., 2014).

KCs initiate immune-mediated injury but also exhibit a protective role and play an important part in removal of apoptotic cell debris (Heymann and Tacke, 2016; Krenkel et al., 2014; Krenkel and Tacke, 2017). Following liver injury, DAMPS released from injured hepatocytes activate KCs which release

an array of pro-inflammatory cytokines (e.g. TNF-α, IL-1β, IL-6), reactive oxygen species (ROS) and chemokines, thus promoting influx of circulating immune effector cells to sites of tissue damage (**Fig. 1.2**) (Kubes and Mehal, 2012). Patients with AALF exhibit an expansion of hepatic macrophages, that localize in areas of necrosis, which is not only due to the proliferation of the resident KCs but also through a chemokine, CCR2 and CCR5, dependent recruitment of circulating monocytes to the liver (Antoniades et al., 2012; Choi et al., 2015a; Dambach et al., 2002; Holt et al., 2008; Mossanen et al., 2016; Zigmond et al., 2014).

Experimental studies revealed that after KC activation, there is an expansion of hepatic macrophages at 12 hours post paracetamol-induced liver injury in mice, and this is mainly due to MoMFs rather than proliferation of KCs (Holt et al., 2008; Karlmark et al., 2009; Zigmond et al., 2014). In parallel to the monocyte influx, KCs are decreased numerically between 24-48 hours post injury while full recovery takes place by 120 hours, which does not rely on CCR2+Ly6C^{high} infiltrating monocytes but is achieved through self-renewal of KCs (Dambach et al., 2002; Ramachandran et al., 2012; Zigmond et al., 2014). These findings concur with previous human data demonstrating a significant proliferative activity of CD68+ KCs in explanted liver tissue (Antoniades et al., 2012). Moreover, gene expression analysis of KCs during the recovery stages of acute liver injury revealed a pro-restorative phenotype that express a repertoire of tissue-repair associated genes (Zigmond et al., 2014).

It is proposed that F4/80 and CD11b expression levels can be used to define developmentally distinct macrophage populations. Cells that are F4/80^{high} CD11b$_{low}$ represent the liver-resident KCs while F4/80$_{low}$ CD11b^{high} cells represent the MoMFs (Holt et al., 2008; Ramachandran et al., 2012). Differential Ly6C expression was recently suggested as marker of the differentiation state of MoMFs (Zigmond et al., 2014). In addition to liver KCs and Ly6C^{high} infiltrating monocytes, a third distinct Ly6C$_{low}$ hepatic macrophage population exists in the liver of mice following APAP-induced liver injury. These CX3CR1+F4/80^{high}Ly6C$_{low}$ macrophages are entirely derived from Ly6C^{high} monocytes and are characterized by a gene expression profile distinct from both infiltrating monocytes and

resident KCs (Zigmond et al., 2014). Ly6C^{high} infiltrating monocytes have a mixed "M1/M2" phenotype, and upon differentiation into Ly6C$_{low}$ MoMFs, reprogramming occurs towards a pro-restorative phenotype with increased expression of "M2" genes.

MoMFs are important for tissue-repair/resolution processes in acute liver injury: firstly, through secretion of mediators involved in extracellular matrix remodeling, angiogenesis and hepatocyte regeneration, and secondly by neutrophils suppression and their subsequent clearance. Accordingly, selective ablation of MoMFs results in impaired recovery manifested by greater hepatotoxic damage and significantly increased neutrophil numbers (Holt et al., 2008; Zigmond et al., 2014). In line with this, recent studies employing murine models of sterile liver injury demonstrate that the initially inflammatory monocytes topographically form ring-like structures around the injured liver areas and can differentiate into CCR2$_{low}$CX3CR1+Ly6C$_{low}$ MoMFs, which promote resolution and tissue-repair processes (Dal-Secco et al., 2015; Ramachandran et al., 2012).

As discussed above, during sterile liver injury MoMFs and KCs contribute to tissue inflammation and regeneration (Rehermann, 2017). Recently, Wang and Kubes using a model of thermal sterile liver injury, where hepatocyte necrosis results in DAMP release (e.g. cytosolic ATP, mitochondrial DNA) and innate immune activation, identified peritoneal macrophages as a third population that responds to liver injury (Wang and Kubes, 2016). They demonstrate that wound healing and tissue regeneration are aided by a specialized subset of GATA6+ peritoneal macrophages that moves directly through the visceral endothelium of the liver and not through the vasculature. These cells arrive at the injury site within 1 hour, in a chemokine independent manner, undergo rapid expansion and up-regulate CD273, CD206, and arginase-1 expression along with a tissue-repair macrophage transcriptional profile. They dismantle the nuclei of necrotic cells, thereby releasing DNA to cover the necrotic area and contributing to liver regeneration (Wang and Kubes, 2016). Thse findings are not limited to thermal injury close to the surface of the liver but may extend to other models of acute or chronic liver injury, hence this new paradigm of avascular recruitment of mature macrophages opens many avenues for future research and potential new therapeutic applications (Rehermann, 2017).

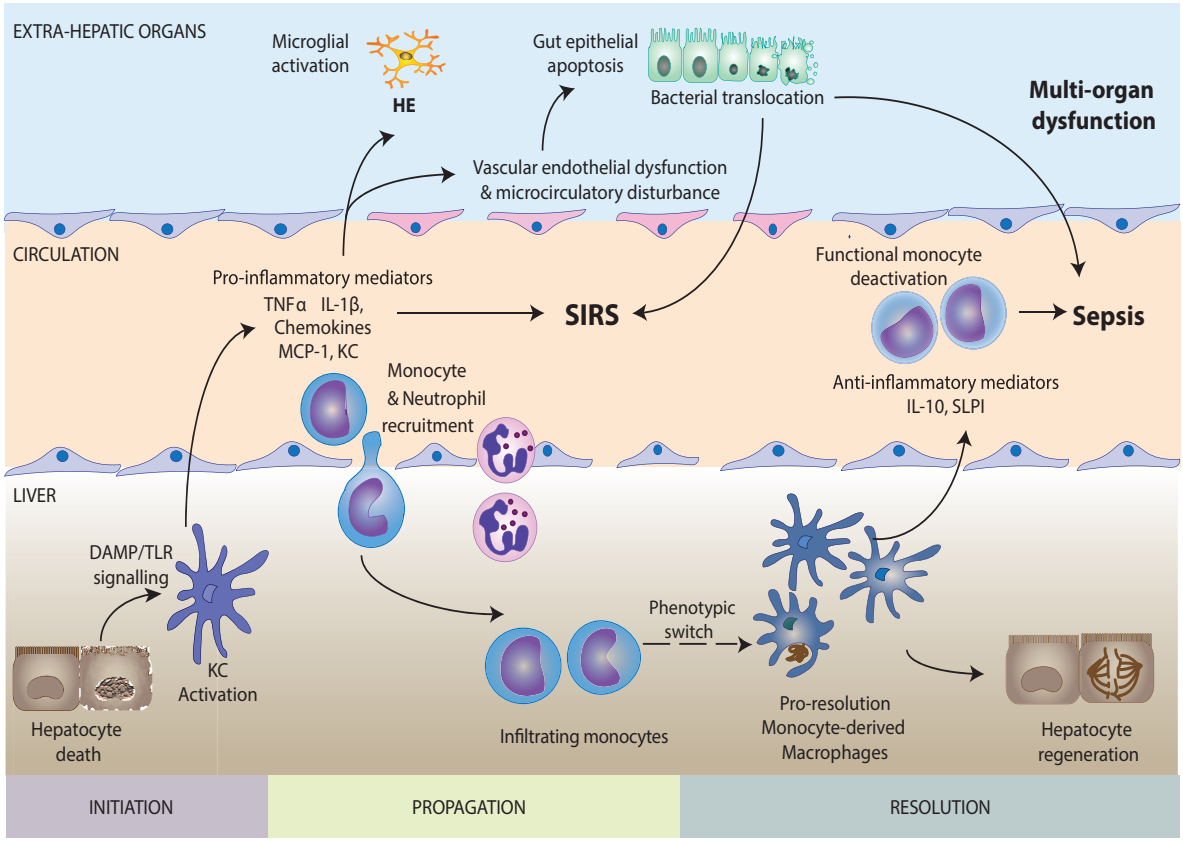

Figure 1.2 Role of monocytes and hepatic macrophages in acute liver failure.

KCs detect hepatocyte death through DAMP/TLR signaling and initiate a pro-inflammatory response. Bone-marrow derived monocytes traffic to the liver to contribute to an expanded macrophage population which are initially pro-inflammatory. During the propagation phase, immune activation is self-perpetuating with recruitment of effectors driving further cytokine and chemokine production. The release of cytokines and vasoactive mediators into the systemic circulation provokes SIRS. Macrophage-derived mediators contribute to vascular endothelial dysfunction and microcirculatory disturbances that result in extra-hepatic organ dysfunction [from: (Possamai et al., 2014b)].

1.3 Neutrophils and NK/NKT cells during liver injury

1.3.1 Neutrophil functions

Neutrophils are large polymorphonuclear cells that belong to the granulocyte family of leukocytes. They are derived from the bone marrow, where they remain for 4–6 days, and then circulate in the peripheral blood surviving for a short period of time (12-18 hours half-life) (Liaskou et al., 2012). The profound susceptibility to bacterial and fungal infections resulting from neutropenia or defects in neutrophil trafficking demonstrates their essential role in host defense (Heymann and Tacke, 2016; Kubes and Mehal, 2012). Neutrophils are key effectors of the innate immune system during infective and sterile inflammation that result in their trafficking and localization to sites of tissue injury. These cells are uniquely endowed with high phagocytic capacity and a vast arsenal of rapidly synthesized cytotoxic antimicrobial molecules stored in their cytoplasmic granules, e.g. perforin and granzyme (Xu et al., 2014). However, this potent arsenal exhibits poor specificity and can cause collateral damage to host tissues.

1.3.2 Neutrophils and liver inflammation

1.3.2.1 Neutrophil recruitment

Immunity is beneficial when is well contained and tightly regulated. Excessive neutrophil recruitment at sites of liver injury contributes fundamentally to the pathogenesis of a variety of liver diseases (**Fig. 1.3**). Neutrophils do not always functionally contribute to liver inflammation but they can aggravate liver disease through secretion of pro-inflammatory cytokines (e.g. IL-1β and TNF-α) and cytotoxic reactive oxygen and nitrogen species (Xu et al., 2014). Tissue damage and hepatocyte death result in the release of DAMPs that guide neutrophils to injury site, leading to a multistep process that involves activation of the inflammasome, adhesion molecule upregulation (ICAM-1 and VCAM-1), formation of a chemokine gradient (CXCL1, CXCL2, CXCL8) and formyl-peptide signals in areas of necrosis (Kubes and Mehal, 2012; Marra and Tacke, 2014; McDonald et al., 2010). In a recent study Slaba et

al. used multichannel spinning disk microscopy which enabled them to track platelets and neutrophils in a model of sterile thermal liver injury; interestingly they noted a rapid accumulation of platelets within blood vessels (Slaba et al., 2015). Whereas their initial intuition was that platelets were occluding the sinusoids and preventing perfusion, their data revealed that neutrophil recruitment in areas of necrosis depends on platelets which can aid and/or erminate the recruitment of the first (Slaba et al., 2015). Furthermore, studies using murine models of acute and chronic liver injury show that neutrophils are directly activated by nuclear DNA through TLR-9 signaling and patrol DNA-rich necrotic areas (Marques et al., 2012). Also, a TLR-2 and S100A8–S100A9 signaling pathway acts as key regulator of intrahepatic CXCL2 and TNF-α expression that drive subsequent neutrophil liver infiltration (Moles et al., 2014). However, the molecular mechanisms that allow neutrophils to home to the liver, and affect their functions therein, are yet not fully understood.

1.3.2.2 Neutrophils in chronic liver disease

Due to their early activation and distribution in the circulation, neutrophils also trigger recruitment of other leukocytes, such as monocytes, therefore are of great importance in the overall initiation of the intrahepatic immune responses (Heymann and Tacke, 2016). In addition to bacterial phagocytosis and release of antimicrobial proteins, neutrophils form extracellular traps (NETs) which are composed of DNA decorated with histones and proteases that can trap and kill bacteria (Sorensen and Borregaard, 2016). Following systemic infections, NETs are formed within the liver sinusoids, remaining anchored to the vascular wall via von Willebrand factor, thus enabling the liver to protect the body from infection, by efficiently clearing bacteria (Kolaczkowska et al., 2015; McDonald et al., 2012) and viral particles (Jenne et al., 2013). Furthermore, in experimental acute liver injury (ischaemia-reperfusion model), NETs were recently described to exacerbate acute tissue damage through activation of the inflammasome (Huang et al., 2015). The role of neutrophils in other chronic liver diseases remains unclear. Although infiltration of neutrophils is commonly seen in sterile inflammatory conditions of the liver, such as alcohol-induced steatohepatitis (Jaeschke, 2002), NASH (Liang et al., 2014), ischaemia reperfusion injury and toxin mediated halothane hepatitis (You et al.,

2006), Concanavalin-A (ConA) induced hepatitis (Bonder et al., 2004), these cells seem to be dispensable for establishing chronic inflammation and hepatic fibrosis (Moles et al., 2014).

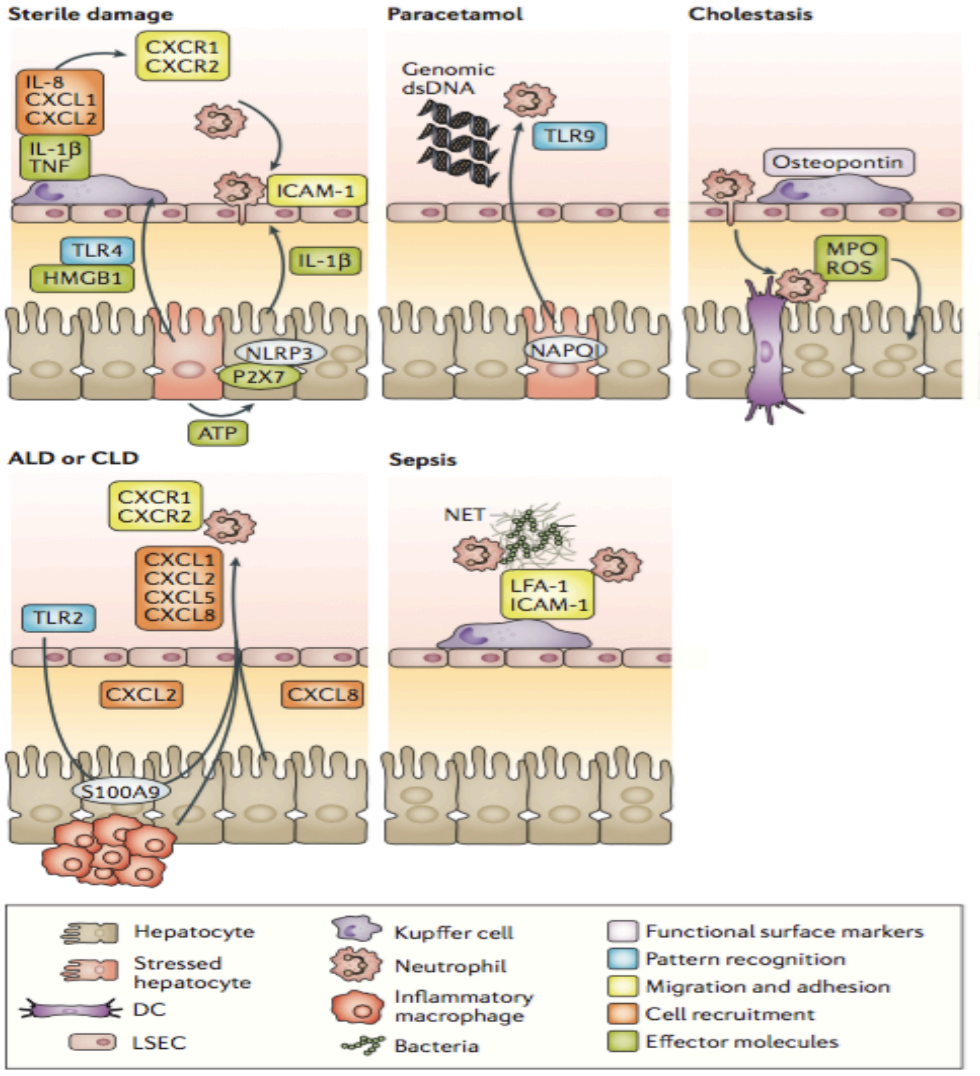

Figure 1.3 Neutrophils in liver inflammation.

Neutrophils respond to primary liver injury as well as TLR-mediated signaling and are subsequently recruited via and LFA-1–ICAM-1 into the tissue. Their activation leads to secretion of oxidative stress response mediators (ROS, MPO), which can further aggravate hepatocellular damage. During bacterial infections, neutrophils release DNA to form NETs, which are involved in antimicrobial defence. ALD, alcoholic liver disease; CLD, chronic liver disease; DC, dendritic cell; HMGB1 high mobility group box protein 1; ICAM-1, intracellular adhesion molecule 1; LFA, lymphocyte function associated antigen; LSEC, liver sinusoidal endothelial cell; MPO, myeloperoxidase; NET, neutrophil extracellular traps; ROS, reactive oxygen species; TLR, Toll-like receptor [from (Heymann and Tacke, 2016)].

1.3.3 Neutrophils in acute liver failure

The role of neutrophils in acetaminophen-induced ALF remains controversial, with some studies suggesting they promote while others that they have no effect on the severity of acute liver injury (Jaeschke et al., 2013). The early recruitment of neutrophils into the liver of mice, within 6 hours post paracetamol, is well documented (Liu et al., 2006; Marques et al., 2012; Williams et al., 2014a). Early studies indicated that neutrophils are not activated following APAP-induced liver injury, showing that circulating neutrophils did not up-regulate CD11b/CD18 expression levels, the β integrins required for endothelial adhesion and adhesion-dependent target cell killing (Lawson et al., 2000). Also, mice treated with anti-CD18 blocking antibody or $CD18^{-/-}$ mice are not protected from liver injury (Lawson et al., 2000; Williams et al., 2010a). Another recent report showed that CD11b is up-regulated in both circulating and hepatic neutrophils between 24-48 hours post APAP and they exhibit a lack of ROS priming, suggesting they cannot exert cytotoxic effects and do not contribute to liver injury (Williams et al., 2014b). Moreover, strategies administrating endotoxin and a pharmacological dose of IL-1β as 'second hits' following APAP dosing augmented neutrophil recruitment to the liver, with no changes in the extent of liver injury (Williams et al., 2010a; Williams et al., 2010b).

In contrast, research from others demonstrates that neutrophils exert cytotoxic effects on hepatocytes during the initial phases of paracetamol toxicity and thus contribute to the severity of liver injury. Mice treated with neutropaenia-inducing antibodies prior to paracetamol dosing are partially protected from liver damage (Ishida et al., 2006; Liu et al., 2006; Marques et al., 2012), however there is not such an effect if neutropaenia is induced after paracetamol dosing (Cover et al., 2006). Of note, this work has received criticism for likely off-target effects of the neutropaenia-inducing antibodies supporting that the documented protection is due to priming of liver-resident KCs by circulating cellular debris from depleted neutrophils that may induce the expression of protective genes in the liver, thus attenuating the response to the secondary inflammatory insult of paracetamol-induced hepatocyte damage (Jaeschke and Liu, 2007). Recently, in a model of carbon tetrachloride induced acute liver inflammation, neutrophil depletion dramatically reduced liver damage in mice underlying

their critical role in this type of liver injury (Moles et al., 2014). In addition, strategies aimed to inhibit neutrophil recruitment to liver have shown amelioration of liver injury. Combined blockade of CXCR2 and formyl peptide receptor 1 (FPR1) was found to be protective in APAP-treated mice (Marques et al., 2012). ICAM-1 deficient mice also exhibit reduced neutrophil recruitment following liver injury and reduced indices of liver injury (Liu et al., 2006).

1.3.4 NK and NKT cell functions

NK cells are enriched in the human liver representing the ~30–50% of total lymphocytes and consist a key component of hepatic innate immunity having unique phenotypic and functional features (Tian et al., 2013). Human NK cells are defined as CD56+CD3- lymphocytes and are classified into CD56-low-expressing ($CD56^{dim}$) with preferential cytolytic activities and CD56-high-expressing ($CD56^{bright}$) with release of immune-modulatory cytokines (Zimmermann et al., 2013). Liver NK cells are distinct from circulating NK cells with respect to their origin, phenotype and function (Heymann and Tacke, 2016). Approximately 90% of circulating NK cells are $CD56^{dim}$ whereas in the liver only 50% of NK cells are $CD56^{dim}$ and the other 50% are $CD56^{bright}$ (Tian et al., 2013). The underlying mechanisms of their enrichment and special characteristics remain largely unknown, however these differences may relate to the high hepatic expression of NK cell-recruiting chemokines and the cross-talk of NK cells with other hepatic cell types (Krueger et al., 2011; Maghazachi, 2010). Compared to their circulatory counterparts, liver-resident NK cells display an increased killing activity, secrete high concentrations of cytotoxic mediators and express higher levels of CD69 (Tian et al., 2013).

Liver NK cells share many similarities with innate lymphoid cells (ILCs), a subpopulation of lymphocytes with immune-regulatory properties that are commonly found on mucosal surfaces (Peng and Tian, 2015). In the mouse liver, liver NK cells seem to be similar to mucosal ILC1 cells since they depend on T-bet, express NK1.1 (CD161), NKp46, CD69 and TRAIL, but not DX5 (CD49d) or T-cell and/or B-cell markers (Heymann and Tacke, 2016). These ILCs secrete IFN-γ and TNF, but have a poor cytolytic capacity. The human counterpart of mouse liver NK cells is probably the

CD49a+ NK-cell subset, which expresses high levels of CD69 and granzyme B and produces high amounts of IFN-γ, TNF and GM-CSF (Marquardt et al., 2015).

NK cells exert a key effector function by killing target cells through their cytotoxicity and cytokine production, that is pivotal for host defense against pathogens and tumors (Heymann and Tacke, 2016). This ability is determined by the opposing signals from inhibitory and stimulatory NK cell receptors and their interactions with their respective ligands on target cells (Lanier, 2005). NK cell inhibitory receptors (e.g. CD94 and Ly49A) interact with inhibitory ligands [e.g. major-histocompatibility-complex-class 1 (MHC-1)] expressed on the target cells and suppress NK cell function whereas stimulatory receptors [e.g. NK group 2D (NKG2D) NKp46, NKp30, and NKp44] interact with the stimulatory ligands on target cells and promote NK cell activity (Lanier, 2005). The expression of inhibitory/stimulatory NK cell receptors and their ligands on hepatocytes and non-parenchymal cells is altered during a variety of liver disease and contributes to their pathogenesis (Tian et al., 2013). NK cells also act as regulatory cells by interacting directly (cell-to-cell contact) or indirectly (cytokine production) with other liver cell types such as tumor cells, stressed hepatocytes and HSCs (Tian et al., 2013). They can influence DCs, KCs/macrophages, T/B cells and endothelial cells by producing various cytokines (IFN-γ, TNF-α and IL-10), chemokines and growth factors or through innate immune recognition, as summarized in (**Fig. 1.4**).

Natural killer T (NKT) cells is a subpopulation of T cells, expressing surface markers and cytokines characteristic for NK cells, that is particularly enriched in the liver and regulates hepatic immune responses in the context of autoimmunity, cancer and microbial infection (Heymann and Tacke, 2016). During homeostasis, mouse liver NKT cells crawl along the sinusoids and can interact with the hepatic endothelium (Krenkel et al., 2014); for example CXCR6+ NKT-cell trafficking into the liver is guided by CXCL16 secreted from HSECs and KCs (Wehr et al., 2013). Liver DCs also interact with patrolling NKT cells via glycolipid receptors such as CD1d, triggering both IL-4 and IFN-γ secretion from NKT cells (Schmieg et al., 2005; Trobonjaca et al., 2001). In contrast to the highly abundant CD1d-restricted Vα14Jα18 mouse liver NKT cells, which can constitute up to 40% of

hepatic lymphocytes, their human counterpart, Vα24Vβ11 NKT cells are less frequent in the human liver and represent a minority (0.5–10%) of hepatic lymphocytes (Tian et al., 2013). Vα14Jα18 NKT cells are highly restricted to antigen presentation via non-classic glycolipid antigen receptors such as CD1d. Tumour-infiltrating human NKT cells express CD56, NK1.1 and show signs of activation by expressing CD69 and pro-inflammatory cytokines such as TNF and IFN- γ, indicating a role in anti-tumour defence (Kenna et al., 2003) . Furthermore, invariant mouse NKT cells are substituted by mucosal-associated invariant T (MAIT) cells in human liver. MAIT cells are clearly enriched in human liver and are usually identified as CD3+γδ−CD4−CD161+Vα7.2+ lymphocytes (Le Bourhis et al., 2010).

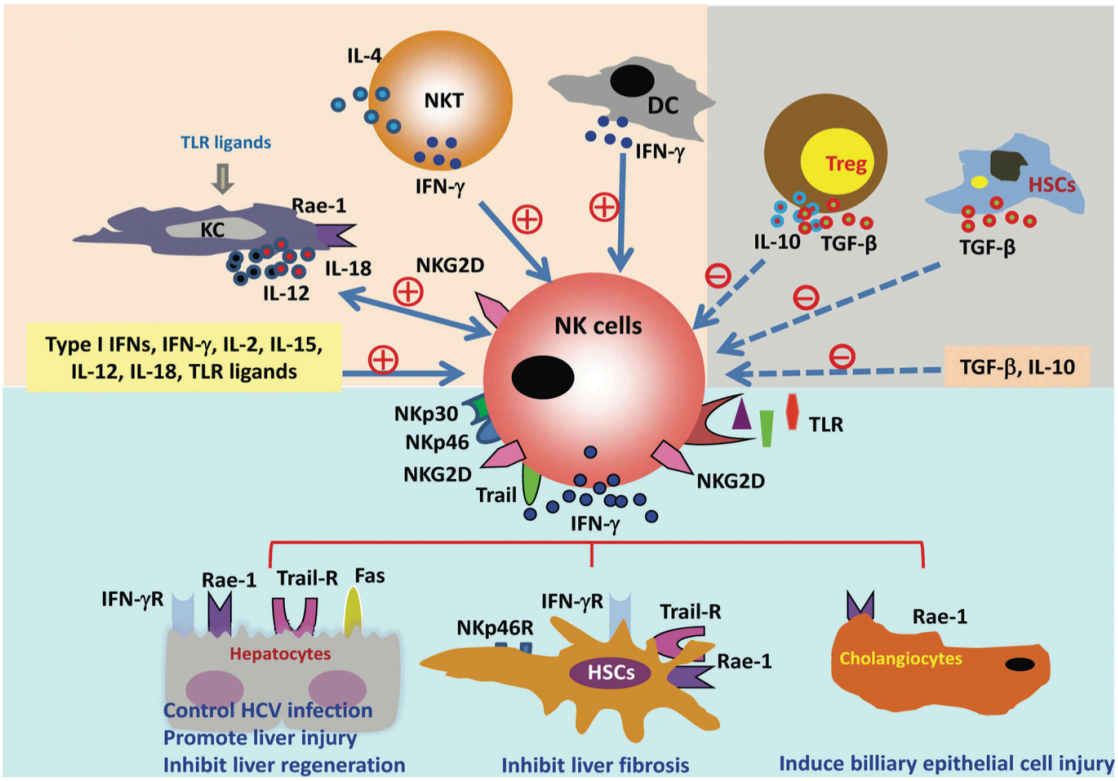

Figure 1.4 Regulation and functions of liver NK cells.

Top panel: regulation of NK cells. The left side of the top panel illustrates that activated KCs, DCs, and NKT cells can induce NK cell activation by the production of a variety of cytokines. Several cytokines that activate NK cells are also listed. The right side of the top panel illustrates that Tregs and activated HSCs can inhibit NK cell functions by the production of several cytokines. TGF-b is a potent inhibitor of NK cell functions. Bottom panel: functions of NK cells in the liver. Activated NK cells target hepatocytes, HSCs, and cholangiocytes and perform a variety of important functions in the pathogenesis of liver disease [from (Tian et al., 2013)].

1.3.5 NK/NKT cells in chronic liver disease

Accumulating evidence suggests that NK/NKT cells play beneficial roles in controlling viral hepatitis, liver fibrosis and cancer while contribute to the pathogenesis of acute liver inflammation and injury (Heymann and Tacke, 2016; Tian et al., 2013). In viral hepatitis, human and murine studies propose an NK-cell-mediated immunity both for controlling viral infection and for mediating cytopathogenic effects. Evidence shows an NK-cell-mediated control of HCV replication by NKp46^{bright} NK cells but also for harmful NK-cell activation, that is, HCV-associated loss of anti-fibrotic activity by CXCR3+CD56^{bright} NK cells and increased fibrogenesis (Eisenhardt et al., 2012; Kramer et al., 2012) Upon HBV infection, NK cells are demonstrated to limit viral infection by targeting HBV-infected hepatocytes (Dunn et al., 2007), however they can deplete HBV-antigen specific CD8+ T cells via TRAIL-receptor 2, therefore suppressing the cytotoxic T-cell response against the virus (Peppa et al., 2013). In mice, NKT cells enhance T and B cell responses in a model of HBV infection, probably through sensing of HBV-induced modified self-lipids on infected hepatocytes (Zeissig et al., 2012).

NK cells exert crucial hepatoprotective functions in chronic liver disease. Hepatocyte-derived DNA leads to engagement of TLR9 and following CpG-mediated NK cell activation, pro-fibrotic HSCs were efficiently killed by NK cells, thereby attenuating liver fibrosis *in vivo* (Abu-Tair et al., 2013). NKT cells infiltrating in areas of necrosis via the CXCL16/CXCR6 axis are mostly pro-inflammatory and lead to increased liver inflammation and fibrosis (Wehr et al., 2013), however, dependent on the stimulus and the stage of fibrosis progression, NKT cells can also exert anti-inflammatory functions (Park et al., 2009). These contradictory findings may be explained by the fact that NKT cells release IL-4 and IFN-γ that mediate partially opposing effects on neutrophil recruitment and liver injury (Wang et al., 2013). Accumulation of invariant NKT cells in human livers has been associated with disease progression especially in NASH-related cirrhosis (Syn et al., 2010) while NKT might promote steatosis through increased hepatocyte lipid uptake and contribute to progression from steatohepatitis to hepatocellular carcinoma, by activating the canonical and non-canonical NF-κB pathway (Wolf et al., 2014).

1.3.6 NK/NKT cells in acute liver failure

The role of NK cells in acute liver inflammation is yet not fully explored. In principle, lymphoid cells contribute to APAP-induced liver injury by secreting IFN-γ and depleting the glutathione storages in hepatocytes via Fas/FasL; of note, IFN-γ and FasL expression are two effector mechanisms of hepatic NK/NKT cells (Heymann and Tacke, 2016). Murine studies that suggested a direct pathogenic role for NK/NKT cells after APAP overdose (Liu et al., 2004) could later be linked to the use of dimethyl-sulfoxide (DMSO) as a solvent, as DMSO alone leads to the activation of NK/NKT cells which are characterized by increased IFN-γ and granzyme B expression (Masson et al., 2008). These findings suggest a role of IFN-γ in the pathogenesis of ALF and mice treated with anti-IFN-γ antibodies or IFN-γ deficient mice show attenuated liver injury after APAP overdose (Ishida et al., 2002).

NKT cells show immunogenic or protective functions in acute liver inflammation. In mice, hepatic inflammation induced by α-galactosylceramide results in IL-17 secretion by NKT cells and IL-17 blocking leads to increased liver inflammation, enhanced influx of neutrophils and monocytes and upregulation of CXCL5/CCL2 (Wondimu et al., 2010). Furthermore, mice lacking Stat4, a negative regulator of NKT cells, were found more susceptible to ConA-induced hepatitis (Wang et al., 2014) while retinoic acid was shown to alleviate ConA-induced hepatitis and differentially regulate effector production in NKT cells inducing IL-4 and IFN-γ but not TNF (Lee et al., 2012a). Murine studies using NKT deficient mice revealed they are more susceptible to APAP-induced acute liver injury, however the exact underlying mechanisms remain unclear (Martin-Murphy et al., 2013).

1.4 Resolution of inflammation

1.4.1 Inflammation

Inflammation is a pathophysiological response to infection and tissue injury and a key component of many human diseases such as rheumatoid arthritis, asthma, cancer and in liver injury, as discussed above (Heymann and Tacke, 2016; Ortega-Gomez et al., 2013). Local and systemic inflammatory responses aim to eliminate the inciting stimulus, promote tissue-repair and wound healing processes, and in the case of infection to establish immune memory for the host's future encounter of pathogens (Fullerton and Gilroy, 2016). An acute inflammatory response is a complex but highly coordinated sequence of events that involves molecular, cellular and physiological alterations and which unfolds in several phases.

Initially, tissue-resident cells including macrophages, DCs, lymphocytes, endothelial cells and mast cells produce soluble mediators such as complement, chemokines, cytokines and free radicals in the injured or infected tissue, thus alarming the innate immune system (Ortega-Gomez et al., 2013). Concomitantly, cell adhesion molecules are upregulated on circulating leukocytes and endothelial cells that promote the exudation of proteins and recruitment of neutrophils from the blood. Upon their arrival, neutrophils become activated and primarily act to phagocytose tissue debris and eliminate microorganisms, through intracellular mechanisms including degranulation and ROS production (oxidative burst) and extracellular mechanisms such as NET formation (Fullerton and Gilroy, 2016). Recruited neutrophils further promote the recruitment of inflammatory monocytes and neutrophils to the injured site and potentiate the pro-inflammatory environment. Monocytes follow, able to link the innate and adaptive immune responses, and govern whether the intial insult can be overcome with or without adaptive immunity. The type and number of effector cells as well as their ability to neutralize the inciting stimuli probably signal the resolution phase that follows (Gilroy and De Maeyer, 2015).

1.4.2 Principles of resolution

In order to prevent the progression from acute to chronic inflammation, the inflammatory response must be actively resolved in order to quell further tissue damage and restore organ function and homeostasis. The period between peak inflammatory cell influx and their clearance from the injured site and the restoration of functional homeostasis, classically defined as resolution, is no longer considered a passive process (Buckley et al., 2014). This involved chemokine gradients' dilution over time, thus circulating leukocytes would no longer sense gradients and be recruited to the site of injury (Gilroy and De Maeyer, 2015). Instead, nowadays resolution of inflammation is considered a complex and tightly regulated active process while deficiency in any of its steps may lead to uncontrolled persistent inflammation. Resolution occurs in overlapping phases and is governed by the spatial and temporal production of pro-resolving mediators present in the microenvironment (Headland and Norling, 2015). Molecules which fall under this umbrella are diverse in nature including: lipid mediators [lipoxins (A_4 and B_4), resolvins (E1, D1 and D2) protectin D1, maresins and PGD_2], proteins (D6, galectin1 and annexin A1), gaseous mediators (hydrogen sulphide and carbon monoxide), adenosine as well as changes of NF-κB, PI3K, ERK1/2, CDKs and cAMP intracellular signaling pathways, the function of which is extensively reviewed in (Fullerton and Gilroy, 2016; Headland and Norling, 2015).

Macrophages and neutrophils are key cellular components of the resolving process following acute tissue inflammation, the interplay between which is critical for resolution (**Fig. 1.5**). First, elimination of the inciting stimulus is a critical requirement for the inflammatory response to switch off, failure of which may lead to chronic inflammation (Gilroy and De Maeyer, 2015). Effectively dispensing of the injurious insult will signal a cessation of pro-inflammatory/toxicant mediator synthesis and increase of their catabolism, in parallel with counter-regulation of chemokines, through proteolytic cleavage, and abrogation of neutrophil influx (Ortega-Gomez et al., 2013). Induction of neutrophil apoptosis and their subsequent clearance next take place, followed by a macrophage functional switch towards a resolution-like type, return of non-apoptotic cells to the vasculature or lymphatics and initiation of the

healing processes (Fullerton and Gilroy, 2016; Headland and Norling, 2015). Multiple intricate signaling mechanisms and factors control each of these processes and the balance between them, including cell-to-cell receptor binding and humoral mediators, that culminate in a return to tissue homeostasis (Buckley et al., 2014).

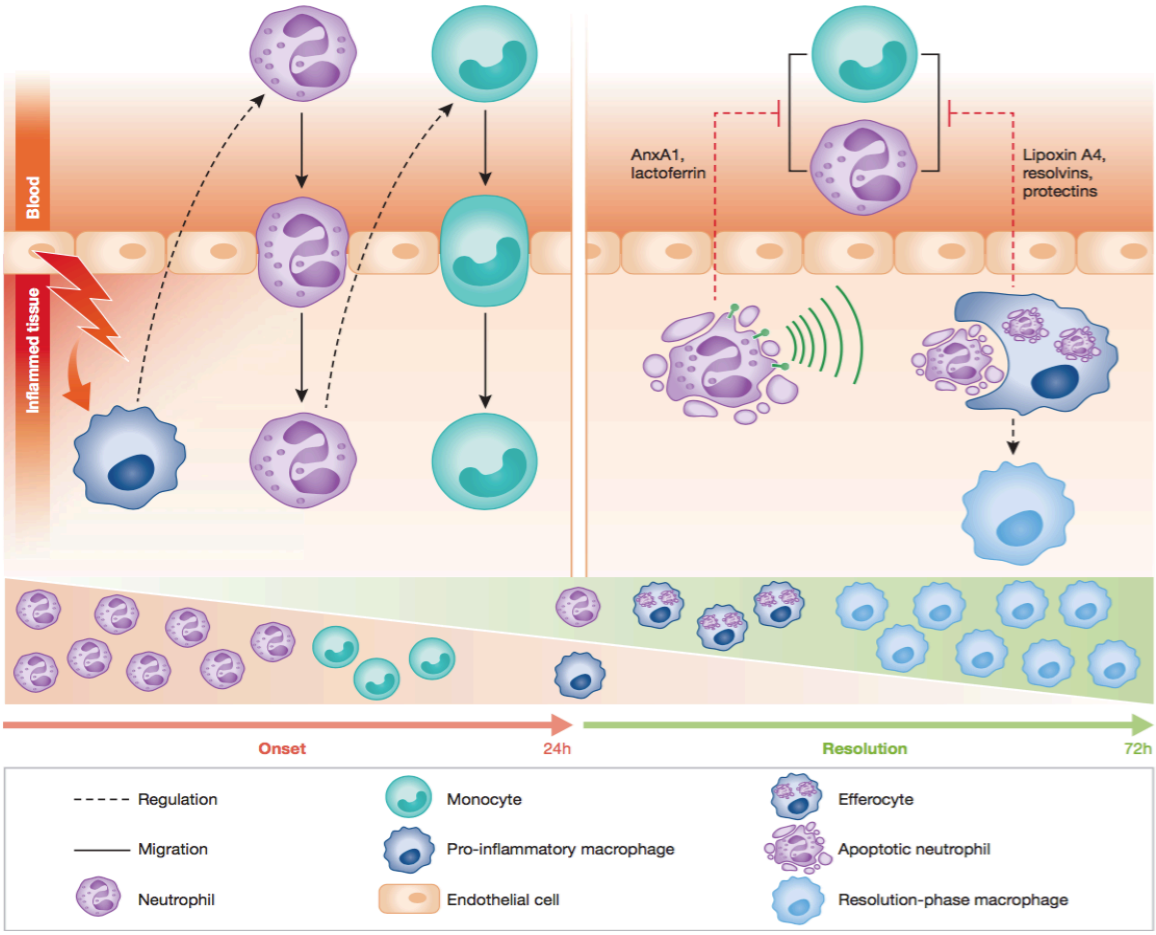

Figure 1.5 Neutrophil/macrophage interplay during resolution of inflammation.

Overview of cellular processes during onset (left) and resolution (right) of inflammation. During the early phases of inflammation tissue-resident cells sense damage/insult and launch the release of signals that induce a rapid neutrophil and delayed monocyte recruitment. Resolution is initiated when neutrophils become apoptotic, thus secreting mediators that inhibit continued neutrophil infiltration. Ingestion of apoptotic neutrophils changes the macrophage phenotype towards a resolution-phase macrophage, which promotes return to tissue homeostasis. [Adapted from: (Ortega-Gomez et al., 2013)]

1.4.3 Neutrophil apoptosis and tissue clearance

Aborted neutrophil influx and their apoptosis is but one of the steps required to restore tissue homeostasis. Neutrophils are short-lived cells but once extravasated into specific tissue sites, they reprogram their gene and product repertoire and can extend their lifespan considerably, influenced by the local inflammatory environment (Fox et al., 2010; Geering and Simon, 2011). Within an inflamed tissue, many extracellular signals can extend the lifespan and functional longevity of neutrophils, including cytokines, bacterial products and low oxygen tensions (Headland and Norling, 2015). Macrophages can importantly control the lifespan of neutrophils by secreting death receptor ligands such as TNF-α, Fas (FasL) and TNF-related apoptosis-inducing ligand (TRAIL) (Renshaw et al., 2000; van den Berg et al., 2001). At low concentrations FasL prolongs neutrophils' lifespan but also recruits neutrophils to injured tissue sites. TRAIL is a type II membrane protein that is expressed by leukocytes and while its genetic deletion delays neutrophil apoptosis and resolution responses (McGrath et al., 2011). In this regulatory pathway, phosphoinositide 3-kinase (PI3K)-mediated ROS production is the key event in controlling cell survival and triggering apoptosis (Geering and Simon, 2011). Physiological hypoxia induces increased neutrophil lifespan via oxygen-sensing enzymes that stabilize hypoxia-inducible factor pathways (e.g. HIF-1) (Walmsley et al., 2011). Other micro-environmental mediators such as granulocyte-macrophage colony-stimulating factor (GM-CSF) and neutrophil-derived proteins including annexin A1 and lactoferrin are also reported to regulate neutrophil lifespan (Fullerton and Gilroy, 2016; Headland and Norling, 2015).

Apoptotic neutrophils promote their own clearance by macrophage, termed efferocytosis, by producing "find-me" and "eat-me" signals. Find-me signals are secreted factors that attract scavengers and to date, four of them have been identified including lysophosphatidyl-choline (LPC), sphingosine 1-phosphate (S1P), fractalkine (CX3CL1), and the nucleotides ATP and UTP (Ortega-Gomez et al., 2013). These find-me signal gradients guide the macrophage towards the dying cell through the involvement of G2A, S1P1-5, CX3CR1, and P2Y2 receptors, respectively. During apoptosis, the dying cell loses surface expression of repellent "don't-eat-me" cell-surface molecules such as CD31

and CD47 (Brown et al., 2002; Gardai et al., 2005) and upregulates expression of various "eat-me" signals such as phospholipids, nucleotides and phosphatidylserine (PtdSer) (Fadok et al., 2001). The interaction between macrophages and these signals ensures that apoptotic cells are efficiently removed from the tissue before membrane rupture and the release of cytotoxic mediators that could perpetuate the inflammatory response (Fadok et al., 2001; Fadok and Henson, 2003; Gregory and Pound, 2010).

1.4.4 Macrophage reprogramming following efferocytosis of apoptotic cells

Recruitment of monocytes and their differentiation into macrophages at sites of inflammation are key events in determining the outcome of the inflammatory response and restoring tissue homeostasis. One of macrophages' primary roles during resolution is clearance of apoptotic cells. This process is essential to prevent further tissue injury, with a great impact on macrophage reprogramming that is crucial for efficient resolution (Gilroy and De Maeyer, 2015). Macrophages exhibit great functional and phenotypic plasticity and that becomes apparent during the resolution phase of inflammation (Ginhoux et al., 2016). Phagocytosis of apoptotic cells triggers the functional switch of phagocytosing macrophages towards an immune-regulatory or pro-resolution phenotype (Bellingan et al., 2002; Bystrom et al., 2008), maintaining immune tolerance both locally and in draining lymphoid organs, and limiting potential collateral tissue damage (Bellingan et al., 1996; Bellingan et al., 2002; Schif-Zuck et al., 2011). This post-phagocytosis macrophage phenotype is typified by: a) increased expression of co-inhibitory molecules (PDL1 and ICOS ligand), b) release of anti-inflammatory cytokines/mediators such as IL-10, TGF-β and SLPI, c) secretion of PCNA-associated factor, PGE2 and cAMP and d) release of reduced levels of pro-inflammatory cytokines including TNF-α, GM-CSF, IL-1β, IL-12 and IL-18 (Ashcroft et al., 2000; Bystrom et al., 2008; Fadok et al., 1998; Fadok and Henson, 1998). Moreover, macrophages that have ingested apoptotic cells also release pro-resolving lipid mediators such as RvE1, protectin D1 and maresins that contribute to termination of the inflammatory process (Schwab et al., 2007; Serhan et al., 2012).

Transcriptomic analysis of murine resolution-phase macrophages (rM) shed light on their features during the resolution phase, revealing that they possess *in vivo* a hybrid phenotype of alternative activation, mannose receptor expression and IL-10 and arginase 1 synthesis (M2, anti-inflammatory) with high cyclooxygenase-2 **(**COX2) and iNOS expression (M1, pro-inflammatory) (Stables et al., 2011). This study suggested a role of these cells in antigen processing/presentation, T- and B-lymphocyte recruitment, clearance of inflammatory cells and subsequent restoration of tissue homeostasis, highlighting the naivety of trying to categorize such plastic cells in a dynamic environment (Stables et al., 2011). Resolving macrophages exhibit lower CD11b expression levels, enhanced ability to engulf apoptotic neutrophils, reduced responsiveness to microbial challenge (Schif-Zuck et al., 2011). Clearly, the latter two studies indicate heterogeneity of resolution-phase macrophages.

1.4.5 Targeting resolution pathways

Many aspects of the resolution cascade can be therapeutically targeted to alter the inflammatory profile without compromising the host's immune tolerance. Modulation of any of these events along with supplementation of, or catabolic inhibition of, soluble pro-resolving mediators represents a strategy to invoke resolution and has dominated drug research for inflammatory diseases in the last decades (Buckley et al., 2014; Fullerton and Gilroy, 2016). An ideal immunoresolvent would limit continued neutrophil infiltration, counter-regulate pro-inflammatory mediators, enhance the efferocytosis of cell debris and apoptotic neutrophils, and promote restoration of tissue homeostasis (Ortega-Gomez et al., 2013). Pro-resolving mediators administered exogenously have proved efficacious at improving disease and inflammatory outcomes in a variety of experimental models, including periodontitis, colitis, myocardial infarction and reperfusion injury and allergic airway disease (Headland and Norling, 2015).

Abrogation of continued leukocyte recruitment is essential to favor the return to tissue homeostasis. AnxA1 dampens neutrophil accumulation through several mechanisms including down-regulation of

trans-endothelial migration, promotion of neutrophil apoptosis and stimulation of their clearance by macrophages (Scannell et al., 2007). In addition, lipoxins and resolvins inhibit neutrophil influx and enhance efferocytosis without compromising host defence (Serhan, 2014) and RvD1, RvD5 and protectin D1 accelerate leukocyte-mediated killing of bacteria and enhance antibiotic efficacy (Chiang et al., 2012). There are several strategies for enhancing neutrophil apoptosis *in vivo*, including CDK inhibition (with roscovitine or AT7519) or inhibition of PI3K, ERK1/2 or NF-κB signaling pathways (Alessandri et al., 2013). For maximum benefit, this must be accompanied by enhanced and effective efferocytosis by macrophages, which can be augmented by melanocortins, glucocorticoids or annexin A1 (Poon et al., 2014). This can also be induced by lipid mediators such as PGJ2 and RvD1 and mimetics based on their mode of action through G protein-coupled receptors represent a very effective target for treating ongoing inflammation (Cash et al., 2014)

Although induction of apoptosis in neutrophils and the resultant reprogramming of macrophages following efferocytosis may be beneficial against tissue injury, resolving inflammation before the tissue is fully immunologically and functionally restored opens a window of potential infectious opportunity (Fullerton and Gilroy, 2016; Grabiec and Hussell, 2016). It is shown that apoptotic cells suppress *in vitro* the phagocytosis and killing of bacteria by alveolar macrophages in a PGE_2-, PGE_2 receptor EP2 subtype (PTGER2) and cAMP-mediated manner (Medeiros et al., 2009). Importantly, intrapulmonary administration of apoptotic thymocytes impaired lung recruitment of neutrophils as well as clearance of *Streptococcus pneumoniae*, also in a PGE2/PTGER2-dependent pathway. These results suggest that additionally to their beneficial homeostatic influence, anti-inflammatory/pro-resolution programs initiated following acute tissue injury, at least in the lung, dampen antimicrobial responses and may lead to host's susceptibility to secondary infections (Medeiros et al., 2009).

1.5 Mer Tyrosine Kinase (MerTK) receptor

1.5.1 The TAM receptor Tyrosine Kinase family

Receptor tyrosine kinases (RTKs) are surface transmembrane receptors possessing a regulated protein tyrosine kinase activity in their cytoplasmic domains. They act as sensors for extracellular ligands the binding of which triggers receptor dimerization and receptor's kinase activation (Lemke and Rothlin, 2008). This leads further to phosphorylation and activation of multiple downstream signaling pathways which affect cell physiology by controlling diverse processes, from cell differentiation to cell death. The TAM family of receptors (TAMs) is a relatively recently identified subfamily of RTKs with diverse biological roles (Lai and Lemke, 1991). Subsequent cloning of full-length cDNAs by different laboratories resulted in a plethora of different TAM names: Tyro3/Dtk/Brt/Sky/Tif/Rse, Tyro7/Axl/Ufo/Ark and Tyro12/v-Ryk/c-Eyk/Mer. However, Tyro3, Axl, and Mer are now being used according to the National Center for Biotechnology Information (NCBI) designations (Rothlin et al., 2015).

TAM signaling pathway functions to restore homeostasis through different mechanisms: it negatively regulates inflammation by limiting the intensity and duration of the immune response (Lemke and Rothlin, 2008). TAMs also function in phagocytosis, specifically the phagocytic removal of apoptotic cells and debris; these receptors bind to phosphatidylserine (PtdSer) exposed on the plasma membrane of apoptotic cells, in association with their respective ligands, that enables the selective uptake and clearance of apoptotic cells (Scott et al., 2001). This action is necessary to prevent continuous inflammation and is a transitional signal from "attack the pathogen" to "tissue-repair/restore organ function" mode. TAMs are mainly expressed by cells of the immune, nervous, reproductive and vascular system (Rothlin et al., 2015). Axl is widely expressed in our body, MerTK is found in hematopoietic cells and in specialized epithelia, including retinal pigmental epithelium (RPE) and Sertoli cells and Tyro3 is strongly expressed in the central nervous system. Importantly, downstream signaling interacts with other growth factor pathways, thus TAMs can be proto-oncogenic and are

overexpressed in many human cancers (Graham et al., 2014). They do not play an essential role in embryonic development but rather function as regulators of cell and tissue homeostasis in fully differentiated organs that are under continuous renewal throughout adult life as discussed below.

1.5.2 TAM receptor structure and signaling features

TAM receptors share structural similarities: from the extracellular N-end to the cytosolic C-end, these receptors display two Ig-like domains, two fibronectin type III (FNIII) domains, a hydrophobic transmembrane domain, and a tyrosine kinase domain (**Fig. 1.5**) (Rothlin et al., 2015). The Ig-like domains are formed by 7-9 antiparallel β-strands and are involved in interactions with the TAM ligands, while FNIII domains are all β-strand structures with similarities to Ig folds. Three tyrosine autophosphorylation sites (Tyr^{749}, Tyr^{753}, and Tyr^{754}) have been identified in MerTK (Ling et al., 1996). These residues are conserved in Axl and Tyro3 and are frequently phosphorylated, yet their requirement for the receptor's kinase activity remains to be examined (Hornbeck et al., 2012). Within their intracellular domains Axl and MerTK, but not Tyro3, carry a conserved ITIM (Immunoreceptor Tyrosine-based Inhibitory Motif, LLYSRL) (Staub et al., 2004). TAM signaling activation is coupled to downstream phosphoinositide 3 kinase (PI3K)/AKT pathway activation and most of this pathway is nucleated through a TAM autophosphorylated Grb2 binding site (Rothlin et al., 2015). Coupling to phospholipase C, ERK1/2, Ras, and MAP kinase activation have been described in many different cells (Keating et al., 2010; Ou et al., 2011).. Macrophages, dendritic cells and other immune cells also express cytokine receptors, such as type I interferon (IFN), that can be coupled to TAMs. Hence, the TAM-activated PI3K/AKT pathway is often dominated by a TAM-activated JAK/STAT pathway in these cells (Lemke and Rothlin, 2008; Rothlin et al., 2007).

1.5.3 TAM ligand structure and receptor specificity

Two ligands that bind and activate the TAM receptors have been identified: growth-arrest-specific 6 (Gas6) and Protein S (Pros1) (Rothlin et al., 2015). Both ligands are large (~80 kD) proteins that are

~42 % identical in amino acid sequence and share the same multi-domain arrangement. Tyro3, Axl, and MerTK can all effectively signal as homodimeric receptors that bind just one ligand dimer (Rothlin et al., 2015). Gas6 and Protein S possess two structural features key to their activity (**Fig. 1.6**). The first is a C-terminal "sex hormone binding globulin" (SHBG) domain that binds to the Ig-like domains of the TAM receptors. The second is an N-terminal "GLA" domain. GLA domains bind in a Ca^{2+}-dependent manner to exposed PtdSer on the surface of apoptotic cells, another crucial feature for TAM activation (Lemke and Rothlin, 2008). Of note, GLA domains are detected in several proteins of the coagulation cascade and Protein S also functions as an anticoagulant in a TAM-independent mechanism (Dahlback, 2000).

The extent to which TAM ligands contribute to TAM signaling has only begun to be dissected. Current evidence indicates that Gas6 is as a ligand for all three TAM receptors and is produced primarily in vascular smooth muscle and endothelial cells (Rothlin et al., 2015). Gas6 can bind and activate Axl without PtdSer, suggesting a function additonal to apoptotic cell clearance (Tsou et al., 2014). During steady state, Gas6 serum concentrations are low (<0.2 nM) but increase dramatically during acute stress or tissue injury such as sepsis (Mukherjee et al., 2016). In contrast, Pros1 is a selective TAM ligand that binds and activates Tyro3 and MerTK (Lew et al., 2014; Tsou et al., 2014). Another difference between TAM ligands is their sites of expression. Pros1 is abundant in the blood, being present at ~ 300 nM in the human circulation whereas Gas6 is nearly absent. Pros1 is produced by hepatocytes, endothelial cells and in tissues that use MerTK-mediated clearance of apoptotic cells (Rothlin et al., 2015). Galectin-3 is a another recently identified TAM ligand, the levels of which are elevated during tissue damage, such as acute and chronic liver injury (Mukherjee et al., 2016). It employs a number of downstream signaling pathways, and to date it's only described to facilitate phagocytosis via MerTK (Caberoy et al., 2012),

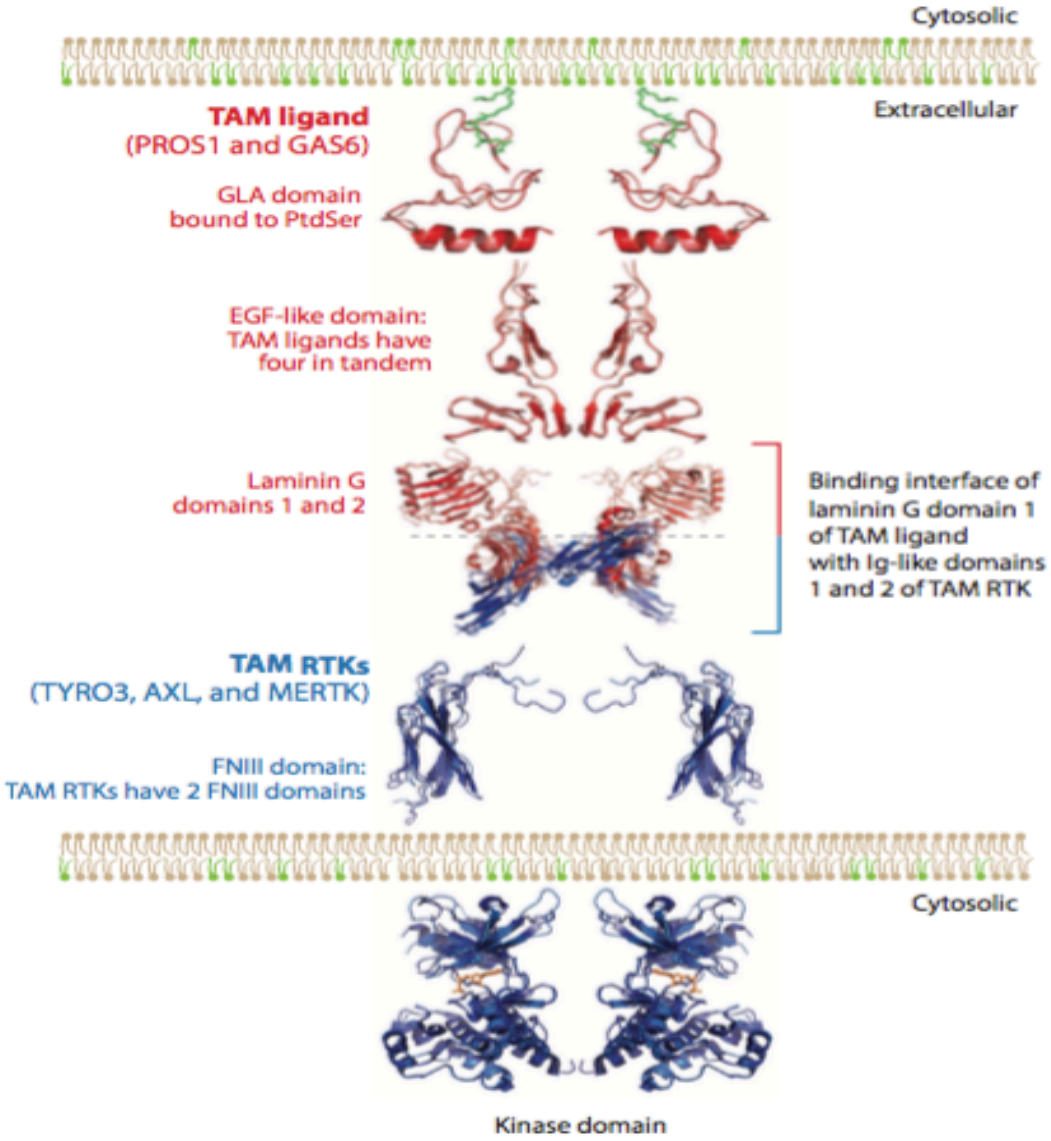

Figure 1.6 Domain organization of TAM receptors and their ligands.

The TAM ligands Gas6 and Pros1 (red) carry an N-terminal GLA domain that binds to PtdSer (green) exposed on the plasma membrane of apoptotic cells. GLA domains are followed by four EGF-like repeats. At the C terminus, the TAM ligands carry two laminin G domains, of which domain 1 interacts with the Ig-like domains of the TAM RTKs to form a heterotetrameric complex. Ig-like domains are followed by two FNIII domains and an intracellular tyrosine kinase domain (blue).. The structure of the whole complex—including PtdSer, TAM ligands, and TAM receptors—remains unknown. Abbreviations: EGF, epidermal growth factor; FNIII, fibronectin type III; RTK, receptor tyrosine kinase; TAM, TYRO3, AXL, and MERTK [from: (Rothlin et al., 2015)].

1.5.4 MerTK-mediated regulation of phagocytosis

TAM signaling plays a critical role in the phagocytosis of apoptotic cells and cellular debris in mature tissues (Lemke and Burstyn-Cohen, 2010; Scott et al., 2001; Zagorska et al., 2014). During this process, TAM ligands serve as a "bridge" to link the TAM receptor, expressed on the surface of the phagocyte, to PtdSer exposed on the surface of the apoptotic cell that will be engulfed (Nagata et al., 2010). Simultaneously, the ligand must activate the TAM receptor tyrosine kinase activity for the process of phagocytosis (Scott et al., 2001). Recent evidence show that "bridging" in the absence of TAM kinase activation and/or kinase activation in the absence of bridging, are insufficient to promote efferocytosis (Zagorska et al., 2014).

The first phenotype described in TAM knockout mice ($TAM^{-/-}$) was male infertility. TAM expression in Sertoli cells is required to clear apoptotic remnants of meiosis in the testes and $TAM^{-/-}$ male mice show inflammatory damage at seminiferous tubules and infertility (Sun et al., 2010; Zhang et al., 2013). $MerTK^{-/-}$ mice show increased accumulation of apoptotic germ cells whereas $Tyro3^{-/-}$ and $Axl^{-/-}$ mice display no apoptotic cell accumulation (Lew et al., 2014). A similarly strong phenotype is detected in the eyes of $MerTK^{-/-}$ mutants which are born with normal retinae. Retinal pigment epithelium (RPE) cells in $MerTK^{-/-}$ mice differentiate normally but fail to clear apoptotic cells and debris. This leads to death of nearly all photoreceptors (PRs), pro-longed inflammation, fibrosis, and retinal degeneration (Duncan et al., 2003; Prasad et al., 2006). Within the central nervous system MerTK-lacking microglial cells are unable to clear ineffective synaptic connections, leading to impaired hippocampal development and neuronal damage (Ji et al., 2013).

TAMs play important roles in the clearance of apoptotic cells by macrophages and other phagocytes (Scott et al., 2001). Axl and MerTK are the two most important receptors for the engulfment of apoptotic cells by macrophages and dendritic cells (Lemke and Burstyn-Cohen, 2010). Recent studies show that these two act in distinct environments with MerTK receptor mediating homeostatic phagocytosis in tolerogenic settings and Axl functioning in inflammatory microenvironments created

by infection or tissue damage (Zagorska et al., 2014). In those settings in which efferocytosis is Axl-dependent it is also Gas6-dependent whereas Mer-dependent efferocytosis can be stimulated by both Gas6 and Protein S. Incomplete efferocytosis can lead to the accumulation of secondary necrotic cells which constitute a major source of auto-antigens, thus defects in phagocytosis are associated with the development of autoimmune diseases and is a prominent feature of the phenotypes of TAM mutants (Rothlin and Lemke, 2010).

1.5.5 MerTK signaling in immune regulation

TAM receptors and their ligands are essential regulators of the immune system and function at the interface of innate and adaptive immunity, as demonstrated by studies on macrophages and DCs (Rothlin et al., 2007). These cells use pattern recognition receptors (PRRs), such as Toll-like receptors (TLRs), to detect molecular patterns, such as lipopolysaccharide and double-stranded RNA, that are associated with bacteria and other pathogens (Chung et al., 2012). Activation of PRRs leads to the production of pro-inflammatory cytokines, for example type I interferons. However, these cytokines must be tightly controlled after the innate immune response is mobilized because unrestrained cytokine signaling results in chronic inflammation (Rothlin et al., 2015).

Studies using experimental models of sterile and pathogen-induced inflammation have demonstrated that TAM receptor loss can result in exaggerated activation and ineffective resolution, thus leading to excessive inflammatory tissue damage (Mukherjee et al., 2016). In a model of endotoxemia, MerTK-deficient mice almost uniformly succumbed to septic shock and died as a result of tissue damage mediated by excessive levels of TNF-α and IL-1 (Camenisch et al., 1999). Bleomycin-induced lung injury was significantly reduced when MerTK macrophage expression was enhanced in mice, that were also typified by increased anti-inflammatory mediators, such as TGF-β and hepatocyte growth factor (HGF) and reduced TNF-α and IL-1 expression levels (Lee et al., 2012c).

TAMs regulate the innate immune responses through the modulation of cytokine secretion (Rothlin et al., 2015). There is direct evidence that TAMs are significantly upregulated in murine DCs following TLR engagement and that TLR-induced pro-inflammatory cytokine production is attenuated by both MerTK and Axl signaling (Rothlin et al., 2007). The mechanism of TAM action involves the suppressor of cytokine signaling proteins SOCS-1/3 which act as inhibitory proteins at various points in the TLR cascade. Increased SOCS-1/3 expression occurs downstream of TAM signaling and a dynamic feedback loop exists, in which the initial burst of cytokines as products of TLR pathway bind to their respective receptors and activate the transcription factor STAT1. In addition to promoting further the pro-inflammatory cytokine production, STAT1 induces Axl expression. In association with its ligands, Axl interacts with the cytokine receptor interferon (IFN)-associated receptor and this protein complex appears to differentially activate STAT1, redirecting its downstream genetic targets toward SOCS-1/3 and crucially acting as a brake for TLR-evoked cytokine production by pathogens (Rothlin et al., 2007). Hence, this braking mechanism is not available at the onset of inflammation, but manifests only following initiation and propagation of the immune response.

MerTK signaling in macrophages also skews their cytokine secretion profile following efferocytosis to promote tissue-repair and wound healing processes. MerTK-mediated efferocytosis promotes anti-inflammatory cytokine productions (IL-4, IL-10, and TGF-β) that promote tissue-repair and resolution of inflammation (Filardy et al., 2010), and this depends upon inhibition of nuclear factor (NF)-kB signaling and activation of the phosphatidylinositol 3-kinase pathway (Sen et al., 2007). In addition, IL-10 further acts in an autocrine manner on macrophages by inducing MerTK expression and propagating an anti-inflammatory response to tissue damage (Zizzo et al., 2012). Gas6 and Protein S are also secreted in an autocrine manner by macrophages and DCs, following activation of both MerTK and Axl, thus further amplify TAM signaling at sites of tissue inflammation (Rothlin et al., 2007). Recent work proposed that differential TAM receptor expression by different immune cells may indicate specificity in biological function (Zagorska et al., 2014). Axl is more abundant in murine DCs whereas MerTK is predominantly expressed in macrophages. Axl expression is increased in response to TLR ligands lipopolysaccharide (LPS) and poly(I:C) whilst MerTK expression is induced

following the uptake of apoptotic cells and IL-10 (Zizzo et al., 2012). These findings support that MerTK enables phagocytic clearance in homeostatic settings and Axl functions in antigen-presenting cells in response to acute inflammatory tissue damage (Zagorska et al., 2014)

1.5.6 MerTK signaling and human disease

1.5.6.1 MerTK in autoimmunity

Autoimmune diseases such as systemic lupus erythematosus (SLE) are linked with accumulation of apoptotic cell debris (Rothlin and Lemke, 2010). Not surprisingly, the delayed efferocytosis of apoptotic cells and loss of the regulation of the inflammatory response are associated with the development of a lupus-like syndrome in TAM triple knock out (TKO) mice (Cohen et al., 2002; Lu and Lemke, 2001). These TKO mice are show elevated titers of circulating auto-antibodies (anti-chromatin and anti-double and single stranded DNA antibodies), uncontrolled B and T cell proliferation and accumulation of lymphocytes in secondary lymphoid organs (Cohen et al., 2002; Lu and Lemke, 2001). This phenotype appears to be cell non-autonomous with respect to lymphocytes, since T and resting B cells and do not express TAMs. In humans SLE, there is defective clearance of autoreactive lymphocytes in germinal centers of lymph nodes by tingible body macrophages that express MerTK (Gaipl et al., 2006; Rahman et al., 2010). Genetic studies also showed polymorphisms in the MerTK gene, that are tied to SLE and development of multiple sclerosis (Cheong et al., 2007; Ma et al., 2011). Furthermore, deficiencies in the TAM ligand Pros1 have also been frequently detected in SLE patients, suggesting a role for impaired TAM signaling in its pathogenesis (Song et al., 2000), and recent evidence has highlighted a further role for MerTK in innate and adaptive immunity. Cytotoxic T lymphocytes in mice produce Pros1 and externalize patches of PtdSer, thereby activate MerTK on antigen-presenting cells, dampening pro-inflammatory cytokines and antigen-specific responses (Carrera Silva et al., 2013).

1.5.6.2 MerTK in viral infection

TAM receptors and their ligands have been described on affecting viral infectivity. TAMs function as entry factors for the Ebola/Marburg family of hemorrhagic fever filoviruses (Rothlin et al., 2015). Similar results are obtained following cell infection with lentiviral vectors pseudotyped with Sindbis virus, vesicular stomatitis virus, Ebola, and Marburg virus glycoproteins and for infection by the flaviviruses Dengue virus and West Nile virus (Rothlin et al., 2015). Enveloped viruses, mentioned above, employ a strategy to evade the immune system, known as "apoptotic mimicry", where they expose PtdSer on their surface (Mercer and Helenius, 2010). This allows them to use TAM ligands as "bridging molecules" and link themselves to TAMs expressed on target cells. It is shown that Gas6 and Pros1 as well as their binding to exposed PtdSer is required for TAM-mediated viral infection (Bhattacharyya et al., 2013; Morizono et al., 2011). The expression of kinase dead receptors or the addition of a TAM inhibitor to the cell culture reduced the capacity of TAMs to favor viral infection *in vitro* (Meertens et al., 2012).

Most studies have examined the ability of TAMs to promote viral replication *in vitro*, however their role *in vivo* remains controversial. $Axl^{-/-}$ mice are more susceptible to herpes simplex virus (HSV)-1 infection maybe due to reduced capacity of $Axl^{-/-}$ DCs to cross-present viral antigen (Subramanian et al., 2014). In contrast, systemic administration of an anti-Axl antibody to WT mice infected with a lethal dose of PR8 influenza virus strain led to reduced mice mortality (Shibata et al., 2014). Similarly, administration of anti-Axl antibody reduced the lung pathology upon respiratory syncytial virus infection in mice (Shibata et al., 2014). Moreover, no significant differences were detected in the response to lymphocytic choriomeningitis virus infection between WT and $Axl^{-/-}$ mice (Sullivan et al., 2013).

1.5.6.3 MerTK in cancer

TAM-mediated regulation of immune responses is implicated in antitumor immunity with existing literature focused on TAM function in tumor cells and tumor-associated immune cells, describing both pro-oncogenic and anti-oncogenic roles (Linger et al., 2010; Rothlin et al., 2015). Tumor-associated macrophages secrete higher Gas6 levels compared to their splenic counterparts while mediators (i.e, IL-10 and M-CSF) enriched in the tumor microenvironment may further upregulate their Gas6 production (Loges et al., 2010). Of note, Gas6 levels are elevated in a number of different solid tumors (Graham et al., 2014). TAMs also possess non–tumor cell autonomous roles; MerTK ablation in a model of breast cancer, or syngeneic transplantation of melanoma and colon cancer cells in $MerTK^{-/-}$ mice, led to reduced tumor burden and fewer metastases (Cook et al., 2013) and *in vivo* administration of a TAM inhibitor reduced both tumor and metastatic burden, as result of enhanced NK cell activation and anti-tumor activity (Paolino et al., 2014). In contrast, an anti-inflammatory and anti-tumor TAM function is supported in colorectal cancers. $Gas6^{-/-}$ mice showed increased susceptibility to inflammation-induced colon carcinogenesis, as a result of azoxymethane (AOM) and dextran sodium sulfate (DSS) treatment, characterized by a greater number of PCNA/c-Myc-positive polyps, higher TNF-α levels, increased NF-κB activation and reduced survival (Akitake-Kawano et al., 2013). Accordingly, $Axl^{-/-}$ $Mer^{-/-}$ mice post AOM-DSS treatment had more and larger polyps, increased tumor score and their colons exhibited increased number of apoptotic Ly6G+ neutrophils and increased IFN-γ and TNF-α production, compared to WT (Bosurgi et al., 2013).

1.5.6.4 MerTK in liver disease

TAM-mediated immune regulation in the liver is vital for maintaining hepatic immune tolerance. The liver is a central immunological organ with high exposure to circulating antigens and endotoxins derived from the gut, hence several mechanisms during homeostasis ensure suppression of hepatic immune responses, resulting in tolerance (Heymann and Tacke, 2016). This important function is orchestrated by the resident population of antigen-presenting cells, adapted epithelial cells and an enriched NK cell population (Kubes and Mehal, 2012). Importantly, all TAM receptors have been

identified in the livers of mice: MerTK is expressed in liver-resident KCs and sinusoidal endothelial cells, but not in hepatocytes, Axl is expressed by all three cell types whereas Tyro3 is restricted to macrophages (Qi et al., 2013; Rothlin et al., 2015). TAM TKO mice develop autoimmune hepatitis, by six months of age, with elevated transaminases and titers of autoantibodies (Qi et al., 2013). Histological analysis reveals a rich infiltrate of autoreactive CD4 T cells and circulatory macrophages, while hepatocytes show elevated pro-inflammatory cytokines such as IL-6, IL-1β, TNF-α, and IFNs through NF-κB and IFN regulatory factor 3 upregulation. However, this phenotype was not observed when the bone marrow of TAM TKO mice was transplanted with WT stem cells (Qi et al., 2013).

TAM signaling is also studied in chronic and acute liver inflammation. A genome-wide association study in patients with chronic hepatitis C virus (HCV) infection identified several susceptibility loci for severity and progression of liver fibrosis (Patin et al., 2012). The strongest was homozygosity for rs4374383 G>A single nucleotide polymorphism, a non-coding variant in the MerTK locus, that was associated with the protection against fibrosis progression in HCV (Patin et al., 2012). Another study found that the MerTK rs4374383 AA genotype, associated with lower hepatic MerTK expression, is protective against stage F2-F4 fibrosis in patients with NAFLD (Petta et al., 2016). MerTK was overexpressed in *in vivo* models of fibrogenesis whereas exposure of cultured human HSCs to the MerTK ligand Gas6, increased cell migration and induced procollagen expression, effects that were counteracted by MerTK inhibition and resulted in apoptotic HSC death, thus proposing a MerTK-dependent modulation of HSC activation (Petta et al., 2016). In a murine model of hepatic ischemia, serum Gas6 levels rose shortly after arterial ligation and western blot analyses after ischemic insult revealed an increase in hepatic phosphorylated MerTK over Axl levels, indicating a preferential activation of MerTK signaling (Llacuna et al., 2010). Compared to WT, $Gas6^{-/-}$ animals had higher mRNA levels of pro-inflammatory cytokines (IL-1α and TNF-α) and more frequently succumbed to fulminant hepatic failure after only partial ischemic insult. Recombinant Gas6 administration protected these mice from fulminant disease, however it is unclear if this was due to TAM signaling in liver immune cells or parenchyma (Llacuna et al., 2010).

Recently, MerTK signaling was also studied in human acute-on-chronic liver failure (AoCLF). There is an expansion of MerTK+ monocytes in AoCLF patients, compared to healthy and cirrhotic controls, with a concomitant increase in all TAM ligands as well as phosphorylated MerTK levels, that indicate an active TAM signaling (Bernsmeier et al., 2015). Monocytes in AoCLF exhibited an attenuated response to microbial challenge while blocking MerTK with a small molecule inhibitor restored their TNF-α and IL-6 secretion. The authors also showed that MerTK+ monocytes have enhanced migration abilities across hepatic endothelium, thus they proposed a dynamic model in which monocytes are recruited to the inflamed liver, resulting in increased MerTK expression in response to liver tissue damage. However, in the setting of a systemic inflammatory response, endothelial dysfunction enables their reverse transmigration back into the circulation and local lymph nodes, potentially contributing to immuneparesis and susceptibility to sepsis (Bernsmeier et al., 2015).

Although TAM signaling is beneficial during liver homeostasis and perhaps in response to acute liver injury, research on chronic liver disease suggests it is potentially deleterious. HSC activation is pivotal in progression of chronic liver injury by promoting fibrogenesis and cirrhotic transformation (Tacke and Zimmermann, 2014). In a murine model of CCL_4-induced chronic liver injury, HSC activation was shown to rely upon Gas6-mediated Axl activation that leads to upregulation of signaling via protein kinase B and NF-kB. There was increased Axl transcription and translation as well as activation of the downstream signaling in both hepatic macrophages and stellate cells (Barcena et al., 2015; Fourcot et al., 2011). In another model where mice develop steatohepatitis, following a choline-deplete ethionine-supplemented diet, $Gas6^{-/-}$ mice exhibited a reduction in HSC activation and TGF-β expression and their onset of necroinflammation and steatosis was delayed, compared with WT mice (Fourcot et al., 2011).

TAM function, in particular Axl, is studied in chronic HCV infection where Axl is shown to regulate IFN signaling and IFN-stimulated gene (ISG) expression. Of note, chronically infected HCV patients, characterized by prolonged activation of type I/III IFN signaling and high expression of ISGs before treatment, are less likely to achieve sustained virological response (Read et al., 2015a; Read et al.,

2015b). Using *in vitro* and *in vivo* models, Read et al. showed that Axl expression was upregulated in chronically HCV infected hepatocytes; in particular, hepatocytes from "non-responder" patients showed higher Axl levels than hepatocytes from "responders" (Read et al., 2015a; Read et al., 2015b). Axl overexpression in hepatocytes *in vitro* resulted in reduced phosphorylation of STAT1 and subsequent ISG expression. Together, these results propose that IFN-induced Axl expression mediates a negative feedback loop, down-regulating IFN signaling, in a similar manner to that previously shown in DCs (Rothlin et al., 2007). This does not appear to be via SOCS-1/3 in hepatocytes but may be an effect of Axl on IFN signaling pathways (Read et al., 2015a; Read et al., 2015b).

1.6 Secretory leukocyte protease inhibitor (SLPI)

1.6.1 Structure and expression of SLPI

Secretory leukocyte protease inhibitor (SLPI) is a 107-amino acid-long protein with two homologous whey acidic protein (WAP) domains (**Fig. 1.7)**. Each one is characterized by eight cysteine residues that form four characteristic intramolecular disulfide bonds. The WAP II (C-terminal) domain is mainly responsible for SLPI's inhibitory function against proteases and the protease-inhibiting region is localized between residues 67–74 (Majchrzak-Gorecka et al., 2016). The biological function of the WAP I (N-terminal) domain is less understood, although SLPI's antimicrobial activity is thought to reside in it (Scott et al., 2011a). SLPI is secreted by epithelial cells, including those cells lining the respiratory, digestive or reproductive tracts, as well as those cells of the breast, kidney and skin where it is thought to have homeostatic and protective functions. It is also produced by host-defense myeloid cells, constitutively or transiently, such as macrophages, granulocytes, dendritic cells (DCs) and platelets, as well as in neurons, and skeletal muscle cells (Sallenave, 2010; Scott et al., 2011a).

1.6.2 Regulation of SLPI expression

A variety of pro-inflammatory stimuli that trigger cell responses by binding to pattern recognition receptors, for example TLRs, increase SLPI expression. These include bacteria and bacterial cell wall components [LPS and lipoteichoic acid (LTA)], viral RNA analogs and pathogenic parasites (Majchrzak-Gorecka et al., 2016). Likewise, SLPI expression can be controlled by pro-inflammatory cytokine signals (TNF-α and IL-1β) and thymic stromal lymphopoietin (TSLP) while neutrophil elastase (NE) which is a target of SLPI also increases its secretion during granulopoiesis (Klimenkova et al., 2014). In addition, macrophages secrete SLPI following phagocytosis of apoptotic cells and in response to anti-inflammatory cues (IL-6 and IL-10) (Ashcroft et al., 2000). On the contrary, the pro-inflammatory stimuli IFN-γ inhibits both basal and LPS-induced SLPI secretion by macrophages and may account for the low SLPI levels detected in severe asthma patients (Jin et al., 1997; Raundhal et

al., 2015). Regulation of SLPI at transcriptional and post-transcriptional level is discussed in more detail elsewhere (Majchrzak-Gorecka et al., 2016; Scott et al., 2011a).

1.6.3 Multiple functions of SLPI

1.6.3.1 SLPI as an anti-protease

The most well-documented role of SLPI is the reversible inhibition of neutrophil elastase (NE). SLPI inhibits the enzymatic activity of other serine proteases, albeit with lesser efficiency, such as chymotrypsin, chymase, cathepsin G and trypsin (Wright et al., 1999). SLPI also interferes with the synthesis of proteases; for example, SLPI suppresses the MMP1 and MMP9 expression in monocytes and plays a role in the conversion of protease zymogen form (e.g. serine protease plasmin) where it is shown to block plasminogen activation through its interaction with annexin A2 at the surface of macrophages (Wen et al., 2011; Zhang et al., 1997).

1.6.3.2 SLPI as an inhibitor of NF-kB activity

SLPI possesses a wide functional repertoire such as antimicrobial and immune-modulatory activities, due to its ability to regulate the NF-κB pathway in immune cells. SLPI inhibits the LPS and LTA induced NF-κB activation of human monocytes (Lentsch et al., 1999) while others using anti-protease active-site mutated or truncated SLPI reveal it suppresses macrophage-like cell responses to LPS (Yang et al., 2005). These results suggest that the LPS-antagonizing action of SLPI is independent of its anti-protease effect. SLPI attenuates monocyte/macrophage responses via both intracellular and extracellular mechanisms. Outside the cell, SLPI can bind to and neutralize LPS, thereby can prevent TLR activation (Ding et al., 1999), whereas inside the cell SLPI prevents the degradation of NF-kB inhibitory components (IkBα and IkBβ) (Taggart et al., 2002) or competes with the NF-kB component p65 for binding to the NF-kB sites in the promoter regions of the pro-inflammatory genes TNF-α and CXCL8 (Taggart et al., 2005). The immune-modulatory activity of SLPI is also demonstrated *in vivo*, for example SLPI knockout mice are more susceptible to LPS-induced endotoxin shock and exhibit

higher mortality compared to WT mice (Nakamura et al., 2003). Human experimental and murine studies on acute tissue injury and wound healing, show that SLPI is a key anti-inflammatory mediator in the local micro-environment by directly inhibiting macrophage NF-κB dependent pro-inflammatory responses (Ashcroft et al., 2000; Odaka et al., 2003b; Sano et al., 2000; Sano et al., 2003).

1.6.3.3 Antimicrobial and antiviral actions of SLPI

SLPI is shown to inhibit bacteria/fungal growth and to restrain viral infections. It exerts bactericidal activity against Gram-positive/negative bacteria (Majchrzak-Gorecka et al., 2016); many skin-associated bacteria including *E. coli, Staphylococcus aureus, P. aeruginosa and Staphylococcus epidermidis* are affected by SLPI *in vitro* suggesting it controls the skin microbial burden in the skin (Hiemstra et al., 1996). SLPI also possesses antifungal properties against *Candida albicans* and metabolically active *Aspergillus fumigatus* (Sallenave, 2010; Scott et al., 2011a) and its antimicrobial activity is attributed mainly to its N-terminal (WAP I) domain, as discussed above (Majchrzak-Gorecka et al., 2016; Verma et al., 2007). Another important antimicrobial activity is described by McNeely et al. who found that SLPI inhibited the ability of HIV-1 to infect macrophages (McNeely et al., 1995) since it competitively binds to annexin II, an important cellular co-factor that facilitates HIV infection (Ma et al., 2004).

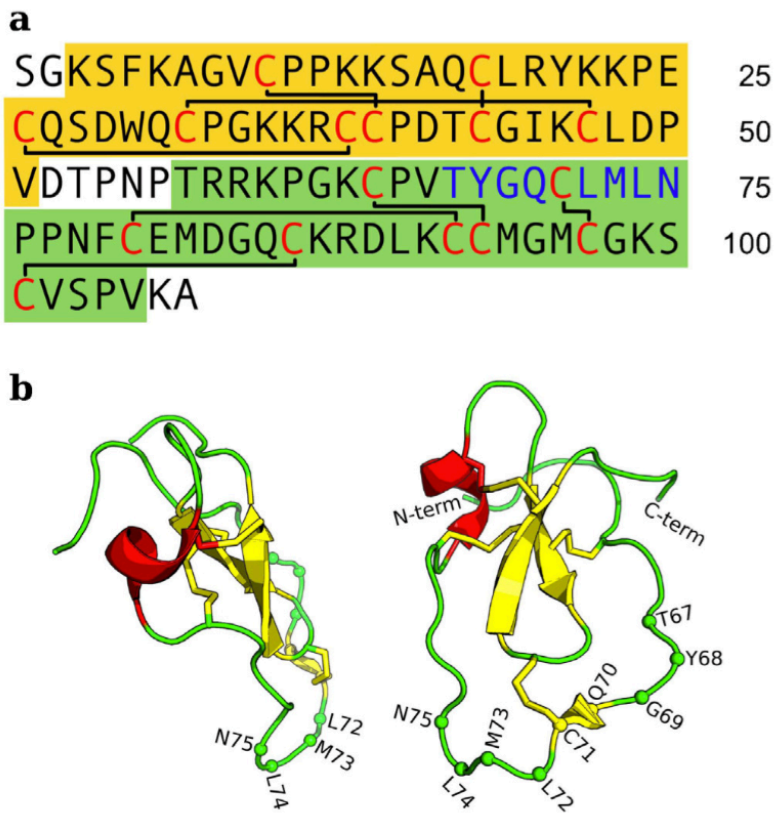

Figure 1.7 Amino acid sequence of human SLPI.

(a) Amino acid sequences of two WAP domains are shown in yellow and green background. Cysteine residues (red) make intradomain disulfide bridges (black lines). The fragment of the WAP II sequence spanning residues from 67 to 74 (blue) corresponds to the protein region involved in interactions with proteases as determined by structural studies. (b) Two orthogonal views of the 3D structure of the WAP II domain are shown. Three b-strands and a short a helix are shown in yellow and red, respectively. Four disulfide bridges are shown as yellow sticks. Alpha carbon atoms of a loop ranging from T67 to N75 are shown as small spheres with appropriate labeling of consecutive amino acid residues. [from: (Majchrzak-Gorecka et al., 2016)].

1.6.4 SLPI in pathological inflammatory responses

1.6.4.1 SLPI in infectious and allergic diseases

The levels and activity of SLPI are altered in numerous inflammatory, infectious, allergic and autoimmune diseases. SLPI is expressed at portals of pathogens where it regulates the epithelial activation threshold in order to protect against microbial signals (Menckeberg et al., 2015). Another homeostatic function at body barriers involves the *in situ* regulation of class switching and antibody production in B cells, that are induced by epithelial cell-derived factors (Xu et al., 2007). SLPI is also crucial in controlling host susceptibility to bacterial infection; serum SLPI levels are elevated in experimental LPS-induced endotoxemia and in patients with sepsis (Grobmyer et al., 2000). $SLPI^{-/-}$ mice were more susceptible to LPS-induced endotoxin shock and sepsis, caused by cecal ligation and puncture and developed more inflammation (Nakamura et al., 2003). In a model of pulmonary infection with *M. tuberculosis*, $SLPI^{-/-}$ mice were less capable of clearing the infection, having high bacterial loads in the lung and spleen and reduced survival (Nishimura et al., 2008). SLPI also mounts an effective immune response to the protozoan parasite *L. major*. $SLPI^{-/-}$ mice did not control the infection, however adenoviral delivery of SLPI to the infected $SLPI^{-/-}$ animals significantly restored their infection resistance (McCartney-Francis et al., 2014).

There is also emerging evidence that SLPI is a negative regulator of inflammation in non-infectious conditions such as allergic asthma. Increased levels of SLPI are detected in sputum and nasal lavage specimens from individuals with allergic asthma and allergic rhinitis. SLPI mRNA expression was lower in epithelial cells from patients with severe asthma (SA), compared to mild-moderate asthma (MMA) patients (Raundhal et al., 2015). Insufficient SLPI levels may lead to loss of tolerance to an allergen and persistent airway inflammation and/or airway hyperresponsiveness (AHR). Accordingly, $SLPI^{-/-}$ mice failed to maintain unresponsiveness to ovalbumin (OVA) protein and this brake in tolerance was attributed to enhanced DC activation in the draining lymph nodes (Samsom et al., 2007). In a mouse model of OVA-induced allergic asthma, researchers using gain-of-function and

loss-of-function approaches demonstrated that SLPI exerts a protective effect against allergic asthma (Marino et al., 2011). A recent study in SA pointed SLPI as a negative regulator of asthma related inflammation; SA is characterized by Th1-dominated responses whereas MMA by Th2-dominated responses. Compared to WT, IFN-$\gamma^{-/-}$ mice subjected to SA failed to mount AHR without an effect on airway inflammation and AHR was unaltered in IL-17ra$^{-/-}$ mice, although airway inflammation was lower (Raundhal et al., 2015). Computer-based analysis tools linked IFN-γ to SLPI, the levels of which inversely correlated in SA patients. In mice with SA, induced SLPI expression decreased AHR in absence of corticosteroids and it was further reduced when SLPI was combined with corticosteroids (Raundhal et al., 2015).

1.6.4.2 SLPI in autoimmunity

SLPI exerts crucial immune-modulatory activities during a variety of autoimmune diseases by contributing to the host's responses to "self-antigens" through DC activation and inhibition of NET formation. In a rodent model of experimental autoimmune encephalomyelitis, analysis of the spinal cord transcriptome revealed significantly up-regulated SLPI levels, suggesting it as an endogenous factor for disease outcome progression (Mueller et al., 2008). In another model of streptococcal cell wall-induced arthritis increased SLPI levels were found in affected joints of rats, during the early acute and the chronic destructive phase, although its expression was barely detected in the interval preceding chronic destructive disease (Song et al., 1999). Others have also linked SLPI with skin psoriasis, suggesting it contributes to the host response to "self-antigens" by enabling DCs to sense extracellular DNA, which is typically not immunogenic, and controlling deposition of this potentially harmful stimulus (Skrzeczynska-Moncznik et al., 2013; Skrzeczynska-Moncznik et al., 2012). SLPI expression is elevated in psoriatic skin, mostly in keratinocytes, and found to localizes in NETs, thus proposed to trigger the DNA-mediated activation of plasmacytoid DCs (Skrzeczynska-Moncznik et al., 2013; Skrzeczynska-Moncznik et al., 2012; Wingens et al., 1998). Importantly, SLPI inhibits NET formation, a process that requires chromatin de-condensation during which NE, a SLPI's target, plays a key role (Sorensen and Borregaard, 2016). SLPI detected in the granules and cytoplasm of resting

neutrophils can translocate to the nucleus upon neutrophil activation and restrain NET release; this inhibitory function is partially attributed to SLPI's anti-NE activity (Zabieglo et al., 2015b). SLPI also inhibited NET formation (NETosis) *in vitro*, in human neutrophils and $SLPI^{-/-}$ murine bone marrow-derived neutrophils while a similar effect of SLPI was observed *in vivo* in an experimental model of psoriasis in which more neutrophils producing NETs were detected in the affected skin of $SLPI^{-/-}$ mice compared to WT animals (Zabieglo et al., 2015b).

1.6.4.3 SLPI in wound healing and tissue repair

Numerous studies underline the important role of SLPI in wound healing with contributions at all of its phases starting as early as coagulation, since $SLPI^{-/-}$ mice have significantly prolonged plasma clotting time (Schulze et al., 2004). $SLPI^{-/-}$ mice subjected to cutaneous injury exhibit delayed skin wound healing that is reversible by SLPI administration to cutaneous wounds (Ashcroft et al., 2000). Use of anti-TGF-β and anti-TNF-α neutralizing antibodies *in vivo* largely reversed this impaired healing, thus suggesting a SLPI-mediated control of TGF-β and TNF-α levels is required for cutaneous wound healing (Ashcroft et al., 2012; Ashcroft et al., 2000). Also, SLPI is involved in the growth phase of the healing cascade following dermal injury where it is likely to protect growth factors from protease cleavage. Such a mechanism is proposed for NE, SLPI and proepithelin which at its intact form is a growth factor for epithelial cells that also inhibits neutrophil activation (Zhu et al., 2002). Similarly, TSLP-deficient mice have reduced SLPI levels in the colon and fail to recover from colon damage when challenged with dextran sulfate sodium (DSS). This may be due to increased NE activity during the recovery phase and an imbalance in proepithelin/epithelin conversion (Reardon et al., 2011). Moreover, SLPI is implicated in controlling the inflammation associated with axonal damage and promoting axonal regeneration following injury in the central nervous system (Hannila et al., 2013).

1.6.4.4 SLPI in regulating various aspects of cell biology

SLPI may also influence various aspects of cell biology. Several studies propose a role for SLPI in controlling cell growth, however opposing results are reported, exemplified by its effects on cancer cells where it can support and antagonize tumor growth (Bouchard et al., 2006). SLPI supports the growth of different epithelial cell types, hematopoietic cell precursors or B cells while it impacts on the differentiation, proliferation and survival of neural stem cells and early granulocytes (Klimenkova et al., 2014; Mueller et al., 2008; Nakamura et al., 2003). Emerging evidence suggest a regulatory role of SLPI in granulocytic differentiation. Low levels of NE and SLPI are found in myeloid cells and plasma of severe congenital neutropenia patients where SLPI is shown to control myeloid differentiation through regulation of NFkB, ERK1/2:LEF-1, and c-myc activation (Klimenkova et al., 2014). SLPI is also shown to regulate apoptosis in mature granulocytes and monocytic cells, in an antiprotease-independent manner, however the mechanisms remain largely obscure (McGarry et al., 2015; Subramaniyam et al., 2011).

1.7 Summary and aims

ALF is a clinical syndrome characterized by overwhelming hepatocyte death. Drug-induced liver injury, particularly AALF, is the commonest cause of ALF (Bernal et al., 2015), with a high mortality rate, due to activation of SIRS and its attendant complications of multi-organ failure and recurrent infection, generated by uncontrolled immune-mediated liver injury (Antoniades et al., 2008; Vaquero et al., 2003). Central to the pathogenesis of ALF is liver inflammation, where infiltration of myeloid cells in areas of necrosis is contrasted by immune cell depletion and dysregulation in the systemic circulation (Antoniades et al., 2012). At steady state monocytes traffic to the liver, augmenting the local macrophage pool, a process that is markedly increased during ALF (Holt et al., 2008; Zigmond et al., 2014). ALF patients have an expansion of hepatic macrophages, localized in areas of necrosis, that is through chemokine-dependent recruitment of MoMFs and proliferation of resident KCs (Antoniades et al., 2012; Choi et al., 2015a; Dambach et al., 2002; Holt et al., 2008; Mossanen et al., 2016; Zigmond et al., 2014). Studies in humans and mice show that hepatic macrophages orchestrate both tissue-destructive and resolution/repair responses following acute liver injury (Antoniades et al., 2014; Antoniades et al., 2012; Mossanen et al., 2016; Zigmond et al., 2014).

MerTK, expressed predominantly by macrophages, dampens innate immune responses and promotes the clearance of apoptotic cells (efferocytosis) following acute tissue injury (Rothlin et al., 2015). Engagement and activation of MerTK inhibits signaling pathways triggered by cytokines toll-like receptor ligands (Lemke and Rothlin, 2008). MerTK recognizes the exposed phosphatidylserine on the surface of apoptotic cells, in association with its ligands, while their efferocytosis induces a macrophage functional switch towards resolution/tissue-repair responses (Zagorska et al., 2014). SLPI, secreted by epithelial and myeloid cells, suppresses monocyte/macrophage pro-inflammatory responses through inhibition of NF-κB signaling (Ashcroft et al., 2000; Nakamura et al., 2003; Sallenave, 2010; Scott et al., 2011b). SLPI is shown to exert immune-modulatory activities during tissue inflammation in a variety of diseases, such as sepsis, asthma and cancer (Majchrzak-Gorecka et

al., 2016) while it was recently identified that SLPI, secreted in the liver by biliary epithelial cells and hepatic macrophages, is a key modulator of circulating monocyte function in human ALF (Antoniades et al., 2014).

The aim of the research described in this thesis is to investigate, using a combination of human and murine experimental models, the role of MerTK during resolution of inflammation following acute liver injury and examine how SLPI, as a pro-resolving mediator, governs this immunological response between macrophages and neutrophils. Hence, I aimed to examine the:

- Phenotypic/functional profile, migratory characteristics and tissue topography of monocytes and hepatic macrophages in ALF patients.
- Phenotype of hepatic macrophages in WT mice following APAP-induced acute liver injury and the biological relevance of MerTK+ cells for resolution of hepatic inflammation using WT and MerTK-deficient mice.
- Effects of micro-environmental triggers including biliary epithelial cells, apoptotic cell debris and SLPI, detected in the inflamed ALF liver, on skewing monocytes/macrophages towards a $MerTK^{high}$ resolution-like type.
- Direct and indirect effects of SLPI on the innate immune function and survival of neutrophils.
- Effects of SLPI administration in WT mice, with APAP-induced acute liver injury, on the hepatic macrophage phenotype and the activation/apoptosis state of neutrophils.
- Examine the circulating and hepatic micro-environmental milieu and characterize the hepatic immune cell infiltrate in SALF patients and pathological controls.

CHAPTER 2

2. PHENOTYPIC AND FUNCTIONAL CHARACTERIZATION OF MONOCYTES AND MACROPHAGES IN PATIENTS WITH ACUTE LIVER FAILURE

2.1 Background and aims

Central to the pathogenesis of ALF is liver inflammation where the infiltration of myeloid cells in areas of hepatic necrosis is contrasted by immune cell depletion and dysregulation in the circulation (Antoniades et al., 2006; Antoniades et al., 2008). During steady state, monocytes traffic to the liver augmenting the local macrophage pool, a process that is markedly increased during experimental ALF (Holt et al., 2008; Zigmond et al., 2014). Consistently, ALF patients show an expansion of hepatic macrophages, due to the chemokine-dependent recruitment of monocytes and proliferation of resident KCs (Antoniades et al., 2012; Choi et al., 2015a; Dambach et al., 2002; Holt et al., 2008; Mossanen et al., 2016; Zigmond et al., 2014). Several studies suggest that hepatic macrophages orchestrate both tissue-destructive and resolution responses following acute liver injury (Antoniades et al., 2014; Antoniades et al., 2012; Mossanen et al., 2016; Zigmond et al., 2014).

In the past decade, research in human ALF started to explore the role of monocytes and macrophages in the pathophysiology of the disease (Possamai et al., 2014b). Compared to healthy controls (HC) and chronic liver disease (CLD) patients, monocytes and hepatic macrophages in ALF have an anti-inflammatory $CD163^{high}HLA\text{-}DR_{low}$ phenotype and functional characteristics, typified by reductions in NF-κBp65, TNF-α and IL-6 levels and preserved IL-10 secretion following microbial challenge (Antoniades et al., 2006; Antoniades et al., 2014; Antoniades et al., 2012). These data implicated monocytes/macrophages in the resolution and tissue-repair processes during human ALF (Antoniades et al., 2014; Antoniades et al., 2012).

MerTK, expressed predominantly by tissue macrophages, dampens innate immune responses and promotes clearance of apoptotic cells following acute tissue injury (Rothlin et al., 2015). Recently, a

study on acute-on-chronic liver failure (AoCLF) patients revealed that these patients are characterized by monocyte dysfunction and attenuated pro-inflammatory responses to microbial challenge, similar to ALF patients (Bernsmeier et al., 2015). In particular, it described increased numbers of MerTK+ monocytes/macrophages, showing that these cells contribute to down-regulation of innate immune responses in AoCLF. This immune-regulatory subset was detected in both circulatory and tissue (liver and lymph-node) compartments of AoCLF patients, exhibited an anti-inflammatory $CD163^{high}HLA\text{-}DR_{low}$ phenotype, echoing the one observed in ALF (Antoniades et al., 2014; Antoniades et al., 2012). Interestingly, this MerTK+ monocyte subset was also detected, remarkably at higher levels than the AoCLF study group, in the circulation of ALF patients (Bernsmeier et al., 2015).

Hypothesis and aims:

Given the previous and new findings on circulating monocytes and hepatic macrophages in human ALF, I hypothesized that this MerTK+ immune-regulatory subset is expanded in ALF, and is detected at both circulatory and tissue compartments of these patients. In addition, these cells fundamentally contribute to the resolution of hepatic inflammation processes following acute liver injury. Hence, in this chapter I aimed to:

- Examine the phenotypic/functional profile of circulating monocytes and liver-derived hepatic macrophages isolated from ALF patients, healthy and disease controls.
- Assess the migratory characteristics across hepatic endothelium of monocytes in healthy controls and ALF.
- Determine the topography and phenotypic profile of monocytes/macrophages in liver and mesenteric lymph-node tissue derived from pathological controls and ALF patients.

2.2 Materials and methods

2.2.1 Patient recruitment

Acetaminophen-induced ALF (AALF, n=23) and non-acetaminophen-induced ALF (NAALF, n=9) patients, as detailed in **(Table 2.1),** were recruited into the study within 24 hours following admission to the Liver Intensive Care Unit at King's College Hospital (London, UK). Chronic liver disease (CLD, n=10) inpatients, none with acute-on-chronic liver failure **(Table 2.1),** and healthy volunteers (HC, n=15) served as pathological and healthy controls, respectively. Exclusion criteria were age <18 or >65 years, neoplasia and immunosuppressive therapy. AALF patients were identified for transplantation according to the King's College Hospital criteria (Bernal et al., 2002).

The study was approved by the NRES Health Research Authority (12/LO/0167). Assent was obtained by the patients'nominated next of kin if they were unable to give informed consent themselves. All human diseased (06/Q2708/11) and normal donor (06/Q2702/61) liver tissue and blood samples (04/Q2708/41) obtained through the Liver Unit at the Queen Elizabeth Hospital (Birmingham, UK) were collected with local research ethics committee approval and patient consent. Clinical, hematological and biochemical parameters were determined in patients using a hematology analyzer (Siemens Advia 2120, Berks, UK).

2.2.2 Isolation of peripheral blood mononuclear cells, monocytes and neutrophils

Whole blood was obtained from healthy volunteers and ALF patients, recruited at King's College Hospital, in order to isolate peripheral blood mononuclear cells (PBMCs) using Ficoll-Paque Plus (GE Healthcare) and neutrophils using Polymorphprep (Axis-Shield, Norway), as recommended by the manufacturers. Cell viability was >95% according to trypan blue staining. CD14+ cells were isolated from healthy PBMCs using CD14 magnetic beads (Miltenyi Biotec, UK). In addition, purity of monocytes and neutrophils was assessed by flow cytometry (90-95%) by using monoclonal antibodies against CD14 and CD66b, respectively (BD Biosciences, UK). After isolation, PBMCs, monocytes and neutrophils were washed in PBS (Life Technologies, UK).

2.2.3 Isolation of hepatic mononuclear cells

Hepatic mononuclear cells (HMCs) were isolated from approximately 120-150 g of human liver tissue, as previously described (Liaskou et al., 2013). The tissue was washed in cold sterile phosphate-buffered saline and was cut into small pieces in order to be mechanically digested in RPMI-1640 medium using a Stomacher400 Circulator (Cole-Parmer Instrument, United Kingdom) for 5 min at 260 speed. The tissue homogenate was then filtered and HMCs were purified further by density gradient centrifugation using Lympholyte (Cedarlane Laboratories, Canada) for 20 min at 550x*g*. HMCs were washed in phosphate-buffered saline and were further examined for their phenotype and function or cultured.

2.2.4 Flow cytometry of immune cells

Human PBMCs and HMCs were incubated with mouse anti-human monoclonal antibodies [CD14-PE-Cy7, CD16-APCH7, CD163-PE, CCR2-AF647, CCR5-FITC, CCR7-FITC (BD Biosciences, UK); HLA-DR-PerCP (eBioscience, UK); MerTK-APC, Tie-2-PE (R&D Systems, UK)] for 20 min at room temperature in the dark and then assessed by flow cytometry for surface marker expression. Cells were washed and re-suspended in phosphate-buffered saline supplemented with 1% fetal bovine serum. Cells were fixed and permeabilized for intracellular cytokine staining (BD Biosciences, UK). Also, TNF-α and IL-6 levels (BD Biosciences, UK) were determined by flow cytometry using intracellular cytokine staining (BD Biosciences, UK) following 6h LPS (100 ng/ml) stimulation (Sigma-Aldrich, UK).

2.2.5 Gene expression analysis

Gene expression analysis was performed using the NanoString nCounter® GX Human Immunology V2 assay (NanoString Technologies, Inc., Seattle, WA) profiling 594 immunology-related genes. FACS-separated cells from HC and ALF patients (n=3 each) were lysed in RLT lysis buffer (Qiagen,

Dusseldorf, Germany) (max 50.000 cells / 2µl) and were stored at -80°C. The cell lysates were incubated with reporter and capture probe sets overnight and afterwards were immobilized on a cartridge using the nCounter® Prep Station (NanoString Technologies, Inc., Seattle, WA). Cartridges were scanned on the nCounter® Digital Analyzer at 600 fields of view at the UCL Nanostring Facility (University College London, UK). The differential gene expression was calculated and plotted as heatmap using the nSolver™ Analysis Software 3.0 (NanoString Technologies, Inc., Seattle, WA). Statistically relevant results are considered with $P < .05$ and a fold-change of 50% higher or lower.

2.2.6 Measurement of inflammatory mediator and cytokine levels

Human quantikine ELISA was used to measure SLPI levels (R&D Systems, UK) in PBMC culture supernatants from ALF patients and HC, following 6h LPS (100 ng/ml) stimulation (Sigma-Aldrich, UK). The MSD Human Pro-inflammatory 10-plex panel was also used to assess (IFN-γ, IL-1β, IL-2, IL-4, IL-6, IL-8, IL-10, IL-12p70, IL-13 and TNF-α) cytokine levels in culture supernatants. ELISA microplates were read using the SoftMax® Pro software (Molecular Devices, USA). MSD plates were read on the Sector Imager 2400 apparatus (Gaithersburg, MD). All experiments were performed in duplicates and according to the manufacturer's instructions.

2.2.7 Tissue sampling, immunohistochemistry and imaging

Human liver tissue was obtained from ALF patients undergoing orthotopic liver transplantation (OLT), diseased liver tissue from CLD patients while normal liver tissue was derived from hepatic resection margins of colorectal malignancies. For phenotypic characterization of liver-derived macrophages, HMCs were isolated from fresh ALF (n=8), CLD (n=10) and NL (n=6) explant liver tissue. For immunohistochemistry (IHC), liver and mesenteric lymph node (LN) tissue was obtained from ALF (n=6) and hepatic resections, serving as pathological controls (PC, n=4).

Single-epitope enzymatic immunohistochemistry for detection of MerTK, CD163, and HLA-DR expressing cells. FFPE tissue was cut at 4 μm using a Leica RM2235 rotary microtome (Leica Biosystems, UK) and picked up on poly-L-lysine coated slides which were manually stained using a) rabbit monoclonal anti-MerTK primary antibody (# ab52968, Abcam, UK; dilution 1:500), b) mouse monoclonal anti-HLA-DR antibody (# M0746, Dako, UK; dilution 1:100), c) mouse monoclonal anti-CD163 primary antibody (# NCL-L-CD163, Leica Biosystems, UK; dilution 1:100) d) rabbit polyclonal anti-MPO primary antibody (# ab9535, Abcam, UK; dilution 1:50). All slides were dewaxed in xylene, rehydrated, subjected to heat-induced epitope retrieval (HIER) using sodium citrate buffer, pH 6, for 20 min, and allowed to cool, followed by one incubation at room temperature with the primary antibody. The signal was detected using EnVisionTM G/2 Doublestain System, Rabbit/Mouse (DAB+/Permanent Red) (# K536111-2, Dako, UK), and visualized with the Vector VIP peroxidase kit (# SH-600, Vector Laboratories, UK). The slides were then dehydrated with alcohol, cleared with xylene and cover slipped with DPX (Leica Biosystems, UK) after hematoxylin counterstaining. Images were captured with a Nikon Eclipse E600 microscope using the Nuance™ 3.0.2 (PerkinElmer, UK) multispectral imaging technology.

Double-epitope enzymatic immnohistochemistry for detection of MerTK/CD163 and MerTK/HLA-DR expressing cells. FFPE tissue was cut at 4 μm using a Leica RM2235 rotary microtome (Leica Biosystems, UK) and picked up on poly-L-lysine coated slides which were manually stained using a) rabbit monoclonal anti-MerTK primary antibody (# ab52968, Abcam, UK; dilution 1:300) and mouse monoclonal anti-CD163 primary antibody (# NCL-L-CD163, Leica Biosystems, UK; dilution 1:100), b) rabbit monoclonal anti-MerTK primary antibody (# ab52968, Abcam, UK; dilution 1:300) and mouse monoclonal anti-HLA-DR antibody (# M0746, Dako, UK; dilution 1:100). Slides were dewaxed in xylene, rehydrated, subjected to heat-induced epitope retrieval (HIER) using sodium citrate buffer, pH 6, for 20 min, and allowed to cool, followed by 1 MerTK incubation at room temperature with either the anti-HLA-DR or anti-CD163 antibody. The signal was detected using the EnVisionTM G/2 Doublestain System, Rabbit/Mouse (DAB+/Permanent Red) (# K536111-2, Dako, UK), with Permanent Red for visualization. The slides were then incubated for 1 MerTK at room

temperature with the anti-MerTK antibody, and the second signal was detected using the same detection kit but with the Vector VIP peroxidase kit (# SH-600, Vector Laboratories, UK) for visualization. Slides were then dehydrated with alcohol, cleared with xylene and cover slipped with DPX (Leica Biosystems, UK) after hematoxylin counterstaining.

MerTK/CD163 and MerTK/HLA-DR double epitope fluorescent immunostaining. FFPE tissue cut at 4 µm using a Leica RM2235 rotary microtome (Leica Biosystems, UK) was picked up on poly-L-lysine coated slides which were manually stained using a) rabbit monoclonal anti-MerTK primary antibody (# ab52968, Abcam, UK; dilution 1:250) and a mouse monoclonal anti-CD163 antibody (# NCL-L-CD163, Leica Biosystems, UK; dilution 1:100) or b) rabbit monoclonal anti-MerTK primary antibody (# ab52968, Abcam, UK; dilution 1:250) and a mouse monoclonal anti-HLA-DR antibody (# M0746, Dako, UK; dilution 1:100). Slides were dewaxed in xylene, rehydrated, subjected to heat-induced epitope retrieval (HIER) using sodium citrate buffer, pH 6, for 20 min, and allowed to cool, followed by 15 mins avidin and biotin blocking steps using an avidin/biotin blocking kit (# SP-2001, Vector Laboratories, US), and a 1h incubation with 3% skimmed milk in PBS. Slides were first incubated for MerTK at room temperature with the anti-MerTK antibody, followed by an incubation in the same conditions with a biotinylated goat-anti-rabbit secondary antibody (# E043201-8, Dako, UK; dilution 1:200), and another incubation with Alexa Fluor 488-conjugated streptavidin (# S32354, Life Technologies, UK; dilution 1:200). The second primary antibody was then applied (1.5 MerTK at room temperature) followed by an incubation in the same conditions with an Alexa Fluor 594-conjugated goat anti-mouse antibody (# A11032, Life Technologies, UK; dilution 1:200). All slides were counterstained with 4′,6-diamidino-2-phenylindole (DAPI) (# D1306, Life Technologies, UK), cover slipped using a fluorescence mounting medium (# S302380-2, Life Technologies, UK) and imaged using a Zeiss LSM800 confocal microscope (Zeiss, UK).

Assessing MerTK/HLA-DR and MerTK/CD163 expression - multispectral imaging and confocal microscopy. Double-epitope enzymatic immunohistochemistry (MerTK/CD163, MerTK/HLA-DR, MPO/TUNEL) was used to assess co-localization. Distinguishing between red and purple and

unmixing these co-localized chromagens is not feasible with an RGB camera as it only uses 3 channels, so a multispectral approach was used. Nuance camera takes several images over different wavelengths, thus identifying the 'individual spectral signature' of each chromagen, saving and unmixing it from adjacent colours. Once unmixed, images are re-coloured, enabling distinction of chromogens and inverting to a pseudo-fluorescence image. In addition, confocal examination of double epitope fluorescent immunostains was used to confirm MerTK/HLA-DR, MerTK/CD163 and MPO/TUNEL cells co-expression, to overcome a few obstacles such as the thickness of the histological sections which allowed for the overlapping of signals.

2.2.8 Monocyte migration across hepatic endothelium

Trans-endothelial migration of ALF and HC monocytes across stimulated hepatic endothelium were assessed using a recently established *in vitro* migration assay (Bernsmeier et al., 2015; Zimmermann et al., 2015). Collagen plugs were formed in cell culture inserts (Merck Millipore, Germany) placed in 24-well plates (Corning, USA). Human hepatic sinusoidal endothelial cells (HSECs) (5×10^4) were added/grown on the plugs and then were stimulated with TNF-α and IFN-γ (both 10 ng/ml) (R&D Systems, UK) (37^{o}C in 5% CO_2). CD14-isolated monocytes ($2x10^6$) were added on top of the collagen matrix and after 1.5h incubation non-migrated monocytes were harvested. Sub-endothelial monocytes were recovered from the HSEC/collagen matrix after 24h, following incubation with collagenase solution. Monocyte phenotype was determined and cells (cells/µl) were quantified using Count Bright Absolute Counting Beads by flow cytometry (Life Technologies, UK).

2.2.9 Efferocytosis, phagocytosis and oxidative burst

Human neutrophils were isolated as described above (2.2.2) and were re-suspended at 10^6 cells/ml in complete medium, labeled with CellTracker Green CMFDA (Life Technologies, UK) (5 µM in serum-free medium, 45 min, dark) and incubated for 20h (37℃ in 5% CO_2) in 24-well plates (Corning, USA). Annexin V kit (BD Biosciences, UK) was used to determine the percentage of

cultured neutrophils that are actively undergoing apoptosis which was over 70% apoptotic cells. Next, PBMCs from HC or ALF patients were re-suspended and co-incubated in 1:2 ratio for 4 hours with CMFDA-labeled apoptotic neutrophils and flow cytometry was used to quantify the percentage of CD14-labeled monocytes that phagocytosed apoptotic cells. In addition, neutrophil oxidative burst was assessed using the Phagoburst kit (Glycotrope, Germany) and monocyte phagocytosis of bacteria bioparticles using the pHRodo kit (ThermoFisher Scientific, UK) by flow cytometry, according to the manufacturer's instructions.

2.2.10 Statistical analysis

Analysis and graphing of data were performed using GraphPad Prism 6 software (GraphPad Software, La Jolla California, USA). Statistical significance was assessed with non-parametric analysis for data not normally distributed, unless otherwise specified in figure legends. Results are presented as median with interquartile range (IQR), unless otherwise specified in figure legends.

2.3. Results

2.3.1. Patient characteristics

No significant differences were detected in ages between acute liver failure (ALF) patients and healthy controls (HC). Patients with chronic liver disease (CLD) were significantly older compared to both ALF and HC groups [52 (44-65) vs 35 (28-45)/29 (26-45); $p< 0.01$] **(Table 2.1).** Patients with ALF showed significantly higher biochemical and physiological indices of liver injury including international normalized ratio (INR) and creatinine, bilirubin and AST levels, when compared to CLD patients **(Table 2.1).**

2.3.2. Circulating monocytes exhibit a resolution-like MerTK+ phenotype in ALF

The immune-phenotype of circulating monocytes isolated from patients with CLD (n=10), ALF (n=15) and HC (n=15) was assessed using flow cytometry. Monocytes were identified following a previously established gating strategy (Abeles et al., 2012; Antoniades et al., 2014) based upon CD14, CD16 and HLA-DR expression (positive selection) (**Fig. 2.1A**). The expression levels of different surface markers were determined in the total monocyte population and the three monocyte subsets, that exist in human blood and liver: "classical" (CD14+CD16-), "intermediate" (CD14++CD16+) and "non-classical" ($CD14_{low}CD16+$) monocytes (Antoniades et al., 2014; Liaskou et al., 2013).

The immune profiling revealed a significantly increased proportion of MerTK-expressing (MerTK+) circulating monocytes in ALF patients, compared to HC and CLD patients (48.3 vs 8.7/9.3 %, both $p< 0.0001$) **(Fig. 2.1B**). Compared to classical and non-classical monocytes, MerTK expression in ALF was much higher in the intermediate subset (41.0/25.8 vs 70.9 %, both $p< 0.01$) (**Fig. 2.1B**) that is expanded in ALF (Abeles et al., 2012). Moreover, patients with AALF have a higher proportion of MerTK+ monocytes compared to non-acetaminophen induced ALF (NAALF) cases (51.5 vs 36.0 %; $p< 0.01$) **(Table 2.2).** Also, I found that monocyte MerTK expression in ALF patients correlated positively with SIRS score ($r=0.6217$; $p=0.0004$), INR ($r=0.5523$; $p=0.0023$) and negatively with

bilirubin (r=-0.4399; p=0.0192) and monocyte count (r=-0.4117; p=0.0295) (**Fig. 2.1-C**). In contrast with HC and CLD, I show that monocytes in ALF are characterized by a resolution-like (HLA-$DR_{low}CD163^{high}Tie\text{-}2^{high}$) phenotype with enhanced tissue homing ($CCR2^{high}CCR5^{high}CCR7^{high}$) properties (**Fig. 2.1D-E**). These results confirm and extend recent findings in patients with acetaminophen-induced ALF (AALF) and acute-on-chronic liver failure (AoCLF) (Antoniades et al., 2014; Bernsmeier et al., 2015).

Functional *in vitro* analyses revealed that, compared to HC cells, monocytes isolated from ALF patients exhibit enhanced efferocytosis of CMFDA-labelled apoptotic neutrophils (42.4 vs 72.6 %; $p< 0.01$) **(Fig. 2.2A)**, and their MerTK expression strongly correlated with their efferocytosis index ($r=0.78$; $p<0.01$). Compared to HC, $MerTK^{high}$ monocytes in ALF secrete comparable (e.g. IL-10) or elevated levels (SLPI, 46 vs 278 pg/ml, $p< 0.05$) of anti-inflammatory mediators and reduced levels of pro-inflammatory mediators [IFN-γ (703 vs 4), $p< 0.05$; TNF-α (3110 vs 346), $p< 0.0001$; IL-6 (2.544 vs 308), $p< 0.001$; all pg/ml] following microbial challenge **(Fig. 2.2B-C).** Furthermore, using flow cytometry based (CD14+) monocyte intracellular cytokine staining I reveal that compared to MerTK-**,** MerTK+ monocytes secrete significantly reduced TNF-α levels, with an inverse correlation between monocyte MerTK expression and TNF-α secretion ($r=-0.57$; $p<0.05$).

It is also proposed that monocyte MerTK expression may be modulated through activation of cytokine receptors and their ligands (e.g. IL-10) (Lemke and Rothlin, 2008; Zizzo et al., 2012), thus the systemic inflammatory milieu is likely to induce MerTK expression in monocytes. In order to assess those effects on monocyte phenotype, I conditioned healthy monocytes in plasma derived from ALF patients and HC **(Fig. 2.2D)**. Compared to monocytes cultured in HC plasma, I found that monocyte culture in ALF plasma induced the distinct HLA-$DR_{low}CD163^{high}Tie\text{-}2^{high}$ immune-phenotype **(Fig. 2.2D)** with increased tissue/lymph-node homing ($CCR2^{high}CCR5^{+}CCR7^{high}$) marker expression, resembling the phenotype described *ex vivo* for monocytes in ALF **(Fig. 2.1B-D)**.

Table 2-1. Clinical and physiological characteristics of patients with ALF in comparison to CLD and HC groups.

Parameter	ALF	CLD	HC
Number of patients	32	10	15
Age	35* [28-45]	52 [44-65]	29* [26-45]
Sex (M/F)	15:17	6:4	6:9
Aetiology	*Drug-induced:* Acetaminophen [23] Mixed overdose [2] *Non-drug induced:* Pregnancy-related [3] Budd-Chiari [1] Hepatitis B [1] Acute Wilsons [1] Ischaemia [1]	ALD [4] NAFLD [3] HFE [1] PBC [1] PSC [1]	n/a
WCC ($x10^9$/L)	10.4* [6.7-15.5]	4.46 [3.7-5.1]	n/a
Monocytes ($x10^9$/L)	0.22 [0.13-0.4]	0.31 [0.24-0.42]	n/a
Creatinine (µmol/L)	139.5** [90-242]	73 [56-79]	n/a
INR	5.4*** [2.8-8.8]	1.4 [1.15-1.6]	n/a
Bilirubin (µmol/L)	88*** [49.5-177]	49 [12-70]	n/a
AST (IU/mL)	5199*** [1155-8499]	45 [28-55]	n/a
Encephalopathy	2*** [1-3]	1 [0-1]	n/a
Child's Pugh	n/a	9 [8-11]	n/a
MELD	39.5* [33-40]	12 [7-19]	n/a
SOFA	13 [10-16]	n/a	n/a

Abbreviations: INR: international normalized ratio; AST: aspartate aminotransferase; MELD: Model for End stage Liver Disease; SOFA: sequential organ failure assessment; WCC: white (leukocyte) cell count; ALD: alcoholic liver disease; NAFLD: non-alcoholic fatty liver disease; HFE: haemochromatosis; PSC: primary sclerosing cholangitis; PBC: primary biliary cholangitis. *p=0.006; **p=0.001; ***p<0.0001, compared to CLD group.

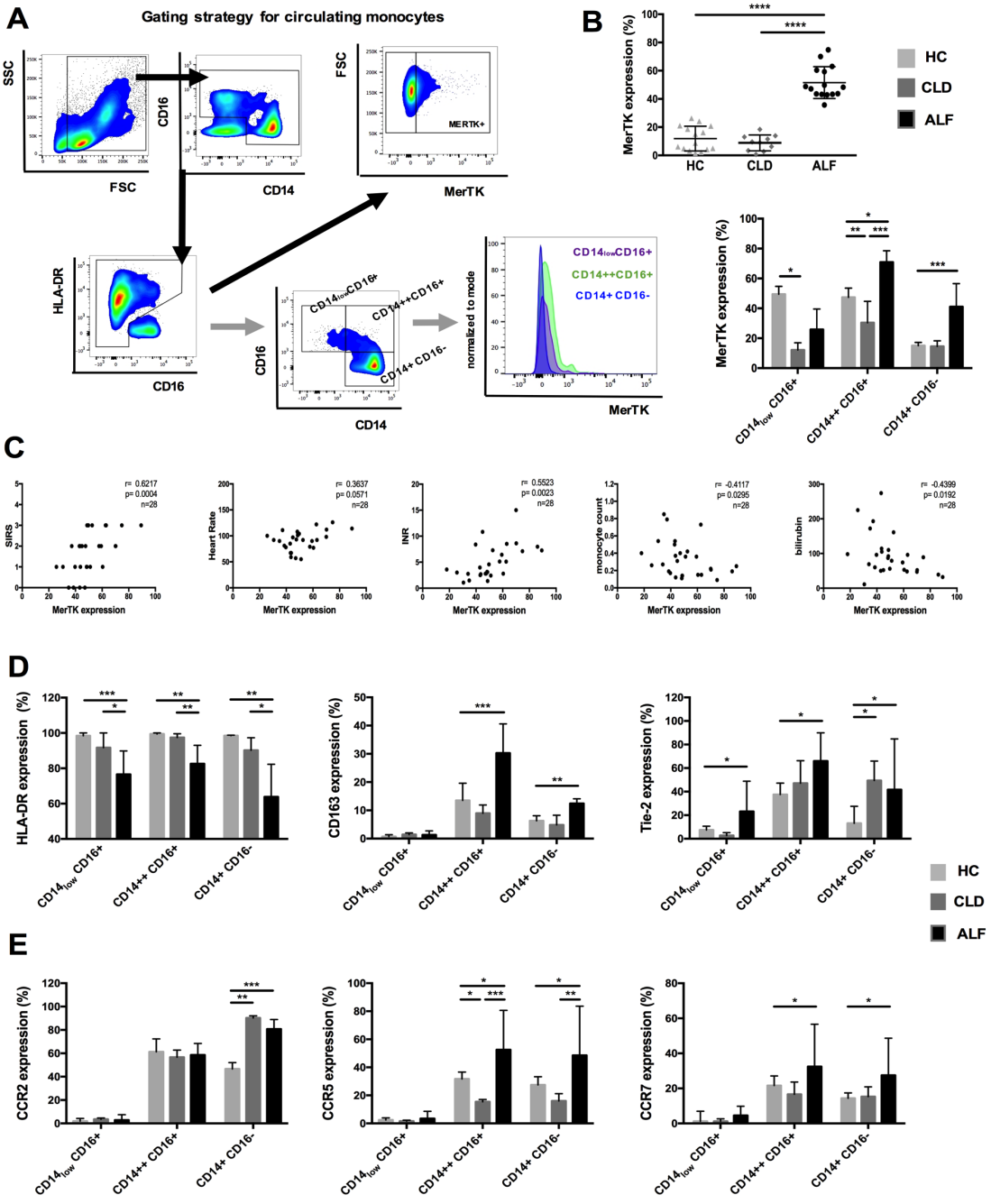

Figure 2.1. Phenotypic characterization of resolution-like MerTK+ monocytes in ALF.

Circulating monocytes were isolated from ALF (n=15), CLD (n=10) patients and HC (n=15) and were phenotypically characterized using flow cytometry. **(A)** Representative flow cytometry analysis and gating strategy used to determine MerTK expression in total circulating monocytes and their subsets [classical (CD14+CD16-), intermediate (CD14++CD16+) and non-classical ($CD14_{low}CD16+$)]. **(B)** Data show monocyte MerTK expression levels in different study groups. **(C)** Correlations of monocyte MerTK expression with different clinical parameters of ALF patients. Data show the percentage of surface expression of **(D)** activation (HLA-DR), pro-resolution (CD163), pro-angiogenesis (Tie-2) and **(E)** tissue (CCR2/CCR5) and lymph-node (CCR7) homing markers in monocyte subsets in all study groups. Non-parametric (Mann-Whitney) statistical analysis was used. Data presented as median values with interquartile range (IQR). * p< .05, ** p< 0.01, *** p< .001, **** p< .0001. SSC: side scatter, FSC: forward scatter.

Table 2-2. Clinical and physiological parameters of acetaminophen-induced ALF (AALF) and non-acetaminophen induced ALF (NAALF) patients.

Parameter	AALF	NAALF
Number of patients	23	9
#patients transplanted/died	8/23	4/9
MERTK monocyte expression (%)	51.50** [40.75-73.75]	35.95 [31.45-52.25]
WCC ($x10^9$/L)	9.57 [6.34-15.96]	11.4 [8.0-18.4]
Monocytes ($x10^9$/L)	0.21** [0.14-0.36]	0.54 [0.31-0.98]
Creatinine (µmol/L)	148 [76.5-237.5]	193 [93-362]
INR	6.4** [3.0-8.4]	2.7 [1.4-4.6]
Bilirubin (µmol/L)	74 [48-96]	172 [42.5-587]
Lactate (mmol/L)	3.0 [2.2-6.8]	2.7 [1.8-4.0]
AST (IU/mL)	5172* [1500-7436]	2088 [432-6176]
Encephalopathy	2* [1-3]	1 [1-2]
SIRS score	2 [1-3]	2 [0-3]
APACHE II	19 [14-25.5]	20 [11-27]
SOFA	12 [10-15.5]	13 [10-16.5]
MELD	40 [33-40]	38 [24-40]

Abbreviations: INR: international normalized ratio; AST: aspartate aminotransferase; MELD: Model for End stage Liver Disease; WCC: white (leucocyte) cell count; APACHE II: acute physiology and chronic health evaluation II score; SOFA: Sequential organ failure assessment score; SIRS: systemic inflammatory response syndrome. * $p<0.05$ and ** $p<0.01$, compared to NAALF group

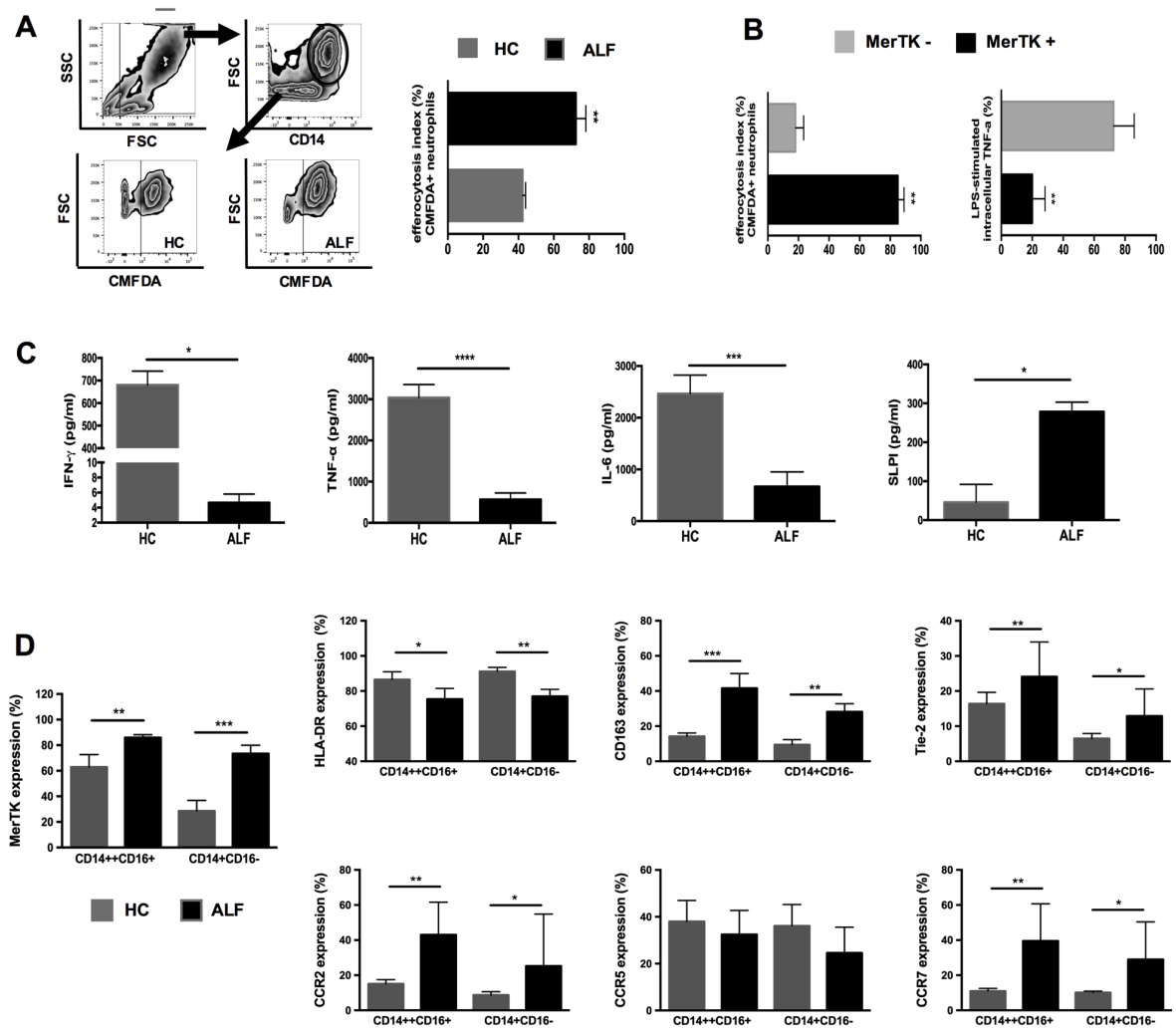

Figure 2.2. Functional characterization of monocytes and effects of the systemic inflammatory microenvironment in ALF.

PBMCs from healthy controls (HC) and ALF patients were co-cultured (4h) with CMFDA-labeled apoptotic neutrophils. **(A)** Representative flow cytometry analysis and data showing the percentage (%) of CMFDA-labeled neutrophils that were phagocytosed by CD14+ monocytes (n=5 each). **(B)** Data show the proportion of MerTK+ vs MerTK- monocytes that phagocytosed CMFDA-labeled neutrophils and that were stained positive for intracellular TNF-α following microbial challenge (LPS 100ng/ml, 6h). **(C)** Inflammatory cytokine secretion in HC and ALF PBMC supernatants (n=5 each) after microbial challenge (LPS 100ng/ml, 6h), as determined by ELISA. **(D)** Healthy CD14-isolated monocytes were cultured in medium containing (25%) plasma from ALF patients compared with HC (n=10 each) for 48 hours. Data show the percentage of surface expression of activation (HLA-DR), pro-resolution (MerTK/CD163), pro-angiogenesis (Tie-2) and tissue (CCR2/CCR5) and lymph-node (CCR7) homing markers, after conditioning monocytes in different plasma, as was assessed by flow cytometry. Non-parametric (Mann-Whitney) statistical analysis was used. Data are expressed as median values with interquartile range (IQR). * P< .05, ** P< 0.01, *** P< .001, **** P< .0001.

2.3.3. Gene expression profile of MerTK+ monocytes in ALF

To fully characterize the MerTK+ population in ALF, I performed FACS-sorting of MerTK± monocytes from HC and ALF patients (**Fig. 2.3A)** and subjected these cells to a quantitative gene expression array. Compared to MerTK-, MerTK+ monocytes at steady state (**Fig. 2.3B-C)**, and in ALF patients (**Fig. 2.4A-B**), have a transcriptional profile consistent with a more differentiated "tissue-like" phenotype, characterized by a significant up-regulation of genes responsible for adhesion (e.g. ICAM2, ITGA4, ITGB1), phagocytosis/pattern-recognition (FCGR2A/C, FCGR3A/B, MSR1, C1q), cell proliferation/survival (e.g C81, LAIR1, SRC), antigen presentation (HLA-DPA1, HLA-DPB1, HLA-DRA) and macrophage M2-like polarization (LGALS3, MARCO, MRC1, CMKLR1, CSF1R) (**Fig. 2.3B-C and 2.4A-B)**.

Comparison of the transcriptional profile between MerTK+ monocytes in ALF patients and HC **(Fig. 2.5A-B)** revealed striking differences in line with the phenotypic and functional readouts (**Fig. 2.1A-E and 2.2A-D).** MerTK+ monocytes in ALF exhibit a marked reduction in a number of regulatory pathways, notably in antigen processing MHC class II associated transcripts (HLA-DMA, HLA-DPA1, HLA-DPB1, HLA-DRA), TLR/NF-kB-dependent pro-inflammatory pathway (NFKBIA, NFKBIZ, TICAM1, TLR4, TLR8), phagocytosis/pattern-recognition (FCGR2A/C, FCGR3A/B) and cytokines/chemokines (CCL5, PTGS2, TNF) **(Fig. 2.5A-B).** Moreover, these cells maintain an M2-like skewed profile (e.g. CD163, MARCO, MRC1), activation of the downstream MerTK/cytokine signaling pathway (IRF3, JAK3) with a concomitant down-regulation in genes linked with cell activation (NLRP3, SMAD3, SRC) **(Fig. 2.5A-B).**

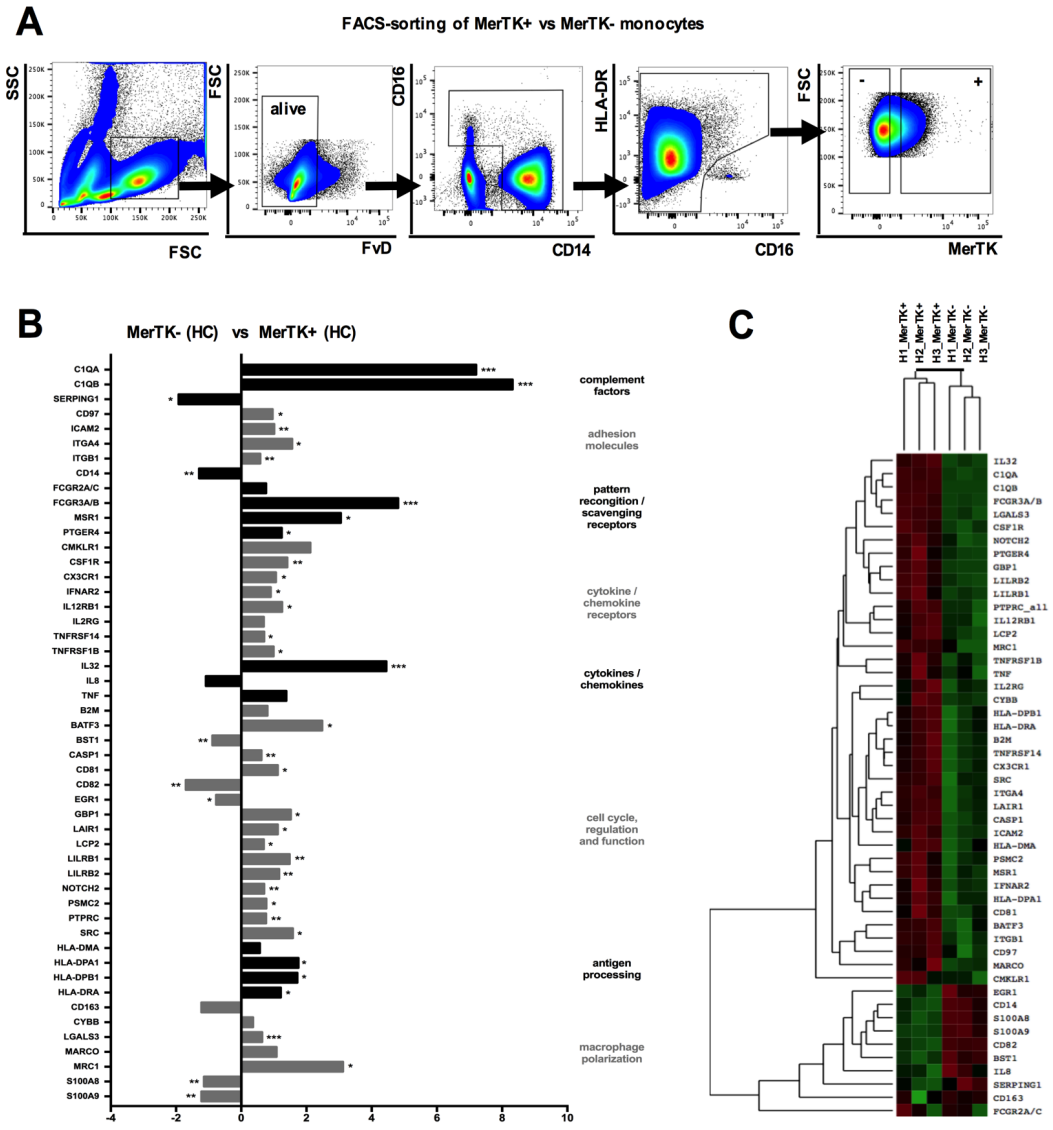

Figure 2.3. Gene expression pattern of MerTK+ versus MerTK- monocytes in healthy controls.

MerTK+ and MerTK- monocytes were FACS-sorted in HC and ALF patients (n=3 each) with a gating strategy displayed by representative flow cytometry plots in **(A)**. Highly pure isolates of the MerTK± subsets were subjected to quantitative microarray gene expression analysis (nCounter® GX Human Immunology V2 kit, profiling 594 immunology-related human genes; NanoString Technologies, Inc., Seattle, WA). **(B-C)** Data show the Log2 fold-change of expression and agglomerative cluster (heatmap, z-Score; green=min/red=max magnitude of expression) of differentially expressed genes, comparing MerTK+ vs MerTK- monocytes in HC. * p< .05, ** p< 0.01, *** p< .001. SSC: side scatter, FSC: forward scatter.

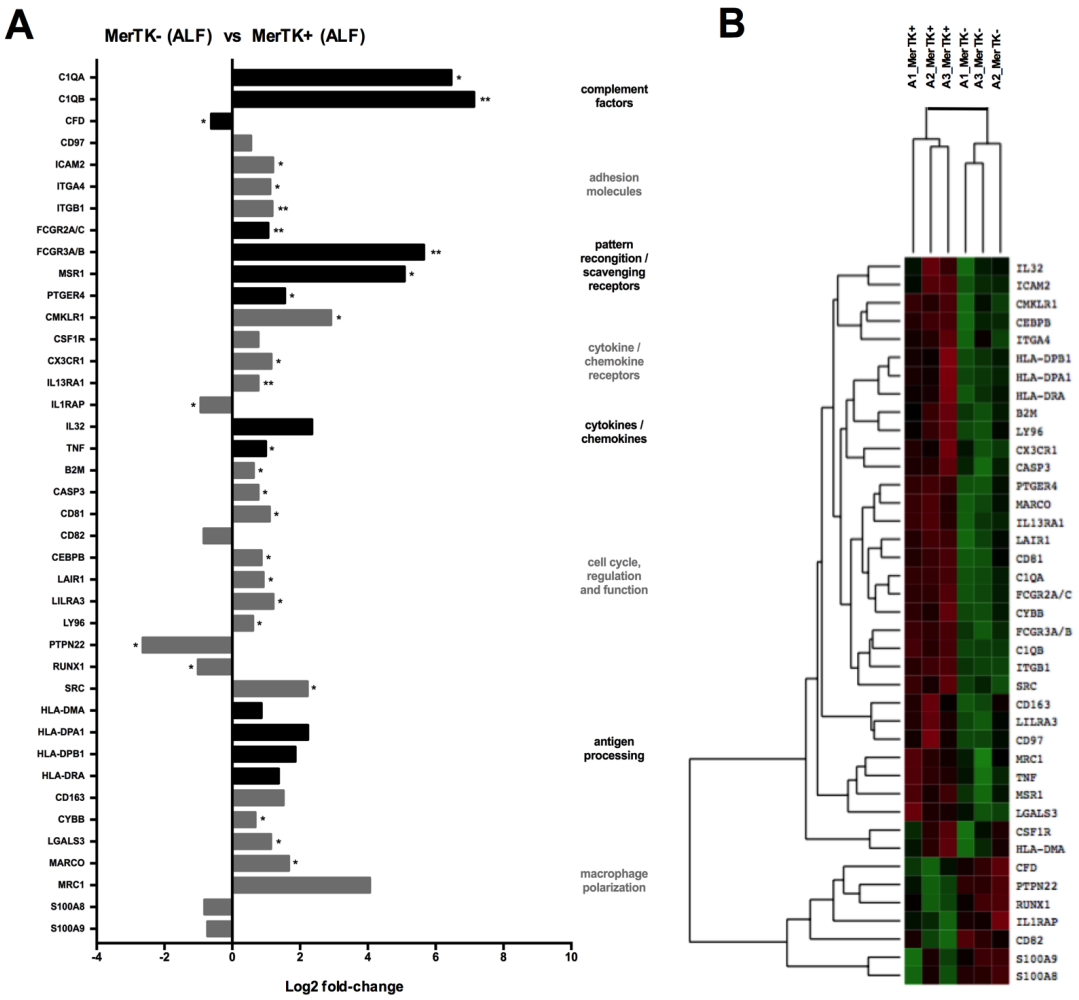

Figure 2.4. Gene expression pattern of MerTK+ versus MerTK- monocytes in ALF.

MerTK+ and MerTK- monocytes were FACS-sorted in HC and ALF patients (n=3 each). Highly pure isolates of the MerTK± subsets were subjected to quantitative microarray gene expression analysis (nCounter® GX Human Immunology V2 kit, profiling 594 immunology-related human genes; NanoString Technologies, Inc., Seattle, WA). **(A-B)** Data show the Log2 fold-change of expression and agglomerative cluster (heatmap, z-Score; green=min/red=max magnitude of expression) of differentially expressed genes, comparing MerTK+ vs MerTK- monocytes in ALF. * p< .05, ** p< 0.01, *** p< .001.

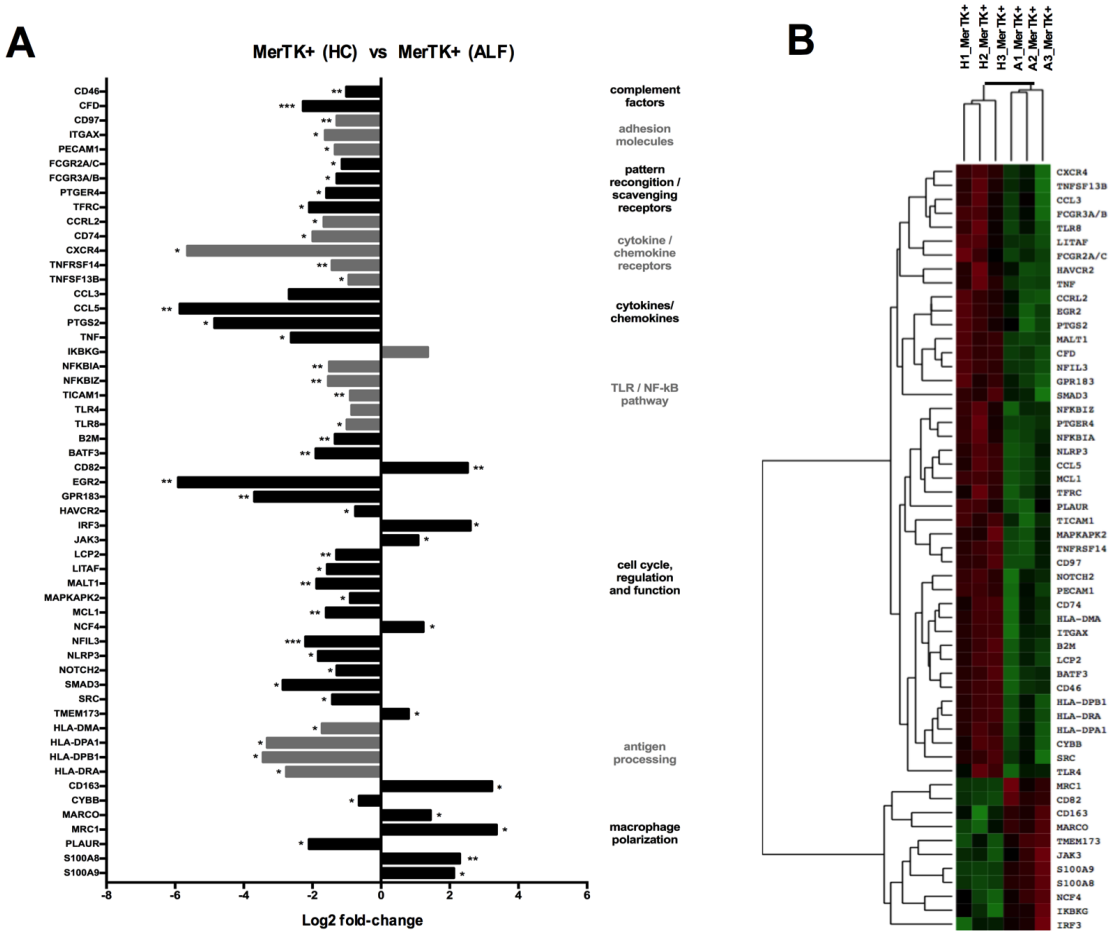

Figure 2.5. Gene expression pattern of MerTK+ monocytes in ALF versus healthy controls.

MerTK+ and MerTK- monocytes were FACS-sorted in HC and ALF patients (n=3 each). Highly pure isolates of the MerTK± subsets were subjected to quantitative microarray gene expression analysis (nCounter® GX Human Immunology V2 kit, profiling 594 immunology-related human genes; NanoString Technologies, Inc., Seattle, WA). **(A-B)** Data show the Log2 fold-change of expression and agglomerative cluster (heatmap, z-Score; green=min/red=max magnitude of expression) of differentially expressed genes, comparing MerTK+ monocytes in ALF and HC. * p< .05, ** p< 0.01, *** p< .001.

2.3.4. Characterization of MerTK+HLA-DR^{high} and MerTK+HLA-DR$_{low}$ subsets

Using flow cytometry, I further characterized the MerTK+ circulating monocytes based upon their HLA-DR expression levels (**Fig. 2.6A**). Interestingly, the analyses identified key differences in the functional profile of these cells. Importantly, peak levels of MerTK+HLA-DR^{high} cells are detected on patients' admission to the Liver Intensive Care Unit and subsequently decline to levels (33.6 vs 17.5 %; $p<0.05$) similar to HC by day 3-5 **(Fig. 2.6B**). In contrast to HC and CLD groups, MerTK+HLA-DR$_{low}$ cells are detected and significantly elevated in the circulation of ALF patients (1.3/0.5 vs 11.3 %; both $p< 0.001$), and remain persistently elevated following their admission **(Fig. 2.6B**).

I demonstrate that compared to HC and MerTK+HLA-DR$_{low}$ cells, MerTK+HLA-DR^{high} monocytes in ALF exhibit enhanced clearance of apoptotic (CMFDA+ Annexin-V^{high} neutrophils) and infective (pHrodo® E. coli BioParticles) material, with attenuated secretion of pro-inflammatory (e.g. TNF-α) mediators following microbial challenge **(Fig. 2.6C**). Compared to HC and CLD, both MerTK+HLA-DR$_{low}$ and MerTK+HLA-DR^{high} cells in ALF have a CD163^{high}Tie-2^{high}CCR2^{high}CCR5^{high}CCR7^{high} phenotype **(Fig. 2.6D**). Taken together, I identify that circulating monocytes in ALF patients exhibit a prorestorative phenotype, characterized by suppressed innate immune responses and enhanced efferocytic and phagocytic capabilities (Antoniades et al., 2006; Antoniades et al., 2012; Bernsmeier et al., 2015).

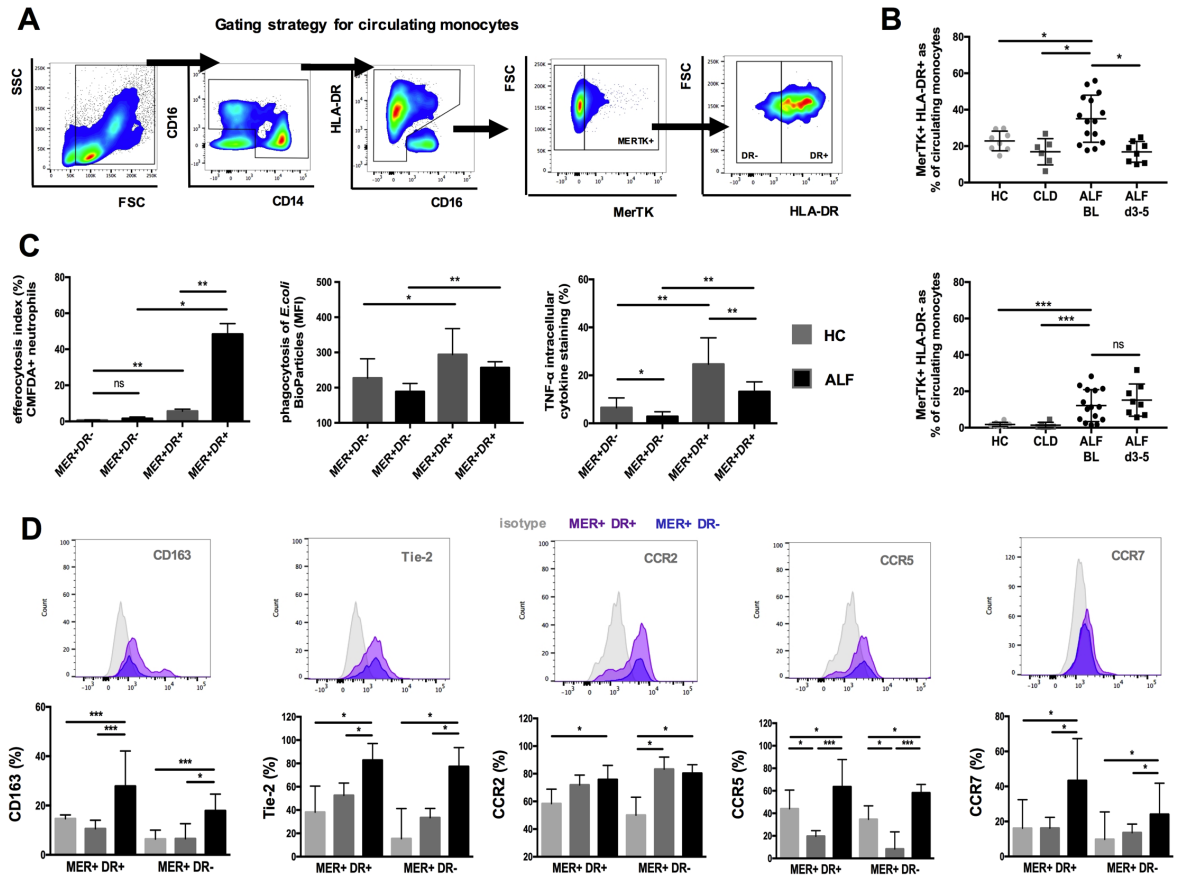

Figure 2.6. Functional characterization of MerTK+HLA-DR^{high} and MerTK+HLA-DR$_{low}$ monocyte subsets in ALF.

Circulating monocytes were isolated from ALF (n=15), CLD (n=10) patients and HC (n=15) and were phenotypically characterized using flow cytometry. **(A)** Representative flow cytometry analysis and gating strategy used to identify MerTK+HLA-DR^{high} and MerTK+HLA-DR$_{low}$ monocyte subsets. **(B)** MerTK+HLA-DR^{high} and MerTK+HLA-DR$_{low}$ subsets as proportion (%) of total circulating monocytes in HC, CLD and ALF patients on admission (n=15) and days 3-5 following their admission (n=8). **(C)** Proportion of MerTK+HLA-DR^{high} and MerTK+HLA-DR$_{low}$ monocytes that efferocytosed apoptotic neutrophils, phagocytosed *E. coli* bioparticles and intracellularly produced TNF-α after microbial challenge in HC and ALF (n=5 each). **(D)** Representative histograms and expression levels (%) of different monocyte surface markers in MerTK+HLA-DR^{high} and MerTK+HLA-DR$_{low}$ subsets in all study groups. Non-parametric (Mann-Whitney) statistical analysis was used. Data presented as median values with interquartile range (IQR). * p< .05, ** p< 0.01, *** p< .001, SSC: side scatter, FSC: forward scatter. ns: non-significant.

2.3.5. MerTK+ monocytes readily migrate across hepatic endothelium in ALF

During steady state and inflammation, circulating monocytes migrate into tissue compartments, where they differentiate into macrophages and promote anti-microbial responses (Gordon and Taylor, 2005), and may subsequently home either to regional lymph nodes or return to the circulatory pool (Gray and Cyster, 2012; Kastenmuller et al., 2012). In addition, human and experimental studies in ALF show that the hepatic macrophage pool is expanded not only due to the proliferation of the resident KCs but also through chemokine-recruited monocytes that give rise to MoMFs (Antoniades et al., 2012; Choi et al., 2015a; Dambach et al., 2002; Zigmond et al., 2014).

Given the evidence above showing that ALF monocytes (**Fig. 2.1E**), as also shown for the MerTK+ subset (**Fig. 2.6D**), highly express tissue (CCR2/CCR5) and lymph node (CCR7) homing receptors, I sought to evaluate their migratory characteristics across cytokine-stimulated hepatic endothelium (**Fig. 2.7**). I employed a novel *in vitro* migration model (Bernsmeier et al., 2015; Zimmermann et al., 2015) where using flow cytometry I assessed the immune-phenotype and kinetics of non-migrated cells, cells entering the sub-endothelial space and cells reverse-migrating back across the endothelial monolayer (**Fig. 2.7A**). Reverse migration is a pivotal *in vivo* process that allows the passage of immune cells out of tissue sites, trafficking either to regional lymph nodes to elicit immune responses, or to re-join the circulatory pool (Gray and Cyster, 2012; Kastenmuller et al., 2012).

The immune profiling of monocytes in ALF showed they were characterized, in all migratory compartments, by the typical $MerTK^{high}CD163^{high}$ phenotype (**Fig. 2.7A**), as observed *ex vivo* in patients (**Fig. 2.1B-E**). Both HC and ALF monocytes preserved their tissue and lymph-node homing marker repertoire ($CCR2^{+}CCR5^{+}CCR7^{+}$) (**Fig. 2.7A**). Using flow cytometry based cell-counting beads, I detected no differences between HC and ALF in the number of total (CD14+) cells migrating across the endothelium (**Fig. 2.7B**). However, compared to HC cells, I found a significantly lower number of sub-endothelial monocytes (75 vs 47 cells/ul; $p<0.001$) and increased number of reverse migrated monocytes in ALF (9 vs 18 cells/ul; $p<0.001$) (**Fig. 2.7B**). Furthermore, analysis of (CD14+)

monocytes based upon their MerTK expression revealed that whilst the number of MerTK+ cells entering into the sub-endothelial compartment was similar between study groups, a significantly higher proportion of MerTK+ cells underwent reverse migration in ALF (4 vs 16 cells/ul; $p<0.01$) (**Fig. 2.7C**). These findings support the hypothesis that in ALF there is an increased proportion of MerTK+ monocytes undergoing trans-endothelial migration from the circulatory compartment and home to sites of acute liver injury.

2.3.6. Liver-derived hepatic macrophages exhibit a resolution-like phenotype in ALF

Using flow cytometry, I assessed the phenotype of liver-derived hepatic macrophages, freshly isolated from explant tissue of patients with ALF (n=8), CLD (n=10) and normal liver (NL, n=6) tissue extracted from hepatic resections (**Fig. 2.8**). Compared to the NL and CLD study groups, I report a significantly increased frequency of CD14++CD16+ hepatic macrophages in the liver of ALF patients (34.6/39.6 vs 44.7 %; $p< 0.05$) with a reciprocal reduction in the CD14+CD16- subset (63.1/57.6 vs 50.9 %; $p< 0.05$) (**Fig. 2.8A-B**). These findings are in accordance with previous studies showing an expansion of the CD14++CD16+ monocyte subset in the circulation of ALF patients (Abeles et al., 2012) and in the inflamed human liver (Liaskou et al., 2013). The phenotypic analysis revealed that liver-derived macrophages in ALF exhibit a resolution-like ($MerTK^{high}CD163^{high}Tie\text{-}2^{high}HLA\text{-}DR_{low}$) phenotype, having augmented tissue/lymph-node homing ($CCR2^{+}CCR5^{high}CCR7^{high}$) characteristics, that was different from macrophages isolated from CLD and NL specimens (**Fig. 2.8C-D**). This macrophage phenotype is similar to that described in circulatory (**Fig. 2.1D-E**) and sub-endothelial compartments (**Fig. 2.7A**) and in line with recent reports (Antoniades et al., 2014; Bernsmeier et al., 2015).

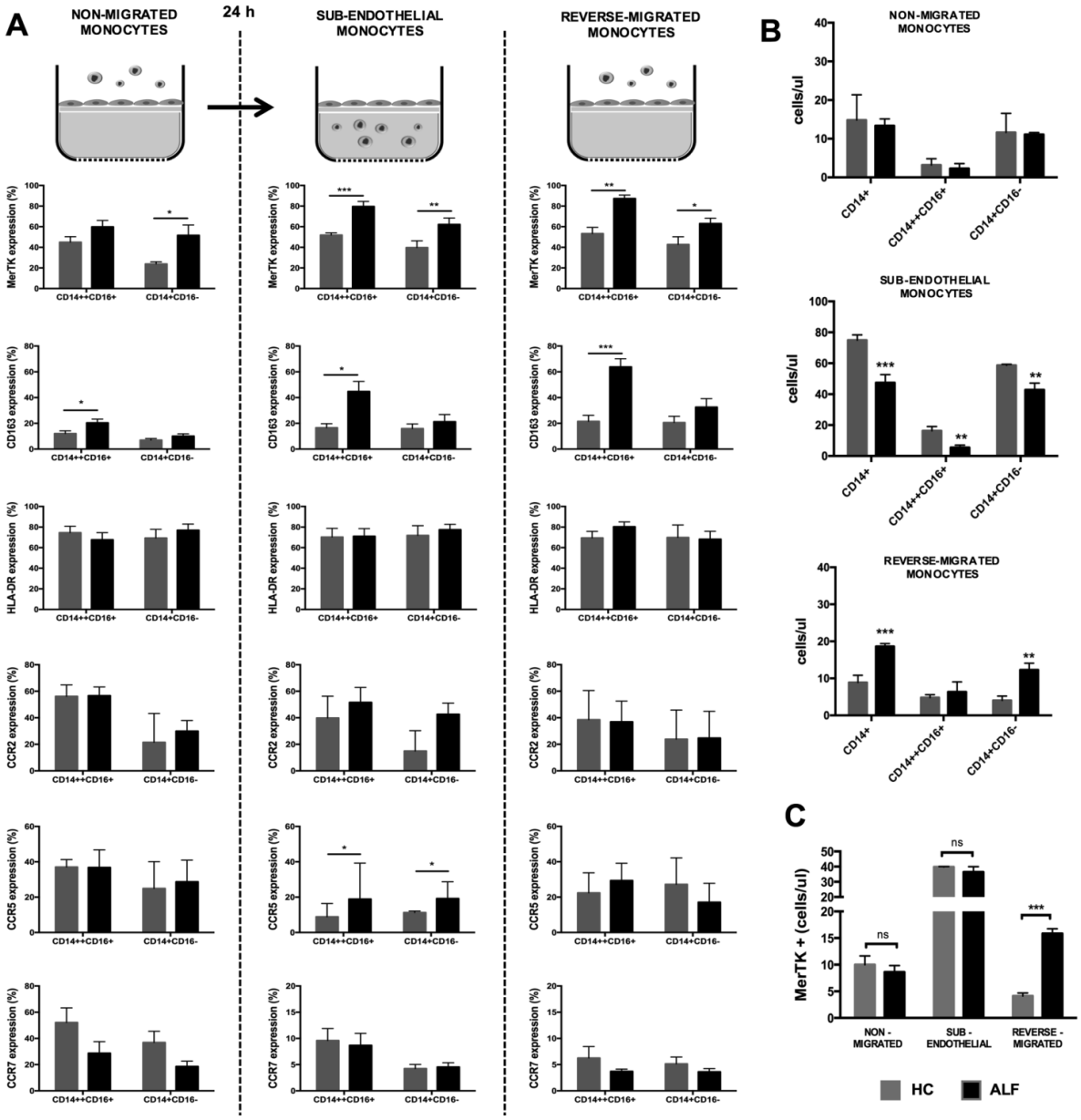

Figure 2.7. Migratory characteristics of circulating monocytes in ALF.

Trans-endothelial migration of ALF (n=12) and HC (n=6) monocytes across hepatic endothelium was determined *in vitro* (n=3). **(A)** Schematic describing the assay: CD14-isolated monocytes are added on top of a cytokine stimulated (TNF-α/IFN-γ) hepatic endothelium monolayer; non-migrated monocytes are harvested 1.5 hours after while sub-endothelial and reverse-migrated monocytes are obtained 24h later. Data show expression levels (percentage, %) of pro-resolution (MerTK, CD163), activation (HLA-DR), tissue (CCR2/CCR5) and lymph-node (CCR7) homing markers of (left panel) non-migrated, (middle panel) sub-endothelial and reverse migrated (right panel) monocytes, as dtermined by flow cytometry. **(B)** Data show the number of monocytes (cells/ul), determined using flow cytometry based cell counting beads, that did not migrate, migrated sub-endothelially migrated and reverse migrated on top of the monolayer. Results are shown for total CD14+ monocytes and monocyte subsets. **(C)** Data show the number of MerTK+ monocytes (cells/ul) at different migratory compartments. Non-parametric (Mann-Whitney) statistical analysis was used. Data are expressed as median values with interquartile range (IQR). * p< .05, ** p< 0.01, *** p< .001. ns: non-significant.

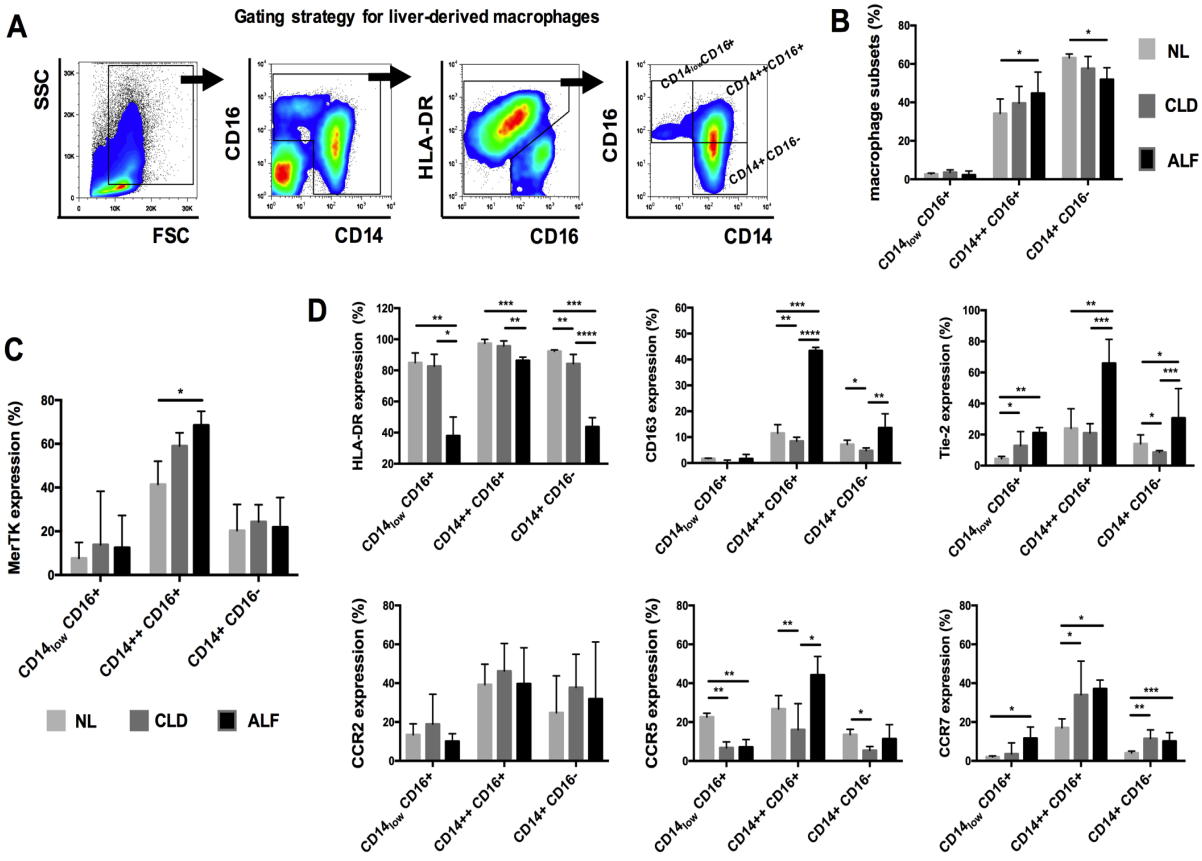

Figure 2.8. Phenotypic characterization of liver-derived hepatic macrophages in ALF

Hepatic macrophages were freshly isolated from human explant liver tissue of ALF (n=8), CLD (n=10) patients and normal liver (NL, n=6) from hepatic resections and were phenotypically characterized using flow cytometry. **(A)** Representative flow cytometry analysis and gating strategy used to identify macrophages and their subsets [classical (CD14+CD16-), intermediate (CD14++CD16+) and non-classical ($CD14_{low}$CD16+)]. **(B)** Data show the proportion (%) of macrophage subsets (classical, intermediate and non-classical) in different study groups. **(C-D)** Data show the percentage (%) of surface expression of MerTK and activation (HLA-DR), pro-resolution (CD163), pro-angiogenesis (Tie-2), tissue (CCR2/CCR5) and lymph-node (CCR7) homing markers of different macrophage subsets in all study groups. Non-parametric (Mann-Whitney) statistical analysis was used. Data presented as median values with interquartile range (IQR). * p< .05, ** p< 0.01, *** p< .001, **** p< .0001. SSC: side scatter, FSC: forward scatter.

2.3.7. MerTK+ hepatic macrophages localize in areas of necrosis in the ALF liver

Having demonstrated an increased proportion of MerTK+ monocytes/macrophages in ALF patients, I used immunohistochemistry, multispectral and confocal imaging in order to delineate the topography and phenotype of these cells in human explant liver tissue, in ALF and pathological controls (PC) (**Fig. 2.9**). Compared to the non-acutely inflamed PC liver tissue, I confirm a numerical increase of MerTK+ intrahepatic cells, of monocyte/macrophage lineage (CD163+), that localize in areas of centrilobular necrosis in ALF (7 vs 35 cells/HPF; p<.0.0001) (**Fig. 2.9A-B),** in keeping with the data on freshly liver-derived hepatic macrophages (**Fig. 2.8C**). Also, the proportion of MerTK+ cells that were derived from infiltrating monocytes (Antoniades et al., 2012), MAC387+MerTK+, was less than 39% in PC liver tissue and similar to circulation-derived cells examined in ALF liver (**Fig. 2.10A).**

Similar to other models of sterile acute liver injury (Dal-Secco et al., 2015; Mori et al., 2009), I demonstrate that hepatic macrophages in ALF form ring-like structures around areas of necrosis **(Fig. 2.9A**). I detected that macrophages populating the outer rim of necrosis show a distinct MerTK+HLA-DR^{high} expression profile that resembles the avidly phagocytic subset described *ex vivo* in ALF patients (**Fig. 2.6C**) whereas cells located in more central and perivenular areas are predominately MerTK+HLA-DR_{low} (**Fig. 2.9A-B**). Enumeration of MerTK+ cells based upon their HLA-DR expression levels, revealed a significant increase in both MerTK+HLA-DR+ and MerTK+HLA-DR- subsets in ALF patients, compared to PC liver tissue (**Fig. 2.9B**). These data are in consistency with the extensively characterized $MerTK^{high}CD163^{high}$HLA-DR_{low} phenotype described ex vivo in ALF (**Fig. 2.1B-E; 2.6B-D; 2.8C-D**).

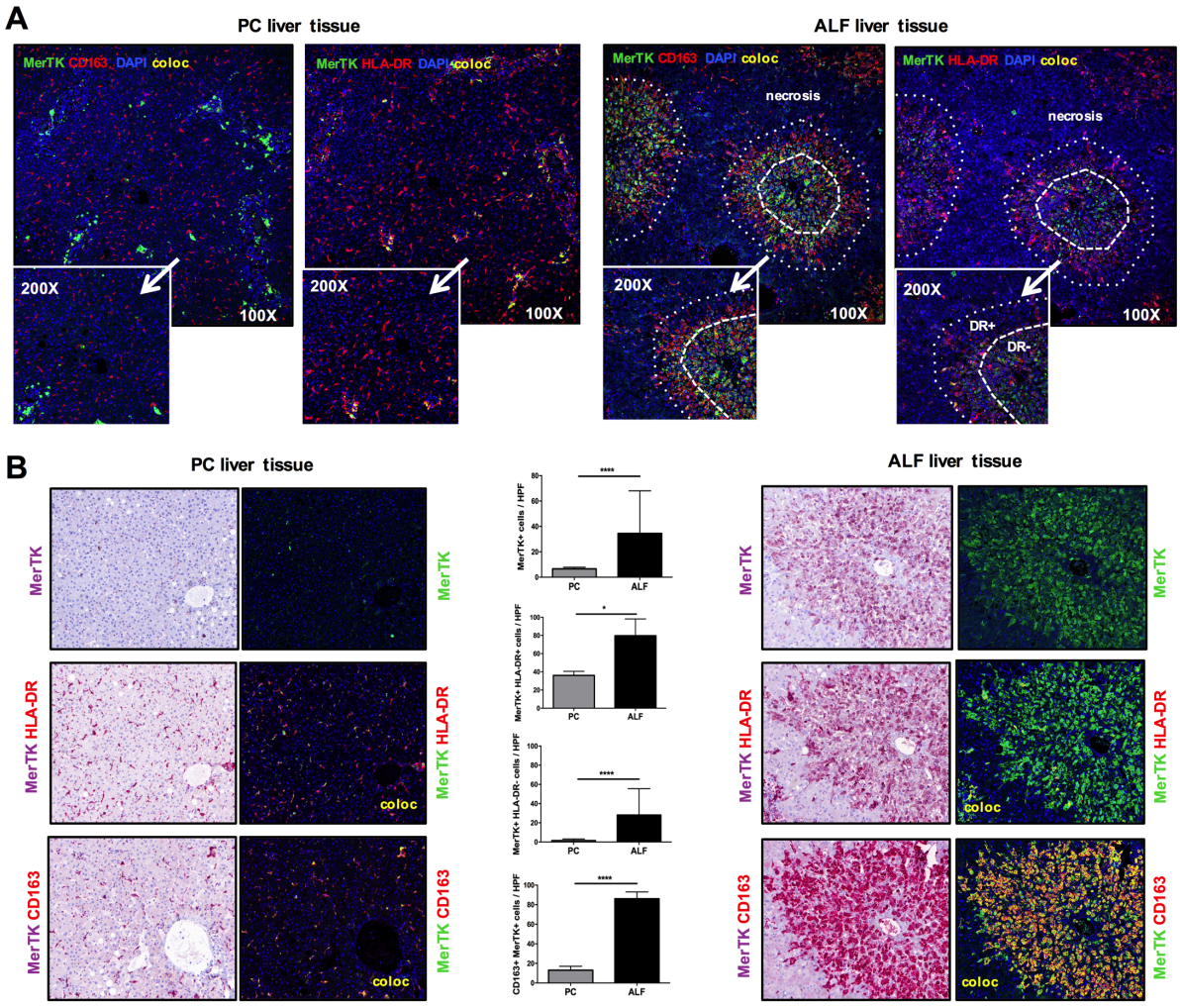

Figure 2.9. Resolution-like MerTK+ hepatic macrophages are expanded in the liver of ALF patients.

(A) Representative confocal images for MerTK (green), CD163 (red), HLA-DR (red), DAPI (blue) and co-localization (yellow) in pathological control (PC, n=4) and ALF (n=6) human liver tissue (100X, inset 200X). **(B)** Representative immunohistochemistry (IHC) images and data showing enumeration of MerTK+, MerTK+HLA-DR± and CD163+MerTK+ cells [positive cells per 5 high-power-field (HPF)] in centrilobular areas of PC and ALF liver tissue, using IHC and multispectral image analysis. RGB images (200X) show MerTK+ (purple), HLA-DR+/CD163+ (red) cells and pseudofluorescent images show MerTK+ (green), HLA-DR+/CD163+ (red) and co-localization (yellow). Non-parametric (Mann-Whitney) statistical analysis was used. Data are expressed as median values with interquartile range (IQR). * p< .05, **** p< .0001.

2.3.8. MerTK+ macrophages are detected in regional lymph-node tissue of ALF patients

During steady state conditions and inflammation, monocytes migrate into tissue compartments and may subsequently home either to regional lymph nodes or return to the circulatory pool, as discussed above (Gray and Cyster, 2012; Kastenmuller et al., 2012). Based on my findings that the expanded MerTK+ monocytes/macrophages in ALF a) have an enhanced ability to cycle in and out of tissue sites (**Fig. 2.7**) and b) express high levels of the lymph node (LN) homing receptor CCR7 (**Fig. 2.1-E; 2.6D; 2.8D**), I used multispectral and confocal imaging in order to detect these cells in LN tissue derived from ALF patients (**Fig. 2.10A-B**).

My results detected a marked expansion, compared to PC, in the number of MerTK+ cells populating sub-capsular sinus and medullary cord areas of peri-portal lymph node tissue derived from ALF patients (68 vs 102 cells/HPF; $p<0.001$) (**Fig. 2.10A-B**). These cells were of monocyte/macrophage lineage (CD163+), with a significant proportion co-expressing the newly-infiltrating monocyte-derived macrophage marker (MAC387) (**Fig. 2.10A**) (Antoniades et al., 2012), as described in explant liver tissue (**Fig. 2.9A-B**). Compared to PC LN tissue, enumeration of MerTK+ HLA-DR-expressing cells revealed decreased numbers of MerTK+HLA-DR+ cells (57 vs 13 cells/HPF; $p<0.0001$) and increased numbers of MerTK+HLA-DR- cells (80 vs 12 cells/HPF; $p<0.001$) in ALF LN tissue (**Fig. 2.10B**). These data support the concept that enhanced tropism of liver and circulation derived MerTK+ cells to regional LN in ALF, may account for the expanded MerTK+HLA-DR_{low} subset, characterized by reduced anti-microbial and efferocytic/phagocytic responses **(Fig. 2.6C**), within the lymphatic compartment, which possibly contributes to the systemic immune dysfunction.

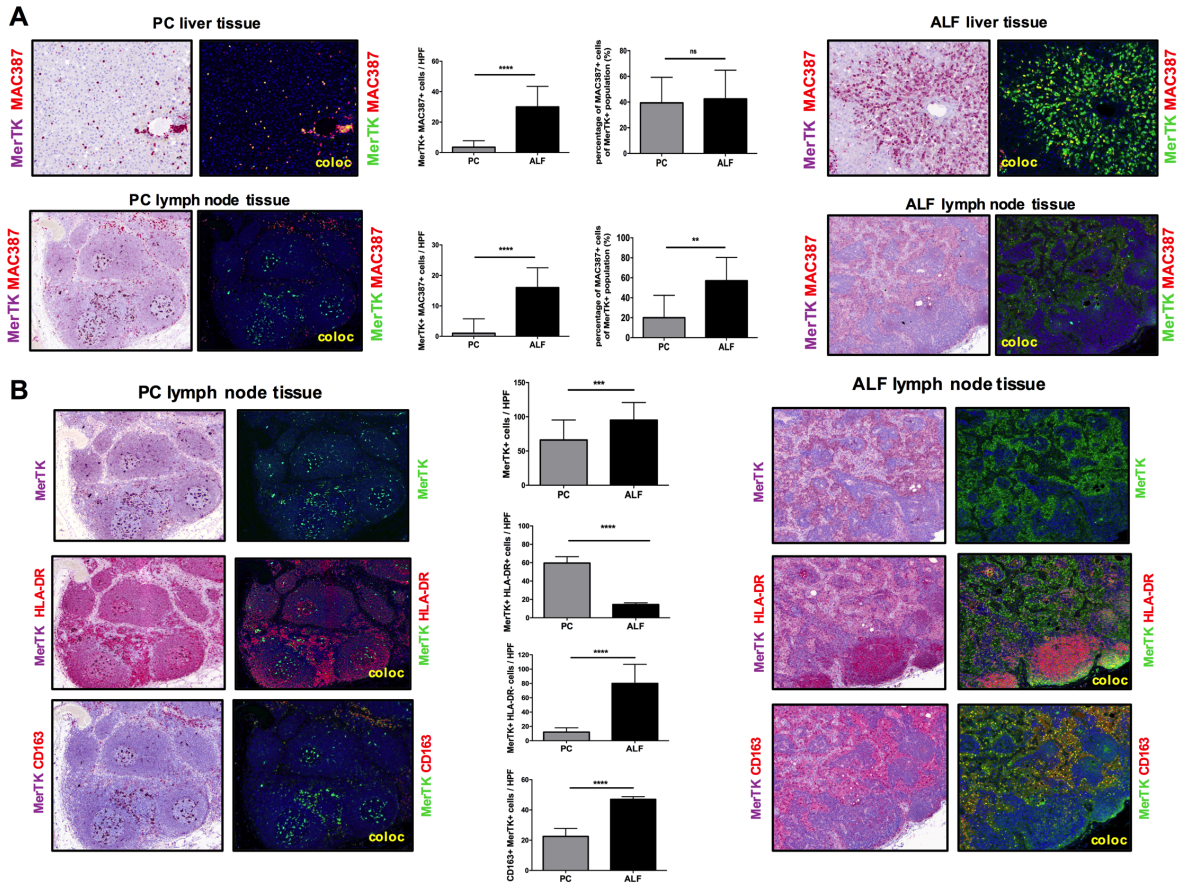

Figure 2.10. Resolution-like MerTK+ macrophages are expanded in the liver and mesenteric lymph nodes of ALF patients.

(A) Representative IHC images and data showing enumeration of MAC387+MerTK+ cells [positive cells per 5 high-power-field (HPF)] and proportion of MAC387+ within the total MerTK+ population in PC (n=4/4) and ALF (n=6/4) explant liver (upper panel) and lymph node (lower panel) tissue, using IHC and multispectral image analysis. RGB images (200X) show MerTK+ (purple) and MAC387+ (red) cells and pseudofluorescent images show MerTK+ (green), MAC387+ (red) and co-localization (yellow). **(B)** Data show representative IHC images and enumeration of MerTK+, MerTK+HLA-DR±, and CD163+MerTK+ cells in mesenteric lymph node tissue from PC (left, n=4) and ALF (right, n=4) patients. For both groups: (left panel) RGB images (100X) showing MerTK+ (purple) and HLA-DR+/CD163+ (red) cells. (right panel) pseudofluorescent images (100X) show MerTK+ (green), HLA-DR+/CD163+ (red) cells and their co-localization (yellow). Non-parametric (Mann-Whitney) statistical analysis was used. Data are expressed as median values with interquartile range (IQR). ** p< 0.01, *** p< .001, **** p< .0001. ns: non-significant.

2.4 Discussion

In this chapter, I identify an expansion of MerTK-expressing (MerTK+) monocytes and macrophages, characterized by resolution-like properties, that are detected in circulatory, hepatic and lymphatic compartments of patients with acetaminophen-induced ALF (AALF). The biological significance of this immune-regulatory subset is highlighted through its strong correlations with physiological and biochemical indices of hepatic injury and with the magnitude of SIRS response. Phenotypic analyses of monocytes and liver-derived macrophages revealed that both have a MerTK^{high}CD163^{high}Tie-2^{high}HLA-DR$_{low}$ phenotype with augmented tissue/lymph-node homing (CCR2^{high}CCR5^{high}CCR7^{high}) characteristics, results that extend previous work in the field (Antoniades et al., 2006; Antoniades et al., 2014; Antoniades et al., 2012; Bernsmeier et al., 2015).

These findings are in line with a recent study in patients with acute-on-chronic liver failure (AoCLF), a form of liver failure that develops in cirrhotic, chronic liver disease, patients (Bernsmeier et al., 2015). Similarly to ALF, patients with AoCLF exhibit monocyte dysfunction, attenuated pro-inflammatory cytokine secretion following microbial challenge and a MerTK^{high}CD163^{high}HLA-DR$_{low}$ anti-inflammatory monocyte phenotype, echoing the one observed in ALF (Antoniades et al., 2014; Antoniades et al., 2012). This work also described an expanded MerTK+ monocyte/macrophage population in circulatory and tissue compartments and proposed that it contributes to the pathogenesis of AoCLF (Bernsmeier et al., 2015).

My data demonstrate marked elevations in the proportion of MerTK+ monocytes in patients with AALF and non-acetaminophen-induced ALF (NAALF). In particular, the highest MerTK levels are detected in AALF, a clinical syndrome characterized by greater severity of acute liver injury and higher degree of hepatic regenerative capability, compared to NAALF cases (Antoniades et al., 2012). Furthermore, peak circulating MerTK levels are detected on admission to the liver unit, which may reflect the extent of hepatic tissue resolution responses following acute hepatocellular necrosis. Future

prospective studies are warranted to assess the utility of MerTK monocyte levels as a mechanistic biomarker of resolution responses and outcome in patients with acute liver injury.

In line with other models of acute tissue injury (Bernsmeier et al., 2015; Choi et al., 2013; Lee et al., 2012c; Wan et al., 2013), functional characterization of MerTK+ monocytes reveals that they possess suppressed innate immune responses to microbial challenge (e.g. TNF-α) but enhanced resolution responses, typified by augmented clearance of cellular/infective material and secretion of anti-inflammatory/tissue-repair mediators (e.g. SLPI) (Antoniades et al., 2006; Antoniades et al., 2012; Bernsmeier et al., 2015). Comparison of the gene expression profiles between MerTK+ and MerTK- cells in steady state and ALF reveal that MerTK+ monocytes have a more differentiated lineage "tissue-like" profile, with increased expression of a number of genes associated with innate and adaptive effector functions. Furthermore, a novel finding in ALF is the identification of two MerTK+ subsets with differential HLA-DR expression that are phenotypically similar but functionally distinct. Compared to MerTK+HLA-DR_{low} cells, MerTK+HLA-DR^{high} monocytes are characterized by higher phagocytic and efferocytic capabilities, with peak circulating levels detected on patients' admission, whereas MerTK+HLA-DR_{low} cells remain persistently elevated following their admission.

Although murine experimental models of acute liver injury provided little evidence that the influx of circulation-derived myeloid cells to areas of necrosis triggers resolution responses (Dambach et al., 2002; Holt et al., 2008; Zigmond et al., 2014), supportive data from human studies is limited and yet remains largely observational (Antoniades et al., 2014; Antoniades et al., 2012). Here, I provide novel insights into the migratory characteristics of circulating monocytes in ALF. First, I show that a significantly high proportion of MerTK+ monocytes and liver-derived hepatic macrophages express tissue (CCR2, CCR5) and lymph-node (CCR7) homing receptors, suggesting they are fully equipped to migrate into tissue compartments. Second, I provide *in vitro* evidence supporting the hypothesis that monocytes in ALF have enhanced trans-endothelial migration capabilities. Particularly, I describe that MerTK+ monocytes efficiently migrate across the hepatic endothelium and subsequently reverse

migrate out of it, bearing the characteristic MerTK^{high}CD163^{high}, results in agreement with the recent findings in AoCLF patients (Bernsmeier et al., 2015).

Furthermore, I reveal that MerTK+ macrophages are significantly expanded and detected within areas of hepatocellular necrosis in human explant liver tissue of ALF patients. These cells form ring-like structures around the areas of injured liver parenchyma with MerTK+HLA-DR^{high} located in the outer rim of necrosis whereas cells in more central and perivenular areas are predominately MerTK+HLA-DR$_{low}$. Of note, these results bear striking similarities with other experimental models of sterile liver injury where the *in situ* reprogramming of monocytes is demonstrated (Dal-Secco et al., 2015; Mori et al., 2009). In particular, the transition of recruited monocytes from outer sites of injured areas towards their center is accompanied by a phenotypic and functional conversion, that is essential to facilitate tissue-repair and wound healing processes (Dal-Secco et al., 2015; Mori et al., 2009). Taken together, I demonstrate in human ALF a preferential recruitment of monocytes, with resolution-like properties, from the circulatory pool to the inflamed liver.

During steady-state or inflammation, monocytes not only migrate into tissues and differentiate into macrophages, but also recirculate out of them homing either to regional lymph nodes or returning back to the systemic circulation (Bellingan et al., 1996; Jakubzick et al., 2013). Of note, lymph-node macrophages serve to filter other tissue and lymph borne pathogens, thus to prevent their systemic translocation and prime innate and adaptive immune responses.(Gray and Cyster, 2012; Kastenmuller et al., 2012). My findings that MerTK+ monocytes/macrophages are characterized *ex vivo* in ALF by increased expression of the lymph-node homing receptor (CCR7) and have an enhanced ability to migrate across hepatic endothelium *in vitro*, may explain why I detected an expansion of circulation-derived MerTK+ cells in both sub-capsular sinus and medullary cord (extrafollicular) areas in the peri-portal mesenteric lymph node from patients with ALF. These data propose that a dynamic circulatory pathway exists, in which MerTK+ cells equipped with enhanced migratory abilities, home from the injured liver to draining regional lymph nodes and/or back into the systemic circulation in ALF (Antoniades et al., 2012; von Andrian and Mempel, 2003; Zigmond et al., 2014). Importantly,

the consequences are likely to be systemic immune suppression and anti-inflammatory responses. Whereas this may help to suppress ongoing systemic inflammation, it will also contribute to the observed immuneparesis and susceptibility to infection in these patients, which is such a devastating complication of ALF.

Recent work from others, using the same i*n vitro* model, indicate that migration of monocytes across hepatic endothelium is a critical process in shaping their phenotype, function and their subsequent fate (Zimmermann et al., 2015). However, I fully recognize the limitations of this assay. I acknowledge that future work is needed in order to assess the migratory characteristics of ALF monocytes *in vivo*. That could be done using the murine model of APAP-induced ALF and other experimental techniques such as live cell imaging by intravital non-invasive microscopy. Furthermore, fluorescent molecular tomography (FMT) could be employed in order to examine the fate of MerTK+ monocytes i*n vivo* during the different phases of APAP-induced acute liver injury, thus allowing to draw more definitive conclusions about the above "re-circulation" hypothesis. Another experiment would be to adoptively transfer MerTK-labelled hepatic macrophages, obtained by flow cytometry based sorting from murine liver tissue at the different phases of APAP-induced acute liver injury, and use the FMT technology to track their fate.

Here, I also detect expanded numbers of MerTK+HLA-DR_{low} cells, in both circulatory and tissue compartments, a subset with impaired both phagocytic and innate immune responses to microbial challenge, during the evolution of human ALF. Given their enhanced lymph-node and tissue homing receptor expression, it is tempting to speculate that these cells are generated following reprogramming within the inflamed liver and subsequently home to extra-hepatic and circulatory compartments where they serve to suppress antimicrobial responses (Kastenmuller et al., 2012). Further work is required to delineate the recruitment and subsequent fate of these MerTK+ myeloid cells during acute liver injury.

To date, the majority of clinical and experimental studies in ALF have focused in drug-induced acute liver injury, in particular AALF, with therapeutic strategies not necessarily being applicable to other cases of ALF. This may be explained by the distinct mechanisms underlying the pathophysiology of liver injury which vary according to the different etiologies of ALF (Tuncer et al., 2013; Wu et al., 2010). In this study, most of the phenotypic and functional analyses in monocytes/macrophages were performed using samples derived from AALF patients. However, the function and role of these cells may differ in other causes of ALF, for example in SALF, an increasingly well-recognized type of ALF with yet unknown etiology (Bernal et al., 2010; Bernal et al., 2013).

SALF is proposed to be caused by a dysregulated immune response to an unidentified hepatotropic or environmental trigger (Donaghy et al., 2013) while it is associated with a lymphocytic infiltrate of effector T cells, NK cells and B cells, suggesting that this drives immune-mediated damage cytotoxic to hepatocytes which culminates in liver necrosis and failure (Tuncer et al., 2013; Wu et al., 2010). I provide recent evidence that SALF is a Th1-cell driven disease, characterized by a macrophage/Th1-lymphocytic rich infiltrate, a profound elevation in circulating and hepatic levels of macrophage and lymphocyte activation markers (Triantafyllou et al., 2014), as it will be discussed below in the present thesis. These histological features and the detection of circulating autoantibodies in SALF are also suggestive of an autoimmune-mediated disorder (Stravitz et al., 2011). Of note, MerTK is crucial for the effective clearance of apoptotic immune cells, thus it has also been implicated in autoimmune disease such as systemic lupus erythematosus and multiple sclerosis (Mukherjee et al., 2016).

Taken together, further work should expand the findings of the present study and investigate the role and function of this prorestorative, MerTK+, monocyte/macrophage subset in SALF or other ALF causes. It would be also interesting to explore this signaling pathway in patients with autoimmune hepatitis who are characterized by impaired immune-regulation and excessive liver inflammation and immune-mediated damage. Future studies, using human and experimental models, could assess the utility of MerTK as an immune-therapeutic target in a variety of hepatic disorders, aimed to quell tissue destructive responses and promote resolution of hepatic inflammation.

CHAPTER 3

3. CHARACTERIZATION OF HEPATIC MACROPHAGES IN MICE WITH ACETAMINOPHEN-INDUCED ACUTE LIVER INJURY

3.1 Background and aims

MerTK is predominantly by monocytes/macrophages and following acute tissue injury it suppresses innate immune responses and by specifically recognizing the exposed phosphatidylserine on apoptotic cells it mediates clearance of apoptotic cells and debris (Rothlin et al., 2015; Zagorska et al., 2014). Experimental studies using models of sterile and pathogen-induced inflammation (e.g. endotoxemia & bleomycin-induced lung injury) show that MerTK loss results in exaggerated immune activation and ineffective resolution, thus leading to excessive inflammatory tissue damage (Camenisch et al., 1999; Lee et al., 2012b; Mukherjee et al., 2016). However, the impact of MerTK on the resolution of hepatic inflammation following acute liver injury is not yet explored.

Hypothesis and aims:

Given my previous human data in ALF (**Chapter 2**), showing a significant expansion of MerTK+ monocytes and tissue macrophages with resolution-like features, I hypothesized that this MerTK+ macrophage subset may also evolve during the time-course of APAP-induced acute liver injury in mice and that is of significant biological relevance for the resolution of acute hepatic inflammation. Hence, in this chapter I aimed to:

- Examine the phenotypic profile of hepatic macrophages isolated from WT mice, following APAP-induced acute liver injury, and determine the MerTK expression of the two distinct (MoMF vs KC) macrophage populations.
- Investigate the biological relevance of MerTK+ macrophages during acute liver injury, by using APAP-treated WT and Mer-deficient ($Mer^{-/-}$) mice and assessing the hepatic myeloid cell infiltrate and biochemical/histological indices of liver injury.

3.2 Materials and methods

3.2.1 Animal treatments and sample collection

All animal experiments were conducted in accordance with the UK laws and with approval of the Home Office and local ethics committees (PPL 70/7578). B6.129-MerTK$^{tm1Grl/J}$ (Mer$^{-/-}$) and wild-type (WT) mice with an identical background (B6.129SF2/J) were obtained from The Jackson Laboratory. Mer$^{-/-}$ and WT mice were age/sex matched (male, 8-10 week-old) for all experiments. Mice were fasted overnight, received an intraperitoneal (i.p.) injection of APAP (300 mg/kg, Sigma-Aldrich, UK) or saline (baseline mice) and were studied at 8, 24 and 48 hours post APAP dose (n=4/group). Groups of mice were culled at the different time points post APAP dosing, being placed under terminal anaesthesia receiving single i.p. injection of 0.2 ml of Pentoject (Centaur Services, UK). Blood was collected from the right ventricle and plasma levels of alanine transaminase were measured using an AU680 chemistry analyzer (Beckman Coulter, UK). The left ventricle was catheterized, an incision was made in the right ventricle and PBS was perfused through the circulation. After visual inspection of blanching of the liver and adequate perfusion, the liver was excised. The median lobe with the gallbladder was separated from the rest of the liver; half was kept in formalin for fixation and half was snap frozen in liquid nitrogen. The remaining liver tissue was kept in cold PBS and was placed on ice to proceed later with the isolation of hepatic immune cells, as described below.

3.2.2 Liver tissue H&E staining and quantification of necrosis

Haematoxylin and eosin staining. Formalin-fixed liver tissue was paraffin-embedded (FFPE) and then was sectioned at 4 μm thickness, using a Leica RM2235 rotary microtome (Leica Biosystems, UK). Liver sections were next stained with haematoxylin and eosin using the following protocol: dewaxing (10 min), rehydration (3 consecutive Et-OH baths with decreasing concentrations followed by a 10

min immersion in distilled water), Harris haematoxylin (5 min), washing (3 min in tap water), acid alcohol (rinse), washing in tap water (3 min), eosin (5 min), washing in tap water (3 min), dehydration (3 different 100% ethanol baths – rinsing), clarification (10 min in xylene), mounting with DPX.

Quantification of necrosis. For the assessment of liver parenchymal injury, H&E stained sections from FFPE liver were imaged and assessment was carried out using ImageJ software. Fifteen low power fields (100X) completely filled with liver were selected, avoiding overlapping and large vessels as much as possible. All micrographs were saved as jpeg. files and randomized. The software was calibrated using a micrograph of a calibration slide taken with the 10× objective. At this magnification and image quality 1mm = 1082.0809 pixels giving each image a field area of 1,236,383.191 μm^2. Large vessels and non-liver parenchyma were hand selected and their area measured using the Analyze → Measure tool. By subtracting this value from the 100× field area we obtained the surface of the liver parenchyma. Then areas of necrosis were hand selected and measured, again by using the Analyze → Measure tool. The measurement was recorded in an Excel spreadsheet. The Edit → Clear Outside tool was used to exclude the non-necrotic liver tissue. Any large vessels or non-liver parenchyma areas within the remaining necrotic areas were again hand selected and measured. Measurements were recorded in the same spreadsheet. The area of necrosis in each field was calculated as the difference between the two recorded measurements. Necrosis was then expressed as percentage within liver parenchyma, on 15 consecutive low power fields (100×) in all groups, using the ImageJ software (Bethesda, Maryland, USA). Micrographs were obtained using a Leica DMR microscope equipped with a Leica DFC300 FX digital camera (Leica Biosystems, UK).

3.2.3 Liver tissue immunohistochemistry and imaging

MPO single epitope enzymatic immunohistochemistry. FFPE tissue was cut at 4 μm and picked up on poly-l-lysine coated slides which were manually stained using a rabbit polyclonal anti-MPO primary antibody (catalog number ab9535, Abcam, UK; dilution 1:50). Slides were dewaxed in xylene, rehydrated, subjected to heat-induced epitope retrieval (HIER) using sodium citrate buffer, pH 6, for

20 minutes, and allowed to cool, followed by 18-hour incubation at 4°C with the primary antibody. The signal was detected using the EnVisionTM G/2 Doublestain System, Rabbit/Mouse (DAB+/Permanent Red) (product number K536111-2, Dako, UK), and visualized with the Vector VIP peroxidase kit (catalog number SH-600, Vector Laboratories, UK). The slides were then dehydrated with alcohol, cleared with xylene and cover slipped with DPX (Leica Biosystems, UK) after hematoxylin counterstaining. Images were captured and processed with a Nikon Eclipse E600 microscope using the Nuance™ 3.0.2 (PerkinElmer, UK) multispectral imaging technology.

3.2.4 Flow cytometry of hepatic immune cells

Following excision, liver tissue was mechanically dissociated and passed through a 100 µm cell strainer. Tissue homogenates were centrifuged at 60x*g* for 1 min to pellet the hepatocytes. The remaining cells in the supernatant were harvested and next purified using density gradient, prepared from Optiprep (Sigma, UK). Mononuclear cells at the interface were collected, washed and red blood cells in the cell pellet were lysed following incubation with ACK lysis buffer (Lonza, Switzerland). Cells were then blocked with normal mouse serum (Sigma, UK) and were phenotypically characterized using antibodies and flow cytometry [F4/80 - AF488 (Serotec, UK); CD11b - PE-CF594, Ly6G - BV605 (BD Biosciences, UK); Ly6C - PE-Cy7, CD 45.2 - eFluor 450, FVD –eFluor 506, MerTK – PE, MHC II - eFluor 780 (eBioscience, UK)]. Cell acquisition was performed on an LSR Fortessa flow cytometer (BD Biosciences, UK) and data analysis using FlowJo 10.1 software (Treestar Inc, Ashland, OR).

3.3. Results

3.3.1. Characterization of the hepatic myeloid cell infiltrate following APAP-induced acute liver injury

Given my data showing a marked expansion of MerTK+ monocytes and hepatic macrophages with resolution-like properties in human ALF (**Chapter 2**), I sought to determine the phenotype of hepatic macrophages isolated from WT mice following APAP-induced acute liver injury. For these experiments, WT mice were administrated intraperitoneally (i.p.) with a single APAP dose (0 hours), and were sacrificed at several time-points (8, 24 and 48 hours) for tissue sampling while untreated mice served as the baseline control group (**Fig. 3.1A**).

I examined the hepatic (CD45+CD11b+) myeloid cell infiltrate of mice administrated with or without APAP using flow cytometry (**Fig. 3.1B-C**). As discussed above (**Chapter 1**), infiltrating monocytes give rise to monocyte-derived macrophages (MoMF), which are separate from the tissue-resident KC population (Scott et al., 2016; Zigmond et al., 2014). Also, following APAP-induced liver injury in mice, $Ly6C^{high}$ monocytes strongly accumulate in the liver and differentiate into MoMF (Holt et al., 2008; Mossanen et al., 2016; Song et al., 2004; You et al., 2013; Zigmond et al., 2014). In line with these murine experimental data, I confirmed by flow cytometry analysis that (CD11b+Ly6G-F4/80+) total hepatic macrophages had a $Ly6C^{high}$MHCII+ expression profile following APAP administration (**Fig. 3.1B**). Compared to baseline levels, peak hepatic CD11b+Ly6G+ neutrophil (8.2 vs 16.6 %; $p< 0.05$) and CD11b+Ly6G-F4/80+ macrophage (20.9 vs 38.5 %; $p< 0.05$) influx, as proportion of total liver CD45+ leukocytes (%), were detected at 24hours post APAP overdose (**Fig. 3.1C**).

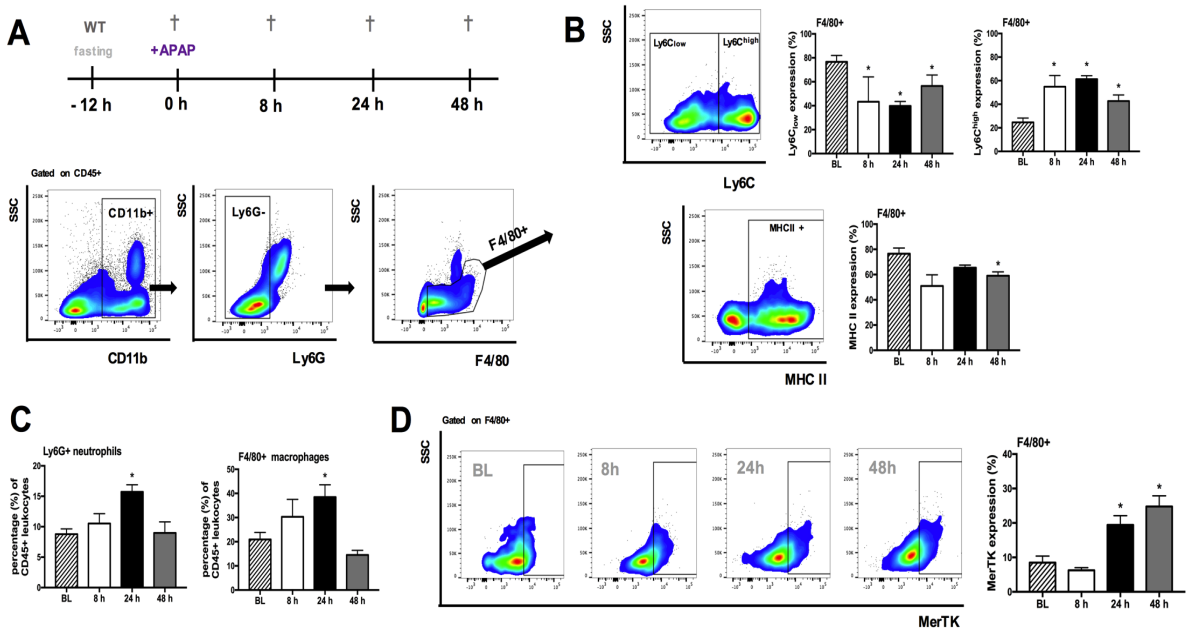

Figure 3.1. MerTK+ hepatic macrophages are expanded during the resolution phase following APAP-induced acute liver injury.

Wild-type (WT) mice dosed with APAP were studied at 8, 24 and 48 hours while untreated mice served as baseline controls (n=4/group). **(A)** Schematic of experimental dosing, representative flow cytometry gating strategy used to identify (CD45+CD11b+Ly6G-) F4/80+ hepatic macrophages and determine their surface marker expression. **(B)** Representative flow cytometry plots and data show Ly6C and MHCclassII expression of F4/80+ macrophages, as determined by flow cytometry. **(C)** (CD45+CD11b+) Ly6G+ neutrophils and (CD45+CD11b+Ly6G-) F4/80+ macrophages as percentage (%) of total liver CD45+ leukocytes, determined by flow cytometry. **(D)** Representative flow cytometry plots and data show MerTK expression of F4/80+ macrophages, as determined by flow cytometry. Non-parametric (Mann-Whitney) statistical analysis was used. Data are presented as median values with interquartile range (IQR). * p< .05. SSC: side scatter.

3.3.2. MerTK+ hepatic macrophages increase during the resolution phase following APAP-induced acute liver injury.

Phenotypic characterization of (CD11b+Ly6G-F4/80+) hepatic macrophages revealed a significant increase in the overall proportion (%) of MerTK-expressing cells at 24 and 48 hours (6.9 vs 19.1 and 26%; both $p< 0.05$) (resolution phase) post APAP administration, compared to baseline levels (**Fig. 3.1D)**. It is previously established that $F4/80^{high}CD11b_{low}$ cells represent the liver-resident KCs while $F4/80_{low}CD11b^{high}$ cells are the MoMFs (Holt et al., 2008; Mossanen et al., 2016; Ramachandran et al., 2012). Therefore, I used this KC vs MoMF macrophage gating strategy and found that WT mice had an increased proportion of MoMFs at 24 hours (56.3 vs 77.1 %; $p< 0.05$) after APAP application while the KC proportion decreased within 24h (42.7 vs 16.3 %: $p< 0.05$) after injury induction (**Fig. 3.2A)**, in keeping with experimental data from other groups (Holt et al., 2008; Mossanen et al., 2016; Zigmond et al., 2014).

Next, I assessed the levels of MerTK expression in hepatic macrophages based on the KC vs MoMF sub-classification. I demonstrate that the increase in MerTK+ cells (**Fig. 3.1D)** is predominantly on the liver-resident KC population (**Fig. 3.2B**). Compared to MerTK+ MoMFs, MerTK+ KCs are characterized by a distinct $MHCclassII^{high}$ $Ly6C_{low}$ expression profile, that was observed at all time points (**Fig. 3.2B**). This phenotype has not only been associated with highly phagocytic (David et al., 2016; Stutchfield et al., 2015) and prorestorative capabilities (Dragomir et al., 2012; Ramachandran et al., 2012), but also bears striking similarities to MerTK+HLA-DR^{high} hepatic macrophages observed in patients with ALF (**Chapter 2**)**.** Furthermore, I show that liver-resident KCs greatly contribute to the increased proportion of MerTK+$MHCclassII^{high}$ macrophages detected at 24 and 48 hours (3.5 vs 11.0 and 17.5 %; both $p< 0.05$), in contrast to the low contribution of MoMFs (0.5 vs 2.2 and 2.5; both $p< 0.05$), compared to baseline levels (**Fig. 3.2C**).

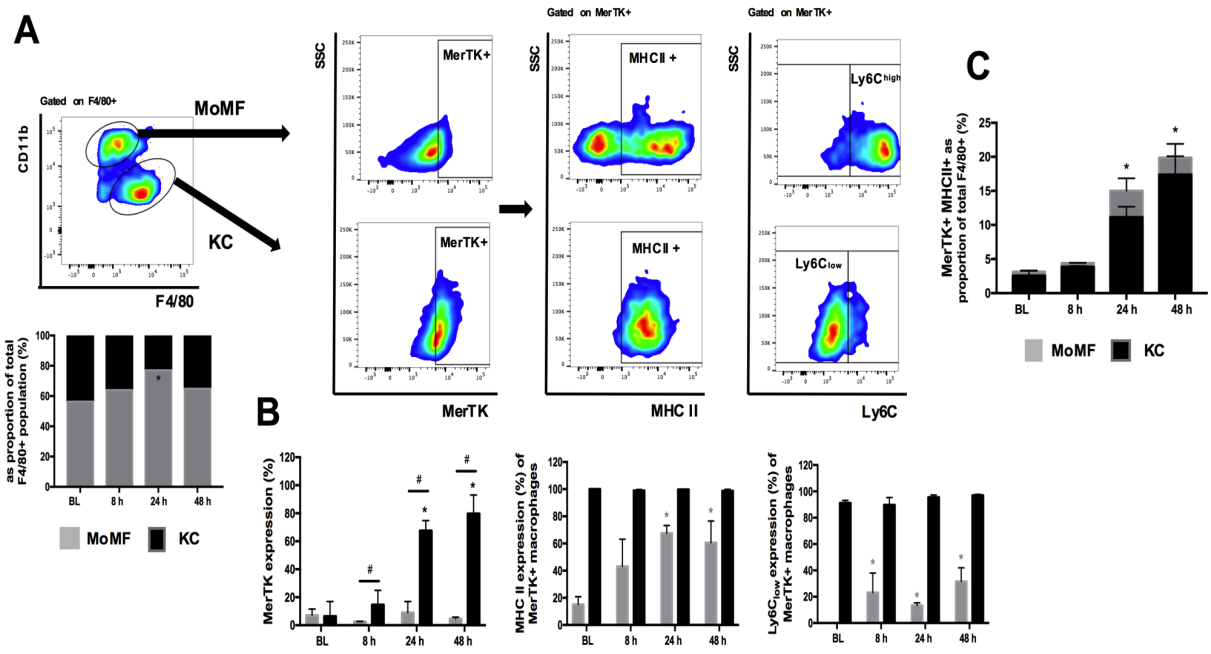

Figure 3.2. Immune-phenotypic characterization of MerTK+ hepatic macrophages during APAP-induced acute liver injury.

Wild-type (WT) mice dosed with APAP were studied at 8, 24 and 48 hours while untreated mice served as baseline controls (n=4/group). **(A)** Representative flow cytometry analysis and gating strategy used to identify ($CD11b_{low}F4/80^{high}$) resident Kupffer cells (KC) and ($CD11b^{high}F4/80_{low}$) monocyte-derived macrophages (MoMF) in order to determine their MerTK expression, and data show their relative proportion (%) within the total F4/80+ macrophage population. **(B)** Further flow cytometry sub-analysis examined the MHC class II and Ly6C expression levels of MerTK+ macrophages in both MoMF (grey bars) and KC (black bars) subsets. **(C)** Data show MerTK+MHCII+ macrophages as proportion of total F4/80+ hepatic macrophages and the relative contribution of MoMF (grey bars) or KC (black bars) within this subset. Non-parametric (Mann-Whitney) statistical analysis was used. Data are presented as median values with interquartile range (IQR). *or $^{\#}$ p< .05. SSC: side scatter.

3.3.3. Mer$^{-/-}$ mice display increased and persistent liver injury following APAP overdose

Having shown that MerTK+ hepatic macrophages are expanded during both human and experimental ALF, I next examined the biological relevance of these cells in APAP-induced acute liver injury by using WT and Mer$^{-/-}$ mice. For these experiments, WT or Mer$^{-/-}$ mice were administrated i.p. with APAP (0 hours) and were sacrificed at several time-points (8, 24 and 48 hours) for tissue sampling while untreated mice served as the baseline control group (**Fig. 3.3A**). I analyzed biochemical and histological indices of liver injury in both study groups, including plasma alanine transaminase (ALT) levels and quantification of liver necrosis (%), respectively (**Fig. 3.3B-D**). My data reveal that APAP administration in Mer$^{-/-}$ mice led to significantly increased and persistent liver injury, compared to APAP-treated WT mice. Specifically, Mer$^{-/-}$ mice exhibited a significantly higher score of hepatic necrosis (%) (32.9 vs 19.8 %; $p< 0.05$) at 8 hours post APAP dose, compared to WT mice (**Fig. 3.3B-C**). Moreover, APAP-treated WT and Mer$^{-/-}$ mice were typified by increased plasma ALT levels at 8 and 24 hours, compared to untreated mice (baseline) in both study groups (**Fig. 3.3D**).

3.3.4 Mer$^{-/-}$ mice show reduced proportion of macrophages and increased numbers of neutrophils following APAP overdose

I demonstrate that Mer$^{-/-}$ mice had a significantly lower proportion of F4/80+ hepatic macrophages, at both steady state and following APAP-induced liver injury, when compared to WT (**Fig. 3.4A**). In addition, using the KC vs MoMF gating strategy described above (Holt et al., 2008; Mossanen et al., 2016; Ramachandran et al., 2012), I reveal that this was attributable to a reduced proportion of the, MHCclassII^{high}Ly6C$_{low}$ (**Fig. 3.2B**) expressing KC population (**Fig. 3.4A-B**). These differences were also reflected in the immune profile of F4/80+ hepatic macrophages of Mer$^{-/-}$ mice, in both KC and MoMF subsets, where these cells were characterized by reduced MHCclassII expression levels (**Fig. 3.4C**). Furthermore, I studied the hepatic neutrophils of both WT and Mer$^{-/-}$ mice. In keeping with the role and importance of MerTK in neutrophil homeostasis and clearance (Hong et al., 2012), Mer$^{-/-}$ mice displayed a significantly higher proportion (Ly6G+) (8 hours, 20.7 vs 9.5 %; $p< 0.05$) (**Fig.**

3.5A) and number of activated (MPO+) neutrophils at peak [(8 hours) 10 vs 3 cells/HPF; $p < 0.05$] and resolution phases [(24 hours) 36 vs 21 cells/HPF; $p < 0.01$] during APAP-induced liver injury, when compared to WT mice (**Fig. 3.5B-C**).

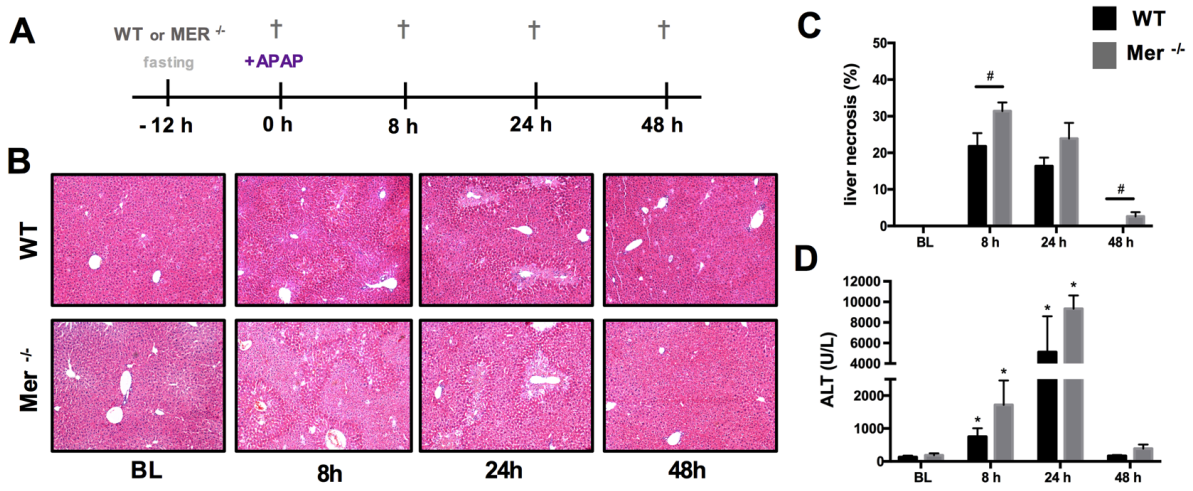

Figure 3.3. Mer$^{-/-}$ mice are characterized by increased and persistent liver injury following APAP overdose.

Wild-type (WT, black bars) and MerTK-deficient (Mer$^{-/-}$, grey bars) mice dosed with APAP were studied at 8, 24 and 48 hours and untreated mice served as baseline controls (n=4/group). **(A)** Schematic of experimental dosing for both study groups. **(B)** Representative images of H&E stained murine liver tissue. **(C)** Quantification of necrosis (%) in murine liver tissue. **(D)** Quantification of plasma alanine transaminase (ALT) levels. Non-parametric (Mann-Whitney) statistical analysis was used. Data are presented as median values with interquartile range (IQR). * or $^{\#}$ P< .05

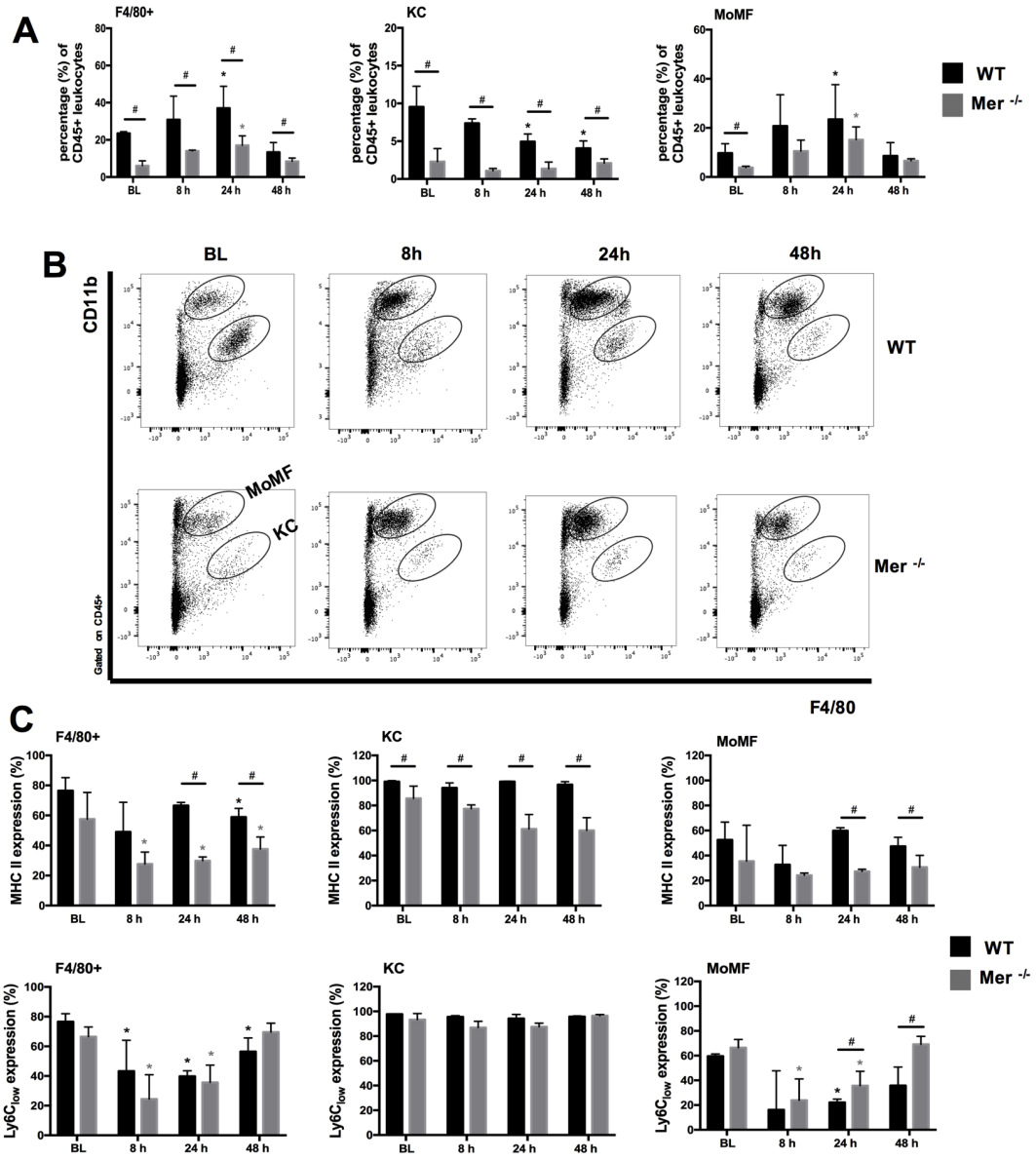

Figure 3.4. Mer$^{-/-}$ mice are characterized by reduced proportion of hepatic macrophages following APAP-induced acute liver injury.

Wild-type (WT, black bars) and MerTK-deficient (Mer$^{-/-}$, grey bars) mice dosed with APAP were studied at 8, 24 and 48 hours and untreated mice served as baseline controls (n=4/group). **(A)** Data show F4/80+ hepatic macrophages, resident Kupffer cells (KC) and monocyte-derived macrophages (MoMF) as percentage (%) of total liver CD45+ leukocytes, determined by flow cytometry. **(B)** Representative flow cytometric analysis from liver CD45+ leukocytes showing the detection of (CD11b^{high}F4/80$_{low}$) MoMF and (CD11b$_{low}$F4/80^{high}) KC. **(C)** Data show the MHC class II and Ly6C$_{low}$ expression of F4/80+ hepatic macrophages, sub-analyzed into the resident KC and MoMF subsets. Non-parametric (Mann-Whitney) statistical analysis was used. Data are presented as median values with interquartile range (IQR). * or # P< .05.

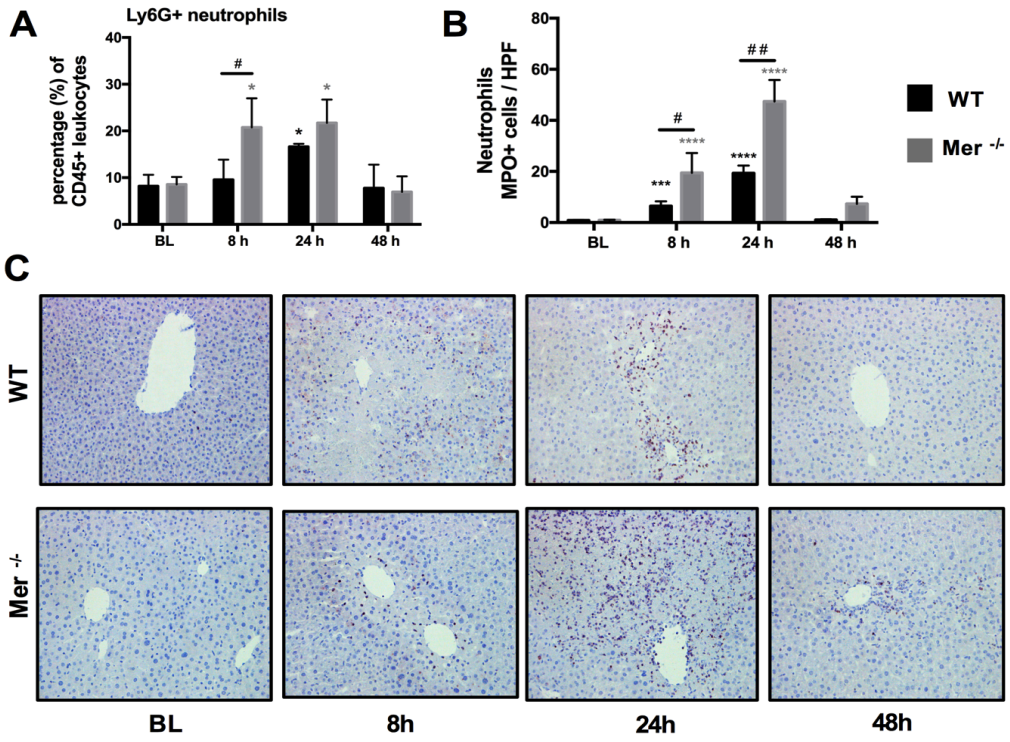

Figure 3.5. Mer$^{-/-}$ mice are characterized by increased proportion of hepatic neutrophils following APAP-induced acute liver injury.

Wild-type (WT, black bars) and MerTK-deficient (Mer$^{-/-}$, grey bars) mice dosed with APAP were studied at 8, 24 and 48 hours and untreated mice served as baseline controls (n=4/group). **(A)** (CD45+CD11b+) Ly6G+ hepatic neutrophils as percentage (%) of total liver CD45+ leukocytes and **(B)** enumeration of MPO+ neutrophils using flow cytometry and immunohistochemistry, respectively. **(C)** Representative images of liver tissue stained for MPO+ (purple) cells (200X). Non-parametric (Mann-Whitney) statistical analysis was used. Data are presented as median values with interquartile range (IQR). * or $^{\#}$ P< .05, $^{\#\#}$ P< .01, *** P< .001, **** P< .0001.

3.4 Discussion

The MerTK receptor signaling pathway is an essential regulator of the immune system, functioning at the interface of both innate and adaptive immunity aimed to restore tissue homeostasis (Lemke and Rothlin, 2008). Following acute tissue injury, MerTK dampens innate immune responses and by recognizing the exposed PtdSer on apoptotic cells it mediates their clearance and promotes resolution of inflammation (Rothlin et al., 2015; Zagorska et al., 2014). Several experimental studies on sterile and pathogen-induced inflammation demonstrate that loss of MerTK results in exaggerated immune activation and ineffective resolution, thus may lead to excessive inflammatory tissue damage.

For instance, in a model of endotoxemia, $Mer^{-/-}$ mice almost uniformly succumbed to septic shock and died as a result of tissue damage mediated by increased TNF-α and IL-1 levels (Camenisch et al., 1999). Bleomycin-induced lung injury was reduced when MerTK macrophage expression was enhanced in mice, that were typified by increased anti-inflammatory mediators such as TGF-β, HGF and reduced TNF-α and IL-1 levels (Lee et al., 2012c). MerTK signaling is also studied in liver inflammation; in a murine model of hepatic ischemia, serum Gas6 levels rose shortly after arterial ligation and western blot analyses after ischemic insult revealed increased hepatic phosphorylated MerTK levels, over Axl, indicating preferential activation of MerTK signaling (Llacuna et al., 2010). However, the temporal evolution of macrophage MerTK expression during acute liver injury and its impact on resolution of hepatic inflammation are not yet explored.

Here, my findings using the murine model of ALF are first to provide novel insights into the identity and role of the MerTK-expressing macrophage population that is significantly expanded in the livers of mice following APAP-induced acute liver injury. I demonstrate that the proportion of MerTK+ hepatic macrophages are specifically increased in the liver-resident Kupffer cells, and not MoMF, population post APAP dose. My data reveal that MerTK+ Kupffer cells exhibit a $MHCclassII^{high}$ $Ly6C_{low}$ expression profile, prior to and during the time course of APAP-induced acute liver injury.

This $Ly6C_{low}$ phenotype is previously associated with prorestorative macrophage properties in murine models of acute and chronic liver injury (Dragomir et al., 2012; Ramachandran et al., 2012). Of note, experiments using flow cytometry, multi-photon intravital microscopy and gene expression analyses have shown that resident Kupffer cells are the dominant phagocytic macrophage population in the liver (David et al., 2016; Stutchfield et al., 2015). Interestingly, the phenotypic data described here in mice bear striking similarities with the expanded pro-phagocytic MerTK+HLA-DR^{high} monocyte and macrophage subset I have identified above in human ALF.

In contrast to KCs, I demonstrate that the MerTK expression levels of the MoMF population do not substantially increase during APAP-induced liver injury. Although MerTK+ MoMFs possess initially a $MHCclassII_{low}Ly6C^{high}$ immune-phenotype at baseline, these cells acquire a $MHCclassII^{high}Ly6C_{low}$ expression profile during the resolution phase of inflammation post APAP administration in mice. These results agree with others revealing that MoMFs upregulate pro-inflammatory proteins such as MHC class II, important for antigen presentation, post APAP dose (Mossanen et al., 2016). This study indicated that $Ly6C^{high}$ MoMFs are distinct from $Ly6C_{low}$ MoMFs and resident KCs, characterized by expression of pro-inflammatory genes, including chemokines, pattern-recognition receptors but also genes involved in liver repair processes (Mossanen et al., 2016).

Accordingly, $Ly6C^{high}$ macrophages show a classically activated pro-inflammatory phenotype typified by increased TNF-α expression, inducible nitric oxide synthase (iNOS) and CCR2, whereas $Ly6C_{low}$ macrophages are alternatively activated, expressing high IL-10 levels, following ALF (Dragomir et al., 2012). As mentioned above, the $Ly6C_{low}$ phenotype is related with prorestorative macrophage functions in liver injury (Dragomir et al., 2012; Ramachandran et al., 2012). Prorestorative $Ly6C_{low}$ hepatic macrophages are key players in resolving fibrosis, shown to accumulate in the liver during the resolution phase following tissue damage, particularly deriving from infiltrating Ly-$6C^{high}$ monocytes/macrophages, following an *in vivo* functional switch during the course of liver injury (Ramachandran et al., 2012). Taken together, the phenotypic transition observed here in MerTK+ MoMFs, from a pro-inflammatory towards a pro-restorative state, during the resolution phase of

APAP-induced acute liver injury is in accord with previous findings on MoMFs and their proposed role in resolving hepatic inflammation (Holt et al., 2008; Zigmond et al., 2014).

The data presented here highlight a significant biological relevance of MerTK+ cells for the effective resolution of hepatic inflammation following ALF, since APAP dosing in MerTK-deficient mice led to markedly increased and persistent liver injury. My results echo recent findings demonstrating that MerTK promotes resolution after acute tissue injury by dampening innate responses and crucially augmenting the clearance of neutrophils (Arandjelovic and Ravichandran, 2015; Choi et al., 2015b; Hong et al., 2012). In a model of sterile zymosan-induced acute inflammation, *in vivo* inhibition using anti-MerTK neutralizing antibody or MerTK deficiency in mice exacerbated local and systemic inflammatory responses, that were associated with reduced abundance of the transcription factors liver-X-receptor LXRα and LXRβ and decreased expression of their target genes in peritoneal macrophages, spleens, and lungs (Choi et al., 2015b). Hence, enhanced MerTK signaling during the recovery phase increases the abundance and activity of LXR to suppress macrophage inflammatory responses (Choi et al., 2015b).

Also, I report a considerably lower proportion of total (F4/80+) hepatic macrophages in $Mer^{-/-}$ mice at both steady state and post APAP dose compared to WT mice. In particular, I demonstrate a significant depletion in prorestorative, $MHCclassII^{high}$ $Ly6C_{low}$, liver-resident KCs, which are protective against acute liver injury (Ju et al., 2002b; You et al., 2013) and exhibit high phagocytic capacity (Stutchfield et al., 2015). This reduction may account for the exaggerated liver injury and inflammation observed in $Mer^{-/-}$ mice post APAP administration. Differences were also detected in the immune profile of hepatic macrophages in $Mer^{-/-}$ animals, as both KC and MoMF subsets were characterized by reduced MHC class II expression levels, which may translate into reduced antigen presentation capacity of macrophages and thereby reducing CD4+ T-cell activation in the liver. To confirm this hypothesis and convince that the lack of the hepatoprotective KCs in $Mer^{-/-}$ mice exaggerates liver injury post APAP, further work is needed to provide evidence that reconstitution of $Mer^{-/-}$ with MerTK+ KCs may revert the phenotype observed in the disease murine model. This could be achieved through bone

marrow transplantation experiments into recipient mice which have previously undergone clodronate-induced liver-resident KC depletion. Furthermore, it would be interesting to investigate if MerTK+ MoMFs and MerTK+ resident KCs have distinct phenotypic and functional profiles throughout the time-course of APAP-induced liver injury. This could be addressed using flow cytometry based sorting of the two subsets, followed by gene expression analyses and time-of-flight mass cytometry (CyTOF) experiments. Furthermore, in view of the role of MerTK in promoting cell survival through activation of anti-apoptotic pathways (Anwar et al., 2009), the above data suggest that activation of MerTK in liver-resident KCs may be important for their differentiation and restoration following acute liver injury. Future studies are warranted to identify the precise mechanisms through which MerTK regulates this process in both human and experimental models of the disease.

The reduction in resident KCs in the liver of $Mer^{-/-}$ mice was detected concomitantly with a reciprocal increase in the proportion/numbers of hepatic neutrophils, importantly not at steady state conditions but only following APAP-induced acute liver inflammation. It is worthy to mention that both MerTK and LXR signaling pathways are shown to coordinately control neutrophil homeostasis (Hong et al., 2012). In this study, *in vitro* and *in vivo* gain- and loss-of-function experiments revealed that LXR positively regulates the efficient clearance of senescent neutrophils by peripheral tissue antigen presenting cells in a MerTK-dependent manner (Hong et al., 2012). In addition, MerTK deficiency was recently associated with reduced LXRα/LXRβ abundance and decreased expression of their target genes in mice (Choi et al., 2015b). Hence, it possible down-regulation of LXR signaling in $Mer^{-/-}$ mice, prior to and post APAP dose, may be responsible for the insufficient clearance of apoptotic neutrophils during liver inflammation and may account for the increased numbers of hepatic detected in the liver of these animals. However, the LXR pathway was not examined in the present study and warrants future work that will perform gene expression analyses of liver tissue from both WT and $Mer^{-/-}$ animals, aimed to assess LXRα/LXRβ levels during the time-course of APAP-induced liver injury. If LXR signaling is down-regulated, it would be interesting to assess if administration of an LXR agonist *in vivo* would protect APAP-treated $Mer^{-/-}$ mice against liver injury.

Together, the experimental data presented and discussed in this chapter indicate that the expanded prorestorative MerTK+ hepatic macrophage population, with enhanced phagocytic capabilities, evolves following acute hepatocellular necrosis, in particular during the resolution phase, and critically serves in driving and promoting the resolution of hepatic inflammation in APAP-induced acute liver injury.

CHAPTER 4

4. LIVER MICRO-ENVIRONMENTAL TRIGGERS INDUCING MERTK^{HIGH} MONOCYTES AND MACROPHAGES IN ACUTE LIVER FAILURE

4.1 Background and aims

SLPI is a small protein secreted by epithelial and myeloid cells that can suppress macrophage pro-inflammatory responses through inhibition of the NF-κB signaling pathway (Ashcroft et al., 2000; Nakamura et al., 2003; Sallenave, 2010; Scott et al., 2011b). Both human and experimental studies have revealed key immune-modulatory functions of SLPI during tissue inflammation, in a variety of diseases including sepsis, asthma and cancer (Majchrzak-Gorecka et al., 2016), as described (**Chapter 1**). SLPI was recently identified as a key micro-environmental modulator of monocytes towards anti-inflammatory responses in human ALF. Compared to HC and CLD, elevated hepatic and circulatory levels of SLPI were detected in ALF that importantly correlated with poor outcome (Antoniades et al., 2014).

Immunohistochemistry-based analysis of ALF liver explant tissue revealed that SLPI is crucially expressed by biliary epithelial cells (BECs) and hepatic macrophages located in areas of necrosis in ALF (Antoniades et al., 2014). Although the involvement of BECs in the pathophysiology of chronic liver disease (CLD) is well documented (Lleo et al., 2014; O'Hara et al., 2013), their role in acute liver injury has not been explored and this study was the first to suggest a potential role for BECs in the pathophysiology of ALF (Antoniades et al., 2014). It is also shown that macrophages secrete SLPI following phagocytosis of apoptotic cells and in response to anti-inflammatory cues such as IL-6 and IL-10 (Ashcroft et al., 2000), that are present in the ALF inflamed liver (Antoniades et al., 2012)

This work also found that monocytes in ALF exhibit an anti-inflammatory phenotype (CD163^{high} HLA-DR$_{low}$) and functional characteristics, typified by reductions in NF-κBp65, TNF-a, and IL-6 levels and preserved IL-10 production following microbial challenge. Culture of healthy monocytes

with ALF liver homogenates, plasma, or rh-SLPI induced monocytes with similar to the *ex vivo* anti-inflammatory characteristics, that were reversed by inhibiting the activity of SLPI (Antoniades et al., 2014). This study proposed that the excessive production of SLPI in the acutely inflamed liver of in ALF is of sufficient magnitude to "spill-over" to the systemic circulation and render monocytes hypo-responsive to microbial challenge, thus may increase the susceptibility to infection encountered in these patients (Antoniades et al., 2014; Possamai et al., 2014a). Furthermore, it was also postulated that SLPI may modulate in an autocrine/paracrine fashion the tissue-resident and newly-infiltrating myeloid cells present in the ALF liver (Antoniades et al., 2014; Possamai et al., 2014b)

Hypothesis and aims:

Given the previous data and proposed role for SLPI in human ALF, I postulated that different micro-environmental triggers within the inflamed ALF liver, including biliary epithelial cells, apoptotic cell debris and SLPI, can re-program both liver-infiltrating monocytes and resident macrophages towards $MerTK^{high}$ resolution-like type. Hence, in this chapter I aimed to:

- Examine the inflammatory cytokine and SLPI secretion levels of BECs isolated from liver tissue of CLD and ALF patients and also to assess their paracrine effects on monocytes.
- Assess the immune-modulatory effects of human apoptotic neutrophils and hepatocytes on monocyte phenotype and function.
- Determine the effects of SLPI on the phenotypic/functional profile of monocytes undergoing migration across hepatic endothelium and of liver-derived hepatic macrophages in culture.

4.2 Materials and methods

4.2.1 Isolation of biliary epithelial cells (BECs) and paracrine effects on monocytes

Biliary epithelial cells (BECs) were isolated from approximately 120-150g of human liver tissue, as previously described (Liaskou et al., 2014). Liver tissue was digested enzymatically with collagenase type 1A (Sigma, United Kingdom), filtered and then was further purified using density gradient centrifugation over 33%/77% Percoll (Amersham Biosciences, United Kingdom). BECs were extracted from the mixed non-parenchymal population via magnetic selection using antibodies against the cholangiocyte-specific receptor HEA-125 (50 μg/mL; Progen Biotechnik, Heidelberg, Germany). Highly pure isolates of HEA-125–positive BECs were next plated in rat-tail collagen-coated flasks and cultured (37 ^{o}C with 5% CO_2) for a week (Liaskou et al., 2014). After first passage, BECs from ALF (n=3) and CLD (n=6) were transferred into rat-tail collagen-coated 6-well plates (500.000 cells/mL) and were cultured (37 ^{o}C with 5% CO_2) up to 24h. Following centrifugation to spin down the cell pellets, BEC culture supernatants were collected at different time points (4h, 8h, and 24h) and were stored at -80^{o}C in order to determine the BEC SLPI and cytokine secretion levels.

Furthermore, BEC culture supernatants (24h) from CLD (n=6) and ALF (n=3) patients were used to culture healthy CD14-isolated monocytes in medium containing 25% BEC supernatants for 48h (37^{o}C with 5% CO_2) which were studied phenotypically and functionally by flow cytometry. In blocking experiments, CD14-isolated healthy monocytes were cultured in medium containing 25% ALF BEC culture supernatants which was pre-incubated with anti-human SLPI neutralizing antibody (α-SLPI) (R&D Systems, UK) (0 and 5 μg/mL) for 1 hour at room temperature, before addition to monocyte cultures, as previously (Antoniades et al., 2014). Phenotype and function of cultured monocytes were assessed by flow cytometry.

4.2.2 Effects of apoptotic neutrophils and hepatocytes on monocytes

Human neutrophils were isolated (2.2.2) and were re-suspended at 10^6 cells/ml in complete medium, labeled with CellTracker Green CMFDA (Life Technologies, UK) (5 μM in serum-free medium, 45 min, dark) and incubated for 20h (37℃ in 5% CO_2) in 24-well plates (Corning, USA) to become apoptotic, as previously described (Zizzo et al., 2012). Human primary hepatocytes (Life Technologies, UK) were thawed using Cryopreserved Hepatocyte Recovery Medium (CHRM) (Life Technologies, UK) and viability was determined using trypan blue staining. Cells were then plated using CHPM medium in a 96-well collagen pre-coated plates at a $0.9x10^6$ cells/ml density for 4h to allow cell adherence, before wash and replacement of CHPM with Williams' E supplemented medium (Life Technologies, UK). Hepatocytes were allowed to further adhere overnight. Cultures were then checked for their cell morphology and monolayer integrity, before being washed and then be supplemented with fresh medium only or medium containing 20 mM acetaminophen (APAP) (Sigma-Aldrich, UK). Annexin V kit (BD Biosciences, UK) was used to determine the percentage of cultured cells that are actively undergoing apoptosis. Next, CD14-isolated healthy monocytes, at 10^6 cells/ml in 24-well plates (Corning, USA) (37^{o}C in 5% CO_2) in fresh complete medium, co-incubated in 1:2 ratio for 4 hours with apoptotic neutrophils or hepatocytes and flow cytometry was used to examine their phenotype.

4.2.3 SLPI effects on migrating monocytes and liver-derived macrophages in culture

Effects of SLPI on migration of healthy monocytes across hepatic endothelium were assessed using the *in vitro* migration assay described above (Bernsmeier et al., 2015; Zimmermann et al., 2015), with the only difference that the collagen plugs were formed containing (rh)-SLPI (0 and 0.5 ug/mL) (R&D Systems, UK). Non-migrated, sub-endothelial and reverse-migrate monocytes were harvested, washed and analyzed further by flow cytometry. In addition, normal liver-tissue derived HMCs and CD14-isolated healthy monocytes were cultured for 48h at 10^6 cells/ml in 24-well plates (Corning, USA) (37^{o}C in 5% CO_2) in fresh complete medium [RPMI-1640 medium containing 10% heat-

inactivated FBS medium and 1% antibiotics (L-glutamine, penicillin, and streptomycin)] (Life Technologies, UK). Effects of recombinant human (rh)-SLPI (R&D Systems, UK) (0 and 0.5 µg/mL) in these culture experiments were assessed. After culture period, cells were harvested, washed with PBS and analyzed for their surface phenotype and function by flow cytometry.

4.2.4 Measurement of SLPI and inflammatory cytokine levels

Human Quantikine ELISA was used for detection of SLPI and HGF levels in HMC and BEC culture supernatants (R&D Systems, UK). The MSD Human Pro-inflammatory 10-plex panel was used to assess (IFN-γ, IL-1β, IL-2, IL-4, IL-6, IL-8, IL-10, IL-12p70, IL-13 and TNF-α) inflammatory cytokine levels as well. ELISA microplates were read using the SoftMax® Pro software (Molecular Devices, USA). MSD plates were read on the Sector Imager 2400 apparatus (Gaithersburg, MD). All experiments were performed in duplicates and according to the manufacturer's instructions.

4.3 Results

4.3.1 Biliary epithelial cells exhibit an anti-inflammatory secretion profile in ALF

Following acute liver injury, biliary epithelial cells (BECs) can modulate the local inflammatory microenvironment by secreting growth factors, cytokines and chemokines that recruit and activate immune cells (O'Hara et al., 2013). Therefore, in order to evaluate the *in vitro* secretion of inflammatory cytokines and mediators by BECs, I isolated BECs from human explant liver tissue and cultured them for up to 24 hours. Compared to CLD, BECs from ALF patients secreted significantly increased levels of SLPI at all time points [(4 hours) 4.405 vs 14756, (8 hours) 4.859 vs 15.108, (24 hours) 6.473 vs 26.912; all pg/ml, $p< 0.0001$] (**Fig. 4.1A)**, in line with previous data showing high intrahepatic SLPI expression by BECs in ALF (Antoniades et al., 2014). Furthermore, I found that compared to CLD, BECs in ALF secreted reduced levels of pro-inflammatory cytokines [TNF-α (6.2 vs 15.2), IL-8 (20.840 vs 39.020) and IL-12p70 (9.3 vs 16.6); all pg/ml, $p< 0.05$] while IL-10 levels were similar between CLD and ALF **(Fig. 4.1B)**. These findings extend the previous human data regarding a skewed anti-inflammatory micro-environmental milieu in the ALF liver (Antoniades et al., 2014; Antoniades et al., 2012).

4.3.2 Biliary epithelial cells induce MerTK+ resolution-like monocytes/macrophages in ALF

I also examined the paracrine effects of BEC-derived supernatants on healthy monocyte phenotype and function. I show that monocytes cultured in ALF BEC-derived supernatants, but not in CLD, were characterized by significantly increased MerTK (82.6 vs 67.5 %; $p< 0.05$) and CD163 (52.8 vs 40; $p< 0.05$) and lower HLA-DR (79.4 vs 68.4 %; $p< 0.05$) expression levels, particularly in the CD14++CD16 subset, as observed *ex vivo* in ALF patients (**Chapter 2**). Also, monocytes cultured in ALF BEC-derived supernatants exhibited reduced secretion of pro-inflammatory cytokines [TNF-α (12.2 vs 27.3 %; $p<0.05$) and IL-6 (29.5 vs 21.2%; $p<0.01$)] following LPS challenge, compared to CLD (**Fig. 4.2A-B**). In order to evaluate whether the SLPI levels derived by ALF BECs serve in

shaping monocyte function, I next cultured healthy monocytes in ALF BEC supernatants that were pre-incubated with anti-SLPI blocking antibody (α-SLPI). I found that inhibition of SLPI's activity in BEC supernatants reversed the up-regulation in CD163 (29.4 vs 16.1 %; $p< 0.05$) and MerTK (49.3 vs 40.8 %; $p< 0.05$) monocyte expression, without affecting HLA-DR levels, while concomitantly increased their TNF-α production (12.7 vs 17.2 %; $p< 0.05$) in response to LPS (**Fig. 4.2C**).

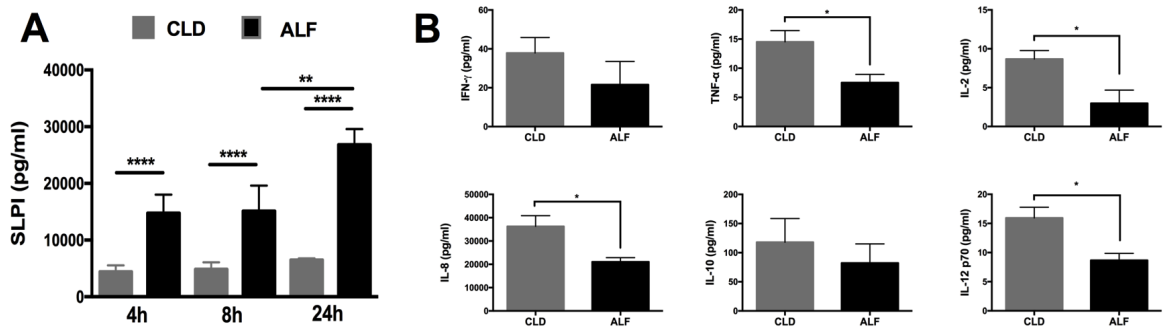

Figure 4.1. Biliary epithelial cells induce monocyte/macrophage MerTK+ resolution responses in a paracrine manner in ALF.

BECs from CLD (n=6) and ALF (n=3) patients were isolated and cultured at different time points (4, 8 and 24 hours). Data show the levels of **(A)** SLPI and **(B)** inflammatory cytokines (pg/ml) that were determined in BEC culture supernatants by ELISA (24h). Non-parametric (Mann-Whitney) statistical analysis was used. Data are expressed as median values with interquartile range (IQR). * P< .05, ** P< 0.01, *** P< .001, **** P< .0001.

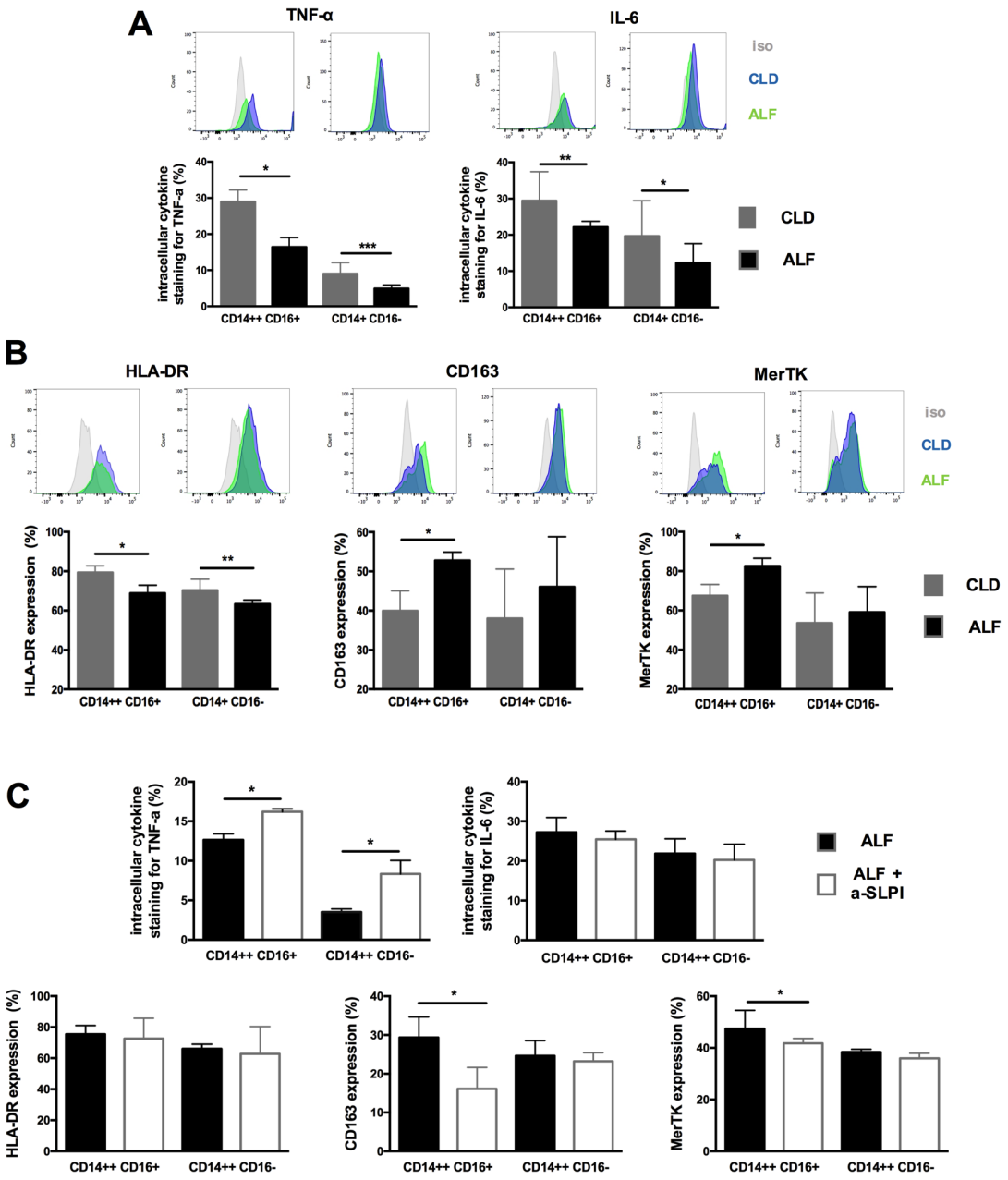

Figure 4.2. Biliary epithelial cells induce monocyte/macrophage MerTK+ resolution responses in a paracrine manner in ALF.

BECs from CLD (n=6) and ALF (n=3) patients were isolated and cultured at different time points (4, 8 and 24 hours). Paracrine effects of ALF and CLD BEC supernatants **(A-B)** and effects of blocking SLPI in BEC supernatants **(C)** were examined on monocytes in culture (n=3 independent experiments). ALF BEC supernatants were pre-incubated with anti-human SLPI neutralizing antibody (+α-SLPI) (0 and 5 ug/mL). Data show LPS-stimulated (100ng/ml, 6h) intracellular cytokine levels, representative flow cytometry histograms and surface marker expression of cultured monocytes. Results expressed as percentage of positive cells. Non-parametric (Mann-Whitney) statistical analysis was used. Data are expressed as median values with interquartile range (IQR). * P< .05, ** P< 0.01, *** P< .001.

4.3.3 Apoptotic cells reprogram monocytes/macrophages towards MerTK+ resolution-like responses

Cell death triggers innate immune activation in ALF where monocytes/macrophages infiltrate necrotic areas to clear cell debris and resolve tissue injury (Antoniades et al., 2012; Possamai et al., 2013; Zigmond et al., 2014) and observational data in humans support this, showing that hepatic macrophages in areas of necrosis contain phagocytosed cell debris (Antoniades et al., 2012). Thus, I hypothesized that monocyte/macrophage reprogramming can occur locally, after exposure and uptake of apoptotic cells and cellular debris that is released following acute liver injury. Therefore, I examined in co-culture experiments the immune-modulatory effects of apoptotic neutrophils and human primary hepatocytes on monocyte phenotype and function (**Fig. 4.3A-B**).

I demonstrate that monocytes are modulated following phagocytosis of either apoptotic neutrophils or hepatocytes. In particular, this functional switch post exposure to apoptotic cells involved acquisition of a MerTK^{high} CD163^{high} HLA-DR+ phenotype (**Fig. 4.3A-B**), characteristic of ALF patients, as shown previously (**Chapter 2**). This change was associated with secretion of higher concentrations of anti-inflammatory and tissue-repair mediators, including SLPI (39 vs 234; pg/ml, $p< 0.001$) and HGF (23 vs 281; pg/ml, $p< 0.001$), and reduced levels of pro-inflammatory (TNF-a, 1.618 vs 1.192; pg/ml, $p< 0.05$) cytokines (**Figure 4.3C**). Taken together, I have identified both biliary epithelial cells and areas of hepatic necrosis containing cell debris in ALF, as key micro-environmental triggers that reprogram monocytes and macrophages towards resolution-like responses within the acutely inflamed liver (Schif-Zuck et al., 2011; Stables et al., 2011).

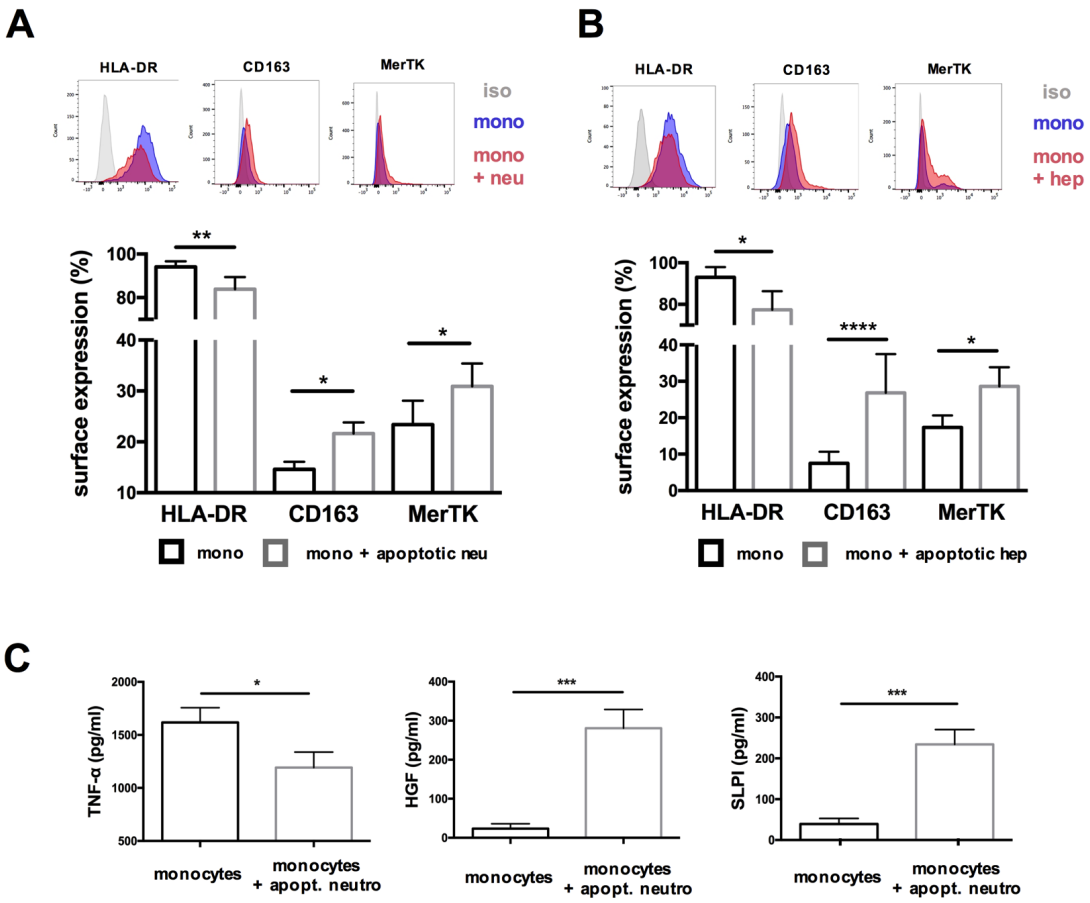

Figure 4.3. Apoptotic cells induce monocyte/macrophage reprogramming towards MerTK+ resolution responses in ALF.

CD14-isolated healthy monocytes co-cultured (4h) in 1:2 ratio with apoptotic neutrophils or apoptotic human primary hepatocytes and their phenotype was determined by flow cytometry (n=3 independent experiments). **(A-B)** Data show representative flow cytometry histograms and total monocyte surface marker expression following co-culture. **(C)** Data show the levels of inflammatory mediators (pg/ml) in monocyte with apoptotic neutrophil co-culture supernatants, as determined by ELISA (n=5). Non-parametric (Mann-Whitney) statistical analysis was used. Data presented as median values with interquartile range (IQR). * P< .05, ** P< 0.01, *** P< .001, **** P< .0001. ns: non-significant. iso: isotype control antibody.

4.3.4 SLPI induces MerTK+ resolution-like monocytes/macrophages

Given the anti-inflammatory role of SLPI on monocytes in ALF (Antoniades et al., 2014) and having identified above the liver micro-environmental triggers of its secretion (**Fig. 4.1-4.3**), here I sought to examine whether SLPI directly induces resolution responses in human circulating monocytes and liver-derived hepatic macrophages, freshly isolated from blood and explant tissue, respectively (**Fig. 4.4**). Several studies in ALF demonstrate that the hepatic macrophage pool is expanded not only due to proliferation of resident Kupffer cells but also through chemokine-dependent recruitment of circulating monocytes (Antoniades et al., 2012; Choi et al., 2015a; Dambach et al., 2002; Zigmond et al., 2014).

I used an *in vitro* migration assay (**Fig. 4.4A-B**) to evaluate the effects of SLPI, present as a micro-environmental mediator, on the phenotype of monocytes migrating across cytokine-stimulated (TNF-α and IFN-γ) hepatic endothelium (Bernsmeier et al., 2015; Zimmermann et al., 2015). I reveal that following trans-endothelial migration, SLPI induced a significant increase in monocyte expression of the pro-resolution markers CD163 [49.3 vs 77.6 (MFI); $p< 0.05$] and MerTK [236.3 vs 303.1 (MFI); $p< 0.05$] selectively within the CD14++CD16+ subset, and only in sub-endothelial cells (**Fig. 4.4B**). Expression levels of HLA-DR remained unaffected while no changes were detected in the monocyte subset frequencies (data now shown) across different migratory compartments and treatments, in line with previous findings (Antoniades et al., 2014).

Culture of normal liver-derived hepatic macrophages with SLPI induced also a selective increase in the expression of CD163 (25.1 vs 43.3 %; $p< 0.05$) and MerTK (32.1 vs 45.9 %; $p< 0.05$), within the CD14++CD16+ subset only (**Fig. 4.4C**) with no changes in HLA-DR expression levels. Consistent with previous data on circulating monocytes (Antoniades et al., 2014), treatment of LPS-stimulated hepatic macrophages with SLPI led to reduced levels of pro-inflammatory cytokines [TNF-α (5.451 vs 3737, $p<0.05$), IL-6 (3.313 vs 2.352, $p<0.05$) and IFN-γ (153 vs 43, $p< 0.01$); all pg/ml], preserved anti-inflammatory/tissue-repair mediator production (IL-10 and TGF-β) and significantly increased

HGF release (190 vs 271; pg/ml, $p < 0.05$) **(Fig. 4.4D)**. Taken together, I identify SLPI as a liver micro-environmental trigger produced by epithelial cells and hepatic macrophages that promotes the development of a monocyte/macrophage phenotype that is associated with dampened innate immune responses.

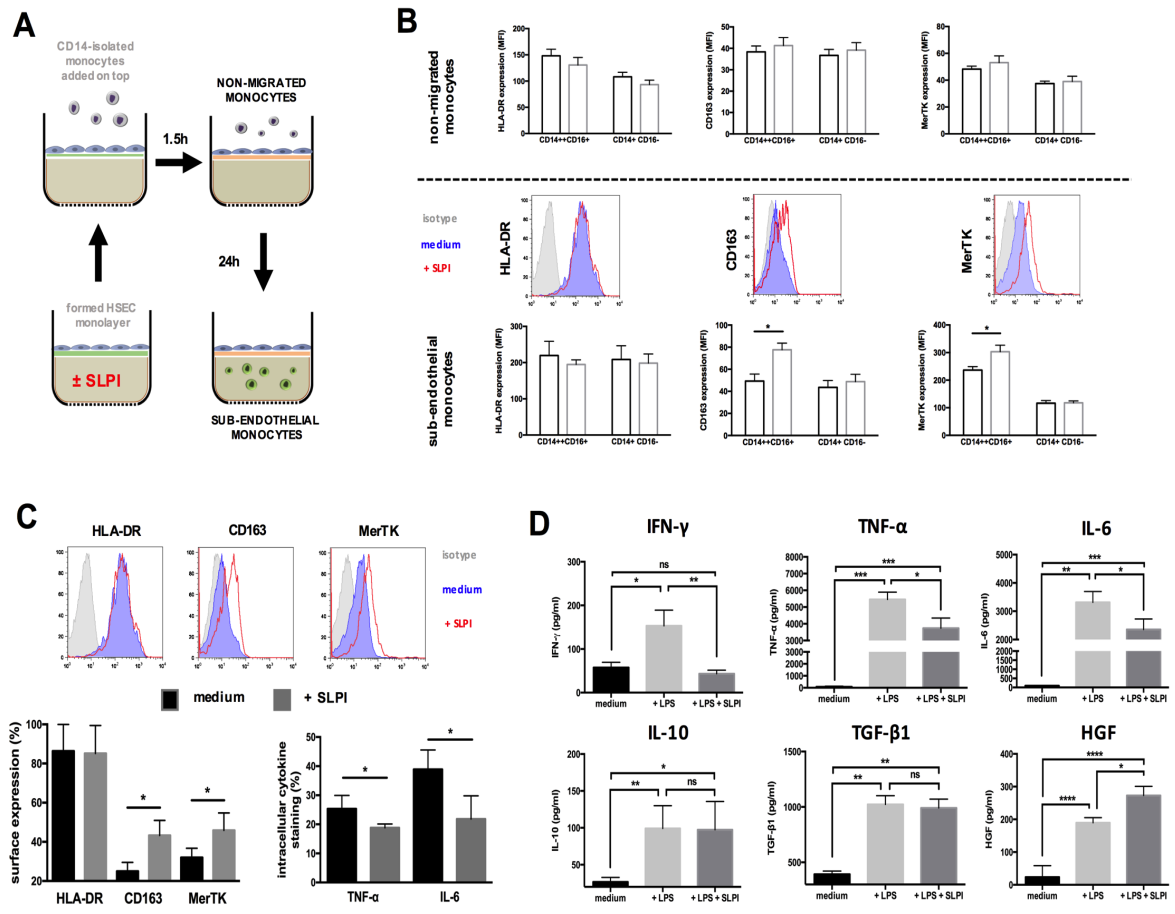

Figure 4.4. SLPI induces a MerTK^{high}HLA-DR^{high} phenotype in monocytes/macrophages.

(A-B) Effects of (rh)-SLPI (0 and 0.5 ug/mL) on monocyte migration across hepatic endothelium were determined (n=3 independent experiments). **(A)** Schematic of migration assay: CD14-isolated monocytes are added on top of a pre-formed hepatic endothelium monolayer; non-migrated monocytes are harvested 1.5 hours after while sub-endothelial monocytes are obtained 24h later. **(B)** Data show HLA-DR, CD163 and MerTK expression levels and representative histograms of the CD14++CD16+ subset, for (top panel) non-migrated and (lower panel) sub-endothelial monocytes. Results expressed as mean fluorescence intensity (MFI). **(C-D)** Effects of (rh)-SLPI (0 and 0.5 ug/mL) on hepatic macrophages isolated from normal liver explant tissue were assessed (n=5). **(C)** Data show representative histograms and surface marker expression in the CD14++CD16+ subset and intracellular cytokine levels in total monocytes following microbial challenge (LPS 100ng/ml). **(D)** LPS-stimulated inflammatory cytokine levels (pg/ml) in hepatic mononuclear cell culture supernatants, as determined by ELISA. Non-parametric (Mann-Whitney) statistical analysis was used. Data presented as median values with interquartile range (IQR). * P< .05, ** P< 0.01, *** P< .001, **** P< .0001. ns: non-significant. iso: isotype control antibody.

4.4 Discussion

In this chapter I have identified three key micro-environmental processes that may take place in the inflamed liver of ALF patients and can drive monocytes/macrophages towards a resolving program. First, the secretion of immune-regulatory/anti-inflammatory molecules (e.g. SLPI) by biliary epithelial cells (BECs). Second, the exposure/phagocytosis of apoptotic immune and epithelial cells and debris that can cause a functional switch in MerTK+ cells from an HLA-DR^{high} to HLA-DR_{low} expression status. Third, the induction of a MerTK+HLA-DR^{high} phenotype by SLPI, which is produced by both BECs and post-phagocytic macrophages, that counter-regulates the production pro-inflammatory cytokines whilst promoting resolution/tissue-repair mediator release

BECs actively sense and react to the inflammatory environment associated with liver injury as well as to bile bioactive and exogenous (microbe-derived, xenobiotic) molecules (Lleo et al., 2014; O'Hara et al., 2013). They respond through the secretion of a repertoire of pro-inflammatory cytokines and growth factors and TGF-β (Hirschfield et al., 2010). These molecules act in an autocrine and/or paracrine manner to mediate proliferation, apoptosis and fibrosis, processes that are associated with the biliary repair response. Secretion of such mediators can also modify the local microenvironment surrounding BECs and leads to activation and recruitment of innate and adaptive immune cells, in order to protect against liver injury and/or infection (O'Hara et al., 2013).

Although the function and involvement of BECs in the pathophysiology of chronic liver disease (CLD), such as primary sclerosing cholangitis (PSC) and primary biliary cirrhosis (PBC), are well documented (Lleo et al., 2014; O'Hara et al., 2013), their role in acute liver injury is not explored. Here, my data highlight a novel immune-regulatory role for BECs in the ALF liver, as I show that they drive monocytes/macrophages towards resolution responses in a paracrine fashion, recapitulating the phenotype detected *ex vivo* in monocytes and hepatic macrophages in ALF. In particular, these epithelial cells induce the development of the prorestorative MerTK+ phenotype and exhibit an anti-

inflammatory cytokine/mediator profile, including the release of high SLPI levels, results that agree with the anti-inflammatory liver micro-environmental milieu in ALF (Antoniades et al., 2014; Antoniades et al., 2012). It would be interesting to assess in future work with co-culture experiments also the direct, cell-to-cell contact, effects of ALF BECs on monocyte phenotype and function, that was not addressed in the present study.

Phagocytosis of apoptotic cells or cell debris can trigger a macrophage functional switch towards an immune-regulatory phenotype, associated with pro-resolution and tissue-repair properties, aimed to maintain immune tolerance and restore tissue homeostasis (Bellingan et al., 2002; Bystrom et al., 2008). Human and experimental models in ALF indicate that cell death is a central trigger of hepatic innate immune activation where monocytes/macrophages infiltrate necrotic areas in the liver in order to clear cell debris and resolve tissue injury (Antoniades et al., 2012; Possamai et al., 2013; Zigmond et al., 2014). In addition, observational data in humans support this hypothesis by demonstrating through scanning electron microscopy in liver tissue that hepatic macrophages in areas of necrosis contain phagocytosed cellular debris (Antoniades et al., 2012). Here, I recapitulate the resolution-like phenotype described *ex vivo* in ALF patients, showing that phagocytosis of both apoptotic neutrophils and hepatocytes induces a macrophage phenotypic switch, typified by loss of HLA-DR and up-regulation of MerTK expression levels. Similar to other models of sterile acute liver injury (Dal-Secco et al., 2015), I demonstrate that MerTK+ hepatic macrophages form ring-like structures around necrotic areas in ALF. MerTK+HLA-DR^{high} cells that possess avid phagocytic and efferocytic capabilities are localized around the rim of areas of necrosis whereas MerTK+ cells that populate more central areas of necrosis bear an HLA-DR$_{low}$ phenotype, similar to the *in vitro* "post-phagocytic" subset observed.

Phagocytosis of cellular debris not only induces a phenotypic switch from an HLA-DR^{high} to HLA-DR$_{low}$ expression status but is also associated with enhanced secretion of immune-regulatory/anti-inflammatory mediators (e.g. SLPI, HGF) and reduced pro-inflammatory cytokines (e.g. TNF-α), in line with data from others (Antoniades et al., 2014; Molnarfi et al., 2015; Odaka et al., 2003a; Park et

al., 2012). These results indicate that, whilst monocytes/macrophages are recruited to sites of acute liver injury to clear necrotic debris, they also undergo local reprogramming following phagocytosis, which enables them to further amplify resolution and tissue-repair processes (Antoniades et al., 2012; Gilroy and De Maeyer, 2015; Holt et al., 2008; Stables et al., 2011; Zigmond et al., 2014). However, this hypothesis is based on *in vitro* findings here, in post-phagocytic monocytes, thus I cannot draw definitive conclusions. Future studies are needed to assess *in vivo* the local phenotypic/functional switch of monocytes/macrophages in areas of necrosis, when they are recruited to sites of liver injury and contact cell debris, using the murine model of APAP-induced ALF and live cell imaging via intravital non-invasive microscopy.

Although anti-inflammatory programs initiated following phagocytosis of apoptotic cells and debris are beneficial in resolving tissue injury and inflammation, they may have the undesirable potential to dampen anti-microbial responses (Fullerton and Gilroy, 2016; Grabiec and Hussell, 2016). My data support this notion where I demonstrate that acute liver injury can reprogram hepatic myeloid cells towards MerTK+ resolution responses, that quell tissue inflammation and promote the clearance of debris. As discussed above, MerTK+ monocytes highly express the lymph-node homing receptor (CCR7) and have enhanced abilities to trans-migrate across hepatic endothelium. Accordingly, both MerTK+HLA-DR^{high} and MerTK+HLA-DR$_{low}$ subsets are significantly elevated in the circulatory, hepatic and crucially in lymphatic tissue compartments in ALF patients. Noteworthy, lymph-node macrophages serve to filter other tissue and lymph borne pathogens in order to prevent their systemic translocation and prime innate/adaptive immune responses (Gray and Cyster, 2012; Kastenmuller et al., 2012). Of note, MerTK+HLA-DR$_{low}$ cells, characterized by suppressed anti-microbial responses, remain persistently elevated following patients' admission and are markedly increased in regional lymph nodes in ALF.

Taken together, one can postulate that the functional re-orientation of immune cells in the inflamed ALF liver may lead to expansion of this immune-suppressive MerTK+ subset not only in the hepatic compartment, but given its augmented migratory characteristics, also in regional lymph nodes. Hence,

this local monocyte/macrophage reprogramming is likely to be of biological significance in AALF that is characterized by systemic immune dysregulation, immuneparesis and a marked susceptibility to secondary infections (Antoniades et al., 2014; Antoniades et al., 2012). However, as argued above, this hypothesis is based only on *in vitro* findings and I fully recognize its limitations. Future work could assess the *in vivo* migratory characteristics of ALF monocytes, where for example by using fluorescent molecular tomography (FMT) the fate of MerTK+ monocytes during the different phases of APAP-induced acute liver injury could be examined, thus allowing to draw more definitive conclusions about the "re-circulation" hypothesis stated above.

CHAPTER 5

5. SLPI SUPPRESSES NEUTROPHILS AND PROMOTES THEIR CLEARANCE VIA MERTK^{HIGH} MONOCYTES AND MACROPHAGES

5.1 Background and aims

Acute tissue inflammation is characterized by the presence of neutrophils which rapidly migrate to sites of infection or injury. Importantly, these leukocytes exert key innate immune functions such as bacterial phagocytosis, release of antimicrobial proteins, inflammatory cytokines and cytotoxic ROS (oxidative burst) while they also form NETs to target and kill bacteria (Sorensen and Borregaard, 2016; Xu et al., 2014). However, exaggerated influx of these leukocytes can be deleterious and may disrupt tissue homeostasis (Headland and Norling, 2015). Accordingly, neutrophils play an essential role in liver inflammation while their excessive recruitment at sites of liver injury contributes fundamentally to the pathogenesis of a variety of liver diseases, including ALF (Kubes and Mehal, 2012).

The key histological feature of resolution of inflammation is the removal of neutrophils from inflamed or injured sites (Headland and Norling, 2015). This is achieved through a network of coordinated and active processes that occur in an overlapping fashion aimed at the restoration of tissue integrity and function (Sugimoto et al., 2016). Neutrophils and monocytes/macrophages are key cellular components of this resolving process following tissue injury. Induction of neutrophil apoptosis and clearance of apoptotic neutrophils (efferocytosis) by macrophages are critical steps for successful resolution of inflammation (Fullerton and Gilroy, 2016; Headland and Norling, 2015).

Hypothesis and aims:

Given the suggested role for SLPI, as a liver micro-environmental mediator in ALF, in modulating liver-resident and newly-infiltrating myeloid cells (Antoniades et al., 2014) and having demonstrated here that it crucially modulates monocytes/macrophages towards MerTK^{high} resolution responses

(**Chapter 4**), I hypothesized that SLPI also modulates the function and survival of neutrophils. Hence, in this chapter I aimed to:

- Investigate if SLPI exerts direct or indirect effects, through MerTK^{high} cells, on the innate immune function and survival (apoptosis) of neutrophils.
- Examine the effects of SLPI on altering the phagocytosis of apoptotic cells capacity in monocytes/macrophages, a critical process for successful resolution of inflammation.

5.2 Materials and methods

5.2.1 SLPI effects on neutrophils

Human neutrophils were isolated as described in Chapter 2 (2.2.2) and cultured for 6h at 10^6 cells/ml in 24-well plates (Corning, USA) (37^oC in 5% CO_2) in fresh complete medium. Effects of recombinant human (rh)-SLPI (R&D Systems, UK) (0 and 0.5 μg/mL) were assessed. For surface and intracellular marker expression, neutrophils were harvested, washed and re-suspended in PBS supplemented with 1% fetal bovine serum. Next, they were incubated with mouse anti-human monoclonal antibody against CD66b (BD Biosciences, UK) for 20 min at room temperature in the dark, and following fixation and permeabilization (BD Biosciences, UK) their TNF-α, IL-6 and IL-8 (BD Biosciences, UK) levels were determined by flow cytometry using intracellular cytokine staining (BD Biosciences, UK) following 6h stimulation with LPS (100 ng/ml) (Sigma-Aldrich, UK).

In addition, effects of SLPI-conditioned and ALF plasma-conditioned monocyte culture supernatants on healthy neutrophil survival and function were examined. CD14-isolated monocytes were cultured for 48h at 10^6 cells/ml in 24-well plates (Corning, USA) ($37o^C$ in 5% CO_2) in fresh complete medium containing (rh)-SLPI (R&D Systems, UK) (0 and 0.5 μg/mL) or 25% human plasma from ALF patients (n=10). The plasma samples were pre-incubated with anti-human SLPI neutralizing antibody (R&D Systems, UK) (0 and 5 μg/ml) for 1 hour at room temperature, as previously described (Antoniades et al., 2014).

5.2.2 Measurement of cytokine levels

Human quantikine ELISA was used to measure IL-6, IL-8 and TNF-α levels (R&D Systems, UK) in neutrophil culture supernatants following 6h stimulation with LPS (100 ng/ml) (Sigma-Aldrich, UK).

ELISA microplates were read using the SoftMax® Pro software (Molecular Devices, USA). All experiments were performed in duplicates and according to the manufacturer's instructions.

5.2.3 Neutrophils apoptosis and oxidative burst

Cell apoptosis kit (BD Biosciences, UK) was used to quantitatively determine the percentage of neutrophils in culture that are actively undergoing apoptosis. Discrimination of total apoptotic cells (Annexin-V+), early apoptotic cells (7-AAD-Annexin-V+) and end stage apoptotic cells (7-AAD+Annexin-V+) was based on 7-AAD and Annexin-V staining. Phagocytosis and oxidative burst. Neutrophil oxidative burst was assessed using the Phagoburst kit (Glycotrope, Germany) by flow cytometry, according to the manufacturer's instructions.

5.2.4 Neutrophil extracellular traps (NETs)

NET formation and extracellular DNA quantification. Neutrophils (2 x 10^5) were stimulated with 25 nM PMA (Sigma-Aldrich, UK) or 100 ng/mL LPS (Sigma-Adlrich, UK) in the absence and presence of (rh)-SLPI (0, and 0.5 μg/mL) (R&D Systems, UK) for 3 hours, 37°C, 5% CO_2. Supernatants were then removed and centrifuged at 2,200x*g* for 10 min. Extracellular DNA content was analyzed by incubation with 5μM SYTOX Green Dye (Life Technologies, UK) for 10 min and fluorometrically examined using a BioTek Synergy HT plate reader (NorthStar Scientific Ltd, UK) at 485/528nm. Samples were calibrated to a λ-DNA (Fisher Scientific, UK) standard curve.

NET visualization by fluorescent microscopy. Neutrophils (2 x 10^5) were seeded onto glass coverslips (VWR International, UK) and were stimulated with 25 nM PMA (Sigma-Adlrich, UK) or 100 ng/mL LPS (Sigma-Aldrich, UK) with and without the presence of (rh)-SLPI (0, and 0.5 μg/mL) (R&D Systems, UK) for 3 hours, 37°C, 5% CO_2 before fixation with 4% paraformaldehyde. Neutrophils were then permeabilised with 0.1% Triton X-100, stained with 1μM SYTOX Green Dye (Life

Technologies, UK), fixed with fluoromount medium and visualized by Zeiss Axiovert 200M microscope (Carl Zeiss Ltd, UK).

5.2.5 Monocyte uptake of apoptotic neutrophils and hepatocytes

Human neutrophils were isolated, as described in (2.2.2), and were re-suspended at 10^6 cells/ml in complete medium, labeled with CellTracker Green CMFDA (Life Technologies, UK) (5 μM in serum-free medium, 45 min, dark) and incubated for 20h (37℃ in 5% CO_2) in 24-well plates (Corning, USA). Annexin V kit (BD Biosciences, UK) was used to quantitatively determine the percentage of neutrophils in culture actively undergoing apoptosis. The composition of neutrophils obtained after incubation was over 70% apoptotic cells, according to Annexin V staining (BD Biosciences, UK).

Huh-7 hepatoma cells were cultured in DMEM medium (containing 1% PenStrep, 1% NEAA, pyruvate, 1% L-glutamine and 10% FBS) (Life Technologies, UK) in vented culture flasks under normal culture conditions (37°C, 5% $C0_2$). Cells were passaged no more than 3 times before used in experiments. Huh-7 cells were seeded on glass cover slips in 24-well plates and allowed to grow until confluent (~$0.2x10^6$). Huh-7 cells were washed with PBS and then were labeled with CellTracker Green CMFDA (Life Technologies, UK) (5 μM in serum-free DMEM, 45 min, dark). Cells were washed again and then were given 300 μl serum-free DMEM containing 20 μM staurosporine (STS) (Sigma-Aldrich, UK), which is shown previously to induce apoptosis in murine hepatocytes (Feng and Kaplowitz, 2002), or equal volume of DMSO. Cells were cultured for 16h, as described (Feng and Kaplowitz, 2002), and then were fixed with 1% PFA (Sigma-Aldrich, UK) in PBS for 5 min, and mounted on microscope slides with Prolong Gold antifade mounting reagent (Life Technologies, UK). Cells were imaged using a Zeiss LSM 780 microscope at x40 magnification using 0.6 zoom or x63 magnification under normal zoom.

Human primary hepatocytes (Life Technologies, UK) were first thawed using Cryopreserved Hepatocyte Recovery Medium (CHRM) (Life Technologies, UK) in order to determine cell count and viability using trypan blue staining. Cells were then plated using CHPM medium in a 96-well collagen pre-coated plates at a $0.9x10^6$ cells/ml density for 4 h to allow cell adherence, before wash and replacement of CHPM with Williams' E supplemented medium (Life Technologies, UK). Hepatocytes were allowed to further adhere overnight. Cultures were then checked for their cell morphology and monolayer integrity before being washed and then be supplemented with fresh medium only or medium containing 20 mM acetaminophen (APAP) (Sigma-Aldrich, UK) (Khamri et al., 2017). After completion of the 24h treatment period, cells were washed and pre-labeled with CellTracker Green CMFDA (Life Technologies, UK) (5 μM in serum-free medium, 45 min, dark) before co-culture with monocytes.

5.3. Results

5.3.1 Effects of SLPI on neutrophil function and survival

Having demonstrated that SLPI induces MerTK^{high}HLA-DR^{high} monocytes/macrophages (**Chapter 4**), I determined whether SLPI can also modulate the function and survival of neutrophils, a critical step to initiate resolution of inflammation (Fullerton and Gilroy, 2016). First, I assessed the numbers of hepatic neutrophils in human liver explant tissue. Compared to pathological controls, I found that ALF patients are characterized by an increased infiltrate of (MPO+) neutrophils (98 vs 336 cells/HPF; $p< 0.05$), with a significantly higher degree of apoptosis (MPO+TUNEL+ cells, 3.7 vs 15.2 %; $p <0.0001$) (**Fig. 5.1A**). Next, I examined in culture the direct effects of SLPI on healthy neutrophil survival and innate immune functions. I found that neutrophil treatment with SLPI did not alter their apoptosis rate (**Fig. 5.1B**) neither impaired their LPS-stimulated pro-inflammatory (TNF-α, IL-6 and IL-8) cytokine secretion (**Fig. 5.1C**) or oxidative burst (**Fig. 5.1D**). However, in line with a recent report describing an inhibitory effect of SLPI on formation of NETs (Zabieglo et al., 2015a), I also show that SLPI, used at physiological concentrations detected in ALF patients (Antoniades et al., 2014), reduced the formation of NETs either without stimulation [73.3 vs 32.4 (DNA, ng/ml), $p< 0.01$] or following stimulation with phorbol-myristate-acetate (PMA) [148.7 vs 77.8 (DNA, ng/ml), $p< 0.05$] or microbial challenge (LPS) (59.2 vs 22.8 (DNA, ng/ml), $p< 0.05$) (**Fig. 5.1E**).

5.3.2 SLPI-induced MerTK^{high} monocytes/macrophages suppress neutrophil function and survival in a paracrine manner

In order to investigate whether SLPI could modulate neutrophils in a paracrine manner through the induction of a MerTK^{high}HLA-DR^{high} monocyte/macrophage phenotype, I evaluated the: (a) direct effects of untreated or SLPI-treated monocytes in co-culture (cell-to-cell-contact) with neutrophils and (b) the indirect (paracrine) effects of soluble mediators released from untreated or SLPI-treated

monocytes, on neutrophil survival and innate immune responses**.** My data here demonstrate that neutrophils co-cultured with SLPI-treated monocytes had a similar survival rate, LPS-stimulated pro-inflammatory cytokine levels and oxidative burst, compared to those co-cultured with untreated monocytes (**Fig. 5.1F**).

However, I found that neutrophils cultured in supernatants derived from SLPI-treated monocytes had unaltered oxidative burst, significantly increased apoptosis (19.1 vs 24.4 %, $p< 0.05$) and decreased PMA-induced NETosis [265.9 vs 157.3 (DNA, ng/ml), $p< 0.05$], compared to neutrophils cultured in supernatants derived from monocytes treated with medium only (**Fig. 5.2A-B**). Taken together, these data suggested a SLPI monocyte-exerted paracrine suppression of neutrophil activation and function. Finally, to determine whether the elevated levels of SLPI, (Antoniades et al., 2014) could account for the observed changes, I repeated these *in vitro* experiments by culturing neutrophils in supernatants derived from ALF-plasma conditioned monocytes following neutralization of SLPI, using an anti-SLPI blocking antibody (α-SLPI). Importantly, I demonstrate that inhibition of SLPI's activity in ALF-derived monocyte supernatants crucially reversed neutrophil apoptosis (26.8 vs 20.5 %, $p< 0.05$) **(Fig. 5.2C)**, augmented PMA-evoked NETosis [173.3 vs 239.3 (DNA, ng/ml), $p< 0.05$)] **(Fig. 5.2D)** and increased LPS-stimulated TNF-α secretion (9.8 vs 15.2 %; $p< 0.05$) **(Fig. 5.2E)**.

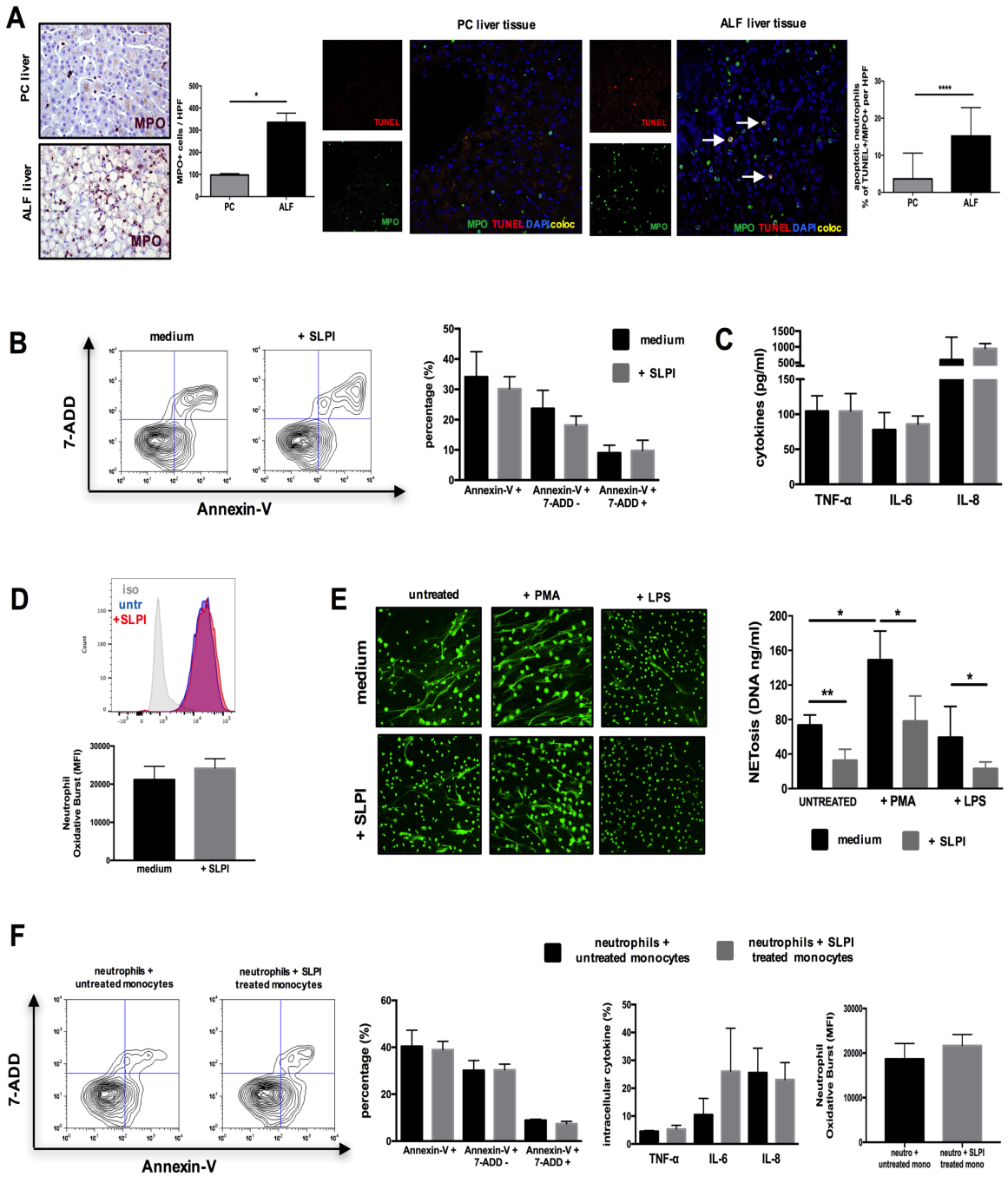

Figure 5.1. Effects of SLPI and SLPI-treated monocytes on neutrophil survival and innate immune responses.

(A) Representative immunohistochemistry (IHC) (left) and confocal (right) micrographs and enumeration of (MPO+) hepatic neutrophils and (MPO+TUNEL+) apoptotic neutrophils in centrilobular areas of pathological control (PC, n=4) and ALF (n=6) human liver tissue. IHC images (400X) show MPO+ (purple) cells. Confocal images show MPO (green), TUNEL (red), DAPI (blue) and co-expression (yellow) (400X). **(B-F)** Effects of (**B-E**) (rh)-SLPI (0 and 0.5 μg/ml) in culture and (**F**) (rh)-SLPI treated (0 and 0.5 μg/ml) monocytes in co-culture, on healthy neutrophil survival and innate immune responses were examined (n=5 independent experiments each). **(B)** Representative Annexin-V/7-AAD staining and percentage of apoptotic neutrophils after 6h culture. **(C)** Levels of LPS-stimulated (LPS 100ng/ml) cytokines (TNF-α, IL-6

and IL-8) detected (pg/ml) in culture supernatants by ELISA. **(D)** Representative histograms of neutrophil oxidative burst in response to *E. coli* after different treatments (3h). Results expressed as mean fluorescence intensity (MFI). **(E)** Neutrophil extracellular trap (NET) formation was determined in culture with or without SLPI after neutrophil stimulation for 3h with PMA (25nM) or LPS (100ng/ml). (left) Representative fluorescence microscopy imaging of NETs using SYTOX Green Dye (1μM). (right) Neutrophil supernatants were stained for extracellular DNA content (ng/ml) with SYTOX Green Dye (5μM) and were fluorometrically examined. (**F**) Effects of (rh)-SLPI treated (0 and 0.5 μg/ml) monocytes were examined in co-culture (4h, 2:1 ratio) with healthy neutrophils. Data show the percentage of apoptotsis, intracellular cytokines (LPS-stimulated TNF-α, IL-6 and IL-8 levels as %) and oxidative burst (MFI) after co-culture, all determined by flow cytometry. Non-parametric (Mann-Whitney) statistical analysis was used. Data are expressed as median values with interquartile range (IQR). * P< .05, ** P< 0.01.

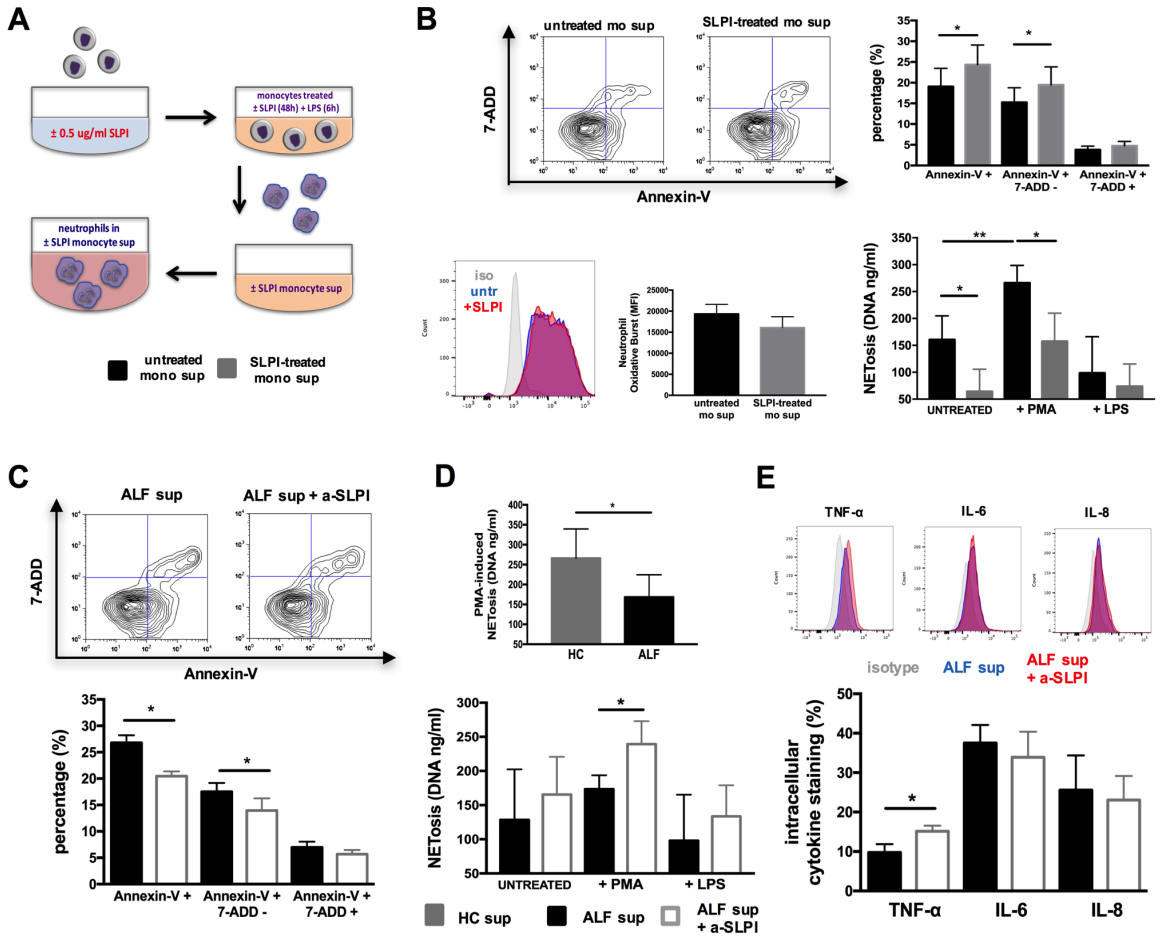

Figure 5.2. SLPI suppresses neutrophils in a paracrine manner through MerTK+ monocytes.

Paracrine effects of untreated or SLPI-treated (0 and 0.5 µg/ml) healthy monocyte supernatants, cultured for 48h, on healthy neutrophil survival and innate immune responses were examined (n=3 independent experiments each). **(A)** Schematic graph describing the paracrine experimental approach undertaken. **(D)** (upper panel) representative Annexin-V/7-AAD staining and percentage of apoptotic neutrophils after 6h culture period, (lower panel, left) representative histograms of neutrophil oxidative burst in response to *E. coli;* results expressed as mean fluorescence intensity (MFI) and (lower panel, right) NET formation (DNA, ng/ml) after stimulation with PMA or LPS of neutrophils cultured (3h) in ± SLPI-treated monocyte supernatants. **(C-E)** Paracrine effects of monocytes on neutrophils were assessed also by blocking the activity of SLPI on monocytes cultured (LPS 100ng/ml for 6h) in ALF plasma (α-SLPI, 5 ug/mL) (n=5 independent experiments each). (**C**) Representative Annexin-V/7-AAD staining and percentage of apoptotic neutrophils (6h), (**D**) NET formation (DNA, ng/ml) after stimulation with PMA or LPS and (**E**) LPS-stimulated (100 ng/ml) intracellular cytokine levels of neutrophils (n=5) cultured in ALF plasma-conditioned monocyte supernatants with or without α-SLPI. Non-parametric (Mann-Whitney) statistical analysis was used. Data are expressed as median values with interquartile range (IQR). * P< .05, ** P< 0.01.

5.3.3 SLPI enhances the efferocytosis of apoptotic neutrophils

Clearance of apoptotic neutrophils by monocytes and macrophages (efferocytosis) is another key step for successful resolution of inflammation (Fullerton and Gilroy, 2016; Headland and Norling, 2015). Having described that SLPI exerts paracrine mediated suppression of neutrophil function, I next aimed to investigate its effect on the process of efferocytosis *in vitro*. For this reason, monocytes previously treated with or without SLPI co-cultured with apoptotic neutrophils and their efferocytosis index was measured using flow cytometry. I demonstrate that similar to MerTK^{high} monocyte analyses in ALF (**Chapter 2**), SLPI-treated monocytes were characterized by significantly increased MerTK expression and by enhanced efferocytosis of CMFDA-labeled apoptotic neutrophils, compared to cells cultured in medium only (37.5 vs 24.5 %; $p< 0.05$) (**Fig. 5.3A-C**). Monocyte treatment with dexamethasone, which is previously shown to augment monocyte/macrophage MerTK expression and efferocytosis (Zizzo and Cohen, 2013), served as a positive control for the assay and not surprisingly led to higher monocyte MerTK expression and efferocytosis index, compared to untreated or SLPI-treated monocytes (**Fig. 5.3A-C**). Furthermore, in separate co-culture experiments, I demonstrate that SLPI did not alter monocyte phagocytosis of CMFDA-labeled staurosporine-treated apoptotic (Feng and Kaplowitz, 2002) Huh7 hepatoma cells (**Fig. 5.3D-E**), when compared to untreated monocytes. Also, treatment of monocytes with SLPI did not affect their phagocytosis of CMFDA-labeled APAP-treated apoptotic/necrotic (Khamri et al., 2017) primary human hepatocytes (**Fig. 5.3F**).

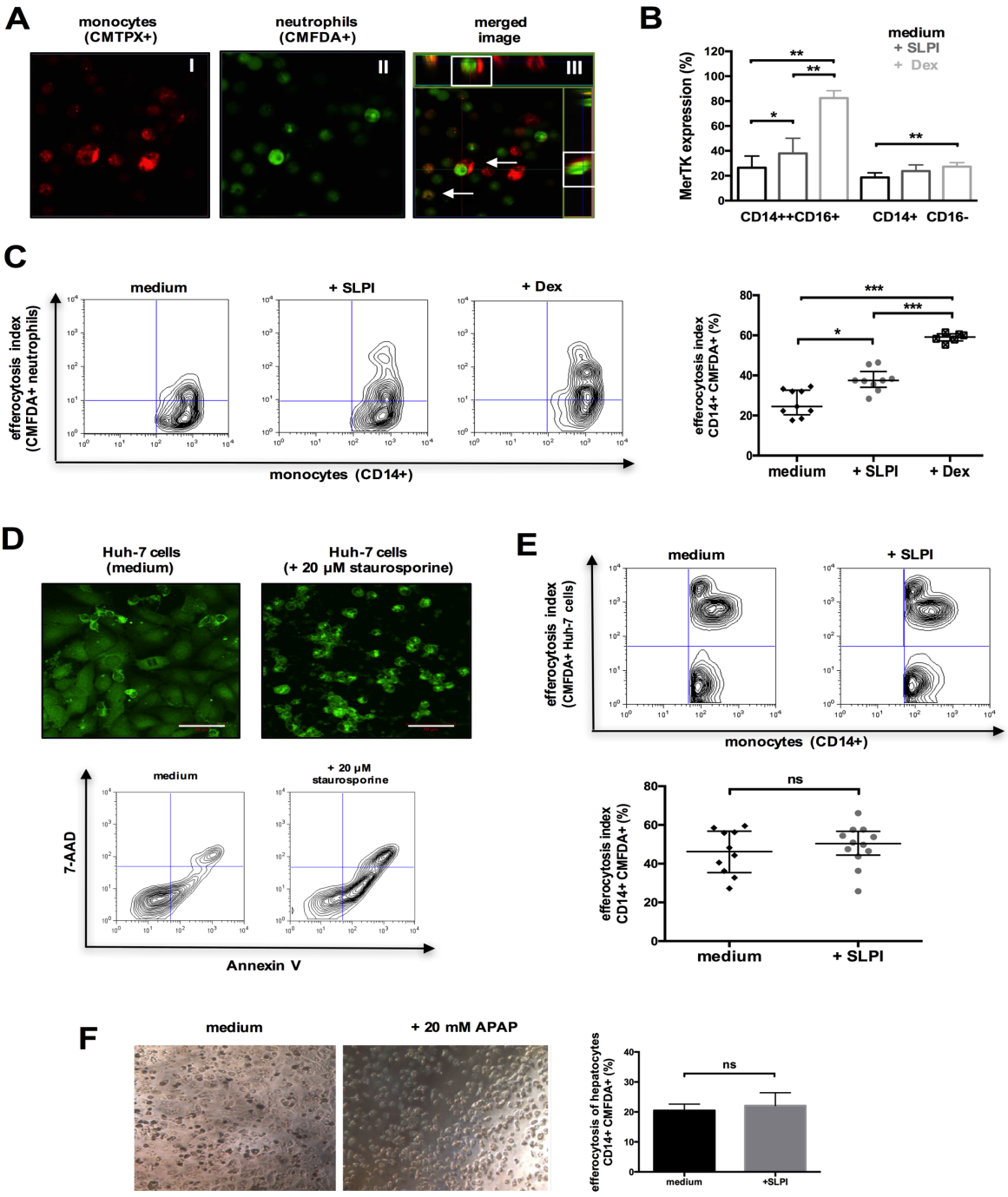

Figure 5.3. SLPI enhances monocyte clearance of apoptotic neutrophils.

CD14-isolated healthy monocytes were pre-cultured with fresh medium, (rh)-SLPI (0.5 µg/ml) or dexamethasone (100nM) and co-incubated with apoptotic neutrophils or Huh-7 hepatoma cells (n=3 independent experiments each). Data show **(A)** Representative confocal microscopy images of CMTPX-labelled monocyte engulfment of CMFDA-labelled apoptotic neutrophils (original magnification x63); merge/z-stack images: arrows showing co-localized/engulfed cells. **(B)** Monocyte MerTK expression in monocyte subsets after 48h culture with different treatments. **(C)** Representative flow cytometry analysis and percentage of monocytes that phagocytosed CMFDA-labeled apoptotic neutrophils. **(D)** Representative confocal microscopy images of CMFDA+ Huh-7 cells treated with or without 20uM STS (50 um, scale bars). **(E)** Representative flow cytometry analysis and percentage of monocytes that phagocytosed CMFDA-labeled (STS-treated)

apoptotic Huh-7 cells. **(F)** (Left) Data show the percentage of CD14-labeled monocytes that phagocytosed CMFDA-labeled APAP-treated (20mM) apoptotic primary hepatocytes (n=2). (Right) Light microscopy images of hepatocytes cultured with/without acetaminophen (APAP, 20mM). Non-parametric (Mann-Whitney) statistical analysis was used. Data are expressed as median values with interquartile range (IQR). * P< .05, ** P< 0.01, **** P< .0001. ns: non-significant.

5.4 Discussion

Recent studies, using the experimental murine model of APAP-induced liver injury, indicate that intrahepatic monocytes/macrophages dampen innate immune activation and promote the clearance of neutrophils following ALF (Arandjelovic and Ravichandran, 2015; Holt et al., 2008; Zigmond et al., 2014). The role of neutrophils during ALF remains controversial, with some experimental studies suggesting these cells promote and others they have no effect on the severity of acute liver injury (Jaeschke et al., 2013). Also, supportive human studies on the role of neutrophils and their clearance during resolution of inflammation following ALF are currently missing. Here, using *in vitro* models of human ALF, I provide novel insights into the role of SLPI as a pro-resolving mediator in the liver micro-environment on shaping the function of myeloid cells and regulating the interplay between them in order to promote resolution of acute hepatic inflammation.

Resolution of inflammation is an active and coordinated anti-inflammatory/pro-resolving program aimed at restoration of tissue homeostasis, integrity and function. Hence, pro-resolving mediators should ideally exert desired pro-resolution actions and fulfill some of the recently established criteria, as further reviewed (Fullerton and Gilroy, 2016; Ortega-Gomez et al., 2013; Sugimoto et al., 2016). Here, I provide evidence that identify SLPI as a pro-resolving mediator in ALF, which fulfills some of these criteria, through induction of MerTK+HLA-DR^{high} monocytes/macrophages, which via both autocrine and paracrine mechanisms: a) counter regulate the production pro-inflammatory cytokines whilst promoting resolution/tissue-repair mediator release b) suppress neutrophil activation and NET formation c) induce neutrophil apoptosis and promote their subsequent clearance.

To date, little is known about the ability of SLPI in modulating apoptosis of myeloid cells. A recent study demonstrated that SLPI can inhibit TNF-α-induced apoptosis in monocytes and this effect is not dependent on its anti-protease activity, since anti-protease deficient variants of SLPI could also inhibit TNF-α-induced apoptosis (McGarry et al., 2015). Another study revealed that SLPI, used at super

physiological concentrations (20–80 mg/mL), induces neutrophil chemotaxis and decreases neutrophil apoptosis rate *in vitro*, without any effects on neutrophil IL-8 secretion or adhesion to fibronectin (Subramaniyam et al., 2011). In contrast to these findings, I show that SLPI, used at the physiological concentrations (0.5 ug/mL) detected in ALF patients (Antoniades et al., 2014), has no direct effect on neutrophil survival. However, I identify a paracrine mechanism of neutrophil suppression whereby SLPI induces neutrophil apoptosis through induction of MerTK^{high} monocytes/macrophages. These results corroborate my analyses of ALF liver tissue where I detect an increased proportion of MerTK+ hepatic macrophages and apoptotic (MPO+TUNEL+) neutrophils within areas of hepatic necrosis (Antoniades et al., 2014).

Furthermore, I show that SLPI promotes the induction of MerTK^{high} monocytes/macrophages whilst concomitantly augments their capacity to efferocytose apoptotic neutrophils, which is critical for the initiation of resolution and tissue-repair processes (Ortega-Gomez et al., 2013; Sugimoto et al., 2016). However, the effect of SLPI on apoptotic cell clearance appears to be highly selective, in view of the fact that SLPI enhances only the efferocytosis of apoptotic neutrophils capacity but does not alter the phagocytosis/clearance of staurosporine-treated apoptotic (Feng and Kaplowitz, 2002) Huh7 cells and APAP-treated apoptotic/necrotic (Khamri et al., 2017) primary hepatocytes, thus providing further support for its importance in hepatic resolution responses. Future work is needed to understand the distinct mechanisms that govern the clearance of parenchymal and non-parenchymal cells following liver injury.

During infectious conditions, in addition to bacterial phagocytosis and antimicrobial protein release, neutrophils form web-like structures composed of decondensed DNA decorated with histones and neutrophil granule proteins, termed NETs, which can trap and kill bacteria (Sorensen and Borregaard, 2016). Peptidyl-arginine-deiminase-4 (PAD4) and NE are essential for NETosis, as NE is shown to cleave histones during this innate process (Papayannopoulos, 2015; Papayannopoulos and Zychlinsky, 2009). Intravital imaging of the liver in mice revealed that following systemic infection, NETs are formed in the liver, in particular within the hepatic sinusoids where they remain anchored to the

vascular wall via von Willebrand factor (VWF), thus enabling the organ to protect the body from infection by efficiently clearing bacteria (Kolaczkowska et al., 2015; McDonald et al., 2012) and viral particles (Jenne et al., 2013). Another study showed that DAMPs released during liver ischaemia-reperfusion result in the formation of NETs, which subsequently exacerbate tissue damage through inflammasome activation (Huang et al., 2015). SLPI, an endogenous inhibitor of NE, was recently described to inhibit both *in vitro* and *in vivo* the formation of NETs (Zabieglo et al., 2015a). Here, I confirm these findings by showing that SLPI, used at physiological concentrations detected in ALF (Antoniades et al., 2014), exerts another pro-resolving function by attenuating *in vitro* NET formation in ALF. Future studies, using human and murine models, might confirm *in vivo* these effects and would allow to examine the systemic and intrahepatic role of NETs during ALF, by addressing if their presence or absence can alter antimicrobial immunity and exaggerate liver tissue injury or promote resolution of liver inflammation following ALF.

CHAPTER 6

6. SLPI INDUCES MERTK+ MACROPHAGES AND PROMOTES HEPATIC RESOLUTION DURING ACETAMINOPHEN-INDUCED ACUTE LIVER INJURY IN MICE

6.1 Background and aims

My previous data indicated that SLPI modulates *in vitro* the function of monocytes/macrophages and alters the activation and survival state of neutrophils, thereby regulating the interplay between those myeloid cells and promoting resolution responses (**Chapters 4 & 5**). In particular, SLPI induces a MerTK+HLA-DR^{high} hepatic macrophage phenotype that suppresses neutrophils and promotes their apoptosis, in a paracrine manner, whilst enhancing their subsequent clearance.

Hypothesis and aims:

Based on the above findings, I hypothesized that SLPI could exert *in vivo* similar pro-resolving effects in mice, following APAP-induced acute liver injury, and promote resolution of hepatic inflammation. Hence, in this chapter I aimed to:

- Investigate the effects of exogenous SLPI administration in WT mice, at both steady state conditions and following APAP overdose, by assessing biochemical and histological indices of acute liver injury.
- Examine if the SLPI-exerted pro-resolving effects could be associated *in vivo* with changes in the hepatic myeloid cell compartment, particularly if it could alter the macrophage phenotype and activation/apoptosis state of neutrophils.

6.2 Materials and methods

6.2.1 Animal treatments and sample collection

All animal experiments were conducted in accordance with the UK laws and with approval of the Home Office and local ethics committees (PPL 70/7578). Wild-type (WT) mice (male, 8-10 week-old, C57BL/6J) were obtained from The Jackson Laboratory. Fasted WT mice received an i.p. injection of APAP or recombinant-human (rh)-SLPI (16.5 μg/kg) (R&D Systems, UK) or APAP plus SLPI at baseline, based on the plasma SLPI levels detected in mice at 8 hours post APAP dose. Mice sacrificed at 24 or 48 hours received a second i.p. injection of saline/SLPI at 8 hours post APAP dose while mice sacrificed at 48 hours received an additional third i.p. injection of saline/SLPI at 24 hours. Groups of mice were culled at the different time points post APAP dosing, being placed under terminal anaesthesia receiving single i.p. injection of 0.2 ml of Pentoject (Centaur Services, UK). Blood was collected from the right ventricle and plasma levels of alanine transaminase were measured using an AU680 chemistry analyzer (Beckman Coulter, UK).

6.2.2 Liver tissue H&E staining and quantification of necrosis

Haematoxylin and eosin staining. Formalin-fixed liver tissue was paraffin-embedded (FFPE) and then was sectioned at 4 μm thickness, using a Leica RM2235 rotary microtome (Leica Biosystems, UK). Liver sections were next stained with haematoxylin and eosin using the following protocol: dewaxing (10 min), rehydration (3 consecutive Et-OH baths with decreasing concentrations followed by a 10 min immersion in distilled water), Harris haematoxylin (5 min), washing (3 min in tap water), acid alcohol (rinse), washing in tap water (3 min), eosin (5 min), washing in tap water (3 min), dehydration (3 different 100% ethanol baths – rinsing), clarification (10 min in xylene), mounting with DPX. *Quantification of necrosis*. For the assessment of liver parenchymal injury, H&E stained sections from FFPE liver were imaged and assessment was carried out using ImageJ software, as previously described in Chapter 3 (3.2.2).

6.2.3 Liver tissue immunohistochemistry and imaging

MPO single epitope enzymatic immunohistochemistry. FFPE tissue was cut at 4 μm and picked up on poly-l-lysine coated slides which were manually stained using a rabbit polyclonal anti-MPO primary antibody (catalog number ab9535, Abcam, UK; dilution 1:50). Slides were dewaxed in xylene, rehydrated, subjected to heat-induced epitope retrieval (HIER) using sodium citrate buffer, pH 6, for 20 minutes, and allowed to cool, followed by 18-hour incubation at 4°C with the primary antibody. The signal was detected using the EnVisionTM G/2 Doublestain System, Rabbit/Mouse (DAB+/Permanent Red) (product number K536111-2, Dako, UK), and visualized with the Vector VIP peroxidase kit (catalog number SH-600, Vector Laboratories, UK). The slides were then dehydrated with alcohol, cleared with xylene and cover slipped with DPX (Leica Biosystems, UK) after hematoxylin counterstaining. Images were captured and processed with a Nikon Eclipse E600 microscope using the Nuance™ 3.0.2 (PerkinElmer, UK) multispectral imaging technology.

*TUNEL/MPO double-epitope fluorescent immunostaining***.** FFPE tissue cut at 4 μm using a Leica RM2235 rotary microtome (Leica Biosystems, UK) was picked up on poly-L-lysine coated slides which were manually stained using an apoptosis staining kit (# C10618, Molecular Probes, UK), according to manufacturer's instructions, followed by an immunofluorescent stain using a rabbit polyclonal anti-MPO antibody (# ab9535, Abcam, UK; dilution 1:25). After TUNEL staining, the slides were incubated overnight at 4°C with the anti-MPO antibody. The second day the slides were incubated for 2 hours at room temperature with a biotinylated goat-anti-rabbit secondary antibody (# E043201-8, Dako, UK; dilution 1:100). This was followed by a 1hour incubation at room temperature with Alexa Fluor 488-conjugated streptavidin (Life Technologies, UK; dilution 1:100). All slides were counterstained with 4′,6-diamidino-2-phenylindole (DAPI) (# D1306, Life Technologies, UK), cover slipped using a fluorescence mounting medium (# S302380-2, Life Technologies, UK) and imaged using a Zeiss LSM800 confocal microscope (Zeiss, UK).

6.2.4 Flow cytometry of hepatic immune cells

Following excision, liver tissue was mechanically dissociated and passed through a 100 μm cell strainer. Tissue homogenates were centrifuged at 60x*g* for 1 min to pellet the hepatocytes. The remaining cells in the supernatant were harvested and next purified using density gradient, prepared from Optiprep (Sigma, UK). Mononuclear cells at the interface were collected, washed and red blood cells in the cell pellet were lysed following incubation with ACK lysis buffer (Lonza, Switzerland). Cells were then blocked with normal mouse serum (Sigma, UK) and were phenotypically characterized using antibodies and flow cytometry [F4/80 - AF488 (Serotec, UK); CD11b - PE-CF594, Ly6G - BV605 (BD Biosciences, UK); Ly6C - PE-Cy7, CD45.2 - eFluor450, MerTK - PE (eBioscience, UK)]. Cell acquisition was performed on an LSR Fortessa flow cytometer (BD Biosciences, UK) and data analysis using FlowJo 10.1 software (Treestar Inc, Ashland, OR).

6.3. Results

6.3.1 SLPI administration reduces indices of liver injury in mice with APAP-induced acute liver injury

Having shown that SLPI acts as pro-resolving mediator in human ALF (**Chapters 4 & 5**), I aimed to assess *in vivo* the effects of exogenous SLPI administration in WT mice, following APAP-induced acute liver injury, regarding the resolution of hepatic inflammation. For these experiments, APAP-treated WT mice were given SLPI (or saline) at 0 and 8 hours post APAP dose and were sacrificed at 24 hours for tissue sampling while untreated mice served as the baseline controls. WT mice that were sacrificed at 48 hours were additionally dosed with SLPI (or saline) at 24 hours post APAP dose (**Fig. 6.1A)**.

I first analyzed biochemical and histological indices of liver injury, including plasma ALT levels and quantification of hepatic necrosis (%), respectively. Here, I demonstrate that administration of SLPI alone did not induce any liver injury in mice, compared to the control animals, either at 24 or 48 hours post SLPI dose, as indicated by their similar ALT levels and no detection of liver necrosis in these study groups (**Fig. 6.1A-C**). My results also showed comparable levels of those indices at the 24-hour time point, between APAP-treated and APAP plus SLPI treated mice (**Fig. 6.1A-C**). However, SLPI administration in APAP-mice led to a significant reduction in both ALT levels (290 vs 102; U/L, $p< 0.05$) and score/percentage of hepatic necrosis (4.2 vs 1.9 %, $p< 0.05$) during the resolution phase (48 hours) following APAP-induced acute liver injury (**Fig. 6.1A-C**).

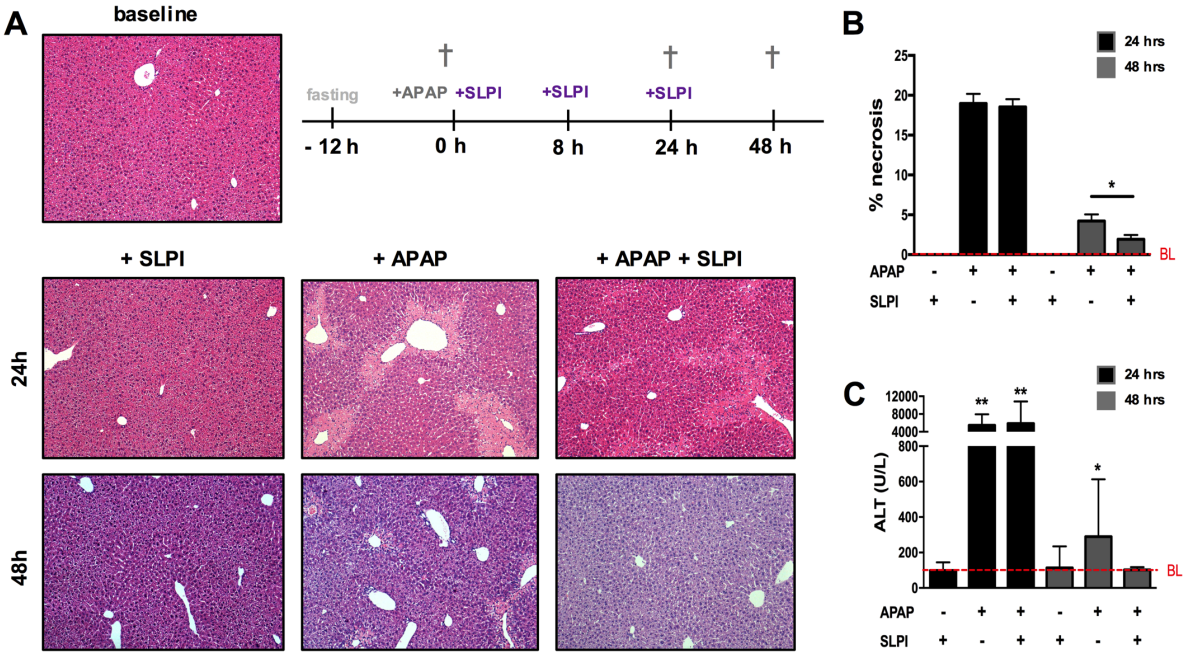

Figure 6.1. SLPI administration in mice reduces indices of liver injury following APAP overdose.

Wild-type (WT) mice were dosed with SLPI (-/+) or APAP (+/-) or APAP plus SLPI (+/+) while untreated mice (-/-) served as baseline controls (n=6/group). Mice were studied at baseline (red, BL), 24 hours (black bars) and 48 hours (grey bars). **(A)** Schematic of experimental dosing for all study groups and representative images of H&E stained livers. **(B)** Quantification of necrosis (%) murine liver tissue. **(C)** Quantification of plasma alanine transaminase (ALT) levels. Non-parametric (Mann-Whitney) statistical analysis was used. Data are presented as median values with interquartile range (IQR). * P< .05, ** P< 0.01.

6.3.2 SLPI administration in mice induces MerTK+ hepatic macrophages *in vivo*

In order to investigate if SLPI induces prorestorative macrophages *in vivo*, as the *in vitro* human data describe above, here I phenotypically characterized the hepatic macrophages isolated from WT mice exogenously dosed with SLPI a) at steady-state conditions (no APAP treatment) and b) following APAP-induced acute liver injury (with or without SLPI treatment) (**Fig. 6.2**). Analysis of the hepatic non-parenchymal cell population, extracted from liver digests of mice at different time points, was performed using flow cytometry. Hepatic macrophages were identified as (CD45+CD11b+Ly6G-) F4/80+ cells while eosinophils that are characterized as $F4/80^{int}$ SSC^{high} cells were excluded by my gating strategy (**Fig. 6.2A**) (Crane et al., 2014). Compared to baseline control levels, I show that SLPI induces a significant increase in the overall proportion of (F4/80+) MerTK+ hepatic macrophages at steady state following SLPI treatment for 24/48 hours (4.1 vs 24.5/26.1 %; both $p< 0.01$) (**Fig. 6.2A**). I found that SLPI administration in APAP-treated mice did not alter the (F4/80+) macrophage MerTK expression at 24 hours post APAP (**Fig. 6.2B**). However, SLPI induced an increase in the proportion of (F4/80+) MerTK+ cells at 48 hours post APAP dose (19.2 vs 11.5 %: $p< 0.05$), compared to the APAP-treated mice at 48 hours (**Fig. 6.2B**).

Furthermore, I used the KC vs MoMF gating strategy, as previously (Holt et al., 2008; Mossanen et al., 2016; Ramachandran et al., 2012), in order to identify the ($F4/80^{high}CD11b_{low}$) liver-resident KCs and ($F4/80_{low}CD11b^{high}$) MoMFs and to determine their MerTK expression. I reveal that the increase in MerTK+ hepatic macrophages following SLPI treatment, either at steady state or at 48 hours post APAP dose, is confined to the liver-resident KC population (**Fig. 6.2B**). Here, my results show that although SLPI administration did not alter the MerTK expression levels within the KC subset at 48 hours post APAP, it significant upregulated KC MerTK expression at 48 hours (86.2 vs 62.5 %: $p< 0.05$), compared to KCs derived from APAP-treated mice at 48 hours (**Fig. 6.2B**). In addition, no differences among different groups and treatments were detected for the total (F4/80+) hepatic macrophages, as proportion (%) of total liver CD45+ leukocytes, or in the KC/MoMF ratio within the F4/80+ population (**Fig. 6.2C**).

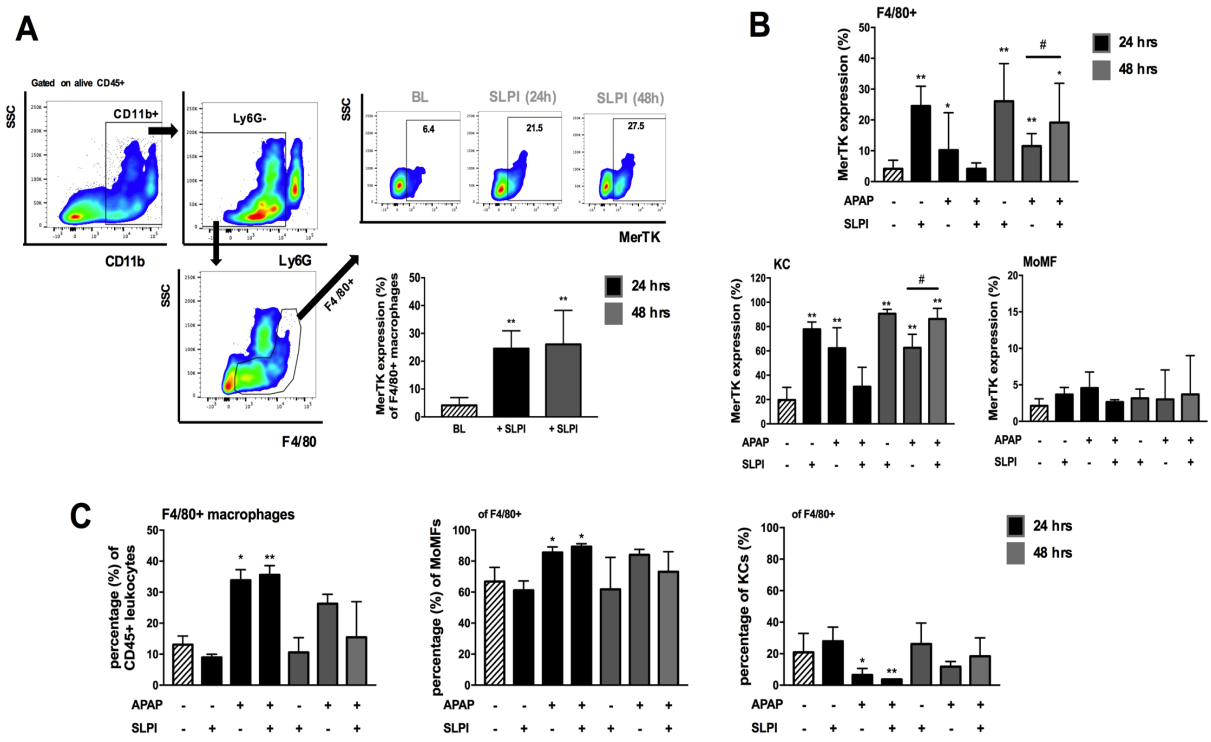

Figure 6.2. SLPI administration in mice induces MerTK expression in hepatic macrophages at steady state and following APAP-induced liver injury.

Wild-type (WT) mice were dosed with SLPI (-/+) or APAP (+/-) or APAP plus SLPI (+/+) while untreated mice (-/-) served as baseline controls (n=6/group). Mice were studied at baseline (white bars), 24 hours (black bars) and 48 hours (grey bars). **(A)** Representative flow cytometry analysis and data showing MerTK expression of F4/80+ macrophages at baseline and following SLPI administration. **(B)** Data show MerTK expression levels of F4/80+ macrophages, sub-analyzed into ($CD11b_{low}F4/80^{high}$) Kupffer cells (KC) and ($CD11b^{high}F4/80_{low}$) monocyte-derived macrophages (MoMF). **(C)** Data show F4/80+ hepatic macrophages as proportion (%) of total CD45+ leukocytes and the percentage (%) of resident KC and MoMF within the F4/80+ population. Non-parametric (Mann-Whitney) statistical analysis was used. Data are presented as median values with interquartile range (IQR). *or # P< .05, ** P< 0.01, **** P< .0001. SSC: side scatter.

6.3.3 SLPI administration in APAP-treated mice leads to increased numbers of hepatic apoptotic neutrophils *in vivo*

In view of the role of SLPI in promoting neutrophil apoptosis and clearance, as shown by *in vitro* human data, I examined the number of hepatic neutrophils using liver tissue immunohistochemistry and confocal imaging (**Fig. 6.3**). I found that APAP-treated mice dosed with SLPI had a significantly lower number of hepatic (MPO+) activated neutrophils at both 24 hours (27 vs 23 cells/HPF, $p< 0.05$) and 48 hours (14 vs 9 cells/HPF, $p< 0.0001$) post APAP, compared to APAP-treated mice (**Fig. 6.3A**). In addition, APAP-treated mice dosed with SLPI had a significantly higher proportion of hepatic (MPO+TUNEL+) apoptotic neutrophils at both 24 hours (7.5 vs 25.3 %, $p< 0.0001$) and 48 hours (7.6 vs 34.6 %, $p< 0.0001$), compared to APAP-treated mice (**Fig. 6.3B**). Similarly, I previously detected an increased proportion of apoptotic neutrophils (MPO+TUNEL+) in areas of necrosis in human ALF liver tissue **(Fig. 5.1A).** Taken together, my results reveal that during experimental APAP-induced liver injury in mice, SLPI administration promotes resolution responses by imprinting a resolution-like, MerTK+, hepatic macrophage phenotype and modulates neutrophil activation and survival.

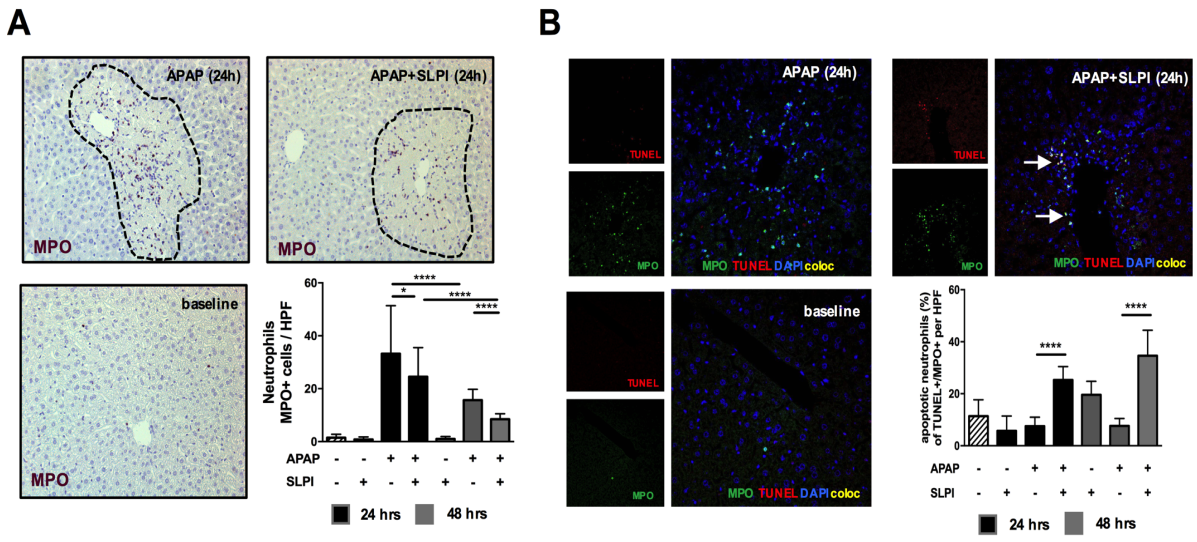

Figure 6.3. SLPI administration in mice induces neutrophil apoptosis following APAP-induced liver injury.

Wild-type (WT) mice were dosed with SLPI (-/+) or APAP (+/-) or APAP plus SLPI (+/+) while untreated mice (-/-) served as baseline controls (n=6/group). Mice were studied at baseline (white bars), 24 hours (black bars) and 48 hours (grey bars). **(A)** Representative liver immunohistochemistry images at baseline and 24 hours (n=5 each) and enumeration of MPO+ (purple) hepatic neutrophils (200X). **(B)** Representative liver confocal micrographs at baseline and 24 hours (n=5 each) stained for MPO (green), TUNEL (red), DAPI (blue); co-expression (yellow) (400X). Data show the percentage of (MPO+TUNEL+) apoptotic neutrophils. Non-parametric (Mann-Whitney) statistical analysis was used. Data are presented as median values with interquartile range (IQR). * P< .05, **** P< .0001.

6.4 Discussion

Several studies using human and experimental models support an immune-modulatory role for SLPI during tissue inflammation in a variety of diseases including sepsis, asthma and cancer (Majchrzak-Gorecka et al., 2016). For instance, $SLPI^{-/-}$ mice are more susceptible to LPS-induced endotoxin shock and sepsis caused by cecal ligation and puncture and develop increased inflammation (Nakamura et al., 2003). During acute tissue injury and wound healing, SLPI is a key anti-inflammatory mediator in the local microenvironment by directly inhibiting the NF-κB dependent pro-inflammatory responses of macrophages (Ashcroft et al., 2000; Odaka et al., 2003b; Sano et al., 2000; Sano et al., 2003).

Furthermore, $SLPI^{-/-}$ mice subjected to cutaneous injury show delayed skin wound healing that is reversible by SLPI administration to wounds. Use of anti-TGF-β and anti-TNF-α antibodies *in vivo* largely reversed this impaired healing, proposing that a SLPI-mediated control of TGF-β and TNF-α levels is required for cutaneous wound healing (Ashcroft et al., 2012; Ashcroft et al., 2000). A critical role of SLPI during the resolution phase of wound healing is described in TSLP-deficient mice, which have reduced SLPI levels in the colon and following DSS-induced colitis they fail to recover from colon damage. That may be due to increased NE activity during the recovery phase and an imbalance in proepithelin/epithelin conversion (Reardon et al., 2011). However, the role of SLPI during the resolution phase of APAP-induced acute liver injury and its potential pro-resolving actions on hepatic inflammation remain unexplored.

Here, my findings are first to describe that exogenous SLPI administration in APAP-treated mice promotes resolution of hepatic inflammation following acute liver injury, by inducing a prorestorative hepatic macrophage phenotype and modulating neutrophil activation and survival. I demonstrate that SLPI, present as a mediator in the liver microenvironment, can increase the proportion of MerTK+ hepatic macrophages at steady state conditions and during APAP-induced liver injury. In particular, I reveal that SLPI administration selectively upregulates MerTK expression within the hepatoprotetive

(Ju et al., 2002b; You et al., 2013), highly phagocytic (Stutchfield et al., 2015), liver-resident Kupffer cell population, and not in monocyte-derived macrophages, either at both steady state or inflammatory conditions post APAP dose. Furthermore, although SLPI administration did not attenuate peak liver injury, it did ameliorate histological/biochemical indices of liver injury at the onset of the resolution phase of inflammation (48 hours) post APAP dose. This time course is consistent with the mechanism I describe by which SLPI promotes the differentiation of macrophages towards a prorestorative state. My data corroborate with previous observations in experimental models of acute tissue injury, which suggest that monocytes promote resolution of inflammation under the correct micro-environmental signals (Crane et al., 2014; Ramachandran et al., 2012; Zigmond et al., 2014).

SLPI administration in APAP-treated mice not only increased the proportion of MerTK-expressing KCs during the resolution phase following acute liver injury but concomitantly decreased the numbers of hepatic neutrophils while increased the numbers of apoptotic neutrophils. These findings agree with, and may be explained by, the described role of MerTK in promoting resolution of inflammation after acute tissue injury by suppressing innate responses and augmenting the clearance of neutrophils (Arandjelovic and Ravichandran, 2015; Choi et al., 2015b; Hong et al., 2012). MerTK possesses a great functional importance for neutrophil clearance where the MerTK/LXR pathway signaling axis is shown to coordinately control neutrophil clearance and homeostasis (Hong et al., 2012). Also, lack of MerTK in mice is associated with reduced LXRα and LXRβ abundance and decreased expression of their target genes (Choi et al., 2015b). However, in the present study, the role of LXR signaling in ALF has not been examined. Further work, including gene expression analyses of liver tissue from mice treated with/without SLPI, would assess if this mediator positively modulates the MerTK/LXR axis during the time-course of APAP model, thus to enhance clearance of neutrophils and promote resolution of acute liver inflammation.

The fact that SLPI administration in APAP-treated mice resulted into increased numbers of apoptotic neutrophils in the liver may be mechanistically explained by my previous human data on SLPI and its actions as a pro-resolving mediator, as discussed above. Precisely, I demonstrated that it can act as a

pro-resolving mediator in the liver microenvironment by modulating the function of hepatic myeloid cells and crucially regulating the interplay between them to promote resolution of liver inflammation. SLPI mediates this via induction of prorestorative (MerTK+ HLA-DR^{high}) hepatic macrophages *in vitro* which counter regulate cytokine secretion towards resolution/tissue-repair, suppress neutrophil activation and induce neutrophil apoptosis, in a paracrine manner, whilst promoting their subsequent clearance. Of note, this SLPI-induced MerTK+ HLA-DR^{high} phenotype in human macrophages bears a remarkable similarity with the *in vivo* effects of SLPI in mice, where it augments the proportion of prorestorative MerTK+ MHCclassII^{high} and highly phagocytic liver-resident KCs at steady state and crucially during the resolution phase following APAP-induced liver injury.

The novel findings about SLPI in this study could be extended further with future work addressing if SLPI administration in APAP-treated mice also alters *in vivo* their liver micro-environmental milieu, as per human data above. That could be performed by using gene expression analyses of murine liver tissue, during the time-course of experimental APAP-induced ALF, in order to assess the expression levels of pro-inflammatory cytokines and resolution/tissue-repairs between the different study groups. In addition, it would be interesting to demonstrate *ex vivo* in these mice, using flow cytometry based techniques, if SLPI treatment leads to increased apoptosis rate of hepatic neutrophils in the liver and also to examine the efferocytic and phagocytic capacity of MoMF and KC macrophage subsets.

CHAPTER 7

7. IMMUNE PROFILING OF PATIENTS WITH SERONEGATIVE ACUTE LIVER FAILURE

7.1 Background and aims

Most studies in human ALF have focused in drug-induced acute liver injury, and in particular AALF, with therapeutic strategies not necessarily being applicable to all ALF causes. This may be explained by the distinct mechanisms underlying the pathophysiology of liver injury which vary according to the different ALF etiologies (Bernal et al., 2010; Bernal et al., 2013). As previously mentioned, SALF is another increasingly well-recognized cause of ALF due to yet unknown etiology. Its current clinical diagnosis is based on exclusion of other causes of hepatocellular injury such as viral, autoimmune or drug-induced hepatitis (Bernal et al., 2010; Bernal et al., 2013) while it is believed that it occurs due to a dysregulated immune response to an unidentified hepatotropic or environmental trigger (Donaghy et al., 2013).

In contrast to the pathogenesis of AALF where the toxic metabolites of paracetamol induce direct hepatocyte damage and necrosis, SALF has been associated with a lymphocytic infiltrate of effector T cells, NK cells and to a lesser extent B cells (Tuncer et al., 2013). That drives immune-mediated cytotoxic damage to hepatocytes that culminates in massive hepatic necrosis and liver failure (Tuncer et al., 2013; Wu et al., 2010). These histological features and the detection of increased circulating levels of autoantibodies also propose SALF as an autoimmune-mediated disorder (Stravitz et al., 2011). In both underlying etiologies of ALF, the recruited immune cells themselves contribute to hepatocyte damage mediated via direct activation of death receptors or cytokine secretion (Bernal et al., 2010; Quaglia et al., 2008). Thus, mechanisms designed to orchestrate liver regeneration and tissue repair can also further amplify liver injury and progression to liver failure (Tuncer et al., 2013).

Hypothesis and aims:

Given the limited data on human SALF and the unexplored role of monocytes/macrophages in its pathogenesis, I hypothesized that the underlying mechanisms of immune-mediated liver injury differ in SALF, compared to AALF, and monocytes/macrophages in SALF are typified by overwhelming pro-inflammatory responses and bear similarities with the macrophage activation syndrome. Hence, in this chapter I aimed to:

- Examine the circulating and hepatic micro-environmental milieu in SALF patients and HC, by measuring the levels of key inflammatory cytokines and mediators.
- Assess the pro-inflammatory cytokine secretion following microbial challenge in SALF, AALF and HC.
- Characterize the hepatic immune cell infiltrate in SALF, AALF and pathological control liver tissue.

7.2 Materials and methods

7.2.1 Isolation of peripheral blood mononuclear cells

Whole blood was obtained from healthy volunteers (HC, n=5) and SALF patients (n=10) (**Table 7.1**) recruited at King's College Hospital and peripheral blood mononuclear cells (PBMCs) were isolated using Ficoll-Paque Plus (GE Healthcare) and were washed in PBS (Life Technologies, UK). Cell viability was >95% according to trypan blue staining.

7.2.3 Measurement of inflammatory mediator and cytokine levels

Human quantikine ELISA (R&D Systems, UK) was used to measure TNF-α and IL-6 levels in PBMC culture supernatants in HC, AALF and SALF patients, following 6h LPS (100 ng/ml) stimulation (Sigma-Aldrich, UK). Human quantikine ELISA (R&D Systems, UK) was also used to measure TGF-β1, sCD163, IL-2Ra levels in human plasma and liver tissue homogenates from pathological controls and SALF patients. The MSD Human Pro-inflammatory 7-plex panel was used to assess (IFN-γ, IL-1β, IL-4, IL-8, IL-10, IL-12p70 and TNF-α) cytokine levels in human plasma and liver tissue homogenates from pathological controls and SALF patients. ELISA microplates were read using the SoftMax® Pro software (Molecular Devices, USA). MSD plates were read on the Sector Imager 2400 apparatus (Gaithersburg, MD). All experiments were performed in duplicates and according to the manufacturer's instructions.

7.2.3 Tissue sampling, immunohistochemistry and imaging

Human liver tissue was obtained from AALF (n=10) and SALF (n=10) patients undergoing orthotopic liver transplantation and from hepatic resection margins of colorectal malignancies, which served as pathological controls (PC, n=5). *Single-epitope enzymatic immunohistochemistry for detection of CD68, CD3, CD4, CD8, MPO, FoxP3, T-bet, CD56 and Perforin expressing cells.* FFPE tissue was cut at 4 μm using a Leica RM2235 rotary microtome (Leica Biosystems, UK) and picked up on poly-

L-lysine coated slides. All slides were dewaxed in xylene, rehydrated, subjected to heat-induced epitope retrieval (HIER) for 20 min, allowed to cool, followed by manual staining using a) mouse monoclonal anti-CD68 primary antibody (# PA0273, Leica Biosystems, UK; ready-to-use), b) rabbit polyclonal anti-CD3 antibody (# A0452, Dako, UK; dilution 1:100), c) mouse monoclonal anti-CD4 primary antibody (# M7310, Dako, UK; dilution 1:200), d) mouse monoclonal anti-CD8 primary antibody (# M7103, Dako, UK; dilution 1:200), e) rabbit polyclonal anti-MPO primary antibody (# ab9535, Abcam, UK; dilution 1:50), f) mouse monoclonal anti-Foxp3 primary antibody (# ab22510, Abcam, UK; dilution 1:100), g) mouse monoclonal anti-T-bet primary antibody (# sc-21749, Santa Cruz Biotechnology, UK; dilution 1:100), h) mouse monoclonal anti-CD56 primary antibody (# 75603, Invitrogen/ThermoFisher, UK; dilution 1:500), i) mouse monoclonal anti-Perforin primary antibody (# 141009, Novocastra/Leica Biosystems, UK; dilution 1:20). All slides were dewaxed in xylene, rehydrated, subjected to heat-induced epitope retrieval (HIER) for 20 min, allowed to cool, followed by incubation at room temperature with the primary antibody. The signal was detected using EnVisionTM G/2 Doublestain System, Rabbit/Mouse (DAB+/Permanent Red) (# K536111-2, Dako, UK) and was visualized with Permanent Red. The slides were then dehydrated with alcohol, cleared with xylene and cover slipped with DPX (Leica Biosystems, UK) after hematoxylin counterstaining. Images were captured with a Nikon Eclipse E600 microscope.

7.2.4 Statistical analysis

Analysis and graphing of data were performed using GraphPad Prism 6 software (GraphPad Software, La Jolla California, USA). Statistical significance was assessed with non-parametric analysis for data not normally distributed, unless otherwise specified in figure legends. Results are presented as median with interquartile range (IQR), unless otherwise specified in figure legends.

7.3. Results

7.3.1 Measurement of circulating and hepatic levels of key inflammatory cytokines in SALF

I examined the levels of circulating key inflammatory cytokines in serum derived from SALF patients (n=10) and healthy volunteers (HC, n=5) (**Table 7.1**). Compared to HC, my results show that SALF patients are characterized by significantly higher circulating levels of pro-inflammatory [IFN-γ (0 vs 0.31), IL-1β (0 vs 0.01), IL-6 (0.02 vs 5.14) and IL-8 (0.46 vs 32.34)] and anti-inflammatory [IL-10 (0.07 vs 17.21) and TGF-β1 (10.57 vs 162.4)] cytokines (all pg/ml; $p<0.01$) (**Fig. 7.1A**). Also, I quantified inflammatory cytokines in liver tissue homogenates in SALF n=10) and PC (n=5). My results reveal that compared to PC, hepatic concentrations of IL-8 (12.72 vs 214.4) and TGF-β1 (0.43 vs 2.75) are significantly elevated in patients with SALF (both pg/ml; $p<0.05$) (**Fig. 7.1B**). In addition, I measured the circulating and hepatic levels of macrophage (sCD163) and T cell (IL-2Rα) activation markers; both were found significantly elevated in SALF in comparison to HC and PC samples (both $p<0.01$) (**Fig. 7.2**).

7.3.2 LPS-induced pro-inflammatory cytokine secretion is unaltered in SALF patients

I determined in culture the LPS-induced pro-inflammatory (TNF-α and IL-6) cytokine secretion of PBMCs in SALF, AALF patients and HC (n=10 per group). In accordance with previous findings (Antoniades et al., 2014), I found that patients with AALF exhibit significantly reduced levels of TNF-α (733 vs 2382) and IL-6 (804 vs 2466) following microbial challenge, compared to HC (pg/ml; $p<0.01$) (**Fig. 7.3**). However, LPS-simulated TNF-α/IL-6 secretion levels of PBMCs were comparable between SALF and HC, suggesting intact pro-inflammatory responses in SALF patients (**Fig. 7.3**).

Table 7-1. Clinical and physiological characteristics of patients with SALF

Parameter	SALF	HC
Number of patients	10	5
Age	58 [50-69]	27 [25-34]
WCC ($x10^9$/L)	8.3 [3.25-19.3]	n/a
Monocytes ($x10^9$/L)	0.66 [0.14-2.42]	n/a
Creatinine (µmol/L)	95.5 [45-264]	n/a
INR	2.3 [1.27-3.9]	n/a
Bilirubin (µmol/L)	402 [261-628]	n/a
AST (IU/mL)	622 [262-1792]	n/a
Encephalopathy	1 [0-3]	n/a
MELD	29 [17-58]	n/a

Abbreviations: INR: international normalized ratio; AST: aspartate aminotransferase; MELD: Model for End stage Liver Disease; WCC: white (leukocyte) cell count.

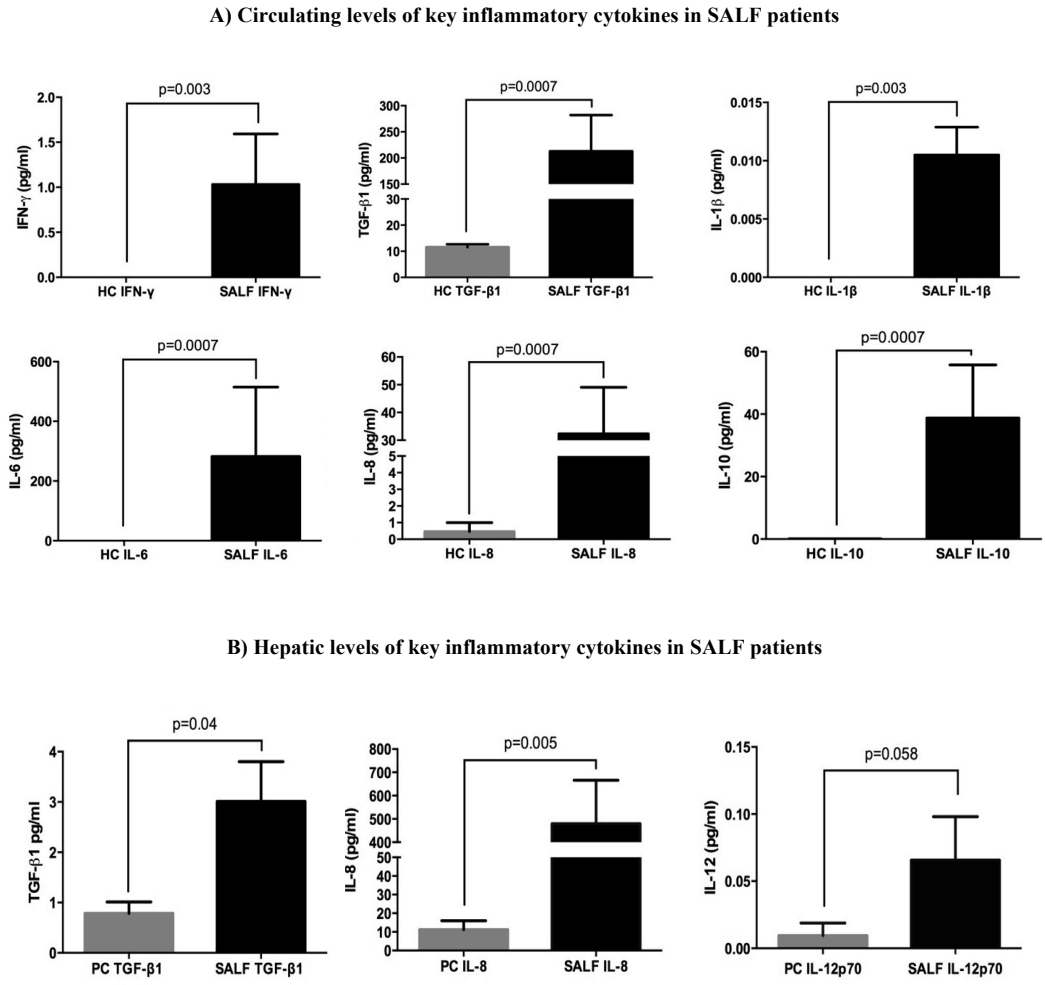

Figure 7.1. Circulating and hepatic levels of key inflammatory cytokines in SALF patients.

Levels of pro-inflammatory (IFN-γ, TNF-α, IL-6, IL-8, IL-12p70) and anti-inflammatory (TGF-β1, IL-10) cytokines (pg/ml) were determined (duplicates) using ELISA in (**A**) serum from SALF patients (n=10) and healthy controls (n=5), and (**B**) liver tissue homogenates from SALF patients (n=10) and pathological controls (n=5). Non-parametric (Mann-Whitney) statistical analysis was used. Data are expressed as median values with interquartile range (IQR). p values are shown.

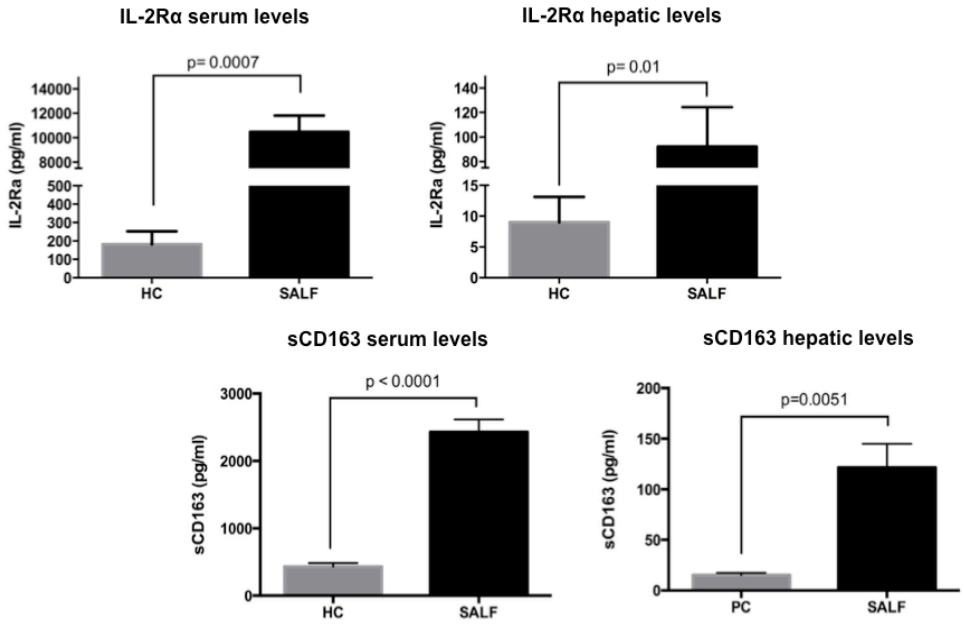

Figure 7.2. Circulating and hepatic levels of macrophage/T-cell activation markers in SALF.

Levels of macrophage (sCD163) and T cell activation (IL-2Ra) markers (pg/ml) were determined (duplicates) using ELISA in a) serum from SALF patients (n=10) and healthy controls (n=5) and b) in liver tissue homogenates from SALF patients (n=10) and pathological controls (n=5). Non-parametric (Mann-Whitney) statistical analysis was used. Data are expressed as median values with interquartile range (IQR). p values are shown.

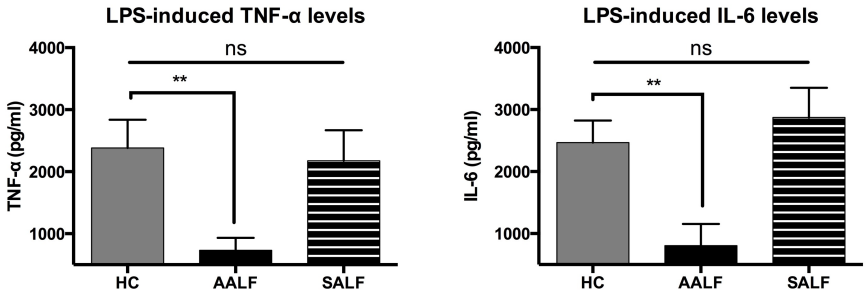

Figure 7.3. Pro-inflammatory cytokine secretion of PBMCs following LPS stimulation in SALF.

PBMCs isolated from patients and healthy volunteers were stimulated with LPS (100 ng/ml) for 6h in culture. Levels of TNF-α and IL-6 (pg/ml) were determined (duplicates) using ELISA in cell culture supernatants from SALF (n=10) and AALF (n=10) patients and healthy controls (n=10). Non-parametric (Mann-Whitney) statistical analysis was used. Data are expressed as median values with interquartile range (IQR). ** p< 0.01, ns: non-significant.

7.3.3 Characterization of the hepatic immune cell infiltrate in SALF

In order to fully characterize the hepatic immune cell infiltrate in SALF patients, I performed single-epitope immunohistochemistry for different markers (CD68, CD3, CD4, CD8, T-bet, MPO, CD56, Perforin and FoxP3) on liver tissue derived from SALF (n=10), AALF (n=10) patients and PC (n=5). My analysis revealed that hepatic macrophages (CD68+) are the predominant inflammatory cell population in SALF, detected in centrilobular and periportal areas at significantly higher numbers compared to PC tissue (**Fig. 7.4**). In addition, lymphocytes (CD3+) and neutrophils (MPO+) were concentrated in portal tracts in SALF, in comparison with PC (**Fig. 7.4**). Interestingly, I demonstrate that there is a Th1 lymphocytic (T-bet+) rich infiltrate in both centrilobular and periportal areas only in the liver of SALF patients, compared to liver tissue derived from AALF patients and PC (**Fig. 7.4**). Finally, SALF patients exhibited lower number of hepatic NK (CD56+) and Perforin+ cells whereas FoxP3+ cells were significantly increased, in both centrilobular and periportal areas, compared to PC liver tissue (**Fig. 7.4**).

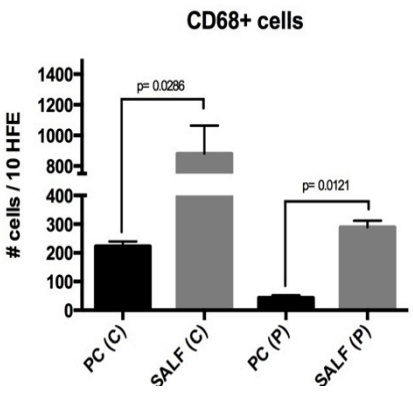
CD68+ cells
cells / 10 HFE
1400
1200
1000
800
400
300
200
100
0
p= 0.0286
p= 0.0121
PC (C)
SALF (C)
PC (P)
SALF (P)

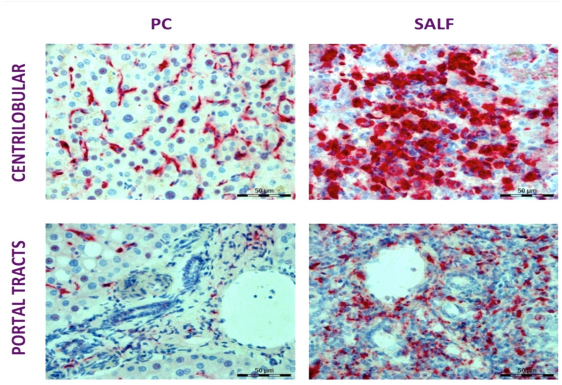
PC
SALF
CENTRILOBULAR
PORTAL TRACTS

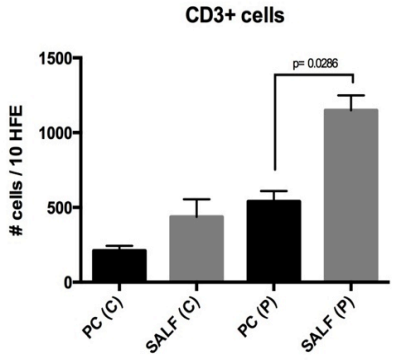
CD3+ cells
cells / 10 HFE
1500
1000
500
0
p= 0.0286
PC (C)
SALF (C)
PC (P)
SALF (P)

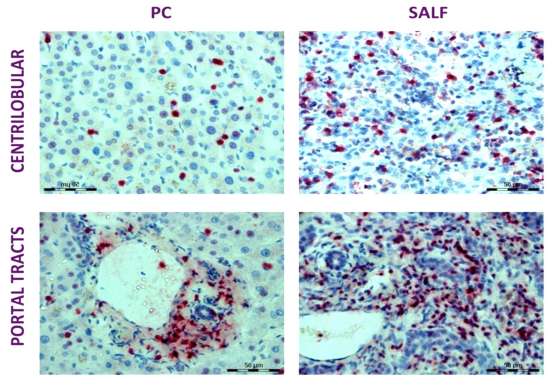
PC
SALF
CENTRILOBULAR
PORTAL TRACTS

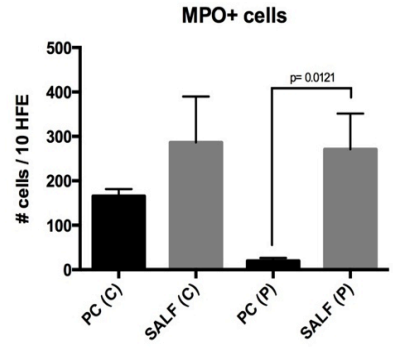
MPO+ cells
cells / 10 HFE
500
400
300
200
100
0
p= 0.0121
PC (C)
SALF (C)
PC (P)
SALF (P)

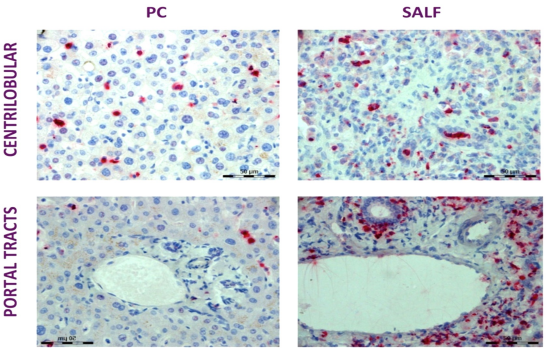
PC
SALF
CENTRILOBULAR
PORTAL TRACTS

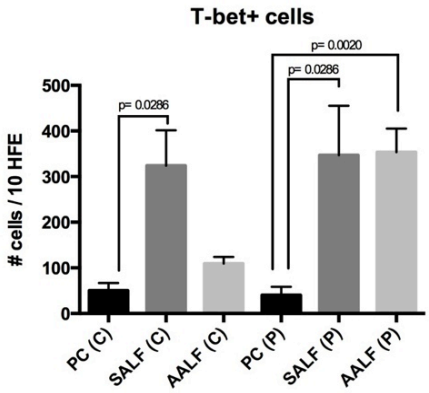
T-bet+ cells
cells / 10 HFE
500
400
300
200
100
0
p= 0.0286
p= 0.0286
p= 0.0020
PC (C)
SALF (C)
AALF (C)
PC (P)
SALF (P)
AALF (P)

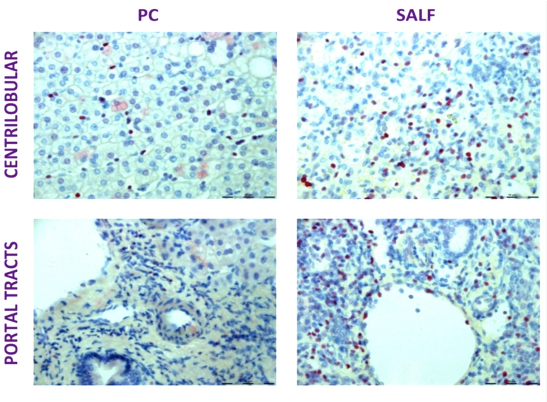
PC
SALF
CENTRILOBULAR
PORTAL TRACTS

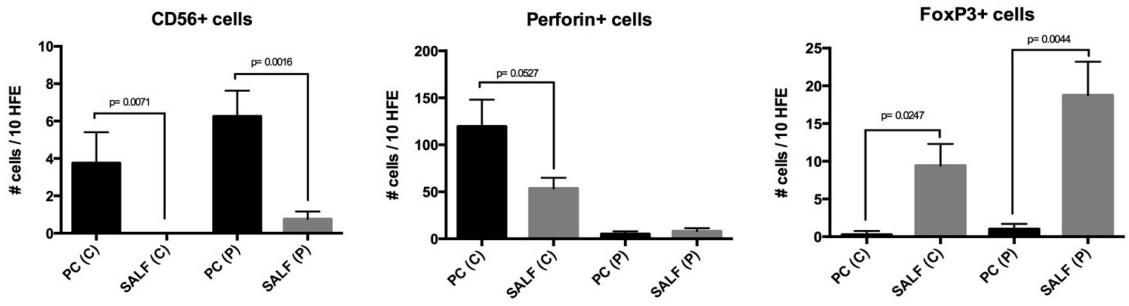

Figure 7.4. Characterization of the immune cell infiltrate in liver tissue of SALF patients.

The characterization of the immune cell infiltrate was performed using single-epitope immunohistochemistry on human explant liver tissue. Left panel: data show the quantification of immune cells within areas of necrosis [C] and portal tracts [P] in tissue from SALF (n=10), AALF (n=10) and pathological controls (n=5). For each section, 10 randomly chosen portal tracts or areas of centrilobular necrosis were assessed at high magnification and the cumulative number of positive cells in 10 fields was recorded. Right panel: representative immunostain images and patterns of expression (red+) of CD68+, CD3+, MPO+, T-bet+, positive cells (magnification X40). Non-parametric (Mann-Whitney) statistical analysis was used. Data are expressed as median values with interquartile range (IQR). p values are shown.

7.4 Discussion

To date, the underlying mechanisms of immune-mediated liver injury in SALF are poorly understood. Phenotypically, these patients present with a marked SIRS response and previous analyses of liver tissue suggest overwhelming pro-inflammatory responses, which in combination with the detection of circulating autoantibodies in SALF, propose that it shares similarities with autoimmune liver disease (Stravitz et al., 2011). Hence, to further characterize this rare cause of ALF, I analyzed the circulating and hepatic inflammatory microenvironment in SALF. My results reveal that SALF patients exhibit higher circulating levels of pro-(IFN-γ, IL-1β, IL-6, IL-8) and anti-(IL-10 and TGF-β1) inflammatory cytokines, compared to healthy controls. Also, they have high levels of macrophage (sCD163) and T cell (IL-2Rα) activation markers. Furthermore, I demonstrate that hepatic concentrations of IL-8, TGF-β1, IL-2Rα and sCD163 are elevated in SALF, compared to pathological controls, while the TNF-α and IL-6 secretion is comparable between SALF and HC, suggesting intact pro-inflammatory responses in SALF patients. The immunohistochemical analysis reveals a macrophage and Th1-lymphocytic rich infiltrate, in both centrilobular and periportal areas in the SALF liver, compared to AALF and pathological controls. Taken together, these data indicate that SALF is a Th1-cell driven disease, as distinct to AALF, characterized by a profound activation of pro-inflammatory responses (Triantafyllou et al., 2014).

Clinically and pathologically, SALF bears similarities with macrophage activation syndrome (MAS). The main pathophysiologic feature of MAS is excessive activation and expansion of T lymphocytes and macrophages, as observed in SALF (Ravelli et al., 2012; Schulert and Grom, 2015). Importantly, these activated immune cells produce large amounts of pro-inflammatory cytokines (IL-1β, IL-6, IL-18, TNF-α, and IFN-γ), creating a "cytokine storm" which is central to the pathogenesis of MAS (Ravelli et al., 2012; Schulert and Grom, 2015). Whatever the upstream events that trigger SALF, the end product is escalating production of pro-inflammatory cytokines that lead to excessive liver damage. Interestingly, cytokine-targeted biologic therapies have been tried in patients with MAS

(Ravelli et al., 2012; Schulert and Grom, 2015). Similarly, monoclonal antibodies directed against pro-inflammatory cytokines (e.g. IL-1β, IFN-γ) or T cell activation marker (IL-2Rα) that is detected here, could be used for therapeutic intervention in SALF. Hence, immunotherapeutic strategies could be assessed in SALF in order to attenuate pro-inflammatory responses and severity of liver failure.

Most clinical and experimental studies in ALF focus in drug-induced acute liver injury, in particular AALF, with therapeutic strategies not necessarily being applicable to all ALF causes. This may be explained by the distinct mechanisms underlying the pathophysiology of liver injury which vary according to the ALF etiologies (Bernal et al., 2010; Bernal et al., 2013). In the present study, most analyses were performed on AALF samples, however the function of monocytes/macrophages may differ between ALF cases (Donaghy et al., 2013), for instance in SALF patients, while the evidence I provide here support also this notion (Triantafyllou et al., 2014). These histological features of SALF and the detection of circulating autoantibodies also suggest it may be an autoimmune-mediated disorder (Stravitz et al., 2011). Of note, MerTK is crucial for the effective clearance of apoptotic immune cells, and has been implicated in autoimmune disease such as SLE and multiple sclerosis (Mukherjee et al., 2016).

Taken together, further studies are needed to characterize the phenotype and function (phagocytosis, efferocytosis and cytokine production) of circulating and hepatic monocytes/macrophages in SALF patients. Future work should expand the findings in AALF of this study, and investigate the role of the prorestorative, MerTK+, monocyte/macrophage subset in SALF or other ALF causes. It would be also interesting to explore this signaling pathway in patients with autoimmune hepatitis that are characterized by impaired immune regulation and excessive liver inflammation and damage. Studies, using human and experimental models, could assess the utility of MerTK as an immune-therapeutic target in a variety of hepatic disorders, aimed to quell tissue destructive responses and promote resolution of hepatic inflammation.

CHAPTER 8

8. GENERAL DISCUSSION

The data presented in this thesis describe a significant expansion of monocytes/macrophages that have a prorestorative MerTK+ phenotype, detected in circulatory, hepatic and lymphatic compartments of ALF patients. The biological significance of this immune-regulatory subset is highlighted through its strong correlations with physiological/biochemical indices of hepatic injury and with the magnitude of SIRS. Immune-phenotypic analyses revealed that MerTK+ cells possess a $CD163^{high}$Tie-2^{high}HLA-DR^{high} expression profile with augmented tissue ($CCR2^{high}CCR5^{high}CCR7^{high}$) homing characteristics, results that extend previous findings (Antoniades et al., 2006; Antoniades et al., 2014; Antoniades et al., 2012; Bernsmeier et al., 2015). Comparison of the gene expression profiles between MerTK+ and MerTK- cells in steady state and ALF reveal that MerTK+ monocytes have a more differentiated lineage "tissue-like" profile, with increased expression of a number of genes associated with innate and adaptive effector functions. My data demonstrate marked elevations in the levels of MerTK+ circulating cells in patients with both acetaminophen (AALF) and non-acetaminophen (NAALF) induced ALF. It is noteworthy that the highest MerTK expression levels are detected in monocytes from AALF patients who exhibit a greater severity of acute liver injury. Peak circulating MerTK levels are detected on admission to the Liver Unit, which may reflect the extent of hepatic tissue resolution responses following acute hepatocellular necrosis. Prospective clinical studies are warranted to assess the utility of MerTK circulating levels as a mechanistic biomarker of resolution responses and outcome in ALF patients.

In keeping with other models of acute tissue injury (Bernsmeier et al.; Choi et al., 2013; Lee et al., 2012c; Wan et al., 2013), functional analyses show that these prorestorative cells suppress innate immune activation whilst concomitantly promote resolution responses by augmenting clearance of cellular/infective material and secreting anti-inflammatory/tissue-repair mediators (e.g. SLPI). Here, I identify two MerTK+ monocyte subsets with differential HLA-DR expression that are phenotypically similar but functionally distinct. Compared to MerTK+HLA-DR_{low}, MerTK+HLA-DR^{high} cells are

characterized by higher phagocytic/efferocytic capabilities with peak circulating levels detected on admission whereas MerTK+HLA-DR$_{low}$ cells remain persistently elevated following admission.

My results show that MerTK+ macrophages are expanded in areas of hepatocellular necrosis in ALF, forming ring-like structures around the areas of injured liver parenchyma, with MerTK+HLA-DR^{high} located in the outer rim of necrosis whereas cells in central and perivenular areas are predominately MerTK+HLA-DR$_{low}$. This echoes recent findings from other experimental models of sterile liver injury where the *in situ* reprogramming of monocytes is shown; the transition of recruited monocytes from outer sites of injured areas towards their center is associated with a phenotypic and functional conversion, essential to facilitate tissue-repair and wound healing processes (Dal-Secco et al., 2015; Mori et al., 2009). Further work is currently planned where by using the APAP experimental model and advanced imaging techniques, including intravital non-invasive microscopy and fluorescent molecular tomography (FMT), I aim to investigate *in vivo* if monocytes/macrophages possess this resolution-like identity prior to homing or acquire, even augment, their phenotypic and functional characteristics *in situ* following recruitment from the circulation to sites of acute liver injury.

Experimental models of acute liver injury provide evidence that the influx of circulatory myeloid cells in areas of necrosis triggers resolution responses (Dambach et al., 2002; Holt et al., 2008; Zigmond et al., 2014), however human data is currently limited (Antoniades et al., 2014; Antoniades et al., 2012). Here, I provide novel insights into the migratory characteristics of ALF monocytes. I show that a high proportion of MerTK+ monocytes/macrophages express tissue and lymph-node (CCR2, CCR5 and CCR7) homing receptors, suggesting they are equipped to migrate into tissues compartments. I provide also evidence that monocytes, particularly MerTK+ cells, efficiently migrate across hepatic endothelium and subsequently reverse migrate out of it, bearing the characteristic MerTK^{high}CD163^{high} phenotype. Accordingly, these cells are expanded in hepatic and lymphatic tissue compartments in ALF patients. These findings suggest a dynamic circulatory pathway, in which MerTK+ cells home from the inflamed liver to regional lymph nodes and/or back into the circulation (Antoniades et al., 2012; von Andrian and Mempel, 2003; Zigmond et al., 2014). To support and prove such hypothesis,

further *in vivo* research is warranted to assess the migratory characteristics of ALF monocytes. This could be also achieved using the APAP experimental model and intravital non-invasive microscopy. Furthermore, FMT could be employed to examine i*n vivo* the fate of MerTK+ monocytes during the different phases of acute liver injury in order to draw more definitive conclusions regarding the "re-circulation" story. In another experiment, I could adoptively transfer MerTK-labelled macrophages, obtained by flow cytometry based sorting from murine liver, during the different phases of APAP-induced acute liver injury and use the FMT technology to track their fate.

This work has identified three key micro-environmental processes in the ALF inflamed liver that drive monocytes/macrophages towards a resolving program. First, I highlight a novel regulatory role for biliary epithelial cells, which through their skewed anti-inflammatory molecule secretion (e.g. SLPI) induce the development of the MerTK+ phenotype. Second, phagocytosis of apoptotic cells triggers a macrophage functional switch towards an immune-regulatory phenotype associated with resolution and tissue-repair properties (Bellingan et al., 2002; Bystrom et al., 2008). Accordingly, I demonstrate that exposure/phagocytosis of apoptotic neutrophils and hepatocytes, detected in the injured ALF liver, cause a functional switch in MerTK+ cells from an HLA-DR^{high} to HLA-DR_{low} expression status, recapitulating the prorestorative phenotype described in ALF. Third, the induction of MerTK+HLA-DR^{high} macrophages by SLPI, that is produced by BECs and hepatic macrophages (Antoniades et al., 2014), which via autocrine/paracrine mechanisms counter regulate cytokine release, suppress neutrophil activation and induce neutrophil apoptosis while promoting their subsequent clearance.

Although anti-inflammatory programs initiated following phagocytosis of apoptotic cells and debris are beneficial in resolving tissue injury and inflammation, they may have the undesirable potential to dampen anti-microbial responses (Fullerton and Gilroy, 2016; Grabiec and Hussell, 2016). My data support this notion where I demonstrate that acute liver injury can reprogram hepatic myeloid cells towards MerTK+ resolution responses, that quell tissue inflammation and promote the clearance of debris. Both MerTK+HLA-DR^{high} and MerTK+HLA-DR_{low} cells, characterized by suppressed anti-

microbial responses, are significantly elevated in the circulatory, hepatic and crucially in lymphatic tissue compartments in ALF. Noteworthy, lymph-node macrophages serve to filter other tissue and lymph borne pathogens in order to prevent their systemic translocation and prime innate/adaptive immune responses (Gray and Cyster, 2012; Kastenmuller et al., 2012). The consequences are likely to be systemic immune suppression and anti-inflammatory responses. Whereas this may help to suppress ongoing systemic inflammation it will contribute to the observed immuneparesis and susceptibility to infection in these patients, which is such a devastating complication of ALF.

My data from the experimental model for this disease are first to provide novel insights into the origin and biological relevance of these regulatory cells during acute hepatic injury. Here, I show that the proportion of MerTK+ cells are specifically increased in the resident Kupffer cell, and not infiltrating macrophage, population following APAP-induced acute liver injury. Moreover, MerTK+ Kupffer cells bear a MHC class II^{high} $Ly6C_{low}$ phenotype which is not only the dominant phagocytic (David et al., 2016; Stutchfield et al., 2015) and prorestorative (Dragomir et al., 2012; Ramachandran et al., 2012) hepatic macrophage population but also bears similarities with "pro-phagocytic" MerTK+HLA-DR^{high} cells identified in humans. Whilst the proportion of MerTK+ MoMFs do not substantially increase over the time course, these cells transit from a (baseline) MHC class II_{low} $Ly6C^{high}$ phenotype during resolution the resolution phase towards an pro-restorative MHC class II^{high} $Ly6C_{low}$ phenotype (Dragomir et al., 2012; Ramachandran et al., 2012), in accord with previous findings and consistently with their proposed role in resolving hepatic inflammation (Holt et al., 2008; Zigmond et al., 2014).

I demonstrate that Mer-deficient mice have a reduced proportion of resident Kupffer cells prior to and following APAP administration. In view of its role in promoting cell survival through activation of anti-apoptotic pathways (Anwar et al., 2009), this data suggest that activation of MerTK in Kupffer cells is of importance in differentiation and restoration following acute liver injury. Further studies are warranted to identify the precise mechanisms through which MerTK regulates this process in both human and experimental models of disease. My findings in APAP-treated Mer-deficient mice echo recent data showing that MerTK promotes resolution of inflammation by dampening innate responses

and augmenting the clearance of neutrophils following experimental acute tissue injury (Arandjelovic and Ravichandran, 2015; Choi et al., 2015b; Hong et al., 2012). In the absence of MerTK, I report a significant depletion in the hepatoprotective MHC class II^{high} $Ly6C_{low}$ liver-resident macrophages (Ju et al., 2002b; You et al., 2013), with the highest phagocytic capabilities (Stutchfield et al., 2015), with a reciprocal increase in hepatic neutrophils and persistent necrosis following APAP administration. Together, these data indicate that the MerTK-bearing cells identify a hepatic macrophage population with enhanced phagocytic capabilities, that evolve following acute hepatocellular necrosis serving to drive hepatic resolution responses.

In both experimental and human models of ALF, I identify SLPI as a micro-environmental mediator that critically regulates the interplay between myeloid cells to promote hepatic resolution responses through the induction of a $MerTK^{high}$ phenotype. Specifically, I demonstrate that SLPI selectively induces MerTK expression in the liver-resident Kupffer cells whilst concomitantly increasing the number of apoptotic neutrophils. However, there is no data on how SLPI modulates neutrophil function. Here, I show that SLPI induces neutrophil apoptosis in a paracrine manner and augments their subsequent clearance through $MerTK^{high}$ cells. The effect of SLPI on cell clearance appears to be highly selective in view of the fact it does not alter the clearance of APAP-treated apoptotic/necrotic parenchymal cells. Future studies could delineate the distinct mechanisms that govern the clearance of parenchymal and non-parenchymal cells following liver injury. Furthermore, I determined that SLPI also drives pro-resolution responses through attenuation of NET formation in ALF; a neutrophil process that exacerbates acute tissue damage through activation of the inflammasome in ischaemia-reperfusion injury (Huang et al., 2015). Human and murine models might confirm *in vivo* these effects and would allow to examine the systemic and liver-specific role of NETs in ALF, addressing if their presence, or absence, can alter antimicrobial immunity, modulate myeloid cell function and promote resolution of liver inflammation in ALF.

Most clinical and experimental studies in ALF focus on drug-induced acute liver injury, in particular AALF, with therapeutic strategies not necessarily being applicable to all ALF causes. This may be

explained by the distinct mechanisms underlying the pathophysiology of liver injury which vary according to the etiologies (Bernal et al., 2010; Bernal et al., 2013). Here, most analyses were performed on AALF samples, however the function of monocytes/macrophages may differ between ALF cases, for instance in SALF, another cause of ALF with yet unknown etiology (Donaghy et al., 2013). SALF is proposed to be due to a dysregulated immune response to an unidentified hepatotropic or environmental trigger (Donaghy et al., 2013) while it is associated with a lymphocytic infiltrate of effector T cells, NK cells and B cells, suggesting that this drives immune-mediated damage cytotoxic to hepatocytes which culminates in liver necrosis and failure (Tuncer et al., 2013; Wu et al., 2010).

I provide recent evidence that SALF is a Th1-cell driven disease, characterized by a macrophage/Th1-lymphocytic rich infiltrate, a profound elevation in circulating and hepatic levels of macrophage and lymphocyte activation markers and intact PBMC pro-inflammatory responses (Triantafyllou et al., 2014). These histological features and the detection of circulating autoantibodies in SALF are also suggestive of an autoimmune-mediated disorder (Stravitz et al., 2011). Of note, MerTK is crucial for the effective clearance of apoptotic immune cells, thus it has also been implicated in autoimmune disease such as SLE and multiple sclerosis (Mukherjee et al., 2016). Together, further work should expand the findings of the present study and investigate the role and function of this prorestorative, MerTK+, monocyte/macrophage subset in SALF or other ALF causes. It would be also interesting to explore this signaling pathway in patients with autoimmune hepatitis who are characterized by impaired immune-regulation and excessive liver inflammation and immune-mediated damage. Future studies, using human and experimental models, could assess the utility of MerTK as an immune-therapeutic target in a variety of hepatic disorders, aimed to quell tissue destructive responses and promote resolution of hepatic inflammation.

This work identified the induction of an immune-regulatory MerTK+ cell subset in ALF that may promote tissue-repair responses, with implications for therapeutic intervention where enhancing the local function of these cells could promote liver repair and regeneration. In this study, I utilized the

pro-resolving actions of SLPI as proof-of-principle in order to highlight the biological significance of the MerTK+ phenotype in promoting resolution responses following acute liver injury. Using targeted strategies to harness the prorestorative abilities of MerTK+ cells represents a promising therapeutic avenue in promoting tissue repair potentially in a number of acute hepatic inflammatory disorders. However, caution would need to be exercised when considering any of these therapeutic approaches given the evidence of peripheral monocyte suppression in ALF (Antoniades et al., 2006; Antoniades et al., 2014), indicating that the timing of therapy would need to be carefully calibrated in order to promote resolution whilst minimizing the impact on immuneparesis. The balance of these biological processes must be rationalized when considering interventional strategies that promote liver repair processes whilst not exacerbating the risk of infection.

In conclusion, the data in this thesis describe a marked expansion of a prorestorative MerTK+ phenotype in circulating monocytes and tissue macrophages during ALF. These immune-regulatory cells evolve in response to micro-environmental cues within the injured liver, as summarized in (**Fig. 8.1**), and represent a novel immunotherapeutic target in acute liver injury to quell tissue destructive responses and promote resolution. Furthermore, I show that SLPI acts as a key micro-environmental mediator by regulating the function of hepatic myeloid cells and promoting resolution responses through induction of MerTK expression within the liver-resident macrophage population.

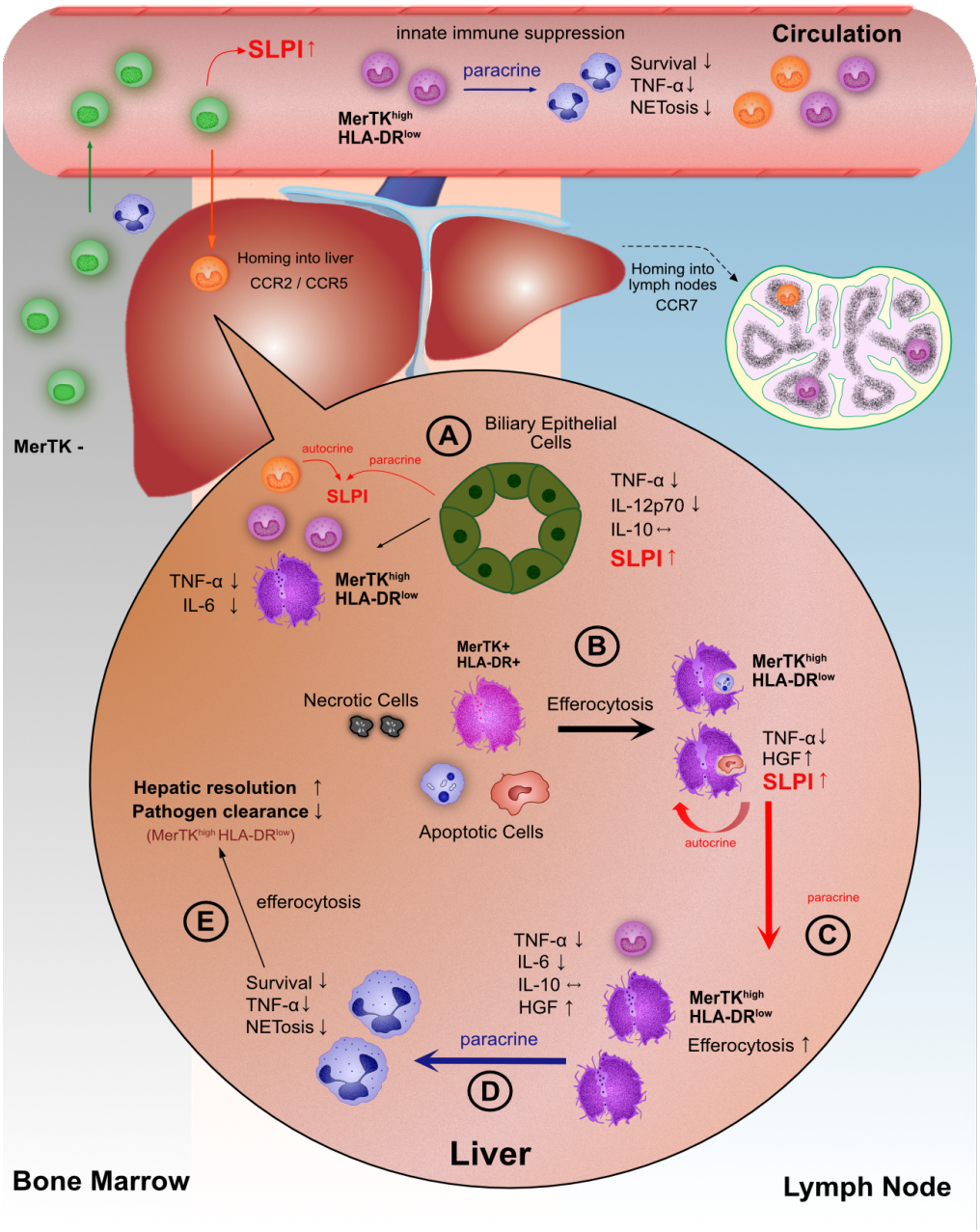

Figure 8.1. Proposed model of hepatic macrophage resolution responses in ALF.

Bone-marrow derived monocytes (MerTK-; green) home to the inflamed liver and acquire a MerTK+ phenotype (MerTK+; orange). Following exposure to multiple micro-environmental triggers, including inflammatory mediators secreted by biliary epithelial cells, notably SLPI [**A**], and contact/uptake of cellular debris [**B**] monocytes/macrophages acquire a resolution-like phenotype (MerTK^{high}; purple). These MerTK^{high} cells [**C**] suppress myeloid cell activation in auto/para-crine manner by: a) counter-regulating the production pro-inflammatory cytokines whilst promoting resolution/tissue-repair mediator release b) suppressing neutrophil activation and NET formation and c) inducing neutrophil apoptosis and enhancing their subsequent clearance [**D**], thereby promoting hepatic resolution responses. Whilst acute liver injury reprograms tissue-infiltrating myeloid cells in a MerTK-dependent manner this may have the undesirable potential to impair anti-microbial responses in lymphatic and other tissue compartments [**E**] that may account for the immuneparesis in ALF patients.

CHAPTER 9

9. REFERENCES

Abeles, R.D., M.J. McPhail, D. Sowter, C.G. Antoniades, N. Vergis, G.K. Vijay, E. Xystrakis, W. Khamri, D.L. Shawcross, Y. Ma, J.A. Wendon, and D. Vergani. 2012. CD14, CD16 and HLA-DR reliably identifies human monocytes and their subsets in the context of pathologically reduced HLA-DR expression by CD14(hi) /CD16(neg) monocytes: Expansion of CD14(hi) /CD16(pos) and contraction of CD14(lo) /CD16(pos) monocytes in acute liver failure. *Cytometry. Part A : the journal of the International Society for Analytical Cytology* 81:823-834.

Abu-Tair, L., J.H. Axelrod, S. Doron, Y. Ovadya, V. Krizhanovsky, E. Galun, J. Amer, and R. Safadi. 2013. Natural killer cell-dependent anti-fibrotic pathway in liver injury via Toll-like receptor-9. *PloS one* 8:e82571.

Acharya, S.K., Y. Batra, S. Hazari, V. Choudhury, S.K. Panda, and S. Dattagupta. 2002. Etiopathogenesis of acute hepatic failure: Eastern versus Western countries. *J Gastroenterol Hepatol* 17 Suppl 3:S268-273.

Akitake-Kawano, R., H. Seno, M. Nakatsuji, Y. Kimura, Y. Nakanishi, T. Yoshioka, K. Kanda, M. Kawada, K. Kawada, Y. Sakai, and T. Chiba. 2013. Inhibitory role of Gas6 in intestinal tumorigenesis. *Carcinogenesis* 34:1567-1574.

Alessandri, A.L., L.P. Sousa, C.D. Lucas, A.G. Rossi, V. Pinho, and M.M. Teixeira. 2013. Resolution of inflammation: mechanisms and opportunity for drug development. *Pharmacol Ther* 139:189-212.

Antoniades, C.G., P.A. Berry, E.T. Davies, M. Hussain, W. Bernal, D. Vergani, and J. Wendon. 2006. Reduced monocyte HLA-DR expression: a novel biomarker of disease severity and outcome in acetaminophen-induced acute liver failure. *Hepatology* 44:34-43.

Antoniades, C.G., P.A. Berry, J.A. Wendon, and D. Vergani. 2008. The importance of immune dysfunction in determining outcome in acute liver failure. *Journal of hepatology* 49:845-861.

Antoniades, C.G., W. Khamri, R.D. Abeles, L.S. Taams, E. Triantafyllou, L.A. Possamai, C. Bernsmeier, R.R. Mitry, A. O'Brien, D. Gilroy, R. Goldin, M. Heneghan, N. Heaton, W. Jassem, W. Bernal, D. Vergani, Y. Ma, A. Quaglia, J. Wendon, and M. Thursz. 2014. Secretory leukocyte protease inhibitor: a pivotal mediator of anti-inflammatory responses in acetaminophen-induced acute liver failure. *Hepatology* 59:1564-1576.

Antoniades, C.G., A. Quaglia, L.S. Taams, R.R. Mitry, M. Hussain, R. Abeles, L.A. Possamai, M. Bruce, M. McPhail, C. Starling, B. Wagner, A. Barnardo, S. Pomplun, G. Auzinger, W. Bernal, N. Heaton, D. Vergani, M.R. Thursz, and J. Wendon. 2012. Source and characterization of hepatic macrophages in acetaminophen-induced acute liver failure in humans. *Hepatology* 56:735-746.

Anwar, A., A.K. Keating, D. Joung, S. Sather, G.K. Kim, K.K. Sawczyn, L. Brandao, P.M. Henson, and D.K. Graham. 2009. Mer tyrosine kinase (MerTK) promotes macrophage survival following exposure to oxidative stress. *Journal of leukocyte biology* 86:73-79.

Arandjelovic, S., and K.S. Ravichandran. 2015. Phagocytosis of apoptotic cells in homeostasis. *Nature immunology* 16:907-917.

Ashcroft, G.S., M.J. Jeong, J.J. Ashworth, M. Hardman, W. Jin, N. Moutsopoulos, T. Wild, N. McCartney-Francis, D. Sim, G. McGrady, X.Y. Song, and S.M. Wahl. 2012. Tumor necrosis factor-alpha (TNF-alpha) is a therapeutic target for impaired cutaneous wound healing. *Wound Repair Regen* 20:38-49.

Ashcroft, G.S., K.J. Lei, W.W. Jin, G. Longenecker, A.B. Kulkarni, T. Greenwell-Wild, H. Hale-Donze, G. McGrady, X.Y. Song, and S.M. Wahl. 2000. Secretory leukocyte protease inhibitor mediates non-redundant functions necessary for normal wound healing. *Nature Medicine* 6:1147-1153.

Aspinall, A.I., S.M. Curbishley, P.F. Lalor, C.J. Weston, M. Blahova, E. Liaskou, R.M. Adams, A.P. Holt, and D.H. Adams. 2010. CX(3)CR1 and vascular adhesion protein-1-dependent recruitment of CD16(+) monocytes across human liver sinusoidal endothelium. *Hepatology* 51:2030-2039.

Baeck, C., A. Wehr, K.R. Karlmark, F. Heymann, M. Vucur, N. Gassler, S. Huss, S. Klussmann, D. Eulberg, T. Luedde, C. Trautwein, and F. Tacke. 2012. Pharmacological inhibition of the chemokine CCL2 (MCP-1) diminishes liver macrophage infiltration and steatohepatitis in chronic hepatic injury. *Gut* 61:416-426.

Barcena, C., M. Stefanovic, A. Tutusaus, L. Joannas, A. Menendez, C. Garcia-Ruiz, P. Sancho-Bru, M. Mari, J. Caballeria, C.V. Rothlin, J.C. Fernandez-Checa, P.G. de Frutos, and A. Morales. 2015. Gas6/Axl pathway is activated in chronic liver disease and its targeting reduces fibrosis via hepatic stellate cell inactivation. *Journal of hepatology* 63:670-678.

Bellingan, G.J., H. Caldwell, S.E. Howie, I. Dransfield, and C. Haslett. 1996. In vivo fate of the inflammatory macrophage during the resolution of inflammation: inflammatory macrophages do not die locally, but emigrate to the draining lymph nodes. *Journal of immunology* 157:2577-2585.

Bellingan, G.J., P. Xu, H. Cooksley, H. Cauldwell, A. Shock, S. Bottoms, C. Haslett, S.E. Mutsaers, and G.J. Laurent. 2002. Adhesion molecule-dependent mechanisms regulate the rate of macrophage clearance during the resolution of peritoneal inflammation. *The Journal of experimental medicine* 196:1515-1521.

Bernal, W., G. Auzinger, A. Dhawan, and J. Wendon. 2010. Acute liver failure. *Lancet* 376:190-201.

Bernal, W., N. Donaldson, D. Wyncoll, and J. Wendon. 2002. Blood lactate as an early predictor of outcome in paracetamol-induced acute liver failure: a cohort study. *Lancet* 359:558-563.

Bernal, W., A. Hyyrylainen, A. Gera, V.K. Audimoolam, M.J. McPhail, G. Auzinger, M. Rela, N. Heaton, J.G. O'Grady, J. Wendon, and R. Williams. 2013. Lessons from look-back in acute liver failure? A single centre experience of 3300 patients. *Journal of hepatology* 59:74-80.

Bernal, W., W.M. Lee, J. Wendon, F.S. Larsen, and R. Williams. 2015. Acute liver failure: A curable disease by 2024? *Journal of hepatology* 62:S112-S120.

Bernsmeier, C., C.G. Antoniades, and J. Wendon. 2014. What's new in acute liver failure? *Intensive care medicine* 40:1545-1548.

Bernsmeier, C., O.T. Pop, A. Singanayagam, E. Triantafyllou, V.C. Patel, C.J. Weston, S. Curbishley, F. Sadiq, N. Vergis, W. Khamri, W. Bernal, G. Auzinger, M. Heneghan, Y. Ma, W. Jassem,

N.D. Heaton, D.H. Adams, A. Quaglia, M.R. Thursz, J. Wendon, and C.G. Antoniades. 2015. Patients with acute-on-chronic liver failure have increased numbers of regulatory immune cells expressing the receptor tyrosine kinase MERTK. *Gastroenterology* 148:603-615 e614.

Bhattacharyya, S., A. Zagorska, E.D. Lew, B. Shrestha, C.V. Rothlin, J. Naughton, M.S. Diamond, G. Lemke, and J.A. Young. 2013. Enveloped viruses disable innate immune responses in dendritic cells by direct activation of TAM receptors. *Cell Host Microbe* 14:136-147.

Biswas, S.K., and E. Lopez-Collazo. 2009. Endotoxin tolerance: new mechanisms, molecules and clinical significance. *Trends in immunology* 30:475-487.

Boltjes, A., D. Movita, A. Boonstra, and A.M. Woltman. 2014. The role of Kupffer cells in hepatitis B and hepatitis C virus infections. *Journal of hepatology* 61:660-671.

Bonder, C.S., M.N. Ajuebor, L.D. Zbytnuik, P. Kubes, and M.G. Swain. 2004. Essential role for neutrophil recruitment to the liver in concanavalin A-induced hepatitis. *J Immunol* 172:45-53.

Bosurgi, L., J.H. Bernink, V. Delgado Cuevas, N. Gagliani, L. Joannas, E.T. Schmid, C.J. Booth, S. Ghosh, and C.V. Rothlin. 2013. Paradoxical role of the proto-oncogene Axl and Mer receptor tyrosine kinases in colon cancer. *Proc Natl Acad Sci U S A* 110:13091-13096.

Bouchard, D., D. Morisset, Y. Bourbonnais, and G.M. Tremblay. 2006. Proteins with whey-acidic-protein motifs and cancer. *Lancet Oncol* 7:167-174.

Brown, S., I. Heinisch, E. Ross, K. Shaw, C.D. Buckley, and J. Savill. 2002. Apoptosis disables CD31-mediated cell detachment from phagocytes promoting binding and engulfment. *Nature* 418:200-203.

Buckley, C.D., D.W. Gilroy, and C.N. Serhan. 2014. Proresolving lipid mediators and mechanisms in the resolution of acute inflammation. *Immunity* 40:315-327.

Bystrom, J., I. Evans, J. Newson, M. Stables, I. Toor, N. van Rooijen, M. Crawford, P. Colville-Nash, S. Farrow, and D.W. Gilroy. 2008. Resolution-phase macrophages possess a unique inflammatory phenotype that is controlled by cAMP. *Blood* 112:4117-4127.

Caberoy, N.B., G. Alvarado, J.L. Bigcas, and W. Li. 2012. Galectin-3 is a new MerTK-specific eat-me signal. *Journal of cellular physiology* 227:401-407.

Camenisch, T.D., B.H. Koller, H.S. Earp, and G.K. Matsushima. 1999. A novel receptor tyrosine kinase, Mer, inhibits TNF-alpha production and lipopolysaccharide-induced endotoxic shock. *Journal of immunology* 162:3498-3503.

Carrera Silva, E.A., P.Y. Chan, L. Joannas, A.E. Errasti, N. Gagliani, L. Bosurgi, M. Jabbour, A. Perry, F. Smith-Chakmakova, D. Mucida, H. Cheroutre, T. Burstyn-Cohen, J.A. Leighton, G. Lemke, S. Ghosh, and C.V. Rothlin. 2013. T cell-derived protein S engages TAM receptor signaling in dendritic cells to control the magnitude of the immune response. *Immunity* 39:160-170.

Cash, J.L., L.V. Norling, and M. Perretti. 2014. Resolution of inflammation: targeting GPCRs that interact with lipids and peptides. *Drug Discov Today* 19:1186-1192.

Cavaillon, J.M., and M. Adib-Conquy. 2006. Bench-to-bedside review: endotoxin tolerance as a model of leukocyte reprogramming in sepsis. *Critical care* 10:233.

Cheong, H.S., S.O. Lee, C.B. Choi, Y.K. Sung, H.D. Shin, and S.C. Bae. 2007. MERTK polymorphisms associated with risk of haematological disorders among Korean SLE patients. *Rheumatology (Oxford)* 46:209-214.

Chiang, N., G. Fredman, F. Backhed, S.F. Oh, T. Vickery, B.A. Schmidt, and C.N. Serhan. 2012. Infection regulates pro-resolving mediators that lower antibiotic requirements. *Nature* 484:524-528.

Choi, D.Y., J.O. Ban, S.C. Kim, and J.T. Hong. 2015a. CCR5 knockout mice with C57BL6 background are resistant to acetaminophen-mediated hepatotoxicity due to decreased macrophages migration into the liver. *Archives of toxicology* 89:211-220.

Choi, J.Y., H.J. Park, Y.J. Lee, J. Byun, Y.S. Youn, J.H. Choi, S.Y. Woo, and J.L. Kang. 2013. Upregulation of Mer receptor tyrosine kinase signaling attenuated lipopolysaccharide-induced lung inflammation. *The Journal of pharmacology and experimental therapeutics* 344:447-458.

Choi, J.Y., J.Y. Seo, Y.S. Yoon, Y.J. Lee, H.S. Kim, and J.L. Kang. 2015b. Mer signaling increases the abundance of the transcription factor LXR to promote the resolution of acute sterile inflammation. *Sci Signal* 8:ra21.

Chung, R.T., R.T. Stravitz, R.J. Fontana, F.V. Schiodt, W.Z. Mehal, K.R. Reddy, and W.M. Lee. 2012. Pathogenesis of liver injury in acute liver failure. *Gastroenterology* 143:e1-7.

Cohen, P.L., R. Caricchio, V. Abraham, T.D. Camenisch, J.C. Jennette, R.A. Roubey, H.S. Earp, G. Matsushima, and E.A. Reap. 2002. Delayed apoptotic cell clearance and lupus-like autoimmunity in mice lacking the c-mer membrane tyrosine kinase. *The Journal of experimental medicine* 196:135-140.

Connolly, M.K., D. Ayo, A. Malhotra, M. Hackman, A.S. Bedrosian, J. Ibrahim, N.E. Cieza-Rubio, A.H. Nguyen, J.R. Henning, M. Dorvil-Castro, H.L. Pachter, and G. Miller. 2011. Dendritic cell depletion exacerbates acetaminophen hepatotoxicity. *Hepatology* 54:959-968.

Cook, R.S., K.M. Jacobsen, A.M. Wofford, D. DeRyckere, J. Stanford, A.L. Prieto, E. Redente, M. Sandahl, D.M. Hunter, K.E. Strunk, D.K. Graham, and H.S. Earp, 3rd. 2013. MerTK inhibition in tumor leukocytes decreases tumor growth and metastasis. *The Journal of clinical investigation* 123:3231-3242.

Cover, C., J. Liu, A. Farhood, E. Malle, M.P. Waalkes, M.L. Bajt, and H. Jaeschke. 2006. Pathophysiological role of the acute inflammatory response during acetaminophen hepatotoxicity. *Toxicology and applied pharmacology* 216:98-107.

Crane, M.J., J.M. Daley, O. van Houtte, S.K. Brancato, W.L. Henry, Jr., and J.E. Albina. 2014. The monocyte to macrophage transition in the murine sterile wound. *PloS one* 9:e86660.

Crispe, I.N. 2009. The liver as a lymphoid organ. *Annual review of immunology* 27:147-163.

Csak, T., A. Pillai, M. Ganz, D. Lippai, J. Petrasek, J.K. Park, K. Kodys, A. Dolganiuc, E.A. Kurt-Jones, and G. Szabo. 2014. Both bone marrow-derived and non-bone marrow-derived cells contribute to AIM2 and NLRP3 inflammasome activation in a MyD88-dependent manner in dietary steatohepatitis. *Liver international : official journal of the International Association for the Study of the Liver* 34:1402-1413.

Dahlback, B. 2000. Blood coagulation. *Lancet* 355:1627-1632.

Dal-Secco, D., J. Wang, Z. Zeng, E. Kolaczkowska, C.H. Wong, B. Petri, R.M. Ransohoff, I.F. Charo, C.N. Jenne, and P. Kubes. 2015. A dynamic spectrum of monocytes arising from the

in situ reprogramming of CCR2+ monocytes at a site of sterile injury. *The Journal of experimental medicine* 212:447-456.

Dambach, D.M., L.M. Watson, K.R. Gray, S.K. Durham, and D.L. Laskin. 2002. Role of CCR2 in macrophage migration into the liver during acetaminophen-induced hepatotoxicity in the mouse. *Hepatology* 35:1093-1103.

David, B.A., R.M. Rezende, M.M. Antunes, M.M. Santos, M.A. Freitas Lopes, A.B. Diniz, R.V. Sousa Pereira, S.C. Marchesi, D.M. Alvarenga, B.N. Nakagaki, A.M. Araujo, D.S. Dos Reis, R.M. Rocha, P.E. Marques, W.Y. Lee, J. Deniset, P.X. Liew, S. Rubino, L. Cox, V. Pinho, T.M. Cunha, G.R. Fernandes, A.G. Oliveira, M.M. Teixeira, P. Kubes, and G.B. Menezes. 2016. Combination of Mass Cytometry and Imaging Analysis Reveals Origin, Location, and Functional Repopulation of Liver Myeloid Cells in Mice. *Gastroenterology* 151:1176-1191.

Davies, L.C., S.J. Jenkins, J.E. Allen, and P.R. Taylor. 2013. Tissue-resident macrophages. *Nature immunology* 14:986-995.

Ding, A., N. Thieblemont, J. Zhu, F. Jin, J. Zhang, and S. Wright. 1999. Secretory leukocyte protease inhibitor interferes with uptake of lipopolysaccharide by macrophages. *Infection and immunity* 67:4485-4489.

Donaghy, L., F.J. Barry, J.G. Hunter, W. Stableforth, I.A. Murray, J. Palmer, R.P. Bendall, A.M. Elsharkawy, and H.R. Dalton. 2013. Clinical and laboratory features and natural history of seronegative hepatitis in a nontransplant centre. *European Journal of Gastroenterology & Hepatology* 25:1159-1164.

Dragomir, A.C., R. Sun, H. Choi, J.D. Laskin, and D.L. Laskin. 2012. Role of galectin-3 in classical and alternative macrophage activation in the liver following acetaminophen intoxication. *Journal of immunology* 189:5934-5941.

Duncan, J.L., M.M. LaVail, D. Yasumura, M.T. Matthes, H. Yang, N. Trautmann, A.V. Chappelow, W. Feng, H.S. Earp, G.K. Matsushima, and D. Vollrath. 2003. An RCS-like retinal dystrophy phenotype in mer knockout mice. *Invest Ophthalmol Vis Sci* 44:826-838.

Dunn, C., M. Brunetto, G. Reynolds, T. Christophides, P.T. Kennedy, P. Lampertico, A. Das, A.R. Lopes, P. Borrow, K. Williams, E. Humphreys, S. Afford, D.H. Adams, A. Bertoletti, and

M.K. Maini. 2007. Cytokines induced during chronic hepatitis B virus infection promote a pathway for NK cell-mediated liver damage. *The Journal of experimental medicine* 204:667-680.

Ehling, J., M. Bartneck, X. Wei, F. Gremse, V. Fech, D. Mockel, C. Baeck, K. Hittatiya, D. Eulberg, T. Luedde, F. Kiessling, C. Trautwein, T. Lammers, and F. Tacke. 2014. CCL2-dependent infiltrating macrophages promote angiogenesis in progressive liver fibrosis. *Gut* 63:1960-1971.

Eisenhardt, M., A. Glassner, B. Kramer, C. Korner, B. Sibbing, P. Kokordelis, H.D. Nischalke, T. Sauerbruch, U. Spengler, and J. Nattermann. 2012. The CXCR3(+)CD56Bright phenotype characterizes a distinct NK cell subset with anti-fibrotic potential that shows dys-regulated activity in hepatitis C. *PloS one* 7:e38846.

Epelman, S., K.J. Lavine, and G.J. Randolph. 2014. Origin and functions of tissue macrophages. *Immunity* 41:21-35.

Fadok, V.A., D.L. Bratton, A. Konowal, P.W. Freed, J.Y. Westcott, and P.M. Henson. 1998. Macrophages that have ingested apoptotic cells in vitro inhibit proinflammatory cytokine production through autocrine/paracrine mechanisms involving TGF-beta, PGE2, and PAF. *The Journal of clinical investigation* 101:890-898.

Fadok, V.A., A. de Cathelineau, D.L. Daleke, P.M. Henson, and D.L. Bratton. 2001. Loss of phospholipid asymmetry and surface exposure of phosphatidylserine is required for phagocytosis of apoptotic cells by macrophages and fibroblasts. *The Journal of biological chemistry* 276:1071-1077.

Fadok, V.A., and P.M. Henson. 1998. Apoptosis: getting rid of the bodies. *Curr Biol* 8:R693-695.

Fadok, V.A., and P.M. Henson. 2003. Apoptosis: giving phosphatidylserine recognition an assist--with a twist. *Curr Biol* 13:R655-657.

Feng, G., and N. Kaplowitz. 2002. Mechanism of staurosporine-induced apoptosis in murine hepatocytes. *Am J Physiol Gastrointest Liver Physiol* 282:G825-834.

Filardy, A.A., D.R. Pires, M.P. Nunes, C.M. Takiya, C.G. Freire-de-Lima, F.L. Ribeiro-Gomes, and G.A. DosReis. 2010. Proinflammatory clearance of apoptotic neutrophils induces an IL-

12(low)IL-10(high) regulatory phenotype in macrophages. *Journal of immunology* 185:2044-2050.

Fletcher, N.F., R. Sutaria, J. Jo, A. Barnes, M. Blahova, L.W. Meredith, F.L. Cosset, S.M. Curbishley, D.H. Adams, A. Bertoletti, and J.A. McKeating. 2014. Activated macrophages promote hepatitis C virus entry in a tumor necrosis factor-dependent manner. *Hepatology* 59:1320-1330.

Fourcot, A., D. Couchie, M.N. Chobert, E.S. Zafrani, P. Mavier, Y. Laperche, and A. Brouillet. 2011. Gas6 deficiency prevents liver inflammation, steatohepatitis, and fibrosis in mice. *Am J Physiol Gastrointest Liver Physiol* 300:G1043-1053.

Fox, S., A.E. Leitch, R. Duffin, C. Haslett, and A.G. Rossi. 2010. Neutrophil apoptosis: relevance to the innate immune response and inflammatory disease. *Journal of innate immunity* 2:216-227.

Fullerton, J.N., and D.W. Gilroy. 2016. Resolution of inflammation: a new therapeutic frontier. *Nat Rev Drug Discov* 15:551-567.

Gaipl, U.S., A. Kuhn, A. Sheriff, L.E. Munoz, S. Franz, R.E. Voll, J.R. Kalden, and M. Herrmann. 2006. Clearance of apoptotic cells in human SLE. *Curr Dir Autoimmun* 9:173-187.

Gardai, S.J., K.A. McPhillips, S.C. Frasch, W.J. Janssen, A. Starefeldt, J.E. Murphy-Ullrich, D.L. Bratton, P.A. Oldenborg, M. Michalak, and P.M. Henson. 2005. Cell-surface calreticulin initiates clearance of viable or apoptotic cells through trans-activation of LRP on the phagocyte. *Cell* 123:321-334.

Geering, B., and H.U. Simon. 2011. Peculiarities of cell death mechanisms in neutrophils. *Cell Death Differ* 18:1457-1469.

Gilroy, D., and R. De Maeyer. 2015. New insights into the resolution of inflammation. *Semin Immunol* 27:161-168.

Ginhoux, F., and S. Jung. 2014. Monocytes and macrophages: developmental pathways and tissue homeostasis. *Nature reviews. Immunology* 14:392-404.

Ginhoux, F., J.L. Schultze, P.J. Murray, J. Ochando, and S.K. Biswas. 2016. New insights into the multidimensional concept of macrophage ontogeny, activation and function. *Nature immunology* 17:34-40.

Gomez Perdiguero, E., K. Klapproth, C. Schulz, K. Busch, E. Azzoni, L. Crozet, H. Garner, C. Trouillet, M.F. de Bruijn, F. Geissmann, and H.R. Rodewald. 2015. Tissue-resident macrophages originate from yolk-sac-derived erythro-myeloid progenitors. *Nature* 518:547-551.

Gordon, S., and P.R. Taylor. 2005. Monocyte and macrophage heterogeneity. *Nature reviews. Immunology* 5:953-964.

Grabiec, A.M., and T. Hussell. 2016. The role of airway macrophages in apoptotic cell clearance following acute and chronic lung inflammation. *Semin Immunopathol* 38:409-423.

Graham, D.K., D. DeRyckere, K.D. Davies, and H.S. Earp. 2014. The TAM family: phosphatidylserine sensing receptor tyrosine kinases gone awry in cancer. *Nat Rev Cancer* 14:769-785.

Gray, E.E., and J.G. Cyster. 2012. Lymph node macrophages. *Journal of innate immunity* 4:424-436.

Gregory, C.D., and J.D. Pound. 2010. Microenvironmental influences of apoptosis in vivo and in vitro. *Apoptosis* 15:1029-1049.

Grobmyer, S.R., P.S. Barie, C.F. Nathan, M. Fuortes, E. Lin, S.F. Lowry, C.D. Wright, M.J. Weyant, L. Hydo, F. Reeves, M.U. Shiloh, and A.H. Ding. 2000. Secretory leukocyte protease inhibitor, an inhibitor of neutrophil activation, is elevated in serum in human sepsis and experimental endotoxemia. *Critical Care Medicine* 28:1276-1282.

Hannila, S.S., M.M. Siddiq, J.B. Carmel, J. Hou, N. Chaudhry, P.M. Bradley, M. Hilaire, E.L. Richman, R.P. Hart, and M.T. Filbin. 2013. Secretory leukocyte protease inhibitor reverses inhibition by CNS myelin, promotes regeneration in the optic nerve, and suppresses expression of the transforming growth factor-beta signaling protein Smad2. *J Neurosci* 33:5138-5151.

Headland, S.E., and L.V. Norling. 2015. The resolution of inflammation: Principles and challenges. *Semin Immunol* 27:149-160.

Heymann, F., L. Hammerich, D. Storch, M. Bartneck, S. Huss, V. Russeler, N. Gassler, S.A. Lira, T. Luedde, C. Trautwein, and F. Tacke. 2012. Hepatic macrophage migration and differentiation

critical for liver fibrosis is mediated by the chemokine receptor C-C motif chemokine receptor 8 in mice. *Hepatology* 55:898-909.

Heymann, F., and F. Tacke. 2016. Immunology in the liver--from homeostasis to disease. *Nat Rev Gastroenterol Hepatol* 13:88-110.

Hiemstra, P.S., R.J. Maassen, J. Stolk, R. Heinzel-Wieland, G.J. Steffens, and J.H. Dijkman. 1996. Antibacterial activity of antileukoprotease. *Infection and immunity* 64:4520-4524.

Hirschfield, G.M., E.J. Heathcote, and M.E. Gershwin. 2010. Pathogenesis of cholestatic liver disease and therapeutic approaches. *Gastroenterology* 139:1481-1496.

Hogaboam, C.M., C.L. Bone-Larson, M.L. Steinhauser, A. Matsukawa, J. Gosling, L. Boring, I.F. Charo, K.J. Simpson, N.W. Lukacs, and S.L. Kunkel. 2000. Exaggerated hepatic injury due to acetaminophen challenge in mice lacking C-C chemokine receptor 2. *Am J Pathol* 156:1245-1252.

Holt, M.P., L. Cheng, and C. Ju. 2008. Identification and characterization of infiltrating macrophages in acetaminophen-induced liver injury. *Journal of leukocyte biology* 84:1410-1421.

Hong, C., Y. Kidani, A.G. N, T. Phung, A. Ito, X. Rong, K. Ericson, H. Mikkola, S.W. Beaven, L.S. Miller, W.H. Shao, P.L. Cohen, A. Castrillo, P. Tontonoz, and S.J. Bensinger. 2012. Coordinate regulation of neutrophil homeostasis by liver X receptors in mice. *The Journal of clinical investigation* 122:337-347.

Hornbeck, P.V., J.M. Kornhauser, S. Tkachev, B. Zhang, E. Skrzypek, B. Murray, V. Latham, and M. Sullivan. 2012. PhosphoSitePlus: a comprehensive resource for investigating the structure and function of experimentally determined post-translational modifications in man and mouse. *Nucleic Acids Res* 40:D261-270.

Hotchkiss, R.S., G. Monneret, and D. Payen. 2013a. Immunosuppression in sepsis: a novel understanding of the disorder and a new therapeutic approach. *Lancet Infect Dis* 13:260-268.

Hotchkiss, R.S., G. Monneret, and D. Payen. 2013b. Sepsis-induced immunosuppression: from cellular dysfunctions to immunotherapy. *Nature reviews. Immunology* 13:862-874.

Huang, H., S. Tohme, A.B. Al-Khafaji, S. Tai, P. Loughran, L. Chen, S. Wang, J. Kim, T. Billiar, Y. Wang, and A. Tsung. 2015. Damage-associated molecular pattern-activated neutrophil extracellular trap exacerbates sterile inflammatory liver injury. *Hepatology* 62:600-614.

Ingersoll, M.A., R. Spanbroek, C. Lottaz, E.L. Gautier, M. Frankenberger, R. Hoffmann, R. Lang, M. Haniffa, M. Collin, F. Tacke, A.J. Habenicht, L. Ziegler-Heitbrock, and G.J. Randolph. 2010. Comparison of gene expression profiles between human and mouse monocyte subsets. *Blood* 115:e10-19.

Ishida, Y., T. Kondo, A. Kimura, K. Tsuneyama, T. Takayasu, and N. Mukaida. 2006. Opposite roles of neutrophils and macrophages in the pathogenesis of acetaminophen-induced acute liver injury. *Eur J Immunol* 36:1028-1038.

Ishida, Y., T. Kondo, T. Ohshima, H. Fujiwara, Y. Iwakura, and N. Mukaida. 2002. A pivotal involvement of IFN-gamma in the pathogenesis of acetaminophen-induced acute liver injury. *FASEB J* 16:1227-1236.

Jaeschke, H. 2002. Neutrophil-mediated tissue injury in alcoholic hepatitis. *Alcohol* 27:23-27.

Jaeschke, H., and J. Liu. 2007. Neutrophil depletion protects against murine acetaminophen hepatotoxicity: another perspective. *Hepatology* 45:1588-1589; author reply 1589.

Jaeschke, H., M.R. McGill, and C.D. Williams. 2013. Pathophysiological relevance of neutrophils in acetaminophen hepatotoxicity. *Hepatology* 57:419.

Jakubzick, C., E.L. Gautier, S.L. Gibbings, D.K. Sojka, A. Schlitzer, T.E. Johnson, S. Ivanov, Q. Duan, S. Bala, T. Condon, N. van Rooijen, J.R. Grainger, Y. Belkaid, A. Ma'ayan, D.W. Riches, W.M. Yokoyama, F. Ginhoux, P.M. Henson, and G.J. Randolph. 2013. Minimal differentiation of classical monocytes as they survey steady-state tissues and transport antigen to lymph nodes. *Immunity* 39:599-610.

Jenne, C.N., C.H. Wong, F.J. Zemp, B. McDonald, M.M. Rahman, P.A. Forsyth, G. McFadden, and P. Kubes. 2013. Neutrophils recruited to sites of infection protect from virus challenge by releasing neutrophil extracellular traps. *Cell Host Microbe* 13:169-180.

Ji, R., S. Tian, H.J. Lu, Q. Lu, Y. Zheng, X. Wang, J. Ding, Q. Li, and Q. Lu. 2013. TAM receptors affect adult brain neurogenesis by negative regulation of microglial cell activation. *Journal of immunology* 191:6165-6177.

Jin, F.Y., C. Nathan, D. Radzioch, and A. Ding. 1997. Secretory leukocyte protease inhibitor: a macrophage product induced by and antagonistic to bacterial lipopolysaccharide. *Cell* 88:417-426.

Ju, C., T.P. Reilly, M. Bourdi, M.F. Radonovich, J.N. Brady, J.W. George, and L.R. Pohl. 2002a. Protective role of Kupffer cells in acetaminophen-induced hepatic injury in mice. *Chem Res Toxicol* 15:1504-1513.

Ju, C., T.P. Reilly, M. Bourdi, M.F. Radonovich, J.N. Brady, J.W. George, and L.R. Pohl. 2002b. Protective role of Kupffer cells in acetaminophen-induced hepatic injury in mice. *Chem Res Toxicol* 15:1504-1513.

Karlmark, K.R., R. Weiskirchen, H.W. Zimmermann, N. Gassler, F. Ginhoux, C. Weber, M. Merad, T. Luedde, C. Trautwein, and F. Tacke. 2009. Hepatic recruitment of the inflammatory Gr1+ monocyte subset upon liver injury promotes hepatic fibrosis. *Hepatology* 50:261-274.

Kastenmuller, W., P. Torabi-Parizi, N. Subramanian, T. Lammermann, and R.N. Germain. 2012. A spatially-organized multicellular innate immune response in lymph nodes limits systemic pathogen spread. *Cell* 150:1235-1248.

Keating, A.K., G.K. Kim, A.E. Jones, A.M. Donson, K. Ware, J.M. Mulcahy, D.B. Salzberg, N.K. Foreman, X. Liang, A. Thorburn, and D.K. Graham. 2010. Inhibition of Mer and Axl receptor tyrosine kinases in astrocytoma cells leads to increased apoptosis and improved chemosensitivity. *Mol Cancer Ther* 9:1298-1307.

Kenna, T., L. Golden-Mason, S.A. Porcelli, Y. Koezuka, J.E. Hegarty, C. O'Farrelly, and D.G. Doherty. 2003. NKT cells from normal and tumor-bearing human livers are phenotypically and functionally distinct from murine NKT cells. *Journal of immunology* 171:1775-1779.

Khamri, W., R.D. Abeles, T.Z. Hou, A.E. Anderson, A. El-Masry, E. Triantafyllou, C. Bernsmeier, F.S. Larsen, A. Singanayagam, N. Kudo, L.A. Possamai, F. Lebosse, G. Auzinger, W. Bernal, C. Willars, C.J. Weston, G. Lombardi, J. Wendon, M. Thursz, and C.G. Antoniades. 2017.

Increased Expression of CTLA4 by T Cells, Induced by B7 in Sera, Reduces Adaptive Immunity in Patients With Acute Liver Failure. *Gastroenterology*

Klimenkova, O., W. Ellerbeck, M. Klimiankou, M. Unalan, S. Kandabarau, A. Gigina, K. Hussein, C. Zeidler, K. Welte, and J. Skokowa. 2014. A lack of secretory leukocyte protease inhibitor (SLPI) causes defects in granulocytic differentiation. *Blood* 123:1239-1249.

Kolaczkowska, E., C.N. Jenne, B.G. Surewaard, A. Thanabalasuriar, W.Y. Lee, M.J. Sanz, K. Mowen, G. Opdenakker, and P. Kubes. 2015. Molecular mechanisms of NET formation and degradation revealed by intravital imaging in the liver vasculature. *Nat Commun* 6:6673.

Kramer, B., C. Korner, M. Kebschull, A. Glassner, M. Eisenhardt, H.D. Nischalke, M. Alexander, T. Sauerbruch, U. Spengler, and J. Nattermann. 2012. Natural killer p46High expression defines a natural killer cell subset that is potentially involved in control of hepatitis C virus replication and modulation of liver fibrosis. *Hepatology* 56:1201-1213.

Krenkel, O., J.C. Mossanen, and F. Tacke. 2014. Immune mechanisms in acetaminophen-induced acute liver failure. *Hepatobiliary surgery and nutrition* 3:331-343.

Krenkel, O., and F. Tacke. 2017. Liver macrophages in tissue homeostasis and disease. *Nature reviews. Immunology* 17:306-321.

Krueger, P.D., M.G. Lassen, H. Qiao, and Y.S. Hahn. 2011. Regulation of NK cell repertoire and function in the liver. *Crit Rev Immunol* 31:43-52.

Kubes, P., and W.Z. Mehal. 2012. Sterile inflammation in the liver. *Gastroenterology* 143:1158-1172.

Lai, C., and G. Lemke. 1991. An extended family of protein-tyrosine kinase genes differentially expressed in the vertebrate nervous system. *Neuron* 6:691-704.

Lanier, L.L. 2005. NK cell recognition. *Annual review of immunology* 23:225-274.

Laskin, D.L., C.R. Gardner, V.F. Price, and D.J. Jollow. 1995. Modulation of macrophage functioning abrogates the acute hepatotoxicity of acetaminophen. *Hepatology* 21:1045-1050.

Lavin, Y., D. Winter, R. Blecher-Gonen, E. David, H. Keren-Shaul, M. Merad, S. Jung, and I. Amit. 2014. Tissue-resident macrophage enhancer landscapes are shaped by the local microenvironment. *Cell* 159:1312-1326.

Lawson, J.A., A. Farhood, R.D. Hopper, M.L. Bajt, and H. Jaeschke. 2000. The hepatic inflammatory response after acetaminophen overdose: role of neutrophils. *Toxicological sciences : an official journal of the Society of Toxicology* 54:509-516.

Le Bourhis, L., E. Martin, I. Peguillet, A. Guihot, N. Froux, M. Core, E. Levy, M. Dusseaux, V. Meyssonnier, V. Premel, C. Ngo, B. Riteau, L. Duban, D. Robert, S. Huang, M. Rottman, C. Soudais, and O. Lantz. 2010. Antimicrobial activity of mucosal-associated invariant T cells. *Nature immunology* 11:701-708.

Lee, K.A., Y.C. Song, G.Y. Kim, G. Choi, Y.S. Lee, J.M. Lee, and C.Y. Kang. 2012a. Retinoic acid alleviates Con A-induced hepatitis and differentially regulates effector production in NKT cells. *Eur J Immunol* 42:1685-1694.

Lee, Y.J., J.Y. Han, J. Byun, H.J. Park, E.M. Park, Y.H. Chong, M.S. Cho, and J.L. Kang. 2012b. Inhibiting Mer receptor tyrosine kinase suppresses STAT1, SOCS1/3, and NF-kappaB activation and enhances inflammatory responses in lipopolysaccharide-induced acute lung injury. *Journal of leukocyte biology* 91:921-932.

Lee, Y.J., S.H. Lee, Y.S. Youn, J.Y. Choi, K.S. Song, M.S. Cho, and J.L. Kang. 2012c. Preventing cleavage of Mer promotes efferocytosis and suppresses acute lung injury in bleomycin treated mice. *Toxicology and applied pharmacology* 263:61-72.

Lemke, G., and T. Burstyn-Cohen. 2010. TAM receptors and the clearance of apoptotic cells. *Annals of the New York Academy of Sciences* 1209:23-29.

Lemke, G., and C.V. Rothlin. 2008. Immunobiology of the TAM receptors. *Nature reviews. Immunology* 8:327-336.

Lentsch, A.B., J.A. Jordan, B.J. Czermak, K.M. Diehl, E.M. Younkin, V. Sarma, and P.A. Ward. 1999. Inhibition of NF-kappaB activation and augmentation of IkappaBbeta by secretory leukocyte protease inhibitor during lung inflammation. *The American journal of pathology* 154:239-247.

Leroux, A., G. Ferrere, V. Godie, F. Cailleux, M.L. Renoud, F. Gaudin, S. Naveau, S. Prevot, S. Makhzami, G. Perlemuter, and A.M. Cassard-Doulcier. 2012. Toxic lipids stored by Kupffer

cells correlates with their pro-inflammatory phenotype at an early stage of steatohepatitis. *Journal of hepatology* 57:141-149.

Lew, E.D., J. Oh, P.G. Burrola, I. Lax, A. Zagorska, P.G. Traves, J. Schlessinger, and G. Lemke. 2014. Differential TAM receptor-ligand-phospholipid interactions delimit differential TAM bioactivities. *eLife* 3:

Liang, W., J.H. Lindeman, A.L. Menke, D.P. Koonen, M. Morrison, L.M. Havekes, A.M. van den Hoek, and R. Kleemann. 2014. Metabolically induced liver inflammation leads to NASH and differs from LPS- or IL-1beta-induced chronic inflammation. *Lab Invest* 94:491-502.

Liaskou, E., L.E. Jeffery, P.J. Trivedi, G.M. Reynolds, S. Suresh, T. Bruns, D.H. Adams, D.M. Sansom, and G.M. Hirschfield. 2014. Loss of CD28 expression by liver-infiltrating T cells contributes to pathogenesis of primary sclerosing cholangitis. *Gastroenterology* 147:221-232 e227.

Liaskou, E., D.V. Wilson, and Y.H. Oo. 2012. Innate immune cells in liver inflammation. *Mediators of inflammation* 2012:949157.

Liaskou, E., H.W. Zimmermann, K.K. Li, Y.H. Oo, S. Suresh, Z. Stamataki, O. Qureshi, P.F. Lalor, J. Shaw, W.K. Syn, S.M. Curbishley, and D.H. Adams. 2013. Monocyte subsets in human liver disease show distinct phenotypic and functional characteristics. *Hepatology* 57:385-398.

Ling, L., D. Templeton, and H.J. Kung. 1996. Identification of the major autophosphorylation sites of Nyk/Mer, an NCAM-related receptor tyrosine kinase. *The Journal of biological chemistry* 271:18355-18362.

Linger, R.M., A.K. Keating, H.S. Earp, and D.K. Graham. 2010. Taking aim at Mer and Axl receptor tyrosine kinases as novel therapeutic targets in solid tumors. *Expert Opin Ther Targets* 14:1073-1090.

Liu, Z.X., S. Govindarajan, and N. Kaplowitz. 2004. Innate immune system plays a critical role in determining the progression and severity of acetaminophen hepatotoxicity. *Gastroenterology* 127:1760-1774.

Liu, Z.X., D. Han, B. Gunawan, and N. Kaplowitz. 2006. Neutrophil depletion protects against murine acetaminophen hepatotoxicity. *Hepatology* 43:1220-1230.

Llacuna, L., C. Barcena, L. Bellido-Martin, L. Fernandez, M. Stefanovic, M. Mari, C. Garcia-Ruiz, J.C. Fernandez-Checa, P. Garcia de Frutos, and A. Morales. 2010. Growth arrest-specific protein 6 is hepatoprotective against murine ischemia/reperfusion injury. *Hepatology* 52:1371-1379.

Lleo, A., L. Maroni, S. Glaser, G. Alpini, and M. Marzioni. 2014. Role of cholangiocytes in primary biliary cirrhosis. *Semin Liver Dis* 34:273-284.

Loges, S., T. Schmidt, M. Tjwa, K. van Geyte, D. Lievens, E. Lutgens, D. Vanhoutte, D. Borgel, S. Plaisance, M. Hoylaerts, A. Luttun, M. Dewerchin, B. Jonckx, and P. Carmeliet. 2010. Malignant cells fuel tumor growth by educating infiltrating leukocytes to produce the mitogen Gas6. *Blood* 115:2264-2273.

Lu, Q., and G. Lemke. 2001. Homeostatic regulation of the immune system by receptor tyrosine kinases of the Tyro 3 family. *Science* 293:306-311.

Ma, G., T. Greenwell-Wild, K. Lei, W. Jin, J. Swisher, N. Hardegen, C.T. Wild, and S.M. Wahl. 2004. Secretory leukocyte protease inhibitor binds to annexin II, a cofactor for macrophage HIV-1 infection. *The Journal of experimental medicine* 200:1337-1346.

Ma, G.Z., J. Stankovich, Australia, C. New Zealand Multiple Sclerosis Genetics, T.J. Kilpatrick, M.D. Binder, and J. Field. 2011. Polymorphisms in the receptor tyrosine kinase MERTK gene are associated with multiple sclerosis susceptibility. *PloS one* 6:e16964.

Maghazachi, A.A. 2010. Role of chemokines in the biology of natural killer cells. *Curr Top Microbiol Immunol* 341:37-58.

Majchrzak-Gorecka, M., P. Majewski, B. Grygier, K. Murzyn, and J. Cichy. 2016. Secretory leukocyte protease inhibitor (SLPI), a multifunctional protein in the host defense response. *Cytokine Growth Factor Rev* 28:79-93.

Marino, R., T. Thuraisingam, P. Camateros, C. Kanagaratham, Y.Z. Xu, J. Henri, J. Yang, G. He, A. Ding, and D. Radzioch. 2011. Secretory leukocyte protease inhibitor plays an important role in the regulation of allergic asthma in mice. *Journal of immunology* 186:4433-4442.

Marquardt, N., V. Beziat, S. Nystrom, J. Hengst, M.A. Ivarsson, E. Kekalainen, H. Johansson, J. Mjosberg, M. Westgren, T.O. Lankisch, H. Wedemeyer, E.C. Ellis, H.G. Ljunggren, J.

Michaelsson, and N.K. Bjorkstrom. 2015. Cutting edge: identification and characterization of human intrahepatic CD49a+ NK cells. *Journal of immunology* 194:2467-2471.

Marques, P.E., S.S. Amaral, D.A. Pires, L.L. Nogueira, F.M. Soriani, B.H. Lima, G.A. Lopes, R.C. Russo, T.V. Avila, J.G. Melgaco, A.G. Oliveira, M.A. Pinto, C.X. Lima, A.M. De Paula, D.C. Cara, M.F. Leite, M.M. Teixeira, and G.B. Menezes. 2012. Chemokines and mitochondrial products activate neutrophils to amplify organ injury during mouse acute liver failure. *Hepatology* 56:1971-1982.

Marra, F., and F. Tacke. 2014. Roles for chemokines in liver disease. *Gastroenterology* 147:577-594 e571.

Martin-Murphy, B.V., D.J. Kominsky, D.J. Orlicky, T.M. Donohue, Jr., and C. Ju. 2013. Increased susceptibility of natural killer T-cell-deficient mice to acetaminophen-induced liver injury. *Hepatology* 57:1575-1584.

Masson, M.J., L.D. Carpenter, M.L. Graf, and L.R. Pohl. 2008. Pathogenic role of natural killer T and natural killer cells in acetaminophen-induced liver injury in mice is dependent on the presence of dimethyl sulfoxide. *Hepatology* 48:889-897.

McCartney-Francis, N., W. Jin, Y. Belkaid, G. McGrady, and S.M. Wahl. 2014. Aberrant host defense against Leishmania major in the absence of SLPI. *Journal of leukocyte biology* 96:917-929.

McDonald, B., K. Pittman, G.B. Menezes, S.A. Hirota, I. Slaba, C.C. Waterhouse, P.L. Beck, D.A. Muruve, and P. Kubes. 2010. Intravascular danger signals guide neutrophils to sites of sterile inflammation. *Science* 330:362-366.

McDonald, B., R. Urrutia, B.G. Yipp, C.N. Jenne, and P. Kubes. 2012. Intravascular neutrophil extracellular traps capture bacteria from the bloodstream during sepsis. *Cell Host Microbe* 12:324-333.

McGarry, N., C.M. Greene, N.G. McElvaney, S. Weldon, and C.C. Taggart. 2015. The Ability of Secretory Leukocyte Protease Inhibitor to Inhibit Apoptosis in Monocytes Is Independent of Its Antiprotease Activity. *Journal of immunology research* 2015:507315.

McGrath, E.E., H.M. Marriott, A. Lawrie, S.E. Francis, I. Sabroe, S.A. Renshaw, D.H. Dockrell, and M.K. Whyte. 2011. TNF-related apoptosis-inducing ligand (TRAIL) regulates inflammatory neutrophil apoptosis and enhances resolution of inflammation. *Journal of leukocyte biology* 90:855-865.

McNelis, J.C., and J.M. Olefsky. 2014. Macrophages, immunity, and metabolic disease. *Immunity* 41:36-48.

Medeiros, A.I., C.H. Serezani, S.P. Lee, and M. Peters-Golden. 2009. Efferocytosis impairs pulmonary macrophage and lung antibacterial function via PGE2/EP2 signaling. *The Journal of experimental medicine* 206:61-68.

Meertens, L., X. Carnec, M.P. Lecoin, R. Ramdasi, F. Guivel-Benhassine, E. Lew, G. Lemke, O. Schwartz, and A. Amara. 2012. The TIM and TAM families of phosphatidylserine receptors mediate dengue virus entry. *Cell Host Microbe* 12:544-557.

Menckeberg, C.L., J. Hol, Y. Simons-Oosterhuis, H.R. Raatgeep, L.F. de Ruiter, D.J. Lindenbergh-Kortleve, A.M. Korteland-van Male, S. El Aidy, P.P. van Lierop, M. Kleerebezem, M. Groeneweg, G. Kraal, B.E. Elink-Schuurman, J.C. de Jongste, E.E. Nieuwenhuis, and J.N. Samsom. 2015. Human buccal epithelium acquires microbial hyporesponsiveness at birth, a role for secretory leukocyte protease inhibitor. *Gut* 64:884-893.

Mercer, J., and A. Helenius. 2010. Apoptotic mimicry: phosphatidylserine-mediated macropinocytosis of vaccinia virus. *Annals of the New York Academy of Sciences* 1209:49-55.

Michael, S.L., N.R. Pumford, P.R. Mayeux, M.R. Niesman, and J.A. Hinson. 1999. Pretreatment of mice with macrophage inactivators decreases acetaminophen hepatotoxicity and the formation of reactive oxygen and nitrogen species. *Hepatology* 30:186-195.

Miura, K., Y. Kodama, S. Inokuchi, B. Schnabl, T. Aoyama, H. Ohnishi, J.M. Olefsky, D.A. Brenner, and E. Seki. 2010. Toll-like receptor 9 promotes steatohepatitis by induction of interleukin-1beta in mice. *Gastroenterology* 139:323-334 e327.

Miura, K., L. Yang, N. van Rooijen, H. Ohnishi, and E. Seki. 2012. Hepatic recruitment of macrophages promotes nonalcoholic steatohepatitis through CCR2. *Am J Physiol Gastrointest Liver Physiol* 302:G1310-1321.

Moles, A., L. Murphy, C.L. Wilson, J.B. Chakraborty, C. Fox, E.J. Park, J. Mann, F. Oakley, R. Howarth, J. Brain, S. Masson, M. Karin, E. Seki, and D.A. Mann. 2014. A TLR2/S100A9/CXCL-2 signaling network is necessary for neutrophil recruitment in acute and chronic liver injury in the mouse. *Journal of hepatology* 60:782-791.

Molnarfi, N., M. Benkhoucha, H. Funakoshi, T. Nakamura, and P.H. Lalive. 2015. Hepatocyte growth factor: A regulator of inflammation and autoimmunity. *Autoimmun Rev* 14:293-303.

Mori, Y., T. Izawa, S. Takenaka, M. Kuwamura, and J. Yamate. 2009. Participation of functionally different macrophage populations and monocyte chemoattractant protein-1 in early stages of thioacetamide-induced rat hepatic injury. *Toxicologic pathology* 37:463-473.

Morizono, K., Y. Xie, T. Olafsen, B. Lee, A. Dasgupta, A.M. Wu, and I.S. Chen. 2011. The soluble serum protein Gas6 bridges virion envelope phosphatidylserine to the TAM receptor tyrosine kinase Axl to mediate viral entry. *Cell Host Microbe* 9:286-298.

Mossanen, J.C., O. Krenkel, C. Ergen, O. Govaere, A. Liepelt, T. Puengel, F. Heymann, S. Kalthoff, E. Lefebvre, D. Eulberg, T. Luedde, G. Marx, C.P. Strassburg, T. Roskams, C. Trautwein, and F. Tacke. 2016. Chemokine (C-C motif) receptor 2-positive monocytes aggravate the early phase of acetaminophen-induced acute liver injury. *Hepatology*

Mosser, D.M., and J.P. Edwards. 2008. Exploring the full spectrum of macrophage activation. *Nature reviews. Immunology* 8:958-969.

Mueller, A.M., X. Pedre, T. Stempfl, I. Kleiter, S. Couillard-Despres, L. Aigner, G. Giegerich, and A. Steinbrecher. 2008. Novel role for SLPI in MOG-induced EAE revealed by spinal cord expression analysis. *J Neuroinflammation* 5:20.

Mukherjee, S.K., A. Wilhelm, and C.G. Antoniades. 2016. TAM receptor tyrosine kinase function and the immunopathology of liver disease. *Am J Physiol Gastrointest Liver Physiol* 310:G899-905.

Murray, P.J., J.E. Allen, S.K. Biswas, E.A. Fisher, D.W. Gilroy, S. Goerdt, S. Gordon, J.A. Hamilton, L.B. Ivashkiv, T. Lawrence, M. Locati, A. Mantovani, F.O. Martinez, J.L. Mege, D.M. Mosser, G. Natoli, J.P. Saeij, J.L. Schultze, K.A. Shirey, A. Sica, J. Suttles, I. Udalova, J.A.

van Ginderachter, S.N. Vogel, and T.A. Wynn. 2014. Macrophage activation and polarization: nomenclature and experimental guidelines. *Immunity* 41:14-20.

Nagata, S., R. Hanayama, and K. Kawane. 2010. Autoimmunity and the clearance of dead cells. *Cell* 140:619-630.

Nakamura, A., Y. Mori, K. Hagiwara, T. Suzuki, T. Sakakibara, T. Kikuchi, T. Igarashi, M. Ebina, J. Miyazaki, T. Takai, and T. Nukiwa. 2003. Increased susceptibility to LPS-induced endotoxin shock in secretory leukoprotease inhibitor (SLPI)-deficient mice. *Journal of Experimental Medicine* 197:669-674.

Negash, A.A., H.J. Ramos, N. Crochet, D.T. Lau, B. Doehle, N. Papic, D.A. Delker, J. Jo, A. Bertoletti, C.H. Hagedorn, and M. Gale, Jr. 2013. IL-1beta production through the NLRP3 inflammasome by hepatic macrophages links hepatitis C virus infection with liver inflammation and disease. *PLoS Pathog* 9:e1003330.

Nishimura, J., H. Saiga, S. Sato, M. Okuyama, H. Kayama, H. Kuwata, S. Matsumoto, T. Nishida, Y. Sawa, S. Akira, Y. Yoshikai, M. Yamamoto, and K. Takeda. 2008. Potent antimycobacterial activity of mouse secretory leukocyte protease inhibitor. *Journal of immunology* 180:4032-4039.

O'Grady, J.G., S.W. Schalm, and R. Williams. 1993. Acute liver failure: redefining the syndromes. *Lancet* 342:273-275.

O'Hara, S.P., J.H. Tabibian, P.L. Splinter, and N.F. LaRusso. 2013. The dynamic biliary epithelia: molecules, pathways, and disease. *Journal of hepatology* 58:575-582.

Odaka, C., T. Mizuochi, J. Yang, and A. Ding. 2003a. Murine macrophages produce secretory leukocyte protease inhibitor during clearance of apoptotic cells: implications for resolution of the inflammatory response. *Journal of immunology* 171:1507-1514.

Odaka, C., T. Mizuochi, J.X. Yang, and A. Ding. 2003b. Murine macrophages produce secretory leukocyte protease inhibitor during clearance of apoptotic cells: Implications for resolution of the inflammatory response. *Journal of Immunology* 171:1507-1514.

Ortega-Gomez, A., M. Perretti, and O. Soehnlein. 2013. Resolution of inflammation: an integrated view. *EMBO molecular medicine* 5:661-674.

Ou, W.B., J.M. Corson, D.L. Flynn, W.P. Lu, S.C. Wise, R. Bueno, D.J. Sugarbaker, and J.A. Fletcher. 2011. AXL regulates mesothelioma proliferation and invasiveness. *Oncogene* 30:1643-1652.

Paolino, M., A. Choidas, S. Wallner, B. Pranjic, I. Uribesalgo, S. Loeser, A.M. Jamieson, W.Y. Langdon, F. Ikeda, J.P. Fededa, S.J. Cronin, R. Nitsch, C. Schultz-Fademrecht, J. Eickhoff, S. Menninger, A. Unger, R. Torka, T. Gruber, R. Hinterleitner, G. Baier, D. Wolf, A. Ullrich, B.M. Klebl, and J.M. Penninger. 2014. The E3 ligase Cbl-b and TAM receptors regulate cancer metastasis via natural killer cells. *Nature* 507:508-512.

Papayannopoulos, V. 2015. Sweet NETs, Bitter Wounds. *Immunity* 43:223-225.

Papayannopoulos, V., and A. Zychlinsky. 2009. NETs: a new strategy for using old weapons. *Trends in immunology* 30:513-521.

Park, H.J., J.Y. Baen, Y.J. Lee, Y.H. Choi, and J.L. Kang. 2012. The TAM-family receptor Mer mediates production of HGF through the RhoA-dependent pathway in response to apoptotic cells. *Molecular biology of the cell* 23:3254-3265.

Park, O., W.I. Jeong, L. Wang, H. Wang, Z.X. Lian, M.E. Gershwin, and B. Gao. 2009. Diverse roles of invariant natural killer T cells in liver injury and fibrosis induced by carbon tetrachloride. *Hepatology* 49:1683-1694.

Patin, E., Z. Kutalik, J. Guergnon, S. Bibert, B. Nalpas, E. Jouanguy, M. Munteanu, L. Bousquet, L. Argiro, P. Halfon, A. Boland, B. Mullhaupt, D. Semela, J.F. Dufour, M.H. Heim, D. Moradpour, A. Cerny, R. Malinverni, H. Hirsch, G. Martinetti, V. Suppiah, G. Stewart, D.R. Booth, J. George, J.L. Casanova, C. Brechot, C.M. Rice, A.H. Talal, I.M. Jacobson, M. Bourliere, I. Theodorou, T. Poynard, F. Negro, S. Pol, P.Y. Bochud, L. Abel, C.C.S.G. Swiss Hepatitis, C.G.C. International Hepatitis, and A.H.C.E.P.G.S.G. French. 2012. Genome-wide association study identifies variants associated with progression of liver fibrosis from HCV infection. *Gastroenterology* 143:1244-1252 e1241-1212.

Peng, H., and Z. Tian. 2015. Re-examining the origin and function of liver-resident NK cells. *Trends in immunology* 36:293-299.

Peppa, D., U.S. Gill, G. Reynolds, N.J. Easom, L.J. Pallett, A. Schurich, L. Micco, G. Nebbia, H.D. Singh, D.H. Adams, P.T. Kennedy, and M.K. Maini. 2013. Up-regulation of a death receptor renders antiviral T cells susceptible to NK cell-mediated deletion. *The Journal of experimental medicine* 210:99-114.

Petta, S., L. Valenti, F. Marra, S. Grimaudo, C. Tripodo, E. Bugianesi, C. Camma, A. Cappon, V. Di Marco, G. Di Maira, P. Dongiovanni, R. Rametta, A. Gulino, E. Mozzi, E. Orlando, M. Maggioni, R.M. Pipitone, S. Fargion, and A. Craxi. 2016. MERTK rs4374383 polymorphism affects the severity of fibrosis in non-alcoholic fatty liver disease. *Journal of hepatology* 64:682-690.

Poon, I.K., C.D. Lucas, A.G. Rossi, and K.S. Ravichandran. 2014. Apoptotic cell clearance: basic biology and therapeutic potential. *Nature reviews. Immunology* 14:166-180.

Possamai, L.A., W. Khamri, E. Triantafyllou, J.A. Wendon, M.R. Thursz, and C.G. Antoniades. 2014a. Could targeting secretory leukocyte protease inhibitor be an effective therapeutic option to prevent infections in acute liver failure? *Immunotherapy* 6:667-669.

Possamai, L.A., M.J. McPhail, A. Quaglia, V. Zingarelli, R.D. Abeles, R. Tidswell, Z. Puthucheary, J. Rawal, C.J. Karvellas, E.M. Leslie, R.D. Hughes, Y. Ma, W. Jassem, D.L. Shawcross, W. Bernal, A. Dharwan, N.D. Heaton, M. Thursz, J.A. Wendon, R.R. Mitry, and C.G. Antoniades. 2013. Character and temporal evolution of apoptosis in acetaminophen-induced acute liver failure*. *Crit Care Med* 41:2543-2550.

Possamai, L.A., M.R. Thursz, J.A. Wendon, and C.G. Antoniades. 2014b. Modulation of monocyte/macrophage function: a therapeutic strategy in the treatment of acute liver failure. *Journal of hepatology* 61:439-445.

Pradere, J.P., J. Kluwe, S. De Minicis, J.J. Jiao, G.Y. Gwak, D.H. Dapito, M.K. Jang, N.D. Guenther, I. Mederacke, R. Friedman, A.C. Dragomir, C. Aloman, and R.F. Schwabe. 2013. Hepatic macrophages but not dendritic cells contribute to liver fibrosis by promoting the survival of activated hepatic stellate cells in mice. *Hepatology* 58:1461-1473.

Prasad, D., C.V. Rothlin, P. Burrola, T. Burstyn-Cohen, Q. Lu, P. Garcia de Frutos, and G. Lemke. 2006. TAM receptor function in the retinal pigment epithelium. *Mol Cell Neurosci* 33:96-108.

Qi, N., P. Liu, Y. Zhang, H. Wu, Y. Chen, and D. Han. 2013. Development of a spontaneous liver disease resembling autoimmune hepatitis in mice lacking tyro3, axl and mer receptor tyrosine kinases. *PloS one* 8:e66604.

Quaglia, A., B.C. Portmann, A.S. Knisely, P. Srinivasan, P. Muiesan, J. Wendon, M.A. Heneghan, J.G. O'Grady, M. Samyn, D. Hadzic, A. Dhawan, G. Mieli-Vergani, N. Heaton, and M. Rela. 2008. Auxiliary transplantation for acute liver failure: Histopathological study of native liver regeneration. *Liver Transplantation* 14:1437-1448.

Rahman, Z.S., W.H. Shao, T.N. Khan, Y. Zhen, and P.L. Cohen. 2010. Impaired apoptotic cell clearance in the germinal center by Mer-deficient tingible body macrophages leads to enhanced antibody-forming cell and germinal center responses. *Journal of immunology* 185:5859-5868.

Ramachandran, P., A. Pellicoro, M.A. Vernon, L. Boulter, R.L. Aucott, A. Ali, S.N. Hartland, V.K. Snowdon, A. Cappon, T.T. Gordon-Walker, M.J. Williams, D.R. Dunbar, J.R. Manning, N. van Rooijen, J.A. Fallowfield, S.J. Forbes, and J.P. Iredale. 2012. Differential Ly-6C expression identifies the recruited macrophage phenotype, which orchestrates the regression of murine liver fibrosis. *Proc Natl Acad Sci U S A* 109:E3186-3195.

Raundhal, M., C. Morse, A. Khare, T.B. Oriss, J. Milosevic, J. Trudeau, R. Huff, J. Pilewski, F. Holguin, J. Kolls, S. Wenzel, P. Ray, and A. Ray. 2015. High IFN-gamma and low SLPI mark severe asthma in mice and humans. *The Journal of clinical investigation* 125:3037-3050.

Ravelli, A., A.A. Grom, E.M. Behrens, and R.Q. Cron. 2012. Macrophage activation syndrome as part of systemic juvenile idiopathic arthritis: diagnosis, genetics, pathophysiology and treatment. *Genes and immunity* 13:289-298.

Read, S.A., E.S. Tay, M. Shahidi, J. McLauchlan, J. George, and M.W. Douglas. 2015a. The Mechanism of Interferon Refractoriness During Hepatitis C Virus Infection and Its Reversal with a Peroxisome Proliferator-Activated Receptor alpha Agonist. *J Interferon Cytokine Res* 35:488-497.

Read, S.A., E.S. Tay, M. Shahidi, K.S. O'Connor, D.R. Booth, J. George, and M.W. Douglas. 2015b. Hepatitis C Virus Driven AXL Expression Suppresses the Hepatic Type I Interferon Response. *PloS one* 10:e0136227.

Reardon, C., M. Lechmann, A. Brustle, M.G. Gareau, N. Shuman, D. Philpott, S.F. Ziegler, and T.W. Mak. 2011. Thymic stromal lymphopoetin-induced expression of the endogenous inhibitory enzyme SLPI mediates recovery from colonic inflammation. *Immunity* 35:223-235.

Rehermann, B. 2017. Mature peritoneal macrophages take an avascular route into the injured liver and promote tissue repair. *Hepatology* 65:376-379.

Renshaw, S.A., S.J. Timmons, V. Eaton, L.R. Usher, M. Akil, C.D. Bingle, and M.K. Whyte. 2000. Inflammatory neutrophils retain susceptibility to apoptosis mediated via the Fas death receptor. *Journal of leukocyte biology* 67:662-668.

Rolando, N., J. Wade, M. Davalos, J. Wendon, J. Philpott-Howard, and R. Williams. 2000. The systemic inflammatory response syndrome in acute liver failure. *Hepatology* 32:734-739.

Rothlin, C.V., E.A. Carrera-Silva, L. Bosurgi, and S. Ghosh. 2015. TAM receptor signaling in immune homeostasis. *Annual review of immunology* 33:355-391.

Rothlin, C.V., S. Ghosh, E.I. Zuniga, M.B. Oldstone, and G. Lemke. 2007. TAM receptors are pleiotropic inhibitors of the innate immune response. *Cell* 131:1124-1136.

Rothlin, C.V., and G. Lemke. 2010. TAM receptor signaling and autoimmune disease. *Current opinion in immunology* 22:740-746.

Sallenave, J.-M. 2010. Secretory Leukocyte Protease Inhibitor and Elafin/Trappin-2 Versatile Mucosal Antimicrobials and Regulators of Immunity. *American Journal of Respiratory Cell and Molecular Biology* 42:635-643.

Samsom, J.N., A.P. van der Marel, L.A. van Berkel, J.M. van Helvoort, Y. Simons-Oosterhuis, W. Jansen, M. Greuter, R.L. Nelissen, C.M. Meeuwisse, E.E. Nieuwenhuis, R.E. Mebius, and G. Kraal. 2007. Secretory leukoprotease inhibitor in mucosal lymph node dendritic cells regulates the threshold for mucosal tolerance. *Journal of immunology* 179:6588-6595.

Sano, C., T. Shimizu, K. Sato, H. Kawauchi, and H. Tomioka. 2000. Effects of secretory leucocyte protease inhibitor on the production of the anti-inflammatory cytokines, IL-10 and

transforming growth factor-beta (TGF-beta), by lipopolysaccharide-stimulated macrophages. *Clinical and Experimental Immunology* 121:77-85.

Sano, C., T. Shimizu, and H. Tomioka. 2003. Effects of secretory leukocyte protease inhibitor on the tumor necrosis factor-alpha production and NF-kappa B activation of lipopolysaccharide-stimulated macrophages. *Cytokine* 21:38-42.

Scannell, M., M.B. Flanagan, A. deStefani, K.J. Wynne, G. Cagney, C. Godson, and P. Maderna. 2007. Annexin-1 and peptide derivatives are released by apoptotic cells and stimulate phagocytosis of apoptotic neutrophils by macrophages. *Journal of immunology* 178:4595-4605.

Schif-Zuck, S., N. Gross, S. Assi, R. Rostoker, C.N. Serhan, and A. Ariel. 2011. Saturated-efferocytosis generates pro-resolving CD11b low macrophages: modulation by resolvins and glucocorticoids. *Eur J Immunol* 41:366-379.

Schmidt, L.E., and F.S. Larsen. 2006. Prognostic implications of hyperlactatemia, multiple organ failure, and systemic inflammatory response syndrome in patients with acetaminophen-induced acute liver failure. *Crit Care Med* 34:337-343.

Schmieg, J., G. Yang, R.W. Franck, N. Van Rooijen, and M. Tsuji. 2005. Glycolipid presentation to natural killer T cells differs in an organ-dependent fashion. *Proc Natl Acad Sci U S A* 102:1127-1132.

Schulert, G.S., and A.A. Grom. 2015. Pathogenesis of macrophage activation syndrome and potential for cytokine- directed therapies. *Annual review of medicine* 66:145-159.

Schulz, C., E. Gomez Perdiguero, L. Chorro, H. Szabo-Rogers, N. Cagnard, K. Kierdorf, M. Prinz, B. Wu, S.E. Jacobsen, J.W. Pollard, J. Frampton, K.J. Liu, and F. Geissmann. 2012. A lineage of myeloid cells independent of Myb and hematopoietic stem cells. *Science* 336:86-90.

Schulze, H., M. Korpal, W. Bergmeier, J.E. Italiano, Jr., S.M. Wahl, and R.A. Shivdasani. 2004. Interactions between the megakaryocyte/platelet-specific beta1 tubulin and the secretory leukocyte protease inhibitor SLPI suggest a role for regulated proteolysis in platelet functions. *Blood* 104:3949-3957.

Schwab, J.M., N. Chiang, M. Arita, and C.N. Serhan. 2007. Resolvin E1 and protectin D1 activate inflammation-resolution programmes. *Nature* 447:869-874.

Scott, A., S. Weldon, and C.C. Taggart. 2011a. SLPI and elafin: multifunctional antiproteases of the WFDC family. *Biochemical Society transactions* 39:1437-1440.

Scott, A., S. Weldon, and C.C. Taggart. 2011b. SLPI and elafin: multifunctional antiproteases of the WFDC family. *Biochemical Society Transactions* 39:1437-1440.

Scott, C.L., F. Zheng, P. De Baetselier, L. Martens, Y. Saeys, S. De Prijck, S. Lippens, C. Abels, S. Schoonooghe, G. Raes, N. Devoogdt, B.N. Lambrecht, A. Beschin, and M. Guilliams. 2016. Bone marrow-derived monocytes give rise to self-renewing and fully differentiated Kupffer cells. *Nat Commun* 7:10321.

Scott, R.S., E.J. McMahon, S.M. Pop, E.A. Reap, R. Caricchio, P.L. Cohen, H.S. Earp, and G.K. Matsushima. 2001. Phagocytosis and clearance of apoptotic cells is mediated by MER. *Nature* 411:207-211.

Sen, P., M.A. Wallet, Z. Yi, Y. Huang, M. Henderson, C.E. Mathews, H.S. Earp, G. Matsushima, A.S. Baldwin, Jr., and R.M. Tisch. 2007. Apoptotic cells induce Mer tyrosine kinase-dependent blockade of NF-kappaB activation in dendritic cells. *Blood* 109:653-660.

Serhan, C.N. 2014. Pro-resolving lipid mediators are leads for resolution physiology. *Nature* 510:92-101.

Serhan, C.N., J. Dalli, S. Karamnov, A. Choi, C.K. Park, Z.Z. Xu, R.R. Ji, M. Zhu, and N.A. Petasis. 2012. Macrophage proresolving mediator maresin 1 stimulates tissue regeneration and controls pain. *FASEB J* 26:1755-1765.

Shibata, T., D.M. Habiel, A.L. Coelho, S.L. Kunkel, N.W. Lukacs, and C.M. Hogaboam. 2014. Axl receptor blockade ameliorates pulmonary pathology resulting from primary viral infection and viral exacerbation of asthma. *Journal of immunology* 192:3569-3581.

Sica, A., and A. Mantovani. 2012. Macrophage plasticity and polarization: in vivo veritas. *The Journal of clinical investigation* 122:787-795.

Skrzeczynska-Moncznik, J., A. Wlodarczyk, M. Banas, M. Kwitniewski, K. Zabieglo, M. Kapinska-Mrowiecka, A. Dubin, and J. Cichy. 2013. DNA structures decorated with cathepsin

G/secretory leukocyte proteinase inhibitor stimulate IFNI production by plasmacytoid dendritic cells. *Am J Clin Exp Immunol* 2:186-194.

Skrzeczynska-Moncznik, J., A. Wlodarczyk, K. Zabieglo, M. Kapinska-Mrowiecka, E. Marewicz, A. Dubin, J. Potempa, and J. Cichy. 2012. Secretory leukocyte proteinase inhibitor-competent DNA deposits are potent stimulators of plasmacytoid dendritic cells: implication for psoriasis. *Journal of immunology* 189:1611-1617.

Slaba, I., J. Wang, E. Kolaczkowska, B. McDonald, W.Y. Lee, and P. Kubes. 2015. Imaging the dynamic platelet-neutrophil response in sterile liver injury and repair in mice. *Hepatology* 62:1593-1605.

Song, K.S., Y.S. Park, and H.K. Kim. 2000. Prevalence of anti-protein S antibodies in patients with systemic lupus erythematosus. *Arthritis and rheumatism* 43:557-560.

Song, X., L. Zeng, W. Jin, J. Thompson, D.E. Mizel, K. Lei, R.C. Billinghurst, A.R. Poole, and S.M. Wahl. 1999. Secretory leukocyte protease inhibitor suppresses the inflammation and joint damage of bacterial cell wall-induced arthritis. *The Journal of experimental medicine* 190:535-542.

Song, Y., Z. Quan, and Y.M. Liu. 2004. Assay of histamine by nano-liquid chromatography/tandem mass spectrometry with a packed nanoelectrospray emitter. *Rapid Commun Mass Spectrom* 18:2818-2822.

Sorensen, O.E., and N. Borregaard. 2016. Neutrophil extracellular traps - the dark side of neutrophils. *The Journal of clinical investigation* 126:1612-1620.

Stables, M.J., S. Shah, E.B. Camon, R.C. Lovering, J. Newson, J. Bystrom, S. Farrow, and D.W. Gilroy. 2011. Transcriptomic analyses of murine resolution-phase macrophages. *Blood* 118:e192-208.

Staub, E., A. Rosenthal, and B. Hinzmann. 2004. Systematic identification of immunoreceptor tyrosine-based inhibitory motifs in the human proteome. *Cell Signal* 16:435-456.

Stravitz, R.T., J.H. Lefkowitch, R.J. Fontana, M.E. Gershwin, P.S.C. Leung, R.K. Sterling, M.P. Manns, G.L. Norman, W.M. Lee, and G. Acute Liver Failure Study. 2011. Autoimmune Acute Liver Failure: Proposed Clinical and Histological Criteria. *Hepatology* 53:517-526.

Stutchfield, B.M., D.J. Antoine, A.C. Mackinnon, D.J. Gow, C.C. Bain, C.A. Hawley, M.J. Hughes, B. Francis, D. Wojtacha, T.Y. Man, J.W. Dear, L.R. Devey, A.M. Mowat, J.W. Pollard, B.K. Park, S.J. Jenkins, K.J. Simpson, D.A. Hume, S.J. Wigmore, and S.J. Forbes. 2015. CSF1 Restores Innate Immunity After Liver Injury in Mice and Serum Levels Indicate Outcomes of Patients With Acute Liver Failure. *Gastroenterology* 149:1896-1909 e1814.

Subramanian, M., C.D. Hayes, J.J. Thome, E. Thorp, G.K. Matsushima, J. Herz, D.L. Farber, K. Liu, M. Lakshmana, and I. Tabas. 2014. An AXL/LRP-1/RANBP9 complex mediates DC efferocytosis and antigen cross-presentation in vivo. *The Journal of clinical investigation* 124:1296-1308.

Subramaniyam, D., C. Hollander, U. Westin, J. Erjefalt, T. Stevens, and S. Janciauskiene. 2011. Secretory leukocyte protease inhibitor inhibits neutrophil apoptosis. *Respirology* 16:300-307.

Sugimoto, M.A., L.P. Sousa, V. Pinho, M. Perretti, and M.M. Teixeira. 2016. Resolution of Inflammation: What Controls Its Onset? *Frontiers in immunology* 7:160.

Sullivan, B.M., M.J. Welch, G. Lemke, and M.B. Oldstone. 2013. Is the TAM receptor Axl a receptor for lymphocytic choriomeningitis virus? *J Virol* 87:4071-4074.

Sun, B., N. Qi, T. Shang, H. Wu, T. Deng, and D. Han. 2010. Sertoli cell-initiated testicular innate immune response through toll-like receptor-3 activation is negatively regulated by Tyro3, Axl, and mer receptors. *Endocrinology* 151:2886-2897.

Syn, W.K., Y.H. Oo, T.A. Pereira, G.F. Karaca, Y. Jung, A. Omenetti, R.P. Witek, S.S. Choi, C.D. Guy, C.M. Fearing, V. Teaberry, F.E. Pereira, D.H. Adams, and A.M. Diehl. 2010. Accumulation of natural killer T cells in progressive nonalcoholic fatty liver disease. *Hepatology* 51:1998-2007.

Tacke, F., and H.W. Zimmermann. 2014. Macrophage heterogeneity in liver injury and fibrosis. *Journal of hepatology* 60:1090-1096.

Taggart, C.C., S.A. Cryan, S. Weldon, A. Gibbons, C.M. Greene, E. Kelly, T.B. Low, J. O'Neill S, and N.G. McElvaney. 2005. Secretory leucoprotease inhibitor binds to NF-kappaB binding sites in monocytes and inhibits p65 binding. *The Journal of experimental medicine* 202:1659-1668.

Taggart, C.C., C.M. Greene, N.G. McElvaney, and S. O'Neill. 2002. Secretory leucoprotease inhibitor prevents lipopolysaccharide-induced IkappaBalpha degradation without affecting phosphorylation or ubiquitination. *The Journal of biological chemistry* 277:33648-33653.

Taylor, N.J., A. Nishtala, G.K. Manakkat Vijay, R.D. Abeles, G. Auzinger, W. Bernal, Y. Ma, J.A. Wendon, and D.L. Shawcross. 2013. Circulating neutrophil dysfunction in acute liver failure. *Hepatology* 57:1142-1152.

Tian, Z., Y. Chen, and B. Gao. 2013. Natural killer cells in liver disease. *Hepatology* 57:1654-1662.

Tomita, K., G. Tamiya, S. Ando, K. Ohsumi, T. Chiyo, A. Mizutani, N. Kitamura, K. Toda, T. Kaneko, Y. Horie, J.Y. Han, S. Kato, M. Shimoda, Y. Oike, M. Tomizawa, S. Makino, T. Ohkura, H. Saito, N. Kumagai, H. Nagata, H. Ishii, and T. Hibi. 2006. Tumour necrosis factor alpha signalling through activation of Kupffer cells plays an essential role in liver fibrosis of non-alcoholic steatohepatitis in mice. *Gut* 55:415-424.

Trey, C., and C.S. Davidson. 1970. The management of fulminant hepatic failure. *Prog Liver Dis* 3:282-298.

Triantafyllou, E., O.T. Pop, R.D. Abeles, W. Khamri, L. Possamai, M. Hussain, W. Bernal, G. Auzinger, M.A. Heneghan, N. Heaton, M. Thursz, J. Wendon, A. Quaglia, Y. Ma, and C.G. Antoniades. 2014. Seronegative Acute Liver Failure Represents a Macrophage-T Cell Activation Syndrome. *Journal of hepatology* 60:S111-S112.

Trobonjaca, Z., F. Leithauser, P. Moller, R. Schirmbeck, and J. Reimann. 2001. Activating immunity in the liver. I. Liver dendritic cells (but not hepatocytes) are potent activators of IFN-gamma release by liver NKT cells. *Journal of immunology* 167:1413-1422.

Tsou, W.I., K.Q. Nguyen, D.A. Calarese, S.J. Garforth, A.L. Antes, S.V. Smirnov, S.C. Almo, R.B. Birge, and S.V. Kotenko. 2014. Receptor tyrosine kinases, TYRO3, AXL, and MER, demonstrate distinct patterns and complex regulation of ligand-induced activation. *The Journal of biological chemistry* 289:25750-25763.

Tu, Z., R.H. Pierce, J. Kurtis, Y. Kuroki, I.N. Crispe, and M.S. Orloff. 2010. Hepatitis C virus core protein subverts the antiviral activities of human Kupffer cells. *Gastroenterology* 138:305-314.

Tuncer, C., Y.H. Oo, N. Murphy, D.H. Adams, and P.F. Lalor. 2013. The regulation of T-cell recruitment to the human liver during acute liver failure. *Liver International* 33:852-863.

van den Berg, J.M., S. Weyer, J.J. Weening, D. Roos, and T.W. Kuijpers. 2001. Divergent effects of tumor necrosis factor alpha on apoptosis of human neutrophils. *Journal of leukocyte biology* 69:467-473.

Vaquero, J., J. Polson, C. Chung, I. Helenowski, F.V. Schiodt, J. Reisch, W.M. Lee, and A.T. Blei. 2003. Infection and the progression of hepatic encephalopathy in acute liver failure. *Gastroenterology* 125:755-764.

Varol, C., S. Yona, and S. Jung. 2009. Origins and tissue-context-dependent fates of blood monocytes. *Immunol Cell Biol* 87:30-38.

Verma, C., S. Seebah, S.M. Low, L. Zhou, S.P. Liu, J. Li, and R.W. Beuerman. 2007. Defensins: antimicrobial peptides for therapeutic development. *Biotechnol J* 2:1353-1359.

von Andrian, U.H., and T.R. Mempel. 2003. Homing and cellular traffic in lymph nodes. *Nature reviews. Immunology* 3:867-878.

Walmsley, S.R., E.R. Chilvers, A.A. Thompson, K. Vaughan, H.M. Marriott, L.C. Parker, G. Shaw, S. Parmar, M. Schneider, I. Sabroe, D.H. Dockrell, M. Milo, C.T. Taylor, R.S. Johnson, C.W. Pugh, P.J. Ratcliffe, P.H. Maxwell, P. Carmeliet, and M.K. Whyte. 2011. Prolyl hydroxylase 3 (PHD3) is essential for hypoxic regulation of neutrophilic inflammation in humans and mice. *The Journal of clinical investigation* 121:1053-1063.

Wan, E., X.Y. Yeap, S. Dehn, R. Terry, M. Novak, S. Zhang, S. Iwata, X. Han, S. Homma, K. Drosatos, J. Lomasney, D.M. Engman, S.D. Miller, D.E. Vaughan, J.P. Morrow, R. Kishore, and E.B. Thorp. 2013. Enhanced efferocytosis of apoptotic cardiomyocytes through myeloid-epithelial-reproductive tyrosine kinase links acute inflammation resolution to cardiac repair after infarction. *Circ Res* 113:1004-1012.

Wan, J., M. Benkdane, F. Teixeira-Clerc, S. Bonnafous, A. Louvet, F. Lafdil, F. Pecker, A. Tran, P. Gual, A. Mallat, S. Lotersztajn, and C. Pavoine. 2014. M2 Kupffer cells promote M1 Kupffer cell apoptosis: a protective mechanism against alcoholic and nonalcoholic fatty liver disease. *Hepatology* 59:130-142.

Wang, H., D. Feng, O. Park, S. Yin, and B. Gao. 2013. Invariant NKT cell activation induces neutrophil accumulation and hepatitis: opposite regulation by IL-4 and IFN-gamma. *Hepatology* 58:1474-1485.

Wang, J., and P. Kubes. 2016. A Reservoir of Mature Cavity Macrophages that Can Rapidly Invade Visceral Organs to Affect Tissue Repair. *Cell* 165:668-678.

Wang, Y., D. Feng, H. Wang, M.J. Xu, O. Park, Y. Li, and B. Gao. 2014. STAT4 knockout mice are more susceptible to concanavalin A-induced T-cell hepatitis. *The American journal of pathology* 184:1785-1794.

Wehr, A., C. Baeck, F. Heymann, P.M. Niemietz, L. Hammerich, C. Martin, H.W. Zimmermann, O. Pack, N. Gassler, K. Hittatiya, A. Ludwig, T. Luedde, C. Trautwein, and F. Tacke. 2013. Chemokine receptor CXCR6-dependent hepatic NK T Cell accumulation promotes inflammation and liver fibrosis. *Journal of immunology* 190:5226-5236.

Wen, J., N.G. Nikitakis, R. Chaisuparat, T. Greenwell-Wild, M. Gliozzi, W. Jin, A. Adli, N. Moutsopoulos, T. Wu, G. Warburton, and S.M. Wahl. 2011. Secretory leukocyte protease inhibitor (SLPI) expression and tumor invasion in oral squamous cell carcinoma. *The American journal of pathology* 178:2866-2878.

Williams, C.D., M.L. Bajt, A. Farhood, and H. Jaeschke. 2010a. Acetaminophen-induced hepatic neutrophil accumulation and inflammatory liver injury in CD18-deficient mice. *Liver international : official journal of the International Association for the Study of the Liver* 30:1280-1292.

Williams, C.D., M.L. Bajt, M.R. Sharpe, M.R. McGill, A. Farhood, and H. Jaeschke. 2014a. Neutrophil activation during acetaminophen hepatotoxicity and repair in mice and humans. *Toxicol Appl Pharmacol* 275:122-133.

Williams, C.D., M.L. Bajt, M.R. Sharpe, M.R. McGill, A. Farhood, and H. Jaeschke. 2014b. Neutrophil activation during acetaminophen hepatotoxicity and repair in mice and humans. *Toxicology and applied pharmacology* 275:122-133.

Williams, C.D., A. Farhood, and H. Jaeschke. 2010b. Role of caspase-1 and interleukin-1beta in acetaminophen-induced hepatic inflammation and liver injury. *Toxicology and applied pharmacology* 247:169-178.

Wingens, M., B.H. van Bergen, P.S. Hiemstra, J.F. Meis, I.M. van Vlijmen-Willems, P.L. Zeeuwen, J. Mulder, H.A. Kramps, F. van Ruissen, and J. Schalkwijk. 1998. Induction of SLPI (ALP/HUSI-I) in epidermal keratinocytes. *J Invest Dermatol* 111:996-1002.

Wolf, M.J., A. Adili, K. Piotrowitz, Z. Abdullah, Y. Boege, K. Stemmer, M. Ringelhan, N. Simonavicius, M. Egger, D. Wohlleber, A. Lorentzen, C. Einer, S. Schulz, T. Clavel, U. Protzer, C. Thiele, H. Zischka, H. Moch, M. Tschop, A.V. Tumanov, D. Haller, K. Unger, M. Karin, M. Kopf, P. Knolle, A. Weber, and M. Heikenwalder. 2014. Metabolic activation of intrahepatic CD8+ T cells and NKT cells causes nonalcoholic steatohepatitis and liver cancer via cross-talk with hepatocytes. *Cancer Cell* 26:549-564.

Wondimu, Z., T. Santodomingo-Garzon, T. Le, and M.G. Swain. 2010. Protective role of interleukin-17 in murine NKT cell-driven acute experimental hepatitis. *The American journal of pathology* 177:2334-2346.

Wong, K.L., J.J. Tai, W.C. Wong, H. Han, X. Sem, W.H. Yeap, P. Kourilsky, and S.C. Wong. 2011. Gene expression profiling reveals the defining features of the classical, intermediate, and nonclassical human monocyte subsets. *Blood* 118:e16-31.

Wright, C.D., J.A. Kennedy, R.J. Zitnik, and M.A. Kashem. 1999. Inhibition of murine neutrophil serine proteinases by human and murine secretory leukocyte protease inhibitor. *Biochem Biophys Res Commun* 254:614-617.

Wu, Z., M. Han, T. Chen, W. Yan, and Q. Ning. 2010. Acute liver failure: mechanisms of immune-mediated liver injury. *Liver International* 30:782-794.

Xu, R., H. Huang, Z. Zhang, and F.S. Wang. 2014. The role of neutrophils in the development of liver diseases. *Cell Mol Immunol* 11:224-231.

Xu, W., B. He, A. Chiu, A. Chadburn, M. Shan, M. Buldys, A. Ding, D.M. Knowles, P.A. Santini, and A. Cerutti. 2007. Epithelial cells trigger frontline immunoglobulin class switching through a pathway regulated by the inhibitor SLPI. *Nature immunology* 8:294-303.

Xue, J., S.V. Schmidt, J. Sander, A. Draffehn, W. Krebs, I. Quester, D. De Nardo, T.D. Gohel, M. Emde, L. Schmidleithner, H. Ganesan, A. Nino-Castro, M.R. Mallmann, L. Labzin, H. Theis, M. Kraut, M. Beyer, E. Latz, T.C. Freeman, T. Ulas, and J.L. Schultze. 2014. Transcriptome-based network analysis reveals a spectrum model of human macrophage activation. *Immunity* 40:274-288.

Yang, J., J. Zhu, D. Sun, and A. Ding. 2005. Suppression of macrophage responses to bacterial lipopolysaccharide (LPS) by secretory leukocyte protease inhibitor (SLPI) is independent of its anti-protease function. *Biochim Biophys Acta* 1745:310-317.

You, Q., L. Cheng, T.P. Reilly, D. Wegmann, and C. Ju. 2006. Role of neutrophils in a mouse model of halothane-induced liver injury. *Hepatology* 44:1421-1431.

You, Q., M. Holt, H. Yin, G. Li, C.J. Hu, and C. Ju. 2013. Role of hepatic resident and infiltrating macrophages in liver repair after acute injury. *Biochemical pharmacology* 86:836-843.

Zabieglo, K., P. Majewski, M. Majchrzak-Gorecka, A. Wlodarczyk, B. Grygier, A. Zegar, M. Kapinska-Mrowiecka, A. Naskalska, K. Pyrc, A. Dubin, S.M. Wahl, and J. Cichy. 2015a. The inhibitory effect of secretory leukocyte protease inhibitor (SLPI) on formation of neutrophil extracellular traps. *Journal of leukocyte biology*

Zabieglo, K., P. Majewski, M. Majchrzak-Gorecka, A. Wlodarczyk, B. Grygier, A. Zegar, M. Kapinska-Mrowiecka, A. Naskalska, K. Pyrc, A. Dubin, S.M. Wahl, and J. Cichy. 2015b. The inhibitory effect of secretory leukocyte protease inhibitor (SLPI) on formation of neutrophil extracellular traps. *Journal of leukocyte biology* 98:99-106.

Zagorska, A., P.G. Traves, E.D. Lew, I. Dransfield, and G. Lemke. 2014. Diversification of TAM receptor tyrosine kinase function. *Nature immunology* 15:920-928.

Zeissig, S., K. Murata, L. Sweet, J. Publicover, Z. Hu, A. Kaser, E. Bosse, J. Iqbal, M.M. Hussain, K. Balschun, C. Rocken, A. Arlt, R. Gunther, J. Hampe, S. Schreiber, J.L. Baron, D.B. Moody, T.J. Liang, and R.S. Blumberg. 2012. Hepatitis B virus-induced lipid alterations contribute to natural killer T cell-dependent protective immunity. *Nat Med* 18:1060-1068.

Zhang, Y., D.L. DeWitt, T.B. McNeely, S.M. Wahl, and L.M. Wahl. 1997. Secretory leukocyte protease inhibitor suppresses the production of monocyte prostaglandin H synthase-2,

prostaglandin E2, and matrix metalloproteinases. *The Journal of clinical investigation* 99:894-900.

Zhang, Y., N. Li, Q. Chen, K. Yan, Z. Liu, X. Zhang, P. Liu, Y. Chen, and D. Han. 2013. Breakdown of immune homeostasis in the testis of mice lacking Tyro3, Axl and Mer receptor tyrosine kinases. *Immunol Cell Biol* 91:416-426.

Zhu, J., C. Nathan, W. Jin, D. Sim, G.S. Ashcroft, S.M. Wahl, L. Lacomis, H. Erdjument-Bromage, P. Tempst, C.D. Wright, and A. Ding. 2002. Conversion of proepithelin to epithelins: roles of SLPI and elastase in host defense and wound repair. *Cell* 111:867-878.

Zigmond, E., S. Samia-Grinberg, M. Pasmanik-Chor, E. Brazowski, O. Shibolet, Z. Halpern, and C. Varol. 2014. Infiltrating monocyte-derived macrophages and resident kupffer cells display different ontogeny and functions in acute liver injury. *Journal of immunology* 193:344-353.

Zimmermann, H.W., T. Bruns, C.J. Weston, S.M. Curbishley, E. Liaskou, K.K. Li, Y.J. Resheq, P.W. Badenhorst, and D.H. Adams. 2015. Bidirectional transendothelial migration of monocytes across hepatic sinusoidal endothelium shapes monocyte differentiation and regulates the balance between immunity and tolerance in liver. *Hepatology*

Zimmermann, H.W., J.R. Mueller, S. Seidler, T. Luedde, C. Trautwein, and F. Tacke. 2013. Frequency and phenotype of human circulating and intrahepatic natural killer cell subsets is differentially regulated according to stage of chronic liver disease. *Digestion* 88:1-16.

Zimmermann, H.W., S. Seidler, N. Gassler, J. Nattermann, T. Luedde, C. Trautwein, and F. Tacke. 2011. Interleukin-8 is activated in patients with chronic liver diseases and associated with hepatic macrophage accumulation in human liver fibrosis. *PloS one* 6:e21381.

Zimmermann, H.W., S. Seidler, J. Nattermann, N. Gassler, C. Hellerbrand, A. Zernecke, J.J. Tischendorf, T. Luedde, R. Weiskirchen, C. Trautwein, and F. Tacke. 2010. Functional contribution of elevated circulating and hepatic non-classical CD14CD16 monocytes to inflammation and human liver fibrosis. *PloS one* 5:e11049.

Zimmermann, H.W., C. Trautwein, and F. Tacke. 2012. Functional role of monocytes and macrophages for the inflammatory response in acute liver injury. *Frontiers in physiology* 3:56.

Zizzo, G., and P.L. Cohen. 2013. IL-17 stimulates differentiation of human anti-inflammatory macrophages and phagocytosis of apoptotic neutrophils in response to IL-10 and glucocorticoids. *Journal of immunology* 190:5237-5246.

Zizzo, G., B.A. Hilliard, M. Monestier, and P.L. Cohen. 2012. Efficient clearance of early apoptotic cells by human macrophages requires M2c polarization and MerTK induction. *Journal of immunology* 189:3508-3520.